

Electronic Thesis and Dissertation Repository

7-18-2011 12:00 AM

Mutant Cx43 in Skin Differentiation and Disease

Jared M. Churko
University of Western Ontario

Supervisor
Dr. Dale W. Laird
The University of Western Ontario

Graduate Program in Anatomy and Cell Biology
A thesis submitted in partial fulfillment of the requirements for the degree in Doctor of
Philosophy
© Jared M. Churko 2011

Follow this and additional works at: <https://ir.lib.uwo.ca/etd>



Part of the [Skin and Connective Tissue Diseases Commons](#)

Recommended Citation

Churko, Jared M., "Mutant Cx43 in Skin Differentiation and Disease" (2011). *Electronic Thesis and Dissertation Repository*. 240.
<https://ir.lib.uwo.ca/etd/240>

This Dissertation/Thesis is brought to you for free and open access by Scholarship@Western. It has been accepted for inclusion in Electronic Thesis and Dissertation Repository by an authorized administrator of Scholarship@Western. For more information, please contact wlsadmin@uwo.ca.

MUTANT Cx43 IN SKIN DIFFERENTIATION AND DISEASE

(Spine title: Mutant Cx43 Expression in Skin)

(Thesis format: Integrated Article)

by

Jared Markam Churko

Graduate Program in Anatomy and Cell Biology

A thesis submitted in partial fulfillment
of the requirements for the degree of
Doctorate of Philosophy

The School of Graduate and Postdoctoral Studies
The University of Western Ontario
London, Ontario, Canada

© Jared M Churko 2011

CERTIFICATE OF EXAMINATION

Supervisor

Examiners

Dr. Dale Laird

Dr. Ross Johnson

Supervisory Committee

Dr. Lina Dagnino

Dr. Martin Sandig

Dr. Dan Belliveau

Dr. David Litchfield

Dr. Paul Walton

The thesis by

Jared Markam Churko

entitled:

Mutant Cx43 in skin differentiation and disease

is accepted in partial fulfillment of the
requirements for the degree of
Doctorate of Philosophy

Date

Chair of the Thesis Examination Board

Abstract

Connexin43 (Cx43) is expressed within keratinocytes, dermal fibroblasts, and the hair follicle epithelium. Since Cx43 is so widely expressed in resident cells of the skin, we speculated that this connexin would play an essential role in skin homeostasis, hair growth and wound healing. Mutations in the gene which encodes Cx43 lead to a disease called oculodentodigital dysplasia (ODDD) and patients expressing the frame-shift mutants (fs230 or fs260) develop a skin disease called palmar plantar hyperkeratosis. In addition, patients with ODDD often develop hair which is dry, sparse, and slow growing. To study skin abnormalities associated with ODDD, hair growth and wound healing assays were performed on a mouse model of ODDD (G60S mice). Cutaneous wounds performed on the G60S mice healed slower than wounds performed on wild-type (WT) littermate mice suggesting that fibroblasts and/or keratinocytes expressing mutant Cx43 may be impaired in their ability to heal wounds. Fibroblasts derived from G60S mice and from two ODDD patients expressing the D3N and V216L Cx43 mutant revealed defects in the ability of fibroblasts to proliferate, migrate, and differentiate into myofibroblasts while keratinocytes derived from the G60S mouse demonstrated an enhancement in cell proliferation but no change in migration. To investigate the ability of keratinocytes expressing mutant Cx43 to differentiate, organotypic epidermal cultures were engineered to express full-length Cx43 or various ODDD mutants (G21R, G138R, G60S, fs230 and fs260). In comparison to full-length Cx43, organotypic epidermal cultures expressing the fs260 mutant significantly lowered the levels of endogenous Cx43, levels of Cx26, and developed nuclei within the stratum corneum. Hair regrowth was also found to be delayed in the G60S mice and this delay was attributed to a reduction in the mitotic activity of hair follicle cells. In addition, hair fibers from G60S mice were thinner, shorter, displayed cuticle degradation in the distal region and nodule formation in the proximal hair fiber region when compared to WT derived hair fibers. Collectively, our results suggest the mutant Cx43 impairs the function of fibroblasts during wound healing and a reduced proliferation of the hair follicle epithelium likely leads to defects in hair growth observed in ODDD patients.

Keywords

Connexin43, Connexin, Mutant, Oculodentodigital Dysplasia, Skin Disease, Hair Follicle, Epidermis, Keratinocyte, Dermal Fibroblast, Proliferation, Migration, Myofibroblast, Differentiation, Wound Healing, Organotypic Epidermal Culture, Palmar Plantar Hyperkeratosis, fs230, fs260, G60S Mouse, Epilation, Scanning Electron Microscopy, Confocal Microscopy, Transepithelial Resistance

Co-Authorship Statement

Chapter 2

Dr. Qing Shao arranged for the transfer of human dermal fibroblasts to the University of Western Ontario, genotyped dermal fibroblasts, performed confocal imaging of vimentin labeled human dermal fibroblasts, and assessed the ability of dermal fibroblasts to transfer dye.

Dr. Xiang-Qun Gong and Dr. Donglin Bai performed conductance measurements on human dermal fibroblasts.

Dr. Katharine Swoboda and Dr. Jacinda Sampson isolated human dermal fibroblast at the University of Utah, shipped the dermal fibroblasts to the University of Western Ontario, and wrote and edited the human ODDD patient descriptions.

Chapter 3

Andrew McDonald performed conductance measurements on primary keratinocytes derived from wild type and G60S mutant mice.

Chapter 4

Dr. Stephanie Langlois contributed by editing the manuscript and teaching me some of the methods used in the study.

Xingue Pan contributed by performing the gap junction plaque counts and measuring the thickness of the organotypic layers generated from rat epidermal keratinocytes.

Dr. Qing Shao contributed by designing many of the Cx43 mutants used in this study.

Chapter 5

Jason Chang measured a large number of hair fibers for length and width thicknesses.

Acknowledgments

I would like to thank the following people:

- My family for their love, offering sage advice and supporting my aspirations
- Jordan Eldred for her love and companionship
- Dr. Dale Laird for accepting me as a PhD student, mentoring me throughout my PhD, funding me throughout my PhD, always having his office door open, editing my writing, supporting my scientific ideas, publishing my work, and ultimately preparing me for a career in science
- Qing Shao for her technical laboratory assistance, keeping the laboratory in a functional state, and for selflessly assisting in multiple research projects
- Kevin barr for his animal handling assistance
- The Laird lab members for troubleshooting and teaching me various laboratory techniques
- The Laird lab members, the gap junction group, and Anatomy and Cell Biology students for their friendship
- Debra Grant, Glenda Ogilvie and Debbie Mayea for the many ways they take care of ACB students
- Natural Sciences and Engineering Research Council of Canada and the province of Ontario for funding multiple years of my PhD

Table of Contents

CERTIFICATE OF EXAMINATION	ii
Abstract.....	iii
Co-Authorship Statement.....	v
Acknowledgments.....	vi
Table of Contents	vii
List of Figures	xii
Abbreviations	xv
Chapter 1	1
1 Connexins, oculodentodigital dysplasia and skin abnormalities.....	1
1.1 Gap junctions.....	1
1.2 Historical perspective on the identification of the gap junction domain.....	4
1.3 Molecular compositions of the gap junction domain	4
1.4 Cx43 and oculodentodigital dysplasia.....	9
1.5 Connexin expression in skin development	13
1.6 Regulation of connexin expression and localization during wound healing.....	17
1.7 Cx43 and Cx26 in keratinocyte proliferation	18
1.8 Cx43 in dermal fibroblast proliferation.....	20
1.9 Cx43 in migration.....	21
1.10 Cx43 in keratinocyte differentiation.....	22
1.11 Cx43 in fibroblast differentiation	23
1.12 Hypothesis and objectives	25
1.13 References	26
Chapter 2.....	36

2	Human dermal fibroblasts derived from oculodentodigital dysplasia patients suggest that patients may have wound-healing defects.....	36
2.1	Introduction	37
2.2	Materials and methods.....	39
2.2.1	Human fibroblast cultures.....	39
2.2.2	Extraction of genomic DNA for sequencing	39
2.2.3	Dye coupling assay	40
2.2.4	Patch-clamp electrophysiology.....	40
2.2.5	Immunocytochemistry and immunohistochemistry.....	41
2.2.6	Wound healing assay	41
2.2.7	Punch biopsy migration	42
2.2.8	Human fibroblast migration.....	42
2.2.9	Fibroblast proliferation	43
2.2.10	TGF β ₁ treatment	43
2.2.11	Western blot analysis	43
2.3	Results	44
2.3.1	Clinical presentation of patients and detection of Cx43 gene mutations.....	44
2.3.2	Characterization of Cx43 in control and mutant fibroblasts.....	45
2.3.3	Both human ODDD-linked mutants reduce GJIC	48
2.3.4	Wound healing is delayed in mice expressing mutant Cx43	48
2.3.5	ODDD mutants reduce dermal fibroblast migration and proliferation.....	55
2.3.6	ODDD mutants hinder the ability of dermal fibroblasts to differentiate into myofibroblasts	60
2.4	Discussion	67
2.4.1	Understanding ODDD	67
2.4.2	Clinical presentation of ODDD in two patients with distinct GJA1 gene mutations	68
2.4.3	Cx43 and GJIC status in control and mutant fibroblasts	68
2.4.4	Cellular consequences of reduced Cx43 function in dermal fibroblasts.....	70
2.5	References	73
	Chapter 3.....	77

3	Mutant Cx43 enhances keratinocyte proliferation without impacting keratinocyte migration	77
3.1	Introduction	78
3.2	Materials and methods.....	79
3.2.1	Cell lines and mice.....	79
3.2.2	Wound healing assay	80
3.2.3	Immunofluorescent labeling of human and mouse skin	80
3.2.4	Primary keratinocyte culture.....	81
3.2.5	Electrophysiology	82
3.2.6	Proliferation Assays	82
3.2.7	Migration.....	83
3.2.8	Western blots	84
3.3	Results	84
3.3.1	Mutant Cx43 disrupts the overall localization pattern of Cx43 in mutant mouse and patient epidermis	84
3.3.2	Mutant Cx43 inhibits gap junctional intercellular communication and enhances the proliferation of primary mouse keratinocytes	87
3.3.3	Migration and the ability of keratinocytes to differentiate is not affected by the expression of the G60S mutant.....	92
3.4	Discussion	99
3.5	References	107
	Chapter 4.....	112
4	The ability of the fs260 Cx43 mutant to impair keratinocyte differentiation is distinct from other disease-linked Cx43 mutants.....	112
4.1	Introduction	113
4.2	Materials and methods.....	115
4.2.1	Cell lines	115
4.2.2	Transfection and infection	115
4.2.3	Antibodies and imaging	116
4.2.4	Microinjection.....	117
4.2.5	Organotypic culture	118

4.2.6	Histological analysis	118
4.2.7	Acetone induced injury	118
4.2.8	Scrape loaded dye transfer assay	119
4.2.9	Transepithelial resistance.....	119
4.2.10	Statistics	119
4.3	Results	120
4.3.1	Localization and functional characterization of REKs expressing mutant Cx43	120
4.3.2	Organotypic epidermal differentiation is affected by REKs expressing mutant Cx43	125
4.3.3	Mutant Cx43 expression reduced the levels of phosphorylated Cx43, Cx26 and loricrin.....	130
4.3.4	Reduced barrier function in REKs expressing G60S, G138R, and fs260 Cx43 mutants.....	133
4.3.5	Organotypic epidermis expressing fs260 increased the vital layer thickness after acetone induced injury	133
4.4	Discussion	138
4.4.1	Understanding skin disease in ODDD patients.....	138
4.4.2	Subcellular localization may reflect the disease burden of ODDD mutants	138
4.4.3	fs260 expressing REKs develop epidermal defects not observed by other ODDD mutants	139
4.4.4	Cx26 cross-talk with Cx43 mutants	140
4.4.5	Decreased levels of Cx43 may lead to epidermal barrier defects.....	141
4.5	References	143
Chapter 5	148
5	The G60S Connexin43 Mutant Regulates Hair Growth and Hair Fiber Morphology in a Mouse Model of Human Oculodentodigital Dysplasia.....	148
5.1	Introduction	149
5.2	Materials and methods.....	150
5.2.1	Skin tissue collection	150
5.2.2	Hematoxylin and eosin staining to determine hair follicle density.....	150
5.2.3	Cx43, phosphorylated histone H3 and cytokeratin 15 immunolabeling.....	151

5.2.4	Hair growth experiment	152
5.2.5	Analysis of coat hair	152
5.2.6	Ultrastructural analysis	153
5.2.7	Statistical analysis	153
5.3	Results	153
5.4	Discussion	164
5.5	References	170
Chapter 6	173
6	Discussion	173
6.1	G60S mice exhibit a delay in wound healing.....	173
6.2	Combined use of multiple ODDD models	175
6.3	Cell type differences.....	176
6.4	Therapeutic implications	178
6.5	References	180
Appendices	182
Copyright and Permission	182
Human Mutation	182
Biochemical Journal	186
Journal of Investigative Dermatology	189
Ethics Approvals	190
Curriculum Vitae	192

List of Figures

Figure 1.1 An overview of the life cycle of connexins.....	2
Figure 1.2 Structural combinations of connexins within a connexon and a gap junction ..	6
Figure 1.3 Schematic composite of reported Cx43 ODDD mutants	10
Figure 1.4 Connexin expression in unwounded and wounded epidermis	14
Figure 2.1 D3, D3N, V216, and V216L cells are fibroblasts	46
Figure 2.2 A large proportion of mutant Cx43 co-localizes with the Golgi apparatus marker GM130.....	49
Figure 2.3 Reduced gap junctional intracellular communication in D3N and V216L fibroblasts.....	51
Figure 2.4 G60S mice wounds heal slower than WT mice wounds	53
Figure 2.5 Fibroblasts from mutant mice exhibited reduced migration on fibronectin and collagen.....	56
Figure 2.6 ODDD-linked human fibroblasts exhibit impaired migration.....	58
Figure 2.7 ODDD-linked human fibroblasts exhibited reduced proliferation.....	61
Figure 2.8 Aberrant Cx43 phosphorylation in mutant expressing fibroblasts	63
Figure 2.9 Reduced smooth muscle actin expression in mutant expressing fibroblasts....	65
Figure 3.1 Reduced Cx43 punctate localization in a human D3N patient skin biopsy and in skin obtained from G60S mutant mice	85
Figure 3.2 Cx43 is maintained localized within intracellular compartments during the wound healing process in G60S mutant mice.....	88

Figure 3.3 Mutant G60S Cx43 impairs the localization of Cx43 and decreases the transjunctional conductance in primary keratinocytes.....	90
Figure 3.4 Mutant G60S Cx43 expression enhances keratinocyte proliferation and overexpression of wild-type Cx43 reduces proliferation.....	93
Figure 3.5 Mutant G60S Cx43 expression does not change the migration of primary keratinocytes	95
Figure 3.6 Rat epidermal keratinocytes engineered to express ODDD mutants exhibited similar levels of migration	97
Figure 3.7 Keratinocyte Cx43 levels decrease under high calcium conditions	100
Figure 4.1 Cx43 mutants display different localization profiles in rat epidermal keratinocytes.	121
Figure 4.2 The fs230 mutant is predominantly localized within the endoplasmic reticulum and reduces the number of endogenous gap junctions and the extent of GJIC.	123
Figure 4.3 Cx43 mutants reduce dye transfer in REKs.	126
Figure 4.4 Cx43 mutant expressing REKs differentiate into organotypic epidermis.	128
Figure 4.5 Assessment of endogenous and mutant Cx43, Cx26 and loricrin protein expression in organotypic epidermis.	131
Figure 4.6 Cx43 mutant expressing REKs exhibited reduced transepithelial resistance	134
Figure 4.7 Acetone treatment increased the vital layer thickness in fs260 expressing organotypic cultures.....	136
Figure 5.1 Cx43 expression in the mouse hair follicle	155
Figure 5.2 A subset of G60S mutant mice have sparse hair in the back and neck regions but overall hair density in mutant mice remains unchanged from wild type mice.	157

Figure 5.3 G60S mutant mice have the same frequency of hair subtypes as WT mice but develop thinner and shorter hair fibers 159

Figure 5.4 Structural defects are observed in hair fibers from human ODDD patients and in the G60S mouse..... 162

Figure 5.5 Hair regrowth is delayed in G60S mice. 165

Abbreviations

α SMA	alpha smooth muscle actin
Δ 244*	truncated carboxy-terminal tail at amino acid position 244 with mutations resulting in a glycine to arginine substitution at amino acid position 58 and a serine to alanine at amino acid position 158
Å	angstrom
ANOVA	analysis of variance
Au	auchene
Aw	awl
asODN	Cx43 antisense oligodeoxynucleotide
BrdU	bromodeoxyuridine
BSA	bovine serum albumin
Ca ⁺²	calcium
CK14	cytokeratin 14
CK15	cytokeratin 15
Cx	connexin
Cx43-GFP	connexin43 linked to green fluorescent protein
D3N	aspartic acid to asparagine substitution at amino acid position 3
D66H	aspartic acid to histidine substitution at amino acid position 66
DAPI	4',6-diamidino-2-phenylindole
DP	dermal papilla
DiI	1'-dioctadecyl-3,3,3'-tetramethylindocarbocyanine perchlorate
DMEM	Dulbecco's modified Eagle's medium
DMSO	dimethyl sulfoxide
DNA	deoxyribonucleic acid
EDTA	ethylene-diamine-tetraacetic acid
EGTA	ethylene glycol tetraacetic acid
ER	endoplasmic reticulum
FBS	fetal bovine serum
Fs230	frame-shift mutation at amino acid position 230
Fs260	frame-shift mutation at amino acid position 260
G21R	glycine to arginine substitution at amino acid position 21
G60S	glycine to serine substitution at amino acid position 60

G138R	glycine to arginine substitution at amino acid position 138
GAPDH	glyceraldehyde 3-phosphate dehydrogenase
G	guard
GFP	green fluorescent protein
G_j	gap junctional conductance
<i>Gjal</i>	Gap junction alpha-1
<i>Gjb3</i>	Gap junction beta-3
GJIC	gap junctional intercellular communication
GM130	Golgi apparatus marker 130
HBSS	Hanks balanced salt solution
HEPES	4-(2-hydroxyethyl)-1-piperazineethanesulfonic acid
HM	hair matrix
I130T	isoleucine to threonine substitution at amino acid position 130
IgG	immunoglobulin G
IRS	inner root sheath
L11P	leucine to proline substitution at amino acid position 138
kD	kilodalton
KO	knockout
mAb	monoclonal antibody
ODDD	oculodentodigital dysplasia
OMIM	online mendelian inheritance in man
Opti-MEM	optimal minimal essential medium
ORS	outer root sheath
PDI	protein disulfide isomerase
PBS	phosphate buffered saline
PCR	polymerase chain reaction
R143W	arginine to tryptophan substitution at amino acid position 143
REKs	Rat epidermal keratinocytes
S255A	serine to alanine substitution at amino acid position 255
S279A	serine to alanine substitution at amino acid position 279
S282A	serine to alanine substitution at amino acid position 282
SDS-PAGE	sodium dodecyl sulfate polyacrylamide gel electrophoresis
SEM	standard error of the mean

shRNA	small hairpin ribonucleic acid
siRNA	small interfering ribonucleic acid
TGF β ₁	transforming growth factor beta one
V	empty viral vector control
V216L	valine to leucine substitution at amino acid position 216
WT	Wild-type
Z	zigzag

Chapter 1

1 Connexins, oculodentodigital dysplasia and skin abnormalities

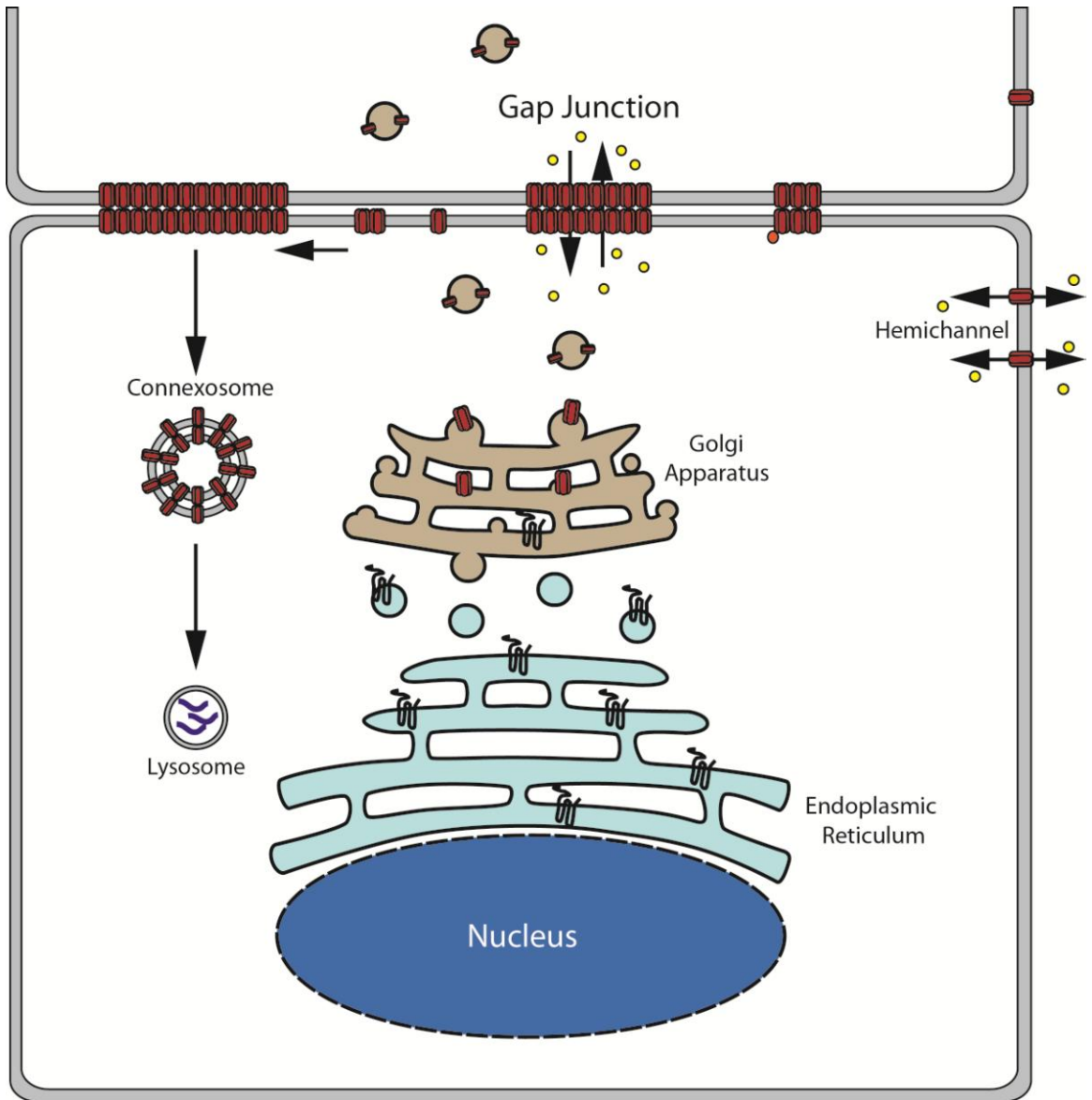
1.1 Gap junctions

Gap junctions are aggregates of protein channels formed between apposing cells that facilitate intercellular communication by allowing the passage of small molecules and metabolites from one cell to another (Alexander and Goldberg, 2003). These intercellular channels assemble from connexin (Cx) subunits named after the molecular weight of each family member (e.g. Cx43 has a molecular weight of 43 kD) (Sohl and Willecke, 2004). Six connexins oligomerize within a cell and are transported to the plasma membrane in a configuration known as a connexon (**Fig. 1.1**). Connexons at the plasma membrane can open and close to exchange molecules with the extracellular environment in a state known as a hemichannel (Goodenough and Paul, 2003). When one connexon docks with a connexon from an adjacent cell, a gap junction channel is formed. These channels laterally diffuse and aggregate into a semi-crystalline state known as the mature gap junction or a gap junction plaque where they open and close to facilitate intercellular communication (reviewed in Herve et al., 2007).

Gap junctions are one of the most interesting and unique structures found between adjoining cells. The importance of these novel structures is highlighted by the fact that virtually all cells found in solid tissues express connexins and assemble gap junctions. The mature gap junction domain itself consists of tightly aggregated connexin channels which are thought to extrude all other integral membrane proteins (Makowski et al., 1984). However, gap junctions are highly dynamic subject to remodeling and rapid turnover (Laird et al., 1991). Nucleation, growth, remodeling, internalization, and turnover of the gap junction domain are all critical for establishing the appropriate physiological levels of intercellular communication in all tissues and organs (reviewed in Laird, 2006).

Figure 1.1 An overview of the life cycle of connexins.

Connexins are co-translationally inserted into the endoplasmic reticulum (ER). Properly folded connexins are transported to the Golgi apparatus where six connexins oligomerize to form a connexon prior to delivery to the plasma membrane. At the plasma membrane connexons may function as hemichannels or dock with connexons from an adjacent cell to form a gap junction channel. Gap junction channels aggregate to form a mature gap junction also commonly referred to as a gap junction plaque. Gap junctions are internalized into specialized double-membrane structures called connexosomes (also called annular gap junctions) prior to delivery to lysosomes for degradation.



1.2 Historical perspective on the identification of the gap junction domain

The term gap junction comes from electron microscopy studies where a between the two electron opaque domains of apposing cells was observed in a junction-rich region between two closely apposed cardiac myocytes (Revel and Karnovsky, 1967). Sometime after this initial observation, low-resolution electron microscopy and X-ray crystallography imaging revealed the first three-dimensional structure of the gap junction channel (Caspar et al., 1977; Makowski et al., 1977). These channels were composed of hexagonal arrays with a central pore embedded into two opposing lipid bilayers. The size of the central pore could be deformed with the addition of the divalent cation chelator EGTA (Unwin and Ennis, 1984), and later analysis of isolated Cx26 gap junctions determined that this pore diameter can decrease from 15 Å to 6 Å after the addition of calcium (Muller et al., 2002). These structural changes in the pore diameter suggested that gap junction channels can be manipulated to form two functional states; the open and closed state. While higher resolution of the gap junction channel was obtained from X-ray diffraction analysis of Cx43 with a portion of the C-terminal tail truncated (Unger et al., 1999), our understanding of the general arrangement of connexins within the connexon has not substantially changed. Confirmation of the structural organization of the connexon in split gap junctions and other gap junction preparations was acquired with the advent of atomic force microscopic imaging where resolution limits of 10 Å were obtained (Hoh et al., 1991; Hoh et al., 1993; Muller et al., 2002; Oshima et al., 2007).

1.3 Molecular compositions of the gap junction domain

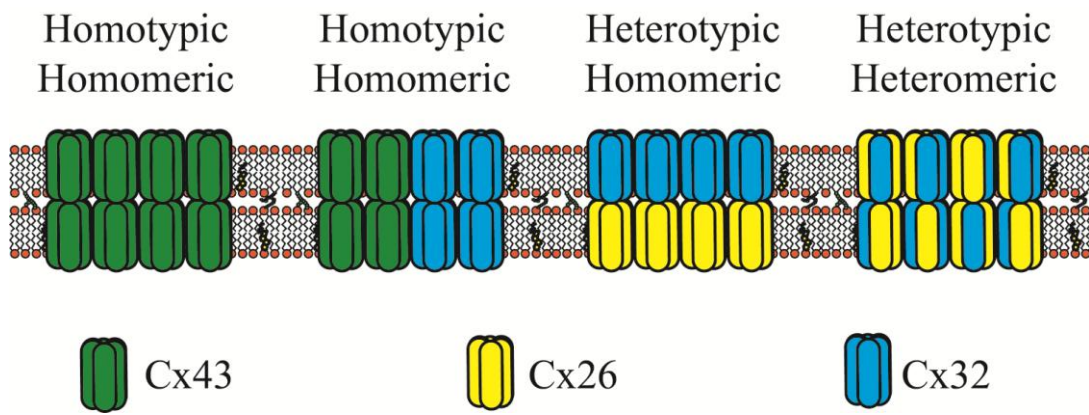
Humans express 21 different members of the connexin family, and the connexin topology in the membrane appears to be essentially the same for all connexin family members (Sohl and Willecke, 2003). Four transmembrane domains subdivide the primary connexin structure into a defined N-terminal, C-terminal, two extracellular, and one intracellular domain. These domains have classically been defined as having unique functional roles and can promote the opening and closing of the gap junction channel. Briefly, the

extracellular loops facilitate the binding of one connexon to a connexon of an adjacent cell (Herve et al., 2007). The N-terminus contributes to voltage gating (Purnick et al., 2000), while the C-terminus and the distal end of the intracellular loop can regulate the channel by sensing the intracellular pH (Ek-Vitorin et al., 1996; Ek et al., 1994). In addition, high-resolution imaging of connexons composed of Cx26 without an N-terminus suggests that the N-terminal domain can physically plug the gap junction channel (Maeda et al., 2009; Oshima et al., 2007). Phosphorylation of the C-terminal has also been shown to promote the opening and closing of the gap junction channel as well as signaling the gap junction to be both assembled and degraded (Solan and Lampe, 2009).

With members of the connexin family being expressed throughout multiple cell types and tissues, it is no surprise that multiple connexins expressed in a single cell may interact with each other. Early immunolocalization studies localized two different connexin family members (Cx26 and Cx32) to the same gap junction plaque (Zhang and Nicholson, 1994), and these connexins were further found to intermix within the same connexon (Sosinsky, 1995) (**Fig. 1.2**). Various combinations of connexins within the gap junction channel can now be classified into distinct groupings (Goodenough and Paul, 2009; Laird, 2006). Connexons containing only one type of connexin are termed homomeric channels, while mixed connexons of two or more different connexins are termed heteromeric (**Fig. 1.2**). If a connexon from one cell is docked with a connexon of a different type from an apposing cell, the resulting channel is heterotypic as opposed to homotypic channels, where the same connexon is found in both cells (Laird, 2006). Although a wide variety of gap junction channels can be formed by these combinations, not all connexins have the ability to oligomerize with each other. For example, Cx40 and Cx43 (He et al., 1999), Cx43 and Cx45 (Martinez et al., 2002), and Cx26 and Cx32 have all been shown to co-oligomerize, but Cx26 cannot oligomerize with Cx43 (Gemel et al., 2004). Restrictions among which connexins can intermix compartmentalize intercellular communication between cells of different origins or functions. The various connexin permutations within a connexon may also play an important role in many normal and disease cellular environments by selectively

Figure 1.2 Structural combinations of connexins within a connexon and a gap junction

Classically, connexins can dock and oligomerize within the same family member and form homotypic, homomeric gap junctions. Some connexin family members are not compatible with each other and will not dock or oligomerize together (Cx26 is not compatible with Cx43 and these two family members will not dock or oligomerize together). Gap junction channels can however be formed by connexon docking with compatible connexons from a different family member. These gap junction channels are termed heterotypic, homomeric channels (Cx26 can dock with Cx32). Finally if Cx26 and Cx32 co-oligomerize and dock, the resulting gap junction channel is both heterotypic and heteromeric.



regulating the transjunctional molecules that are exchanged. Since gap junction channels composed of only one connexin may be specialized for the passage of a specific solute and another connexin may be specialized for the passage of a different solute, varying the ratio of each connexin subunit within a single channel may promote, or even inhibit, the passage of solutes containing intermediate properties of the two solutes. For example, oocytes expressing heteromeric gap junctions composed of both Cx43 and Cx40 are more sensitive to acidification-induced uncoupling than their homomeric channel equivalents (Gu et al., 2000).

Once connexons are transported to the plasma membrane, gap junction channels formed from docked connexons aggregate into dense concentrations of tens to hundreds of gap junction channels (Zampighi et al., 1989). Gap junctions are unique and represent a functional domain distinct from any other junctional complex. Given that the average turnover time for connexins and gap junctions is 1–5 hours, gap junctions are in a constant state of change and dynamically respond to the physiological demands of the cell (Beardslee et al., 1998; Laird et al., 1991). Earlier electron microscopy studies suggest that gap junctions mature from a loosely packed state, termed a formation plaque, to a more densely packed semi-crystalline structure (Johnson et al., 1974). Fluorescent recovery after photobleaching of Cx43-containing plaques also suggests that not all gap junctions possess the same fluidity in the gap junction plaques (Simek et al., 2009) suggestive of immature states of assembly. By measuring the recovery of green fluorescent protein (GFP)-tagged Cx43 in a photobleached region of gap junction plaques (as identified by their punctate fluorescence), the mobility of Cx43 within the gap junction plaque can be classified into two distinct mobile states. Highly mobile GFP-tagged Cx43 may represent immature nascent plaques, while low mobility Cx43 may represent mature densely packed plaques. In addition, connexins have been shown to have multiple protein binding partners, and connexins bound to scaffolding proteins within the gap junction plaque may regulate the surface dynamics of connexons within a gap junction plaque (reviewed in Laird, 2010). For example, the binding of ZO-1 to the distal C-terminal tail of Cx43 has been reported to regulate the gap junction plaque size, and this interaction may further regulate the turnover or stabilization of gap junctions at the plasma membrane (Maass et al., 2007).

1.4 Cx43 and oculodentodigital dysplasia

The most ubiquitously expressed connexin is Cx43 and the expression of Cx43 has been noted in multiple tissues including but not limited to the heart (Manias et al., 2008), bone (Civitelli, 2008), brain (Sohl et al., 2005) and skin (Risek et al., 1992). Given the ubiquitous expression of Cx43 in the human body, it is conceivable that germ line mutations in the *GJA1* gene which encodes for the Cx43 protein can lead to a disease affecting many organs. This was indeed discovered in 2003 when the disease oculodentodigital dysplasia (ODDD) was linked with mutations in the *GJA1* gene (Paznekas et al., 2009).

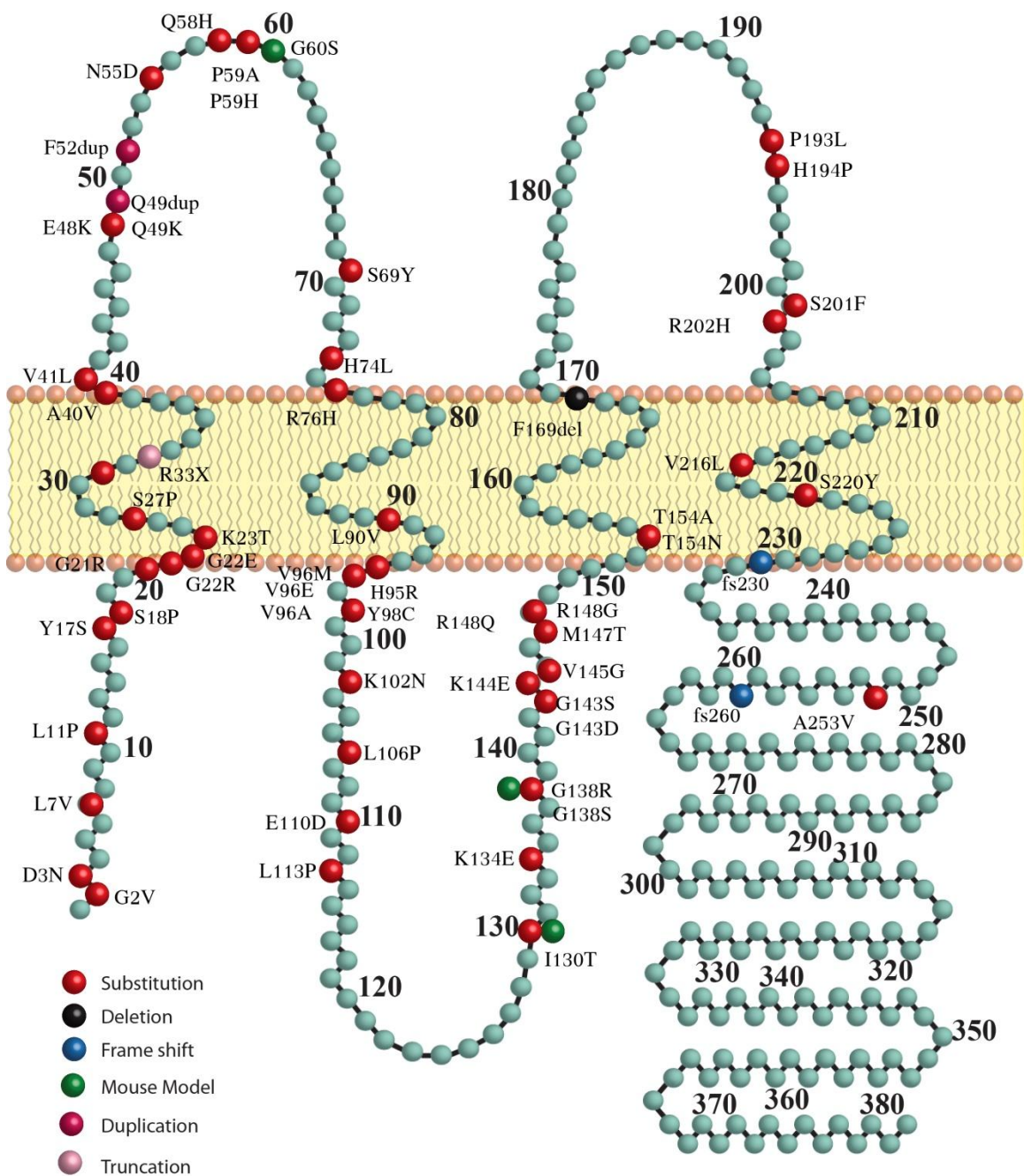
ODDD is a disease which commonly manifests as microphthalmia, microcornea, enamel hypoplasia, and type III syndactyly (Gillespie, 1964). ODDD is a rare condition with less than 1000 cases having been fully documented. In these documentations however, 62 distinct mutations in the gene encoding Cx43 have been reported to cause ODDD and the majority of these mutations are dominant missense mutations (Paznekas et al., 2009) (**Fig. 1.3**).

While ODDD patients commonly develop abnormalities affecting the eyes, teeth and digits, recent studies suggest that other tissues and cell types expressing Cx43 may also demonstrate reduced function or disease. For example, ODDD patients have also been reported to manifest cerebral white matter hypomyelination (Gutmann et al., 1991), incontinence (Loddenkemper et al., 2002), and paresis (Gutmann et al., 1991; Loddenkemper et al., 2002). In addition, Cx43 is highly expressed in the skin and patients with ODDD have also been reported to develop skin disease (van Steensel et al., 2005; Vreeburg et al., 2007).

Palmar plantar hyperkeratosis is a skin disease developed by some ODDD patients. This disease results in an enlarged stratum corneum in the palms and weight bearing areas of the feet (Braun-Falco, 2009). Patients expressing the fs260 (van Steensel et al., 2005) mutant or the fs230 (Vreeburg et al., 2007) mutant have been reported to develop

Figure 1.3 Schematic composite of reported Cx43 ODDD mutants

To date, sixty-two Cx43 mutants have been reported to cause ODDD. These mutations are found throughout multiple regions of the primary Cx43 amino acid sequence and the majority of these mutations are missense mutations. Currently, three ODDD mouse models (G60S, I130T, or the G138R) have been engineered to study ODDD.



palmar plantar hyperkeratosis, however, a recent report of a patient expressing the fs230 mutant did not develop palmar plantar hyperkeratosis (Alao et al., 2010). Since both of these mutants result in a drastic reduction in the C-terminal tail of Cx43, it remains to be determined if C-terminal tail truncations are specifically linked with palmar plantar hyperkeratosis.

Approximately twenty-five percent of patients with ODDD have also been reported to develop hair abnormalities (Paznekas et al., 2009). These patients have been reported to develop hair which is curly, thin, dry, dull, sparse, and slow growing (Gorlin et al., 1963; Kelly et al., 2006; Kjaer et al., 2004; Paznekas et al., 2009; Sugar et al., 1966; Thoden et al., 1977). In addition, hair fiber structural changes (nodules along the hair fiber) were also reported in a patient expressing the L11P mutant (Kelly et al., 2006). Determining how Cx43 affects the growth and differentiation of the hair follicle may lead to successful therapies to treat ODDD-linked hair abnormalities.

To further understand how mutant Cx43 can lead to ODDD, three ODDD mutant mouse models have been developed that harbor single missense mutations (G138R (Dobrowolski et al., 2008), G60S (Flenniken et al., 2005) and I130T (Kalcheva et al., 2007)). These mice display many phenotypic features seen in ODDD patients (syndactyly and craniofacial abnormalities) and these mice are a valuable resource to study how ODDD patients develop skin disease and hair abnormalities. To date, the only reported hair defect observed in these ODDD mouse models was sparse hair observed in approximately 30% of G138R mice (Dobrowolski et al., 2008). It would be interesting to determine if G138R mice also developed defects in hair growth, regeneration, or hair fiber structure or if other ODDD mouse models also develop hair defects. One of my aims was to investigate how mutant Cx43 impacts hair follicle development and hair structure using both the G60S mouse model of ODDD and human hair samples from ODDD patients.

1.5 Connexin expression in skin development

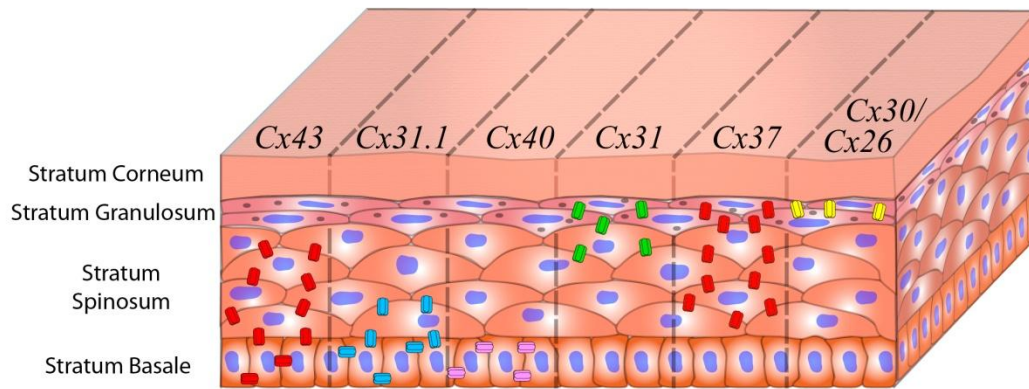
The fully formed epidermis is composed of four distinct layers in thin skin: the stratum basale, stratum spinosum, stratum granulosum, and stratum corneum (**Fig. 1.4**). Together, these layers form a protective coating which blocks many mechanical and environmental insults the human body procures over time. Keratinocytes within the basal layer maintain stem cell-like characteristics and play an important role in the renewal and regeneration of damaged skin (Houben et al., 2007). Keratinocytes in the stratum basale also rest on a basement membrane and have a high proliferative index (Smith, 2003). As keratinocytes in the stratum basale differentiate, they form the stratum spinosum and stratum granulosum. During the formation of the stratum corneum, differentiated keratinocytes in the stratum granulosum, called corneocytes, undergo cell death and release keratins, loricrin, and involucrin. Paradoxically, although this layer contains no living cells, this layer is active. Enzymes such as transglutaminase 1 and 3 crosslink many of these proteins to protect the skin from mechanical insults in this layer (Hitomi, 2005), while lipid ceramides give the skin its waterproof property (Hill et al., 2006).

Nine different connexin family members have previously been reported to be expressed in the rodent epidermis (Cx26, Cx30, Cx30.3, Cx31, Cx31.1, Cx37, Cx40, Cx43, Cx57) (Goliger and Paul, 1994; Kretz et al., 2004; Richard, 2000) and these connexins are expressed in regional and temporal expression patterns during development. During the embryonic E12-E14 stage of rat epidermis development, the epidermis is composed of two cellular layers; the outer periderm and the inner basal layer. Both Cx43 and Cx26 are expressed in these layers and prior to the periderm layer undergoing apoptosis, Cx26 expression is down-regulated (Risek et al., 1992). Later in rodent epidermis development (E17-E20), Cx43, Cx45, Cx31.1, and Cx37 have all been reported to be expressed in the basal layer while Cx26, Cx37, Cx31 and Cx43 are restricted to the stratum spinosum and stratum granulosum (Butterweck et al., 1994; Goliger and Paul, 1994; Risek et al., 1992).

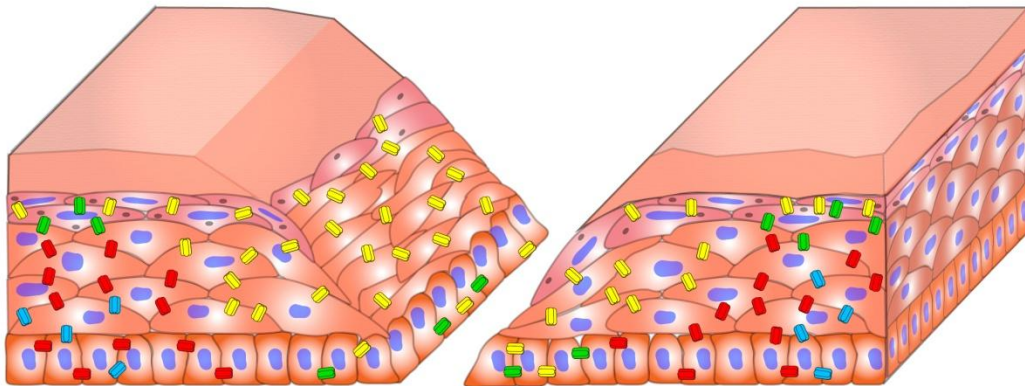
Figure 1.4 Connexin expression in unwounded and wounded epidermis

The epidermis is composed of four layers in thin skin: stratum basale, stratum spinosum, stratum granulosum, and stratum corneum. In unwounded epidermis Cx43 (red), Cx31.1 (blue), Cx40 (purple), Cx31 (green), Cx37 (orange), Cx30 and Cx26 (both in yellow) localize to various epidermal layers in the adult rodent epidermis. Twenty-four hours after the epidermis is wounded, the expression of Cx30 and Cx26 shifts from being expressed in the stratum granulosum to all epidermal layers whereas the expression of Cx31.1 is drastically reduced. Cx40 and Cx43 levels also decrease at the wounded margin and Cx40 is localized to the stratum basale after wounding.

Unwounded



Wounded



In the adult mouse epidermis (**Fig. 1.4**) Cx40 and Cx43 have been reported to be expressed within the stratum basale (Butterweck et al., 1994; Kamibayashi et al., 1993). In humans, 10% of the keratinocytes in the stratum basale do not express Cx43 and these cells are reported to have stem cell like characteristics (Matic et al., 2002). In the stratum spinosum, Cx43 is highly expressed while in the stratum granulosum, no Cx43 expression is observed (Butterweck et al., 1994). Cx37 is expressed in the stratum spinosum and stratum granulosum (Goliger and Paul, 1994) while Cx31.1 was found to be predominantly expressed in the lower basal layer and in the lower stratum spinosum (Goliger and Paul, 1994). Cx26 and Cx30 expression is restricted to the stratum granulosum in the rodent epidermis however, one study observed Cx26 to be expressed in the upper stratum spinosum in human epidermis as well (Wiszniewski et al., 2000) while an additional study could not localize Cx26 to any epidermal keratinocytes (Salomon et al., 1994). In addition, Cx31 was observed to be expressed in the stratum granulosum and in the upper stratum spinosum (Kretz et al., 2003). Immunolocalization of other connexins however, has not been investigated to date.

In the dermis, human dermal fibroblasts are reported to express Cx43, Cx45 and Cx40 (Wright et al., 2009). Cx43 has also been reported to be expressed in the arrector pili muscle, sweat glands, sebaceous glands, and the hair follicle (Choudhry et al., 1997). In the development of the human hair follicle, both Cx26 and Cx43 expression could be observed within the hair peg (Arita et al., 2004). As the hair follicle grows, Cx26 was reported within the outer root sheath and the inner root sheath but absent in the hair matrix. Cx43 however was prominently expressed with the inner root sheath, hair matrix and weakly expressed within the outer root sheath. Later in development (163 days estimated gestational age), intense Cx26 expression was found in the outermost layer of the outer root sheath while Cx43 was highly expressed within the innermost layer of the outer root sheath (Arita et al., 2004). Cx43 expression during the anagen stage of rodent hair follicle growth has also been reported to be expressed in the inner and outer root sheath, the dermal papilla, and the proliferating matrix. However, during catagen, Cx43 expression is absent in the inner root sheath (Risek et al., 1992).

Given that connexins are expressed throughout development in the various layers of the skin, connexins may also play an active role in regulating skin regeneration.

1.6 Regulation of connexin expression and localization during wound healing

When the skin is injured, the epidermis and dermis must reform the wounded area. Complete healing of cutaneous wounds can take up to multiple weeks and the selective expression of different connexins throughout the healing process may play distinct roles. Within the first 24 hours of wounding, Cx26 and Cx30 expression increases in all strata (**Fig. 1.4**). In addition, there is a drastic decrease in the expression of Cx31 and Cx31.1 with Cx31 expression becoming evident in the stratum basale (Goliger and Paul, 1995; Kretz et al., 2003). Cx43 levels previously expressed in the stratum basale and stratum spinosum in the unwounded epidermis, are now lowered in all epidermal layers at the wounded edge (Brandner et al., 2004; Goliger and Paul, 1995; Kretz et al., 2003; Lampe et al., 1998). Keratinocytes residing in the basale layer also selectively express the phosphorylated S368 species of Cx43 to suggest that, not only does the expression pattern of different connexins change during wounding, but also the active state of connexins, as denoted by their state of phosphorylation, may also change (Richards et al., 2004). The differential expression of connexins during wound healing may therefore allow the selective permeability of small molecules to promote either the proliferation or differentiation of keratinocytes. This is supported by a study which demonstrated that when keratinocytes were induced to differentiate under high calcium condition, Cx43 and Cx26 levels decreased while the levels of Cx31 and Cx31.1 increased (Brissette et al., 1994). This change in connexin expression also selectively decreased the gap junction-mediated passage of neurobiotin, carboxyfluorescein and Lucifer yellow dyes but did not affect the ability of keratinocytes to pass the synthetic nucleotide ³⁵S-labeled cytidine triphosphate (Brissette et al., 1994). In the future, determining which molecules selectively pass through various heterotypic and heteromeric gap junction channels will be critical to our understanding of how changes in connexin expression and regional localization can affect the intercellular signaling networks.

The overall mechanisms of how connexins regulate wound healing are not fully known, but some studies suggest that wound healing is enhanced when Cx43 levels are lowered. Since Cx43 null mice die from right ventricular outflow tract abnormalities (Reaume et al., 1995) and Cx26 null mice die in utero due to a placental defect, it is difficult to use these knockout mice to study wound healing. To overcome this early lethality, Cx43 has been conditionally knocked out after birth in mice engineered to express a tamoxifen-induced cre-recombinase in cells with a floxed Cx43 gene (Cx43^{Cre-ER(T)/fl} mice). Tail wounds performed after tamoxifen-induced Cx43 deletion resulted in faster wound healing when compared to the control mice (Kretz et al., 2003). In addition, by wounding mouse skin and applying Cx43 siRNAs and Cx43 targeting antisense, wounds were observed to heal faster (Ghatnekar et al., 2009; Mori et al., 2006; Qiu et al., 2003). Mouse organotypic epidermal cultures also demonstrated faster wound closure after the Cx43 mimetic peptide Gap27 was used to transiently block the interaction between connexons (Kandyba et al., 2008). By deciphering the role that connexins play in keratinocyte or dermal fibroblast proliferation, migration and differentiation, mechanistic insight into how connexins can impact the overall wound healing process could be achieved.

1.7 Cx43 and Cx26 in keratinocyte proliferation

During the initial stages of wound healing (Day 1 to 3 post wound), keratinocytes at the wounded edge increase their proliferation rate (Coutinho et al., 2003) and migrate under the coagulum. Since Cx43 levels go down and Cx26 increase at the wounded edge, these connexins are suggested to play distinct roles during proliferative and migrational events in the early stages of wound healing. Mechanistically it is not surprising to observe a reduction in the plasma membrane pool of Cx43 since it has been documented to play a role in cell to cell adhesion (Prochnow and Dermietzel, 2008). With a net reduction in adhesion, cells would be permitted to proliferate and begin their migration into the wounded area. However, the role of connexins in general is more complex since Cx26 and Cx30 expression increases in all epidermal layers after wounding (Kretz et al., 2003).

The role of Cx26 in keratinocyte proliferation is supported by evidence that persistent Cx26 expression maintains the wounded epidermis in a hyperproliferative state (Djalilian et al., 2006). Cx26 and Cx30 have also been found to be highly expressed in non-healing chronic wounds (Brandner et al., 2004) and in keratinocyte-derived skin tumors (Haass et al., 2006). In addition the expression of Cx30 was up-regulated in human psoriatic skin, irradiated skin, as well as primary keratinocytes subjected to irradiation further supporting the role of Cx30 in hyperproliferation (Lemaitre et al., 2006). While both Cx26 and Cx30 are spatially and temporally co-regulated during wound healing and these connexins can form heterotypic channels, it is possible that mutations in the genes encoding these connexins may result in a similar skin disease phenotype. This turns out to be the case in Clouston syndrome and Vohwinkel's syndrome.

Clouston's syndrome is a disease caused by mutations in the *GJB6* (Cx30) gene. Patients with Clouston's syndrome develop nail dystrophy, palmar plantar hyperkeratosis, slow growing, fine, dry, brittle and sparse hair (Clouston, 1929). Mutant Cx26 expression also causes several skin diseases including Vohwinkel's syndrome (Maestrini et al., 1999). Vohwinkel's syndrome results in starfish-like acral keratoses, papular and honeycomb keratoderma, palmar plantar hyperkeratosis, constricting bands around the digits and moderate hearing loss. One symptom shared by both Clouston's syndrome (Cx30 mutations) and Vohwinkel's syndrome (Cx26 mutations) patients is an epidermal thickening in the palmar and the plantar regions of the hands and feet (palmar plantar hyperkeratosis). This phenotype could also be observed in the tail epidermis of a mouse model of Vohwinkel's syndrome where the D66H mutant Cx26 was expressed in the epidermis under the control of the keratin 10 promoter (Bakirtzis et al., 2003a). While it is tempting to correlate the epidermal expression of Cx26 and Cx30 with the proliferation of keratinocytes and palmar plantar hyperkeratosis, palmar plantar hyperkeratosis is also observed in patients with oculodentodigital dysplasia (van Steensel et al., 2005; Vreeburg et al., 2007) and in patients with erythrokeratoderma variabilis (Cx31, Cx37, Cx31.1 mutations) (Richard et al., 1998; Strober, 2003). Since mutations in the Cx26, Cx30, Cx31, Cx37, Cx31.1 and Cx43 gene can result in palmar plantar hyperkeratosis, functional gap junctional communication may be an important component in order to maintain proper skin homeostasis.

The transient and systematic decrease in Cx43 levels at the wound edge during wound healing suggests that Cx43 expression may slow the proliferation of keratinocytes. In mice expressing 85% lower epidermal Cx43 levels (tamoxifen-induced Cx43^{Cre-ER(T)/fl}) a compensatory increase in Cx30 was observed which appeared to support cell proliferation (Kretz et al., 2003). Mouse wounds treated with an antisense oligodeoxynucleotide against Cx43 also lead to an increase in cell proliferation at the wounded edge (Mori et al., 2006). Furthermore, when a Cx43 mimetic peptide which blocks connexon docking, Gap27, was treated on porcine and human keratinocytes, an increase in proliferation was observed (Pollok et al., 2010). Since Cx43 levels naturally decrease during the initial stages of wound healing, strategic reductions in Cx43 levels appear to also promote keratinocyte proliferation and assist in wound healing.

While *in vivo* studies suggest that down-regulation of Cx43 promotes the proliferation of keratinocytes, sparsely plated human keratinocytes grown *in vitro* however, express Cx43. Only after confluency is reached, was a down-regulation of Cx43 observed (Gibson et al., 1997). In addition, undifferentiated primary mouse keratinocyte cultures also express high levels of Cx43 and these levels go down after Ca⁺² induced differentiation (Brissette et al., 1994). The *in vitro* versus *in vivo* differences observed in the expression of Cx43 suggest that monolayer keratinocyte cultures may not truly represent the basal keratinocyte phenotype present in the *in vivo* environment. Since primary keratinocytes are cultured in media and not subjected to the same air-liquid interface, and/or since cultured keratinocytes may not be grown on the same basement membrane proteins in which keratinocytes interact with *in vivo*, keratinocytes grown in culture may more appropriately represent an active stratum spinosum. Therefore, keratinocytes grown on different extracellular matrix proteins or under organotypic epidermal conditions may be required to more accurately represent the role of Cx43 *in vivo*.

1.8 Cx43 in dermal fibroblast proliferation

While the majority of connexin-linked wound healing studies have focused on the role of connexins in keratinocytes, the role that dermal fibroblasts play in wound healing is less clear. Unlike keratinocytes, Cx43 is up-regulated in dermal fibroblasts at the wound edge

(Coutinho et al., 2003). This suggests that connexin expression and response to injury may be dependent on the cell type assessed. Since fibroblasts proliferate in the wounded area, an increase in Cx43 expression might suggest that Cx43 expression in fibroblasts enhances proliferation. However, the proliferation rate of fibroblast cell lines derived from Cx43-deficient cell lines (Cx43^{+/-}) did not differ from fibroblasts derived from the Cx43-expressing cell lines (Cx43^{+/+}) (Yamakage et al., 1998). In contrast, fibroblasts derived from the murine cardiac tissue from Cx43^{+/-} deficient mice demonstrated an increase in cell proliferation (Zhang et al., 2008). This suggests that not all fibroblast populations are the same and that fibroblasts derived from different organs may be more dependent on the expression of Cx43. By studying a wide variety of Cx43 mutants and by assessing how each mutant affects different cell types, a greater understanding of how Cx43 modulates proliferation may be achieved.

1.9 Cx43 in migration

Keratinocytes, macrophages, neutrophils and fibroblasts all migrate into the wounded skin area to repair the injured tissue. Thus, Cx43 modulation may also manipulate the migration of keratinocytes and fibroblasts after wounding. In a scratch wound assay, connexin mimetic peptides, Gap26 and Gap27 (that reduce the cell surface levels of Cx43) increased the migration rate of both human keratinocytes and human fibroblasts (Wright et al., 2009). In addition Gap27-treated mouse keratinocytes exhibited enhanced migration into a wounded epidermis (Kandyba et al., 2008). The enhancement in cell migration may have involved disrupting the cell adhesion properties (Prochnow and Dermietzel, 2008) or communication properties (Kumar and Gilula, 1996) between cells rather than possibly affecting the intracellular protein binding partner interactions with Cx43 (Laird, 2010). This is supported by a study which demonstrated that reducing total Cx43 by Cx43 antisense oligodeoxynucleotide enhanced the migration of mouse dermal Swiss 3T3 fibroblasts (Mori et al., 2006).

In a wound environment, extracellular matrix proteins may regulate Cx43 levels. Since migrating keratinocytes are not exposed to basement membrane proteins (Larjava et al., 1993) and keratinocytes at the wounded edge have reduced Cx43 levels (Wright et al.,

2009) it is possible that only when keratinocytes are able to synthesize and deposit basement membrane proteins, a decrease in keratinocyte migration (O'Toole et al., 1997) and an increase in Cx43 expression will be observed. This is also supported in a study which demonstrated that human keratinocytes adhered to laminin 332 had greater Cx43 levels and gap junctional coupling in comparison to keratinocytes plated on collagen or fibronectin (Brandner et al., 2004; Lampe et al., 1998).

1.10 Cx43 in keratinocyte differentiation

Once keratinocytes have migrated into the injured area, keratinocytes differentiate into multiple epidermal strata (basale, spinosum, granulosum and corneum) to reform the epidermal barrier. Since connexins are differentially expressed during keratinocyte and fibroblast differentiation, they may also play an important role in regulating this differentiation process. Mice lacking Cx31 (*Gjb3^{-/-}*) develop an epidermis and did not show any skin defects (Plum et al., 2001). In addition, mice lacking both Cx31 and Cx43 were not found to have any epidermal differentiation defects at fetal day 17.5 (Kibschull et al., 2005). Histological analysis of the epidermis in these mice revealed a normal epidermal morphology and did not show any differences in the expression of keratin 14, keratin 10, keratin 6, Cx26, loricrin and filaggrin. While skin abnormalities were not found in the fetal epidermis, connexin expression may regulate epidermal differentiation and regulation after birth.

To investigate if Cx43 reduction can impact the stratification of the epidermis, Langlois et al. knock-downed Cx43 levels by shRNA administration to rat epidermal organotypic cultures (Langlois et al., 2007). Reducing Cx43 in these cultures resulted in a disruption of organotypic epidermal architecture while increasing the terminal differentiation makers loricrin and involucrin (Langlois et al., 2007). This would suggest that not only is the expression of Cx43 important for maintaining epidermal tissue architecture, but disrupting Cx43 expression in the epidermis may also damage the epidermal barrier and thus activate the differentiation pathway to reform the epidermal barrier. Interestingly, the shRNA-induced reduction of Cx43 also resulted in a decrease in Cx26 levels in organotypic cultures. In addition, Cx26 levels were also lower in the adult skin of mutant

mice selected for their heterozygous expression of the Cx43 G60S mutant (Langlois et al., 2007). Thus, the transdominant effect of Cx43 on Cx26 or some sort of cross-talk between these connexins may underlie skin disorders observed in patients with ODDD. While the majority of ODDD-causing Cx43 mutants do not result in clinically diagnosed skin abnormalities, two frameshift mutants have been associated with palmar plantar hyperkeratosis. Since Cx26 is absent in uninjured forearm skin but weakly expressed in the basale layer of plantar skin region (Lucke et al., 1999), the palmar plantar phenotype may be due to the transdominant nature of Cx43 on Cx26 (Lucke et al., 1999; Rouan et al., 2001). The interplay between Cx43 mutants and Cx26 defects is also supported by the observation that tail constricting bands are observed in mice expressing a Cx43 C-terminal truncation (Maass et al., 2004) and in mice expressing the D66H Cx26 mutant (Bakirtzis et al., 2003a). In addition, while only some ODDD-linked Cx43 mutants lead to skin defects, Cx26 mutants are strongly associated with human and mouse skin disease. Mice expressing the D66H Cx26 mutant were shown to have a propensity for premature cell death. This premature cell death may weaken the epidermal barrier of the skin and activate the basale keratinocytes to reform the epidermis. Overstimulation of the keratinocytes may also increase the thickening of the epidermis (Bakirtzis et al., 2003a) and lead to palmar plantar hyperkeratosis. It is interesting to note however that others have shown that Cx26 D66H mutant did not interfere with the formation of the epidermal water barrier during late embryonic development (Bakirtzis et al., 2003b) and that the deafness-associated mutant human Cx26 (R143W) was shown to improve the epithelial barrier in vitro (Man et al., 2007). Evaluation of Cx26 levels in keratinocytes engineered to express skin disease associated Cx43 mutants and Cx43 mutants not associated with skin disease may clarify how some ODDD mutants are more potent at causing skin disease.

1.11 Cx43 in fibroblast differentiation

While most studies have investigated the role that connexins play during epidermal wound healing involving keratinocytes, the role that fibroblasts play in the skin wound healing process cannot be neglected. While dermal fibroblasts are embedded in a collagen mesh, about 30% of fibroblasts were found to be in contact with one another

through fibroblast processes. These fibroblasts were also thought to be in communication with one another since Cx43 was localized at the points of cell to cell contact (Langevin et al., 2004). Since fibroblasts play a crucial role in forming the provisional granulation tissue, long term collagen secretion, and in contracting the wounded area (myofibroblast differentiation), modulation of connexin expression may impact the role that fibroblasts play during wound healing (Darby and Hewitson, 2007).

In Mori et al., knockdown of Cx43 was shown to enhance fibroblast-dependent wound healing (Mori et al., 2006). In this study, mouse wounds treated with Cx43 antisense oligodeoxynucleotide (asODN) had significant increases in the levels of hydroxyproline and mRNA for collagen type alpha1 and TGF β ₁ when compared to control treated wounds. An increase in myofibroblast differentiation and wound contraction was also found after treatment with Cx43-asODN (Mori et al., 2006). In addition, the application of asODN was shown to decrease the amount of granulation tissue and scarring in the wound healing of burns (Coutinho et al., 2005).

In contrast to these studies, other mouse studies suggest that decreasing Cx43 levels impairs the ability of fibroblasts to heal wounds. Fibroblasts derived from Cx43 knockout (KO) mice demonstrated a reduced ability to contract as well as failed to elongate (Ehrlich et al., 2000). In ventricular remodeling after myocardial infarct, Cx43-deficient mice had reduced levels of myofibroblast formation and also were less active in collagen deposition (Zhang et al., 2010). This defect was attributed to impaired TGF β ₁ signaling (Zhang et al., 2010). In addition, reduced myofibroblast differentiation was also found when cardiac fibroblasts were treated with Cx43 antisense oligodeoxynucleotides (Asazuma-Nakamura et al., 2009). This suggests that TGF β ₁ signaling may require normal Cx43 expression to differentiate fibroblasts into myofibroblasts. If this is true, mutant Cx43 expression in fibroblasts may impair the ability of dermal fibroblast to contract a wounded area.

1.12 Hypothesis and objectives

To date, the mechanisms by which mutant Cx43 can impact skin development and differentiation is not fully understood. In addition, cutaneous wound healing in patients with germ line mutation in the Cx43 gene has not been investigated. Since many ODDD-linked Cx43 mutants can traffic to the plasma membrane (McLachlan et al., 2005), the protein binding partners which interact with Cx43 may still be intact (reviewed in Laird, 2010). In addition, ODDD-linked Cx43 mutants act to knockdown but not abolish Cx43-based GJIC (Gong et al., 2006; McLachlan et al., 2005). It will be interesting to determine if mice with chronically reduced levels of Cx43 exhibit differences in their wound healing response. In addition, given that Cx43 is expressed in keratinocytes, dermal fibroblasts, and the hair follicle epidermal cells, mutant Cx43 expression may affect the proliferation, migration and differentiation of these cells. It is therefore hypothesized that the processes which regulate wound healing and hair follicle differentiation in the epidermal and dermal compartment will be impaired by the expression of mutant Cx43.

The specific objectives of the project were to:

1. Determine the role of Cx43 in dermal fibroblast proliferation, migration and differentiation by using human ODDD fibroblasts and a mutant mouse model of ODDD.
2. Determine the role of Cx43 in keratinocyte proliferation, migration and differentiation by using primary keratinocytes derived from a mutant mouse model of ODDD.
3. Determine the role of Cx43 in epidermal maintenance, growth, and differentiation by using epidermal organotypic models of keratinocytes expressing mutant Cx43.
4. Determine whether mice expressing mutant Cx43 display defects in hair follicle structure, growth, and regeneration.

1.13 References

- Alao, M.J., D. Bonneau, M. Holder-Espinasse, C. Goizet, S. Manouvrier-Hanu, A. Mezel, F. Petit, D. Subtil, C. Magdelaine, and D. Lacombe. 2010. Oculo-dento-digital dysplasia: lack of genotype-phenotype correlation for GJA1 mutations and usefulness of neuro-imaging. *Eur.J.Med.Genet.* 53:19-22.
- Alexander, D.B., and G.S. Goldberg. 2003. Transfer of biologically important molecules between cells through gap junction channels. *Curr Med Chem.* 10:2045-2058.
- Arita, K., M. Akiyama, Y. Tsuji, J.R. McMillan, R.A. Eady, and H. Shimizu. 2004. Gap junction development in the human fetal hair follicle and bulge region. *Br J Dermatol.* 150:429-434.
- Asazuma-Nakamura, Y., P. Dai, Y. Harada, Y. Jiang, K. Hamaoka, and T. Takamatsu. 2009. Cx43 contributes to TGF-beta signaling to regulate differentiation of cardiac fibroblasts into myofibroblasts. *Exp Cell Res.* 315:1190-1199.
- Bakirtzis, G., R. Choudhry, T. Aasen, L. Shore, K. Brown, S. Bryson, S. Forrow, L. Tetley, M. Finbow, D. Greenhalgh, and M. Hodgins. 2003a. Targeted epidermal expression of mutant Connexin 26(D66H) mimics true Vohwinkel syndrome and provides a model for the pathogenesis of dominant connexin disorders. *Hum Mol Genet.* 12:1737-1744.
- Bakirtzis, G., S. Jamieson, T. Aasen, S. Bryson, S. Forrow, L. Tetley, M. Finbow, D. Greenhalgh, and M. Hodgins. 2003b. The effects of a mutant connexin 26 on epidermal differentiation. *Cell Commun Adhes.* 10:359-364.
- Beardslee, M.A., J.G. Laing, E.C. Beyer, and J.E. Saffitz. 1998. Rapid turnover of connexin43 in the adult rat heart. *Circ.Res.* 83:629-635.
- Brandner, J.M., P. Houdek, B. Husing, C. Kaiser, and I. Moll. 2004. Connexins 26, 30, and 43: differences among spontaneous, chronic, and accelerated human wound healing. *J Invest Dermatol.* 122:1310-1320.
- Braun-Falco, M. 2009. Hereditary Palmoplantar Keratodermas. *J.Dtsch.Dermatol.Ges.* 7:971-984.
- Brissette, J.L., N.M. Kumar, N.B. Gilula, J.E. Hall, and G.P. Dotto. 1994. Switch in gap junction protein expression is associated with selective changes in junctional permeability during keratinocyte differentiation. *Proc Natl Acad Sci U S A.* 91:6453-6457.

- Butterweck, A., C. Elfgang, K. Willecke, and O. Traub. 1994. Differential expression of the gap junction proteins connexin45, -43, -40, -31, and -26 in mouse skin. *Eur J Cell Biol.* 65:152-163.
- Caspar, D.L., D.A. Goodenough, L. Makowski, and W.C. Phillips. 1977. Gap junction structures. I. Correlated electron microscopy and x-ray diffraction. *J.Cell Biol.* 74:605-628.
- Choudhry, R., J.D. Pitts, and M.B. Hodgins. 1997. Changing patterns of gap junctional intercellular communication and connexin distribution in mouse epidermis and hair follicles during embryonic development. *Dev Dyn.* 210:417-430.
- Civitelli, R. 2008. Cell-cell communication in the osteoblast/osteocyte lineage. *Arch Biochem Biophys.* 473:188-192.
- Clouston, H.R. 1929. A Hereditary Ectodermal Dystrophy. *Can Med Assoc J.* 21:18-31.
- Coutinho, P., C. Qiu, S. Frank, K. Tamber, and D. Becker. 2003. Dynamic changes in connexin expression correlate with key events in the wound healing process. *Cell Biol.Int.* 27:525-541.
- Coutinho, P., C. Qiu, S. Frank, C.M. Wang, T. Brown, C.R. Green, and D.L. Becker. 2005. Limiting burn extension by transient inhibition of Connexin43 expression at the site of injury. *Br J Plast Surg.* 58:658-667.
- Darby, I.A., and T.D. Hewitson. 2007. Fibroblast differentiation in wound healing and fibrosis. *Int Rev Cytol.* 257:143-179.
- Djalilian, A.R., D. McGaughey, S. Patel, E.Y. Seo, C. Yang, J. Cheng, M. Tomic, S. Sinha, A. Ishida-Yamamoto, and J.A. Segre. 2006. Connexin 26 regulates epidermal barrier and wound remodeling and promotes psoriasiform response. *J Clin Invest.* 116:1243-1253.
- Dobrowolski, R., P. Sasse, J.W. Schrickel, M. Watkins, J.S. Kim, M. Rackauskas, C. Troatz, A. Ghanem, K. Tiemann, J. Degen, F.F. Bukauskas, R. Civitelli, T. Lewalter, B.K. Fleischmann, and K. Willecke. 2008. The conditional connexin43G138R mouse mutant represents a new model of hereditary oculodentodigital dysplasia in humans. *Hum Mol Genet.* 17:539-554.
- Ehrlich, H.P., G. Gabbiani, and P. Meda. 2000. Cell coupling modulates the contraction of fibroblast-populated collagen lattices. *J Cell Physiol.* 184:86-92.
- Ek-Vitorin, J.F., G. Calero, G.E. Morley, W. Coombs, S.M. Taffet, and M. Delmar. 1996. pH regulation of connexin43: molecular analysis of the gating particle. *Biophys.J.* 71:1273-1284.
- Ek, J.F., M. Delmar, R. Perzova, and S.M. Taffet. 1994. Role of histidine 95 on pH gating of the cardiac gap junction protein connexin43. *Circ.Res.* 74:1058-1064.

- Flenniken, A.M., L.R. Osborne, N. Anderson, N. Ciliberti, C. Fleming, J.E. Gittens, X.Q. Gong, L.B. Kelsey, C. Lounsbury, L. Moreno, B.J. Nieman, K. Peterson, D. Qu, W. Roscoe, Q. Shao, D. Tong, G.I. Veitch, I. Voronina, I. Vukobradovic, G.A. Wood, Y. Zhu, R.A. Zirngibl, J.E. Aubin, D. Bai, B.G. Bruneau, M. Grynepas, J.E. Henderson, R.M. Henkelman, C. McKerlie, J.G. Sled, W.L. Stanford, D.W. Laird, G.M. Kidder, S.L. Adamson, and J. Rossant. 2005. A Gja1 missense mutation in a mouse model of oculodentodigital dysplasia. *Development*. 132:4375-4386.
- Gemel, J., V. Valiunas, P.R. Brink, and E.C. Beyer. 2004. Connexin43 and connexin26 form gap junctions, but not heteromeric channels in co-expressing cells. *J.Cell Sci*. 117:2469-2480.
- Ghatnekar, G.S., M.P. O'Quinn, L.J. Jourdan, A.A. Gurjarpadhye, R.L. Draughn, and R.G. Gourdie. 2009. Connexin43 carboxyl-terminal peptides reduce scar progenitor and promote regenerative healing following skin wounding. *Regen Med*. 4:205-223.
- Gibson, D.F., D.D. Bikle, J. Harris, and G.S. Goldberg. 1997. The expression of the gap junctional protein Cx43 is restricted to proliferating and non differentiated normal and transformed keratinocytes. *Exp Dermatol*. 6:167-174.
- Gillespie, F.D. 1964. A Hereditary Syndrome: "Dysplasia Oculodentodigitalis". *Arch.Ophthalmol*. 71:187-192.
- Goliger, J.A., and D.L. Paul. 1994. Expression of gap junction proteins Cx26, Cx31.1, Cx37, and Cx43 in developing and mature rat epidermis. *Dev.Dyn*. 200:1-13.
- Goliger, J.A., and D.L. Paul. 1995. Wounding alters epidermal connexin expression and gap junction-mediated intercellular communication. *Mol.Biol.Cell*. 6:1491-1501.
- Gong, X.Q., Q. Shao, C.S. Lounsbury, D. Bai, and D.W. Laird. 2006. Functional characterization of a GJA1 frameshift mutation causing oculodentodigital dysplasia and palmoplantar keratoderma. *J Biol Chem*. 281:31801-31811.
- Goodenough, D.A., and D.L. Paul. 2003. Beyond the gap: functions of unpaired connexon channels. *Nat Rev Mol Cell Biol*. 4:285-294.
- Goodenough, D.A., and D.L. Paul. 2009. Gap junctions. *Cold Spring Harbor Perspect.Biol*. 1:a002576.
- Gorlin, R.J., L.H. Miskin, and G.J. St. 1963. Oculodentodigital dysplasia. *J Pediatr*. 63:69-75.
- Gu, H., J.F. Ek-Vitorin, S.M. Taffet, and M. Delmar. 2000. Coexpression of connexins 40 and 43 enhances the pH sensitivity of gap junctions: a model for synergistic interactions among connexins. *Circ.Res*. 86:E98-E103.

- Gutmann, D.H., E.H. Zackai, D.M. Donald-McGinn, K.H. Fischbeck, and J. Kamholz. 1991. Oculodentodigital dysplasia syndrome associated with abnormal cerebral white matter. *Am.J.Med.Genet.* 41:18-20.
- Haass, N.K., E. Wladykowski, S. Kief, I. Moll, and J.M. Brandner. 2006. Differential induction of connexins 26 and 30 in skin tumors and their adjacent epidermis. *J Histochem Cytochem.* 54:171-182.
- He, D.S., J.X. Jiang, S.M. Taffet, and J.M. Burt. 1999. Formation of heteromeric gap junction channels by connexins 40 and 43 in vascular smooth muscle cells. *Proc.Natl.Acad.Sci.U.S.A.* 96:6495-6500.
- Herve, J.C., N. Bourmeyster, D. Sarrouilhe, and H.S. Duffy. 2007. Gap junctional complexes: from partners to functions. *Prog Biophys Mol Biol.* 94:29-65.
- Hill, J., D. Paslin, and P.W. Wertz. 2006. A new covalently bound ceramide from human stratum corneum -omega-hydroxyacylphytosphingosine. *Int.J.Cosmet.Sci.* 28:225-230.
- Hitomi, K. 2005. Transglutaminases in skin epidermis. *Eur.J.Dermatol.* 15:313-319.
- Hoh, J.H., R. Lal, S.A. John, J.P. Revel, and M.F. Arnsdorf. 1991. Atomic force microscopy and dissection of gap junctions. *Science.* 253:1405-1408.
- Hoh, J.H., G.E. Sosinsky, J.P. Revel, and P.K. Hansma. 1993. Structure of the extracellular surface of the gap junction by atomic force microscopy. *Biophys.J.* 65:149-163.
- Houben, E., K. De Paepe, and V. Rogiers. 2007. A keratinocyte's course of life. *Skin Pharmacol Physiol.* 20:122-132.
- Johnson, R., M. Hammer, J. Sheridan, and J.P. Revel. 1974. Gap junction formation between reaggregated Novikoff hepatoma cells. *Proc.Natl.Acad.Sci.U.S.A.* 71:4536-4540.
- Kalcheva, N., J. Qu, N. Sandeep, L. Garcia, J. Zhang, Z. Wang, P.D. Lampe, S.O. Suadicani, D.C. Spray, and G.I. Fishman. 2007. Gap junction remodeling and cardiac arrhythmogenesis in a murine model of oculodentodigital dysplasia. *Proc Natl Acad Sci U S A.* 104:20512-20516.
- Kamibayashi, Y., M. Oyamada, Y. Oyamada, and M. Mori. 1993. Expression of gap junction proteins connexin 26 and 43 is modulated during differentiation of keratinocytes in newborn mouse epidermis. *J Invest Dermatol.* 101:773-778.
- Kandyba, E.E., M.B. Hodgins, and P.E. Martin. 2008. A murine living skin equivalent amenable to live-cell imaging: analysis of the roles of connexins in the epidermis. *J Invest Dermatol.* 128:1039-1049.

- Kelly, S.C., P. Ratajczak, M. Keller, S.M. Purcell, T. Griffin, and G. Richard. 2006. A novel GJA 1 mutation in oculo-dento-digital dysplasia with curly hair and hyperkeratosis. *Eur J Dermatol.* 16:241-245.
- Kibschull, M., T.M. Magin, O. Traub, and E. Winterhager. 2005. Cx31 and Cx43 double-deficient mice reveal independent functions in murine placental and skin development. *Dev Dyn.* 233:853-863.
- Kjaer, K.W., L. Hansen, H. Eiberg, P. Leicht, J.M. Opitz, and N. Tommerup. 2004. Novel Connexin 43 (GJA1) mutation causes oculo-dento-digital dysplasia with curly hair. *Am J Med Genet A.* 127A:152-157.
- Kretz, M., C. Euwens, S. Hombach, D. Eckardt, B. Teubner, O. Traub, K. Willecke, and T. Ott. 2003. Altered connexin expression and wound healing in the epidermis of connexin-deficient mice. *J Cell Sci.* 116:3443-3452.
- Kretz, M., K. Maass, and K. Willecke. 2004. Expression and function of connexins in the epidermis, analyzed with transgenic mouse mutants. *Eur J Cell Biol.* 83:647-654.
- Kumar, N.M., and N.B. Gilula. 1996. The gap junction communication channel. *Cell.* 84:381-388.
- Laird, D.W. 2006. Life cycle of connexins in health and disease. *Biochem J.* 394:527-543.
- Laird, D.W. 2010. The gap junction proteome and its relationship to disease. *Trends Cell Biol.* 20:92-101.
- Laird, D.W., K.L. Puranam, and J.P. Revel. 1991. Turnover and phosphorylation dynamics of connexin43 gap junction protein in cultured cardiac myocytes. *Biochem J.* 273(Pt 1):67-72.
- Lampe, P.D., B.P. Nguyen, S. Gil, M. Usui, J. Olerud, Y. Takada, and W.G. Carter. 1998. Cellular interaction of integrin alpha3beta1 with laminin 5 promotes gap junctional communication. *J Cell Biol.* 143:1735-1747.
- Langevin, H.M., C.J. Cornbrooks, and D.J. Taatjes. 2004. Fibroblasts form a body-wide cellular network. *Histochem Cell Biol.* 122:7-15.
- Langlois, S., A.C. Maher, J.L. Manias, Q. Shao, G.M. Kidder, and D.W. Laird. 2007. Connexin levels regulate keratinocyte differentiation in the epidermis. *J Biol Chem.* 282:30171-30180.
- Larjava, H., T. Salo, K. Haapasalmi, R.H. Kramer, and J. Heino. 1993. Expression of integrins and basement membrane components by wound keratinocytes. *J Clin Invest.* 92:1425-1435.

- Lemaitre, G., V. Sivan, J. Lamartine, J.M. Cosset, B. Cavelier-Balloy, D. Salomon, G. Waksman, and M.T. Martin. 2006. Connexin 30, a new marker of hyperproliferative epidermis. *Br J Dermatol.* 155:844-846.
- Loddenkemper, T., K. Grote, S. Evers, M. Oelerich, and F. Stogbauer. 2002. Neurological manifestations of the oculodentodigital dysplasia syndrome. *J Neurol.* 249:584-595.
- Lucke, T., R. Choudhry, R. Thom, I.S. Selmer, A.D. Burden, and M.B. Hodgins. 1999. Upregulation of connexin 26 is a feature of keratinocyte differentiation in hyperproliferative epidermis, vaginal epithelium, and buccal epithelium. *J Invest Dermatol.* 112:354-361.
- Maass, K., A. Ghanem, J.S. Kim, M. Saathoff, S. Urschel, G. Kirfel, R. Grummer, M. Kretz, T. Lewalter, K. Tiemann, E. Winterhager, V. Herzog, and K. Willecke. 2004. Defective epidermal barrier in neonatal mice lacking the C-terminal region of connexin43. *Mol.Biol.Cell.* 15:4597-4608.
- Maass, K., J. Shibayama, S.E. Chase, K. Willecke, and M. Delmar. 2007. C-terminal truncation of connexin43 changes number, size, and localization of cardiac gap junction plaques. *Circ.Res.* 101:1283-1291.
- Maeda, S., S. Nakagawa, M. Suga, E. Yamashita, A. Oshima, Y. Fujiyoshi, and T. Tsukihara. 2009. Structure of the connexin 26 gap junction channel at 3.5 Å resolution. *Nature.* 458:597-602.
- Maestrini, E., B.P. Korge, J. Ocana-Sierra, E. Calzolari, S. Cambiaghi, P.M. Scudder, A. Hovnanian, A.P. Monaco, and C.S. Munro. 1999. A missense mutation in connexin26, D66H, causes mutilating keratoderma with sensorineural deafness (Vohwinkel's syndrome) in three unrelated families. *Hum.Mol.Genet.* 8:1237-1243.
- Makowski, L., D.L. Caspar, W.C. Phillips, and D.A. Goodenough. 1977. Gap junction structures. II. Analysis of the x-ray diffraction data. *J.Cell Biol.* 74:629-645.
- Makowski, L., D.L. Caspar, W.C. Phillips, and D.A. Goodenough. 1984. Gap junction structures. V. Structural chemistry inferred from X-ray diffraction measurements on sucrose accessibility and trypsin susceptibility. *J Mol Biol.* 174:449-481.
- Man, Y.K., C. Trollove, D. Tattersall, A.C. Thomas, A. Papakonstantinopoulou, D. Patel, C. Scott, J. Chong, D.J. Jagger, E.A. O'Toole, H. Navsaria, M.A. Curtis, and D.P. Kelsell. 2007. A deafness-associated mutant human connexin 26 improves the epithelial barrier in vitro. *J Membr Biol.* 218:29-37.
- Manias, J.L., I. Plante, X.Q. Gong, Q. Shao, J. Churko, D. Bai, and D.W. Laird. 2008. Fate of connexin43 in cardiac tissue harbouring a disease-linked connexin43 mutant. *Cardiovasc Res.* 80:385-395.

- Martinez, A.D., V. Hayrapetyan, A.P. Moreno, and E.C. Beyer. 2002. Connexin43 and connexin45 form heteromeric gap junction channels in which individual components determine permeability and regulation. *Circ.Res.* 90:1100-1107.
- Matic, M., W.H. Evans, P.R. Brink, and M. Simon. 2002. Epidermal stem cells do not communicate through gap junctions. *J.Invest Dermatol.* 118:110-116.
- McLachlan, E., J.L. Manias, X.Q. Gong, C.S. Lounsbury, Q. Shao, S.M. Bernier, D. Bai, and D.W. Laird. 2005. Functional characterization of oculodentodigital dysplasia-associated Cx43 mutants. *Cell Commun Adhes.* 12:279-292.
- Mori, R., K.T. Power, C.M. Wang, P. Martin, and D.L. Becker. 2006. Acute downregulation of connexin43 at wound sites leads to a reduced inflammatory response, enhanced keratinocyte proliferation and wound fibroblast migration. *J Cell Sci.* 119:5193-5203.
- Muller, D.J., G.M. Hand, A. Engel, and G.E. Sosinsky. 2002. Conformational changes in surface structures of isolated connexin 26 gap junctions. *EMBO J.* 21:3598-3607.
- O'Toole, E.A., M.P. Marinkovich, W.K. Hoeffler, H. Furthmayr, and D.T. Woodley. 1997. Laminin-5 inhibits human keratinocyte migration. *Exp Cell Res.* 233:330-339.
- Oshima, A., K. Tani, Y. Hiroaki, Y. Fujiyoshi, and G.E. Sosinsky. 2007. Three-dimensional structure of a human connexin26 gap junction channel reveals a plug in the vestibule. *Proc Natl Acad Sci U S A.* 104:10034-10039.
- Paznekas, W.A., B. Karczeski, S. Vermeer, R.B. Lowry, M. Delatycki, F. Laurence, P.A. Koivisto, L. Van Maldergem, S.A. Boyadjiev, J.N. Bodurtha, and E.W. Jabs. 2009. GJA1 mutations, variants, and connexin 43 dysfunction as it relates to the oculodentodigital dysplasia phenotype. *Hum Mutat.* 30:724-733.
- Plum, A., E. Winterhager, J. Pesch, J. Lautermann, G. Hallas, B. Rosentreter, O. Traub, C. Herberhold, and K. Willecke. 2001. Connexin31-deficiency in mice causes transient placental dysmorphogenesis but does not impair hearing and skin differentiation. *Dev Biol.* 231:334-347.
- Pollok, S., A.C. Pfeiffer, R. Lobmann, C.S. Wright, I. Moll, P.E. Martin, and J.M. Brandner. 2010. Connexin 43 mimetic peptide Gap27 reveals potential differences in the role of Cx43 in wound repair between diabetic and non-diabetic cells. *J Cell Mol Med.* 15:861-873.
- Prochnow, N., and R. Dermietzel. 2008. Connexons and cell adhesion: a romantic phase. *Histochem Cell Biol.* 130:71-77.
- Purnick, P.E., D.C. Benjamin, V.K. Verselis, T.A. Bargiello, and T.L. Dowd. 2000. Structure of the amino terminus of a gap junction protein. *Arch Biochem Biophys.* 381:181-190.

- Qiu, C., P. Coutinho, S. Frank, S. Franke, L.Y. Law, P. Martin, C.R. Green, and D.L. Becker. 2003. Targeting connexin43 expression accelerates the rate of wound repair. *Curr.Biol.* 13:1697-1703.
- Reaume, A.G., P.A. de Sousa, S. Kulkarni, B.L. Langille, D. Zhu, T.C. Davies, S.C. Juneja, G.M. Kidder, and J. Rossant. 1995. Cardiac malformation in neonatal mice lacking connexin43. *Science.* 267:1831-1834.
- Revel, J.P., and M.J. Karnovsky. 1967. Hexagonal array of subunits in intercellular junctions of the mouse heart and liver. *J.Cell Biol.* 33:C7-C12.
- Richard, G. 2000. Connexins: a connection with the skin. *Exp.Dermatol.* 9:77-96.
- Richard, G., L.E. Smith, R.A. Bailey, P. Itin, D. Hohl, E.H. Epstein, Jr., J.J. DiGiovanna, J.G. Compton, and S.J. Bale. 1998. Mutations in the human connexin gene GJB3 cause erythrokeratoderma variabilis. *Nat Genet.* 20:366-369.
- Richards, T.S., C.A. Dunn, W.G. Carter, M.L. Usui, J.E. Olerud, and P.D. Lampe. 2004. Protein kinase C spatially and temporally regulates gap junctional communication during human wound repair via phosphorylation of connexin43 on serine368. *J.Cell Biol.* 167:555-562.
- Risek, B., F.G. Klier, and N.B. Gilula. 1992. Multiple gap junction genes are utilized during rat skin and hair development. *Development.* 116:639-651.
- Rouan, F., T.W. White, N. Brown, A.M. Taylor, T.W. Lucke, D.L. Paul, C.S. Munro, J. Uitto, M.B. Hodgins, and G. Richard. 2001. trans-dominant inhibition of connexin-43 by mutant connexin-26: implications for dominant connexin disorders affecting epidermal differentiation. *J.Cell Sci.* 114:2105-2113.
- Salomon, D., E. Masgrau, S. Vischer, S. Ullrich, E. Dupont, P. Sappino, J.H. Saurat, and P. Meda. 1994. Topography of mammalian connexins in human skin. *J Invest Dermatol.* 103:240-247.
- Simek, J., J. Churko, Q. Shao, and D.W. Laird. 2009. Cx43 has distinct mobility within plasma-membrane domains, indicative of progressive formation of gap-junction plaques. *J Cell Sci.* 122:554-562.
- Smith, F. 2003. The molecular genetics of keratin disorders. *Am J Clin Dermatol.* 4:347-364.
- Sohl, G., S. Maxeiner, and K. Willecke. 2005. Expression and functions of neuronal gap junctions. *Nat Rev Neurosci.* 6:191-200.
- Sohl, G., and K. Willecke. 2003. An update on connexin genes and their nomenclature in mouse and man. *Cell Commun Adhes.* 10:173-180.

- Sohl, G., and K. Willecke. 2004. Gap junctions and the connexin protein family. *Cardiovasc Res.* 62:228-232.
- Solan, J.L., and P.D. Lampe. 2009. Connexin43 phosphorylation: structural changes and biological effects. *Biochem J.* 419:261-272.
- Sosinsky, G. 1995. Mixing of connexins in gap junction membrane channels. *Proc.Natl.Acad.Sci.U.S.A.* 92:9210-9214.
- Strober, B.E. 2003. Erythrokeratoderma variabilis. *Dermatol Online J.* 9:5.
- Sugar, H.S., J.P. Thompson, and J.D. Davis. 1966. The oculo-dento-digital dysplasia syndrome. *Am J Ophthalmol.* 61:1448-1451.
- Thoden, C.J., S. Ryoppy, and P. Kuitunen. 1977. Oculodentodigital dysplasia syndrome. Report of four cases. *Acta Paediatr Scand.* 66:635-638.
- Unger, V.M., N.M. Kumar, N.B. Gilula, and M. Yeager. 1999. Three-dimensional structure of a recombinant gap junction membrane channel. *Science.* 283:1176-1180.
- Unwin, P.N., and P.D. Ennis. 1984. Two configurations of a channel-forming membrane protein. *Nature.* 307:609-613.
- van Steensel, M.A., L. Spruijt, d.B.I. van, R.S. Bladergroen, M. Vermeer, P.M. Steijlen, and G.M. van. 2005. A 2-bp deletion in the GJA1 gene is associated with oculo-dento-digital dysplasia with palmoplantar keratoderma. *Am.J.Med.Genet.A.* 132A:171-174.
- Vreeburg, M., E.A. de Zwart-Storm, M.I. Schouten, R.G. Nellen, D. Marcus-Soekarman, M. Devies, M. van Geel, and M.A. van Steensel. 2007. Skin changes in oculo-dento-digital dysplasia are correlated with C-terminal truncations of connexin 43. *Am J Med Genet A.* 143:360-363.
- Wiszniewski, L., A. Limat, J.H. Saurat, P. Meda, and D. Salomon. 2000. Differential expression of connexins during stratification of human keratinocytes. *J Invest Dermatol.* 115:278-285.
- Wright, C.S., M.A. van Steensel, M.B. Hodgins, and P.E. Martin. 2009. Connexin mimetic peptides improve cell migration rates of human epidermal keratinocytes and dermal fibroblasts in vitro. *Wound Repair Regen.* 17:240-249.
- Yamakage, K., Y. Omori, C. Piccoli, and H. Yamasaki. 1998. Growth control of 3T3 fibroblast cell lines established from connexin 43-deficient mice. *Mol Carcinog.* 23:121-128.

- Zampighi, G.A., J.E. Hall, G.R. Ehring, and S.A. Simon. 1989. The structural organization and protein composition of lens fiber junctions. *J.Cell Biol.* 108:2255-2275.
- Zhang, J.T., and B.J. Nicholson. 1994. The topological structure of connexin 26 and its distribution compared to connexin 32 in hepatic gap junctions. *J.Membr.Biol.* 139:15-29.
- Zhang, Y., E.M. Kanter, J.G. Laing, C. Aprhys, D.C. Johns, E. Kardami, and K.A. Yamada. 2008. Connexin43 expression levels influence intercellular coupling and cell proliferation of native murine cardiac fibroblasts. *Cell Commun Adhes.* 15:289-303.
- Zhang, Y., H. Wang, A. Kovacs, E.M. Kanter, and K.A. Yamada. 2010. Reduced expression of Cx43 attenuates ventricular remodeling after myocardial infarction via impaired TGF-beta signaling. *Am J Physiol Heart Circ Physiol.* 298:H477-487.

A version of this chapter has been published:

Churko, J.M., Laird, D.W., (2010) "Gap junctions as a Cellular Domain" in Cellular Domains edited by Ivan Robert Nabi, John Wiley & Sons, Inc. N.J. (in press)

Chapter 2

2 Human dermal fibroblasts derived from oculodentodigital dysplasia patients suggest that patients may have wound-healing defects

It is well known that Cx43 is expressed within the epidermis and dermis of the skin and that the expression of Cx43 changes during wound healing. Since ODDD patients systemically express mutant Cx43, mutant Cx43 expression in resident cells of the skin may impair the ability of both fibroblasts and keratinocytes to heal wounds. This chapter focuses on the use of the Cx43 G60S mutant mouse model of ODDD to determine if mutant G60S Cx43 expression impairs the ability of skin wounds to heal. In addition, we have also employed the novel use of ODDD patient and unaffected family member derived fibroblasts to determine if cells expressing the D3N or V216L mutants affect the ability of fibroblasts to proliferate, migrate, and differentiate into myofibroblasts.

A version of this chapter has been published:

Churko, J.M., and Shao, Q., Gong, X., Swoboda, K.J., Bai, D., Sampson, J., and Laird, D.W. (2011) Human dermal fibroblasts derived from oculodentodigital dysplasia patients suggest that patients may have wound-healing defects. *Human Mutation*, Apr;32(4):456-66.

2.1 Introduction

The human *GJA1* gene (OMIM *121014) encodes the gap junction protein Cx43 (Solan and Lampe, 2009). The ubiquitous expression of Cx43 and primary function in establishing gap junctional intercellular communication (GJIC) has led to this connexin being one of the most widely studied members of the connexin family. GJIC plays a critical role in many physiological processes ranging from more passive roles in cell and tissue maintenance to a highly active role in synchronization of electrical coupling (Kizana et al., 2007). Not surprisingly, dysregulation of either connexin expression or mutations in genes encoding connexins has led to a wide array of human diseases.

In 2003, Paznekas and colleagues successfully mapped a developmental disorder known as oculodentodigital dysplasia (ODDD) to mutations in the *GJA1* gene (Paznekas et al., 2003). Presently, 62 mutations have been mapped to the *GJA1* gene and linked to ODDD (Paznekas et al., 2009). ODDD is a rare, mostly autosomal dominant inherited disorder affecting the development of a variety of tissues and organs. Though ODDD patients exhibit some consistent features such as syndactyly, camptodactyly, craniofacial abnormalities, enamel loss and microdontia, other less common features include glaucoma, neurological defects (progressive spastic paraparesis), neurogenic bladder and even heart and skin diseases (Paznekas et al., 2009). Missense mutations are by far the most widely found type of mutations, but two frame-shift mutations have also been identified (van Steensel et al., 2005; Vreeburg et al., 2007). Surprisingly, two autosomal recessive mutations have been reported and one of these results in the premature truncation of Cx43 after only encoding 33 amino acids, effectively resulting in a near complete Cx43 knockout (Richardson et al., 2006). *GJA1* gene mutations are found throughout the expanse of the gene but the vast majority of the mutations occur in the first two thirds of the gene. At present, over 15 specific mutations have been engineered, over-expressed and studied in reference cell systems to assess the ability of the mutant Cx43 to traffic, assemble and form functional channels (Churko et al., 2010; McLachlan et al., 2005). Intriguingly, all of the Cx43 mutants examined under these conditions have severely compromised intercellular channel forming abilities and exhibit moderate to severe dominant-negative effects on co-expressed endogenous Cx43. Thus, these *in vitro*

studies would predict that patients harboring autosomal dominant Cx43 mutants are operating on far less than 50% normal Cx43 function.

A well-documented limitation of mutant overexpression studies is the difficulty in matching the expression level of the mutant and wild-type counterpart to equal the 1:1 expression level expected to be found in patients. To overcome this shortcoming, three mouse models of ODDD have been generated in an attempt to mimic the genotype/phenotype relationship found in the human disease. The first of these models was engineered in 2005 through an ethylnitrosourea screen where a mouse, designated *Gjal*^{Jrt/+}, was found to harbor a G60S point mutation (Flenniken et al., 2005). While this mutation has not yet been identified in the human population, the mouse phenotype was characterized to closely match the clinical symptoms exhibited by ODDD patients. This mouse model has been used extensively and has shed insight into the molecular mechanisms underlying ODDD. In more recent years, two additional mouse models have been engineered to reflect human mutations of interest. The first one was designed to generically express an I130T Cx43 mutant (Cx43^{I130T/+}) (Kalcheva et al., 2007) and the second constitutively expressed the G138R mutant (Cx43^{G138R/+}) (Dobrowolski et al., 2008). Given the recent generation of these mice, they are only beginning to be studied as mouse models of ODDD. Seminal publications describing these mice indicate that while they manifest common characteristics of ODDD, there are unique features to each mouse strain that will require further study.

Although mutant Cx43 expression in reference cell models and genetic mouse models of ODDD are valuable tools to investigate the cell mechanisms associated with ODDD, they may not fully reflect the pathophysiologic aspects of ODDD exhibited by patients. In the current study, we attempt to bridge this shortcoming by isolating and culturing the first primary culture cells from ODDD patients. Here we recruited two ODDD families to obtain human skin tissue specimens for the establishment of matched fibroblast cell lines from both patients and unaffected close relatives. We further compared our findings to fibroblasts derived from the *Gjal*^{Jrt/+} (G60S) mouse model to assess potential human/mouse differences. We found that fibroblasts obtained from these patients are significantly different from their genetically matched control fibroblasts in their

proliferation, migration and differentiation into myofibroblasts. Here we suggest that wound healing in ODDD patients may be delayed and propose a mechanism by which fibroblasts may exacerbate disease in these patients.

2.2 Materials and methods

2.2.1 Human fibroblast cultures

Fresh skin biopsy samples obtained from patients and unaffected relatives were placed in ice cold DMEM (25 mL, Cat#11960-044, Invitrogen, Carlsbad, CA) containing 10% fetal bovine serum (FBS, Cat# A12617DJ, Invitrogen, Carlsbad, CA) prior to being cut into small pieces and transported into a second dish containing DMEM with 10% FBS and 100 U/ml penicillin & 100 µg/ml streptomycin (Cat #15140-122, Invitrogen, Carlsbad, CA), and incubated at 37 °C in a humidified chamber containing 5% CO₂. The media was changed once a week for 3-4 weeks. Cells were subcultured once they reached confluence by treating with trypsin (0.05% trypsin with 0.25 EDTA, Cat# 25200-056 Invitrogen, Carlsbad, CA). For long-term storage, collected cells were resuspended in cryopreservation media (DMEM with 10% FBS, 1x antibiotic/antimycotic and 10% DMSO-filtered (Cat# D2650, Sigma-Aldrich, St. Louis, MO) and aliquoted into cryotubes. Cells were stored in liquid nitrogen. Human fibroblasts were sent to the University of Western Ontario for further analysis as approved by the Office of Research Ethics at the University of Western Ontario. All fibroblasts cells were cultured in DMEM supplemented with 10% fetal bovine serum, 100 U/ml penicillin, 100 µg/ml streptomycin, and 2 mM glutamine and incubated at 37 °C in humidified air with 5% CO₂. In subsequent experiments, results were compared from passage-matched fibroblasts used from passages 2 to 6.

2.2.2 Extraction of genomic DNA for sequencing

Genomic DNA was extracted from peripheral blood leukocytes and/or fibroblast cells of all individuals by standard methods with proteinase K (Cat# 51104, Qiagen DNA Blood kit, Qiagen, Mississauga, Ontario). PCR amplification of the Cx43 gene was performed by using Cx43 primers of the forward 5'-TGGGACAGGAAGAGTTTGAC-3' and

reverse 5'-CACCTGGTGCACTTTCTACAGCAC-3' and the sequencing of Cx43 gene by using primer 1: 5'-GGTGGCCTTCTTGCTGATCC-3', primer 2: 5'-TGGGCAGGGATCTCTTTTGC-5' and primer 3: 5'-GGTTGCCCAAACACTGATGGTG.

2.2.3 Dye coupling assay

A preloading assay was used to quantify GJIC in primary fibroblast cultures as described previously (Goldberg et al., 1995). Briefly, a subpopulation of primary fibroblasts was loaded with the gap junction permeable dye, calcein-AM (Cat# D1430, Molecular Probes, Eugene, OR), and the gap junction impermeable dye, DiI (Cat# D282, Molecular Probes, Eugene, OR). The preloaded cells (~ 100 cells) were seeded onto a monolayer of unlabeled primary fibroblast cells, and after 3 h, samples were observed and images recorded with a Leica DM IRE2 inverted epifluorescence microscope. The instances of calcein dye transfer from the DiI-labeled source cells were counted, and successful dye transfer was declared if there was clear evidence of dye transfer to at least one cell adjacent to DiI donor cell. Three independent trials were performed for each cell line. Standard errors were calculated, and the control and mutant cells were compared with a Student's *t*-test.

2.2.4 Patch-clamp electrophysiology

The intercellular electrical coupling conductance between control or mutant fibroblasts was assessed by using the dual whole cell patch-clamp technique as previously described (Gong et al., 2006). Human fibroblasts were plated on glass coverslips in cell culture dishes at low density for 24-48 hours. Isolated fibroblast cell pairs with side-to-side contacts were chosen for double patch-clamp recording. Data acquisition and analysis were performed via Digidata 1322A interface and pClamp9 software (Axon Instruments Inc., Union City, CA). Gap junctional conductance (G_j) was determined and presented as mean \pm SEM. Online series resistance compensation at 80% was applied to improve the accuracy of measured G_j . A Student's *t*-test was performed to determine statistical significance (**, $p < 0.01$).

2.2.5 Immunocytochemistry and immunohistochemistry

Cells were grown on glass coverslips and fixed with ice-cold 80% methanol/20% acetone at 4°C for 20 min and rinsed with PBS 3 times before immunolabeling. Antibodies to the gap junction protein, polyclonal Cx43 (1:500; Cat# C6219, Sigma-Aldrich, St. Louis, MO) mAb GM130, a 130 kDa Golgi matrix protein antibody (1:100; Cat# 610822, BD Transduction Laboratories, Mississauga, ON), and an intermediate filament, mAb vimentin antibody (1:500; Cat# MAB3400, Millipore, Temecula, CA), were used. Primary antibody binding was detected with appropriate Alexa-488 (anti-mouse Cat# a11017, anti-rabbit Cat# A11008) or Alexa-555–conjugated anti-rabbit (Cat# A21429) or anti-mouse (Cat# A21425) (1:500; Invitrogen, Carlsbad, CA) secondary antibodies. Nuclei were stained with Hoechst 33342 (1:1000; Cat# H3570, Molecular Probes, Eugene, OR) or DAPI (1:1000; Cat# D3571, Molecular Probes, Eugene, OR). Cells were imaged with a Zeiss LSM 510 META confocal microscope as previously described (Simek et al., 2009).

2.2.6 Wound healing assay

The wound healing assay was approved by the Office of Research Ethics at the University of Western Ontario. Eleven adult G60S mutant mice and eleven WT control mice were anesthetized with isofluorane gas and the dorsal back skin surface was shaved using #40 clippers. Prior to performing a punch biopsy, a three stage incision site preparation (betadine soap/alcohol/betadine scrub) was performed on the shaved surface and a sterile disposable 5 mm bore biopsy tool was used to obtain a 5 mm full-thickness excisional epidermal and dermal skin biopsy. Buprenorphine (0.05mg/kg) was administered once during anesthesia recovery, and additional doses (8-12h) were administered if the mice looked stressed. The area of wound closure was measured after day 1, 3, 6, 9, and 12 from images taken at these time points. Wound area calculations were performed using ImageJ and the resulting wound area was graphed using Graphpad Prism 4.0. A two-way ANOVA (repeated measures) from data points Day 3, 6, and 9 with a Bonferroni post-hoc test was performed to determine statistical significance (* $p < 0.05$).

2.2.7 Punch biopsy migration

Circular skin punches were cultured *ex vivo* as previously described (Stephens et al., 1996). Fresh 5 mm dermal punch biopsies from postnatal day 4 WT and G60S littermate mice were placed on culture wells either precoated with 10 $\mu\text{g}/\text{mL}$ fibronectin (Cat# 356008, BD Bioscience, San Jose, CA), 0.3 $\mu\text{g}/\text{mL}$ laminin 332 (V) (Cat# CC-145 Chemicon, Billerica, Massachusetts), or 2 mg/mL bovine collagen type I (Cat# 354236, BD Bioscience, San Jose, CA). Dermal punch biopsies were incubated at 37°C for one hour to facilitate adhesion of the dermal punch biopsy to the culture well and growth medium, (DMEM Cat# 11960-044, Invitrogen, Carlsbad, CA, 10% FBS Cat# A12617DJ, Invitrogen, Carlsbad, CA, 100U/mL pen/strep, Cat# 15140-122, Invitrogen, Carlsbad, CA and 2 mM glutamine, Cat# 25030149, Invitrogen, Carlsbad, CA) was gently added to the culture wells to surround the punch biopsy. Cultures were then incubated at 37°C and 5% CO₂ for 24 hours and extra media was placed in each culture well to fully submerge the punch biopsy. After four days, the growth media was aspirated and cultures were fixed with ice-cold 80% methanol/20% acetone for 10 minutes. Cultures were then washed and stored in PBS until imaged. Eight images were taken around the circumference of the skin explants with a Zeiss 510 microscope and the total area of cellular migration from the explants was calculated. Total cellular area of migration was then graphed using Graphpad Prism 4.0. Student's *t*-test between punch biopsies derived from WT and G60S on the same substrate (collagen I, fibronectin, plastic or laminin 332) was performed to determine statistical significance (**p* < 0.05).

2.2.8 Human fibroblast migration

Human fibroblasts were seeded at cell density of 1×10^4 cells per culture well in a 12-well tissue culture dish. Once confluent, the growth media was removed and a 1000 μL pipette tip was scraped down the center of the culture well. Culture wells were then washed 2X with Opti-MEM (Cat# 11058-021, Invitrogen, Carlsbad, CA) and 1 mL of Opti-MEM was added to each culture well. Time-lapse imaging was performed using a Zeiss 510 microscope equipped with Axiovision software. Time-lapse monolayer closure images were acquired every 15 minutes for 48 hours. Migration was quantified by measuring the

area fibroblasts transversed into the scraped area 24 hour after a scrape was performed. To calculate the average migration distance the area was divided by the field of view height and graphed. Student's *t*-test between D3 and D3N fibroblasts or between V216 and V216L fibroblasts was performed to determine statistical significance (**p* < 0.05).

2.2.9 Fibroblast proliferation

To examine cell proliferation, 1×10^4 control or mutant fibroblasts were plated in 6-well dishes and allowed to grow in growth medium. At days 2, 4 and 6, cells from replicated plates were collected and counted using an automated CountessTM Cell Counter (Invitrogen, Carlsbad, CA). The total cell number during each time point was then graphed using Graphpad Prism 4.0. Student's *t*-test between D3 and D3N fibroblasts or between V216 and V216L fibroblasts after six days of growth was performed to determine statistical significance (**p* < 0.05).

2.2.10 TGF β_1 treatment

D3, D3N, V216 and V216L cells were seeded at a density of 1.5×10^5 cells per well in a 6-well culture dish. Cultures containing each human fibroblast population were either left untreated or treated with 1 ng/mL TGF β_1 (Cat# 240-B, R&D Systems, Minneapolis, MN). After four days, cultures were lysed using a RIPA buffer for Western blot analysis.

2.2.11 Western blot analysis

As previously described (Penuela et al., 2007), total proteins were isolated from human fibroblast cell cultures using a RIPA buffer. Approximately 30 μ g of total protein/lane was separated by electrophoresis on 10% SDS-PAGE gels and transferred to nitrocellulose membrane for immunoblotting. A polyclonal anti-Cx43 antibody (1:5000; Cat# C6219, Sigma-Aldrich, St. Louis, MO) was used to detect endogenous Cx43 species and an anti-alpha smooth muscle actin antibody (1:1000; Cat# A2547, Sigma-Aldrich, St. Louis, MO) to detect alpha smooth muscle actin. The membranes were also probed for GAPDH (1:10,000; Cat# MAB374, Chemicon, Temecula, CA) as a control for protein loading. Primary antibody labeling was detected using IRDye 800 (1:5000; Cat#

611-132-122, Rockland, Glibertsville, PA)) and Alexa Fluor® 680 (1:5000; Cat#A21076, Invitrogen, Carlsbad, CA) goat anti-rabbit and anti-mouse secondary antibodies and the Li-Cor detection system. The relative densitometry intensities were normalized to GAPDH and graphed using Graphpad Prism 4.0. Student's *t*-test between the levels of P2/Total Cx43, alpha smooth muscle actin, or fold change in alpha smooth muscle actin expression was performed to determine statistical significance. Bars denote which groups were compared and achieved significance (* $p < 0.05$).

2.3 Results

2.3.1 Clinical presentation of patients and detection of Cx43 gene mutations

We recruited two families diagnosed with ODDD; one family has multiple members with ODDD while the second family had one isolated case. All affected individuals had the typical craniofacial appearance and limb involvement characteristic of ODDD.

Patient #1

This female individual was born with a tethered tongue, heart murmur and a kidney malfunction. Her motor milestones were normal. She has a narrow nose with hypoplastic alae nasi, and microphthalmia. Her teeth are dysplastic and irregularly enameled, but are in good condition. She had fusion of digits 3-5, with the 5th digit brachydactyly and clinodactyly. Neurologic symptoms of lower extremity paresthesias and weakness are exacerbated by heat and exercise (Uthoff's sign). Neurogenic bladder was managed with tolterodine. At age 14, her neurologic exam was notable for normal strength and gait, but lower extremity hyperreflexia and right Babinski sign, lower extremity hyperesthesia to pinprick but normal vibratory threshold.

Patient #2

This male patient had congenital umbilical hernia, and bilateral fusion of digits 4 and 5 of the hands, but no fusion of toes. He has a narrow nose with hypoplastic alae nasi,

irregular and thinly enameled dentition, but no ocular involvement. Neurologic symptoms began at age 29 with spasticity. He has had episodic gastrointestinal illness and chronic gastrointestinal hypomotility, neurogenic bladder, and also describes Uthoff's sign. He lost ambulation at age 54; his neurologic exam was notable for hyperreflexia, spasticity, Babinski sign, and diminished vibratory threshold in the lower extremities. He has since developed lower extremity lymphedema.

DNA was extracted from each patient's skin fibroblasts. As expected, DNA sequence analysis found that both patients had missense mutations in the *GJA1* gene encoding for Cx43 (**Fig. 2.1A**). Patient 1 exhibited a missense mutation in N-terminal region of Cx43 resulting in the substitution of an aspartic acid at position 3 for asparagine (p.D3N). Patient 2 was found to harbor a mutation in the region of the molecule that would represent the 4th transmembrane domain at residue 216 where valine was replaced by leucine (p.V216L). No mutation was found in the coding region of the *GJA1* gene from fibroblasts of the matched family member of the D3N (the mother of the patient) or V216L patients (the daughter of the patient). Those fibroblasts were used as normal controls and are notated as D3 and V216, respectively.

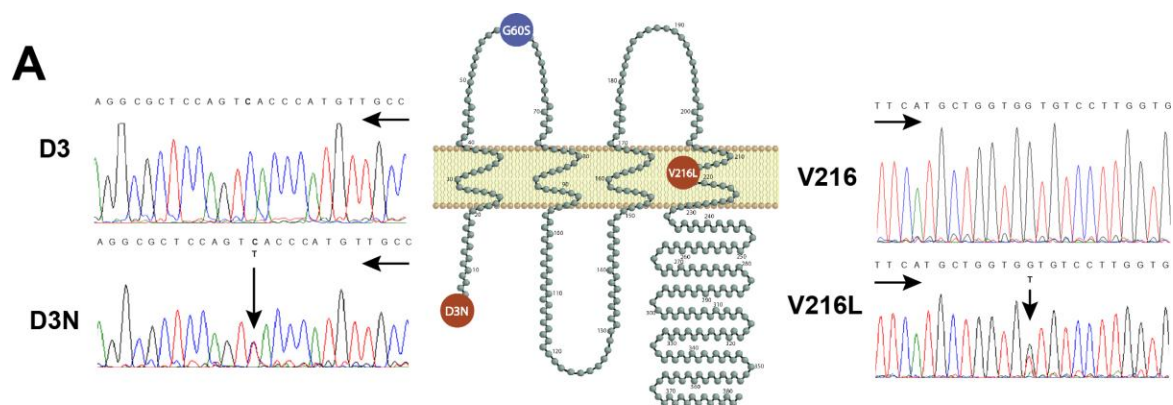
2.3.2 Characterization of Cx43 in control and mutant fibroblasts

Previous studies have reported the existence of the D3N and V216L in ODDD patients but no studies have investigated how human Cx43 mutants affect the trafficking of Cx43 and the assembly of gap junctions (Paznekas et al., 2003; Paznekas et al., 2009). To this end, we established the first use of primary cell culture from patients expressing the D3N and V216L mutant Cx43. Familial matched control fibroblasts (D3 and V216) were also obtained from unaffected relatives to control for the fibroblast source, cell passage and genetic variation which may have otherwise affected the interpretation of our results. Cultured cells were verified as fibroblasts due to their spindle-shaped appearance and positive staining for the intermediate filament, vimentin, confirming their mesenchymal origin (**Fig. 2.1B**).

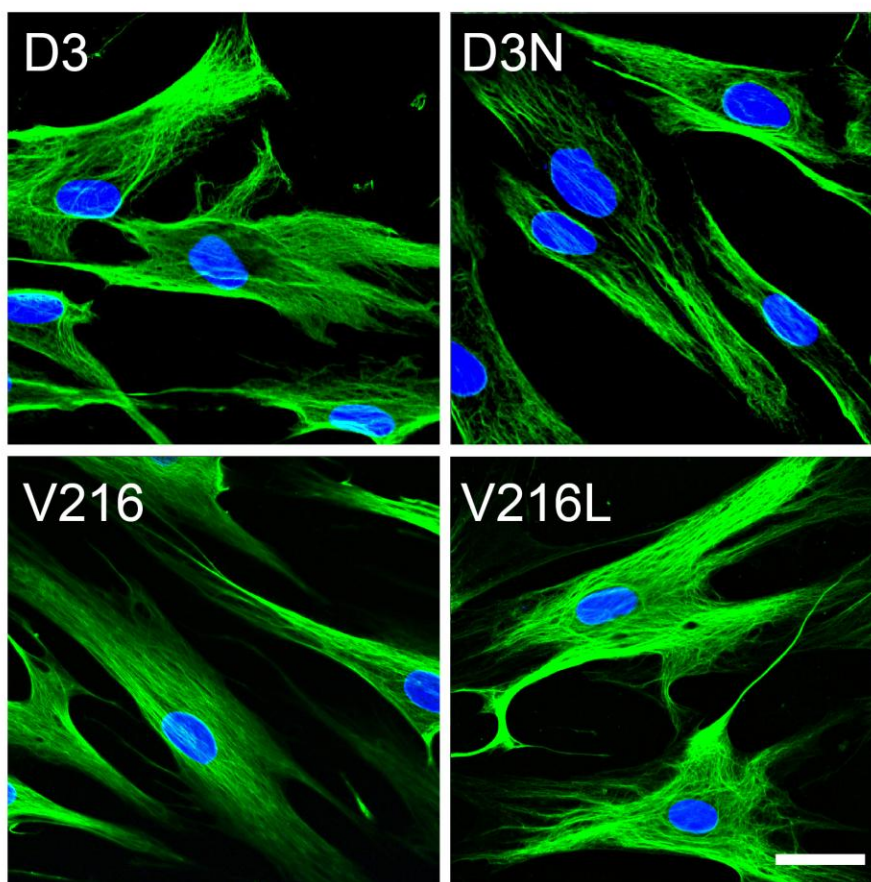
To characterize the subcellular localization of Cx43 in control and mutant fibroblasts, cells were immunofluorescently double-labeled for Cx43 and a resident protein of the

Figure 2.1 D3, D3N, V216, and V216L cells are fibroblasts

A. Genomic DNA was extracted from patient's blood samples or skin fibroblasts. DNA sequence analysis identified the heterozygous missense mutation in the N-terminal coding region of the *GJA1* gene in patient 1 where GAC (Asp, D) changed to AAC (Asn, N) (D3N). The mutation in patient 2 was found in the gene region encoding the fourth transmembrane domain of Cx43 where GTG (Val, V) changed to TTG (Leu, L)(V216L). The G60S mouse mutation is localized within the first extracellular loop domain. B. D3, D3N, V216, V216L cells were immunofluorescently labeled with the mesenchymal marker vimentin (green) and stained with DAPI to denote nuclei (blue). Spindle-like morphology and vimentin-positive labeling support the identification of fibroblasts as the human patient derived cells. Bar = 20 μ m.



B



Golgi apparatus, GM130 (**Fig. 2.2**). In D3, D3N and V216 fibroblasts, Cx43 was localized extensively to punctate structures at sites of cell-to-cell apposition consistent with the formation of gap junction plaques. However, the prevalence of gap junction plaques was greatly reduced in the V216L fibroblasts and a large population of Cx43 co-localized with the resident Golgi protein, GM130. Collectively, these localization studies would suggest that the D3N mutant readily assembles into gap junctions while the V216L mutant is partially impaired from forming gap junctions. All fibroblasts were examined for the presence of Cx26, Cx40 and Cx45 but no specific staining was found for these connexin isoforms (data not shown).

2.3.3 Both human ODDD-linked mutants reduce GJIC

In order to examine GJIC in control and mutant fibroblasts, a preloading assay was performed where calcein-loaded and DiI-labeled donor cells were seeded on fibroblast cultures and the incidents of calcein spread were quantified and compared to control counterparts (**Fig. 2.3A**). In all cases, the incidence of dye transfer in mutant fibroblasts were significantly reduced in comparison to their control counterparts. To further examine the degree of gap junction coupling in control and mutant human fibroblasts, the coupling conductance between cells were measured by double whole cell patch-clamp analysis (**Fig. 2.3B**). Electrical conductance results confirmed that both the D3N and V216L mutants reduced the overall level of gap junction coupling compared to their control counterparts.

2.3.4 Wound healing is delayed in mice expressing mutant Cx43

Since fibroblasts play a crucial role in wound healing (Greenhalgh, 2005; Kretz et al., 2004) and ODDD-linked Cx43 mutants reduced GJIC in dermal fibroblasts, we investigated whether this decrease in GJIC could alter wound healing. To determine if wound healing is altered in an *in vivo* environment, skin punch biopsies were performed on wild-type (WT) and G60S (*Gja1^{Jrt/+}*) mutant Cx43 mice (**Fig. 2.4**) and the wound area

Figure 2.2 A large proportion of mutant Cx43 co-localizes with the Golgi apparatus marker GM130

Fibroblasts denoted as D3, D3N, V216 and V216L were double-labeled for Cx43 (red) and the resident Golgi apparatus protein GM130 (green). Overlaid images reveal that Cx43 was partially localized to the Golgi apparatus especially in cells expressing the V216L mutant. Bar=10 μ m.

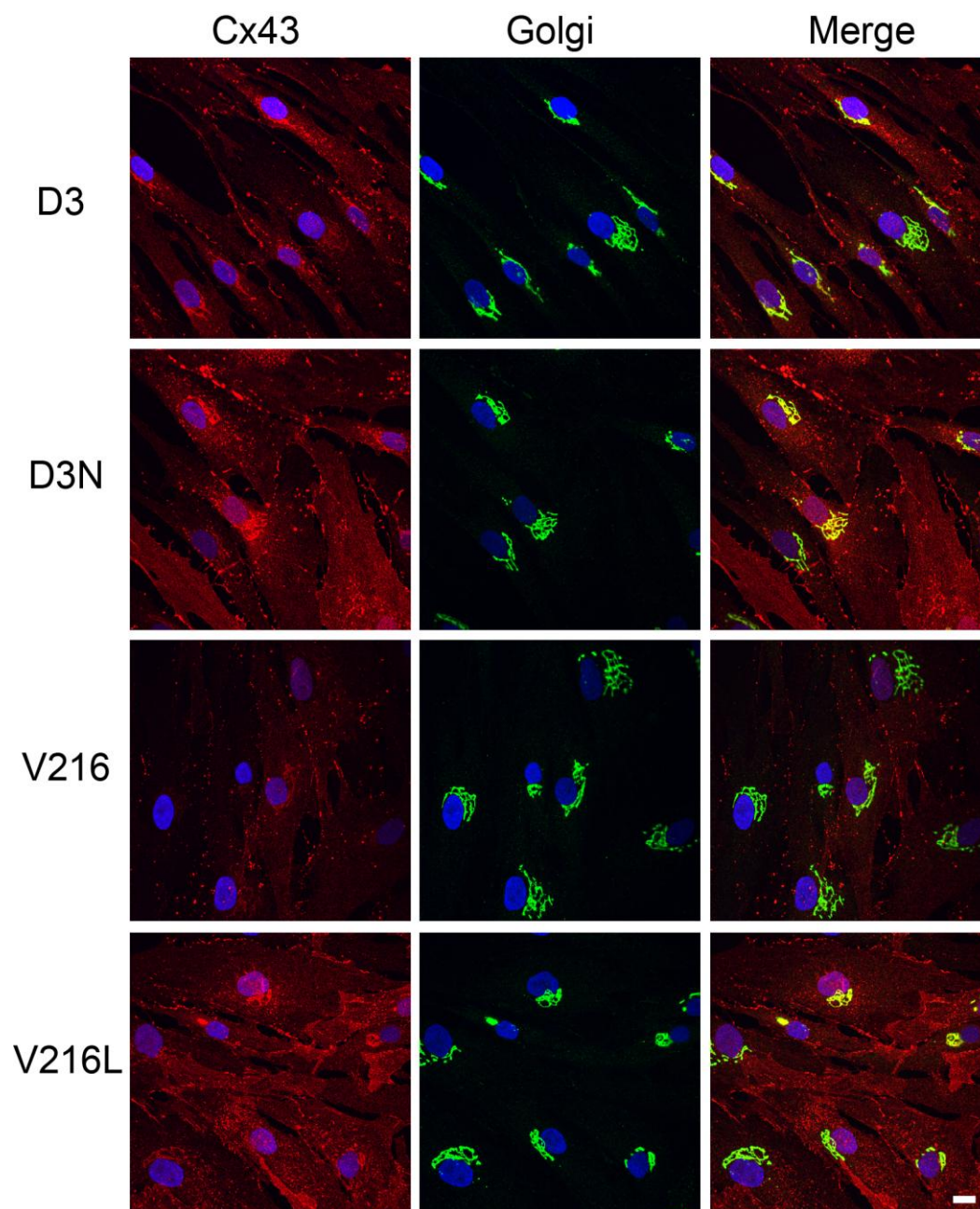


Figure 2.3 Reduced gap junctional intracellular communication in D3N and V216L fibroblasts

(A) D3, D3N, V216 and V216L fibroblasts were preloaded with calcein-AM and DiI, and seeded onto a monolayer of phenotypically-matched fibroblasts for 3 h. Calcein spread from DiI labeled cells was scored as incidences of functional dye transfer. (B) Pairs of D3, D3N, V216 and V216L fibroblasts were double whole cell patch-clamped and assessed for gap junction coupling conductance. Reduced gap junction conductance was found in D3N and V216L fibroblasts when compared to the control D3 and V216 fibroblast counterparts. * $p < 0.05$, ** $p < 0.01$.

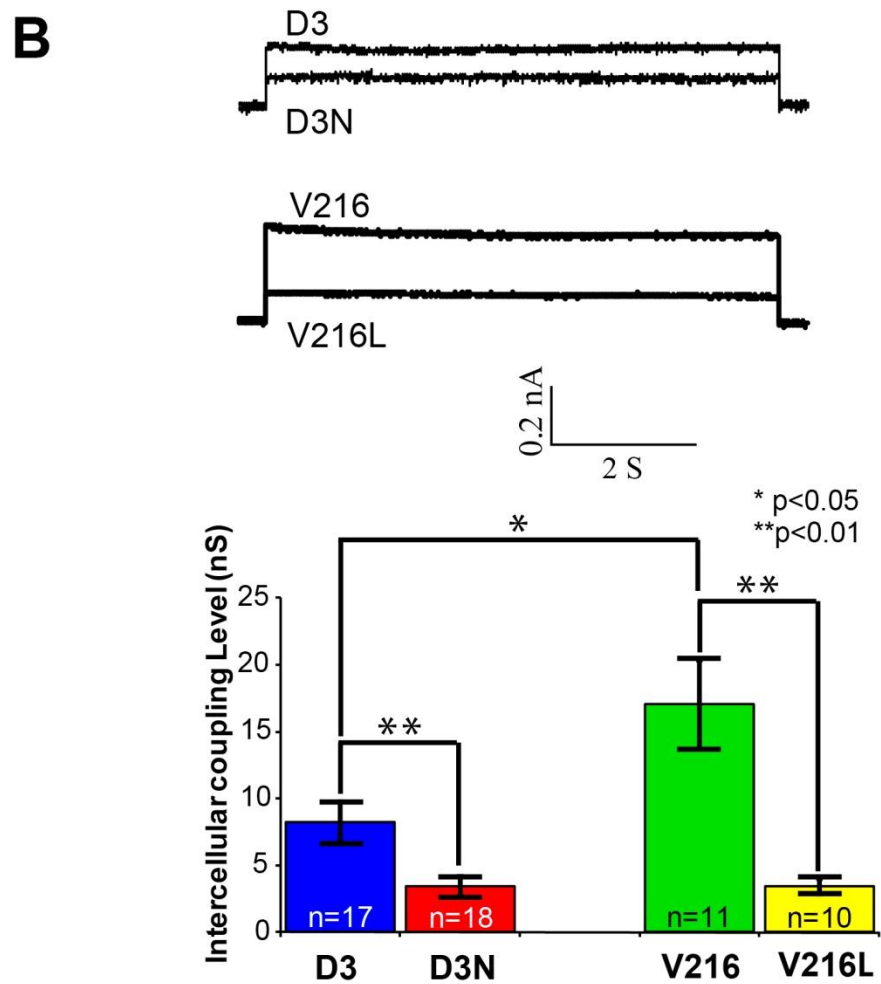
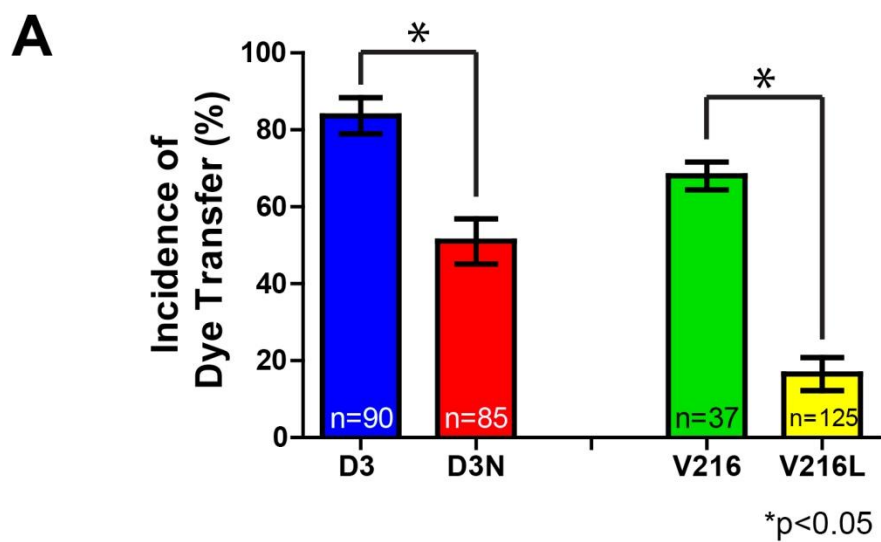
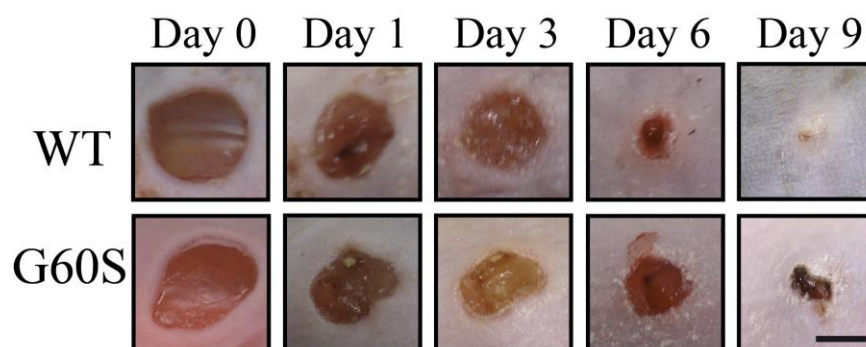
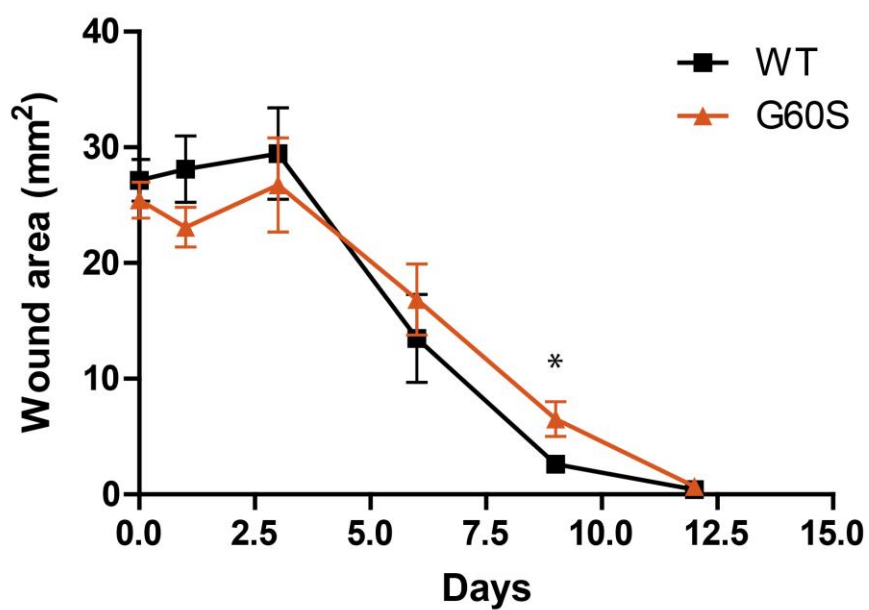


Figure 2.4 G60S mice wounds heal slower than WT mice wounds

Dermal punch biopsies performed on the backs of WT and G60S mice revealed a delay in wound closure in G60S mutant mice. After nine days of healing, the wounds in the G60S mice were significantly larger than the wounds in the WT mice. * $p < 0.05$. Bar = 2.5 mm.



Wound Closure



N=11

was quantified for twelve days after the punch biopsies were performed. One to six days after the punch biopsies were performed; there was no significant difference in the size of the wound between WT and G60S mice. After nine days however, G60S mice wounds were significantly larger than those seen in the WT mice.

Since myofibroblast contraction during the later stages of wound healing is vital to decrease the wound size, we sought to determine whether fibroblasts were responsible for the delay in wound healing observed in the mutant G60S mice. To achieve this, fibroblasts were assessed for their ability to proliferate, migrate and differentiate into myofibroblasts.

2.3.5 ODDD mutants reduce dermal fibroblast migration and proliferation

To assess whether dermal fibroblasts expressing mutant Cx43 can impact the proliferation and migration dependent events which occur during wound healing, explants derived from the WT and G60S punch biopsies were cultured on either plastic, fibronectin, laminin 332 or collagen type I (**Fig. 2.5**). After five days in culture, a fibroblast population could easily be identified surrounding the explants. Quantification of the fibroblast population that migrated from explants derived from WT and mutant mice revealed that mutant harboring fibroblasts migrated less well on fibronectin (**Fig. 2.5B**) and on collagen type I (**Fig. 2.5C**).

To determine if the migration of human dermal fibroblasts was affected by the expression of mutant Cx43, time lapse imaging of scrape-wounded control and mutant fibroblasts was evaluated. When assessed over 48 hours, we observed that migration was delayed in the ODDD mutant containing fibroblast cultures (**Fig. 2.6**). Surprisingly, while migration was analyzed under serum-free conditions, proliferative events were observed after 24 hours as evidenced by the presence of circular shaped cells. To quantify if the proliferation was different in fibroblasts expressing Cx43 mutants, cell counts were performed on human fibroblasts derived from ODDD patients and their familial matched

Figure 2.5 Fibroblasts from mutant mice exhibited reduced migration on fibronectin and collagen

A. Dermal punch biopsies obtained from the backs of WT and G60S mice were plated in uncoated, fibronectin, laminin 332, or collagen-coated culture wells. After punch biopsies were cultured for five days, cellular emigration away from the explants could be observed (blue arrow). In these images the cells appear bright due to the nature of image acquisition. B., C. The area of cellular emigration was quantified around the entire explant and the total cellular emigration area was quantified. There was a significant decrease in the area that fibroblasts derived from the G60S mice migrated out of the skin explants when cultured on fibronectin (B) and collagen type I (C). Bar = 500 μm .

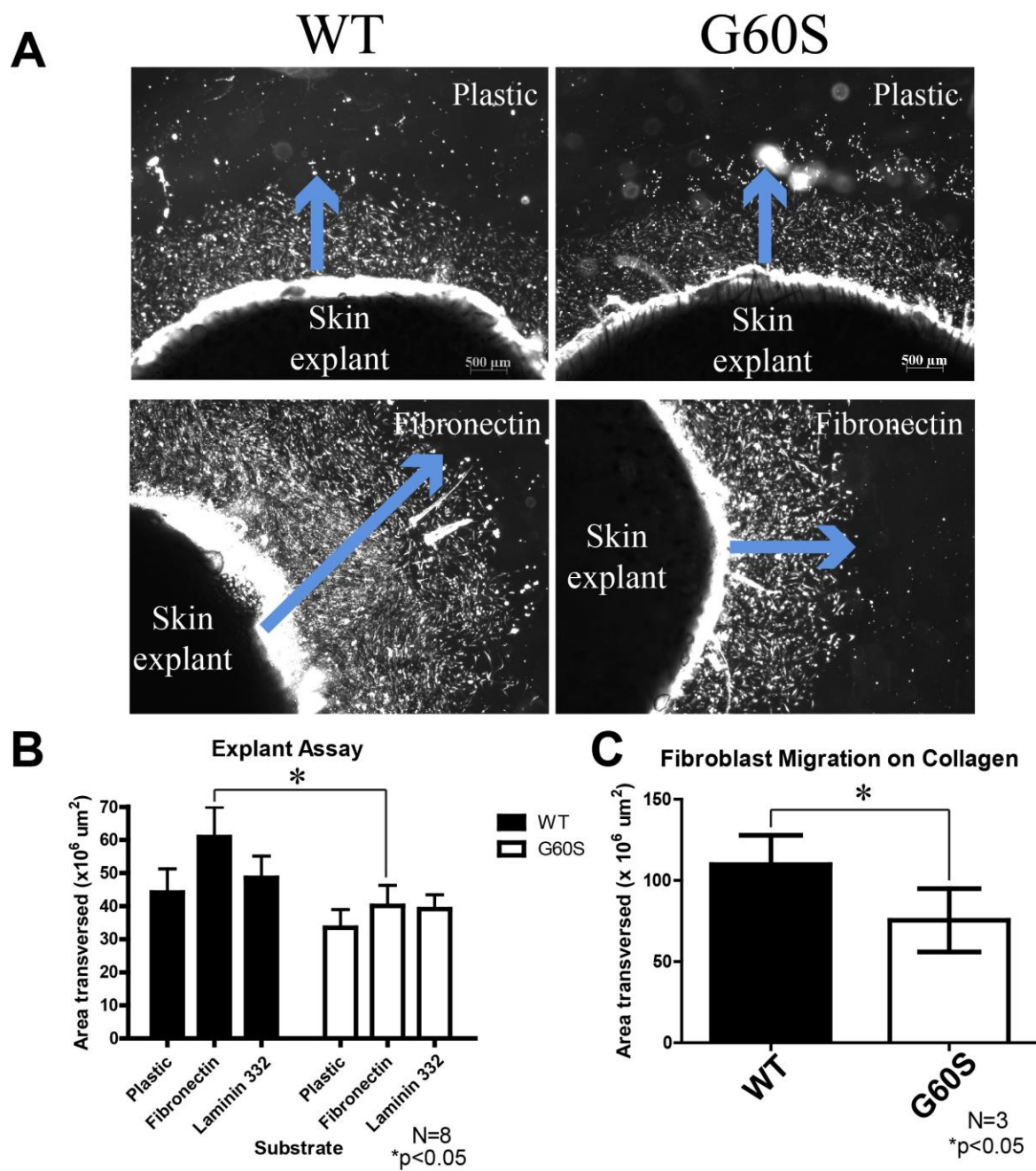
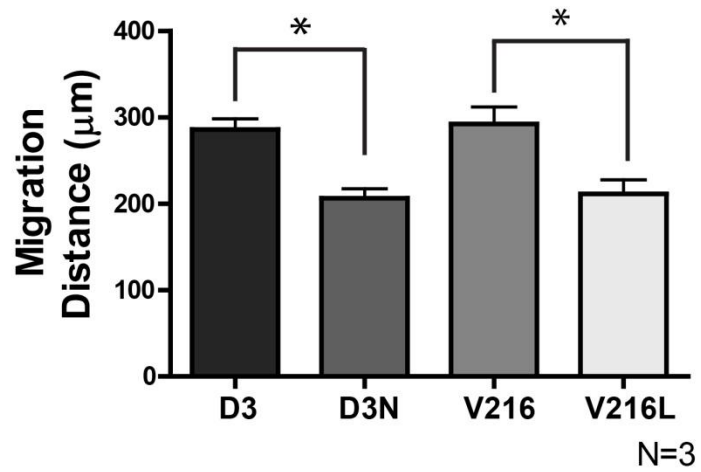
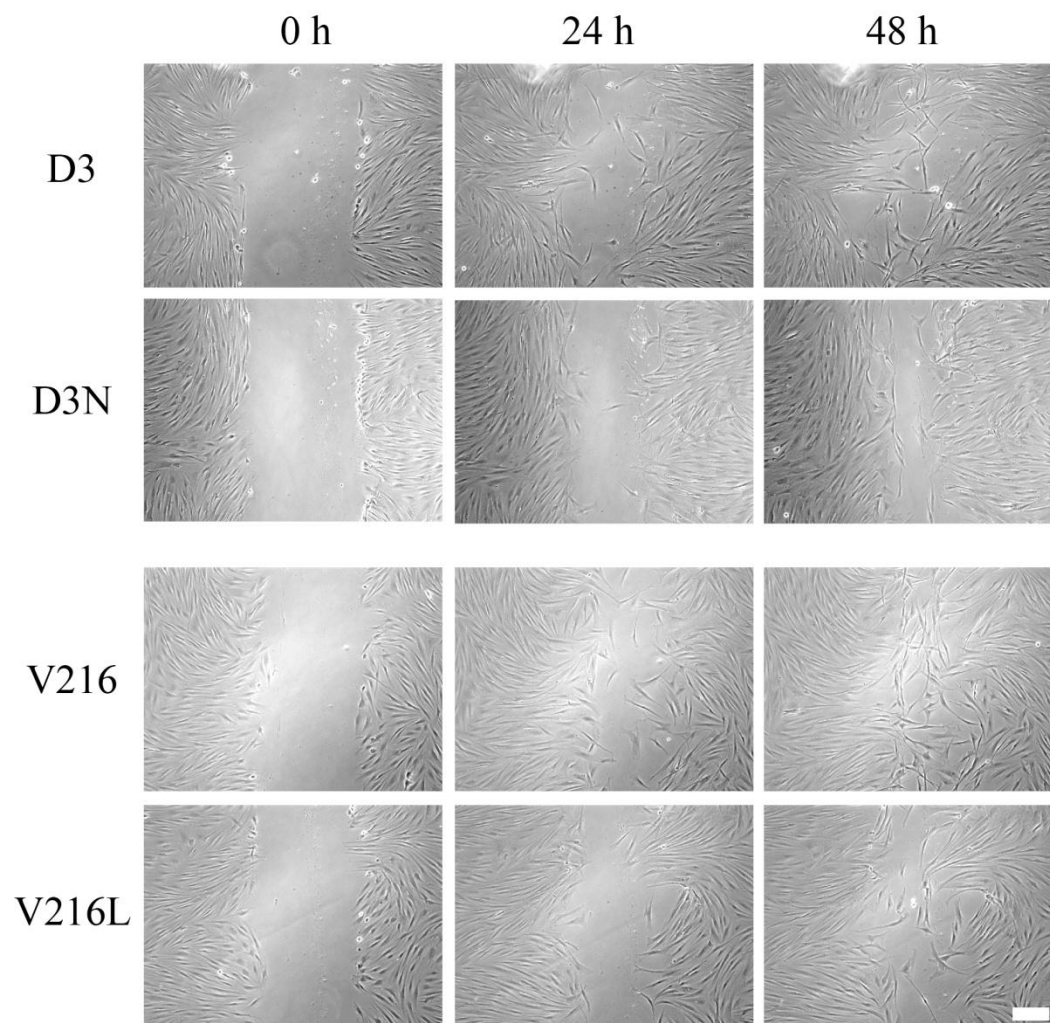


Figure 2.6 ODDD-linked human fibroblasts exhibit impaired migration

Time-lapse imaging of a scrape wound assay was performed using human fibroblasts from ODDD patients (D3N, V216L) and their matched control fibroblasts (D3, V216). After 24 hours it was evident that ODDD-linked fibroblasts migrated into the wound area slower than control fibroblasts. * $p < 0.05$ Bar = 100 μm .



controls (**Fig. 2.7**). All cell lines were seeded at equal densities and cell counts were performed on fibroblasts grown for two, four, and six days. Both mutant fibroblasts were found to proliferate slower than their control counterparts. These results indicate that the expression of mutant Cx43 decreases the proliferative ability of dermal fibroblasts and may contribute to delays in wound healing. We recruited two families diagnosed with ODDD; one family has multiple members with ODDD while the second family had one isolated case. All affected individuals had the typical craniofacial appearance and limb involvement characteristic of ODDD.

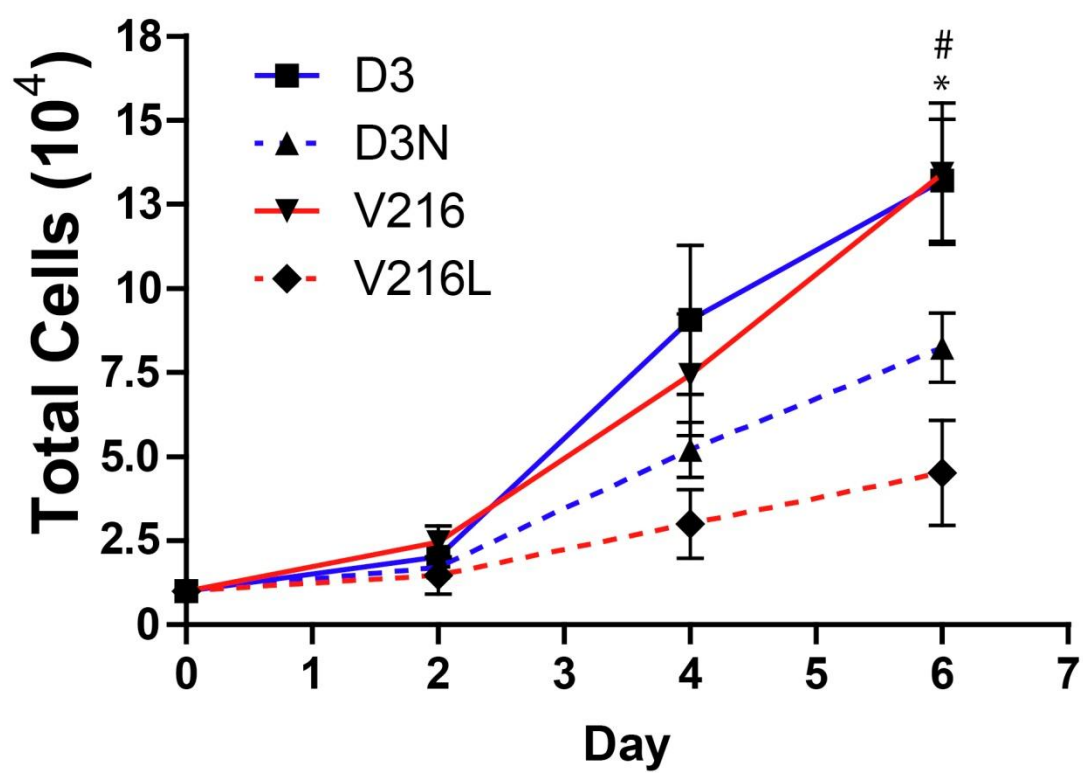
2.3.6 ODDD mutants hinder the ability of dermal fibroblasts to differentiate into myofibroblasts

Wound closure was found to be delayed in the G60S mice nine days after a punch biopsy was performed. At this stage in wound healing, fibroblasts are exposed to TGF β ₁ which facilitates the differentiation of fibroblasts into myofibroblasts. Myofibroblasts in turn express alpha smooth muscle actin which plays a role in contraction of the wounded area (Singer and Clark, 1999). To further investigate the mechanism(s) by which wound healing may be compromised, fibroblasts derived from ODDD patients, as well as their familial matched controls, were treated with TGF β ₁ for four days and Western blots were performed on untreated as well as TGF β ₁-treated fibroblasts to assess the expression of Cx43 and alpha smooth muscle actin. TGF β ₁ treatment elevated the levels of the P2 phosphorylated species of Cx43 (P2) in D3 and V216 fibroblasts. However, in the mutant Cx43 expressing fibroblasts (D3N and V216L), this increase in the P2 species of Cx43 was not observed upon TGF β ₁ treatment (**Fig. 2.8**). To determine if this change in phosphorylation could impact the ability of both familial matched control and ODDD patient derived fibroblasts to differentiate into myofibroblasts, Western blots for alpha smooth muscle actin were performed with and without TGF β ₁ treatment (**Fig. 2.9**). Control fibroblasts (D3 and V216) expressed high levels of alpha smooth muscle actin after TGF β ₁ treatment while ODDD patient-derived fibroblasts exhibited a smaller increase in the expression of alpha smooth muscle actin. In addition, we found that due to the presence of TGF β ₁ in serum (without exogenous administration of TGF β ₁), increases

Figure 2.7 ODDD-linked human fibroblasts exhibited reduced proliferation

D3, D3N, V216 and V216L fibroblasts were plated and counted over a period of 6 days. At day 6, there were significantly fewer cells in the culture wells containing V216L and D3N fibroblasts when compared to V216 and D3 fibroblasts. # D3 vs. D3N $p < 0.05$, * V216 vs. V216L $p < 0.05$.

Cell Count (Proliferation)



D3 vs. D3N $p < 0.05$

* V216 vs. V216L $p < 0.05$

N=6

Figure 2.8 Aberrant Cx43 phosphorylation in mutant expressing fibroblasts

Cx43 levels (green) in untreated and TGF β ₁ treated D3, D3N, V216 and V216L fibroblasts as assessed by Western blot. Three bands of Cx43 are resolved and these bands are noted as different phosphorylation states. The lowest band is notated as P₀, the middle band as P₁ and the highest band as P₂. Four days after D3, D3N, V216, and V216L fibroblasts were treated with TGF β ₁, the levels of the P₂ Cx43 phosphorylated species as compared to total Cx43 levels was significantly increased in D3 and V216 fibroblasts but this increase was not observed in D3N and V216L fibroblasts. GAPDH was used as a loading control (red). *p<0.05.

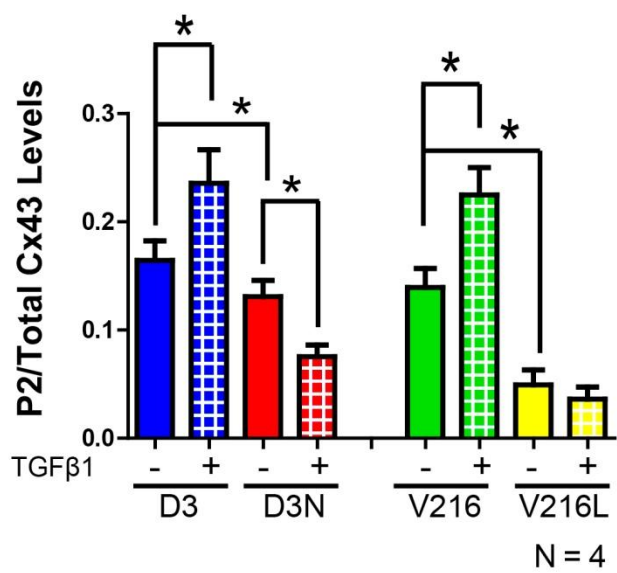
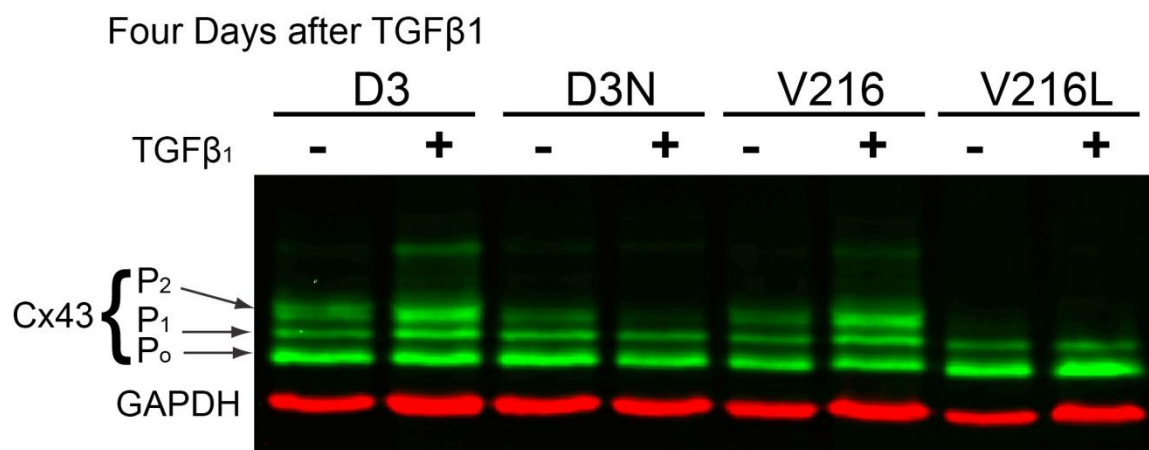
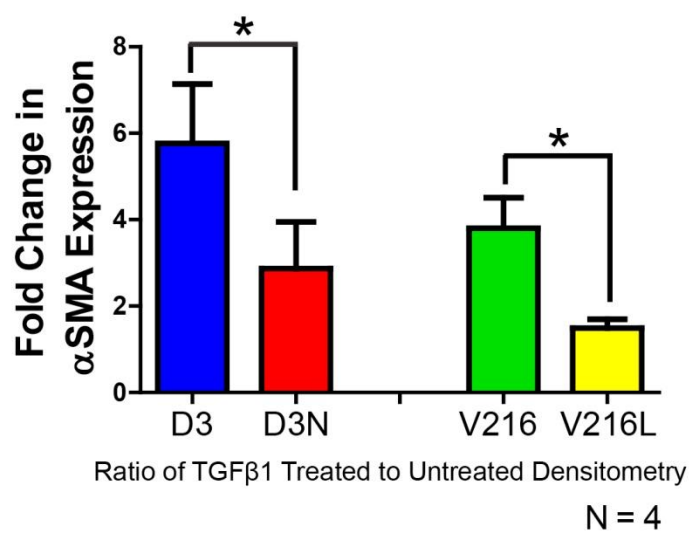
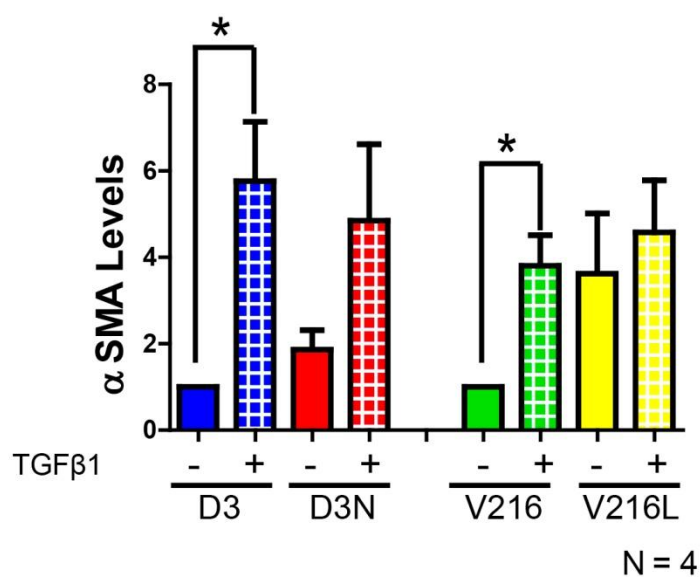
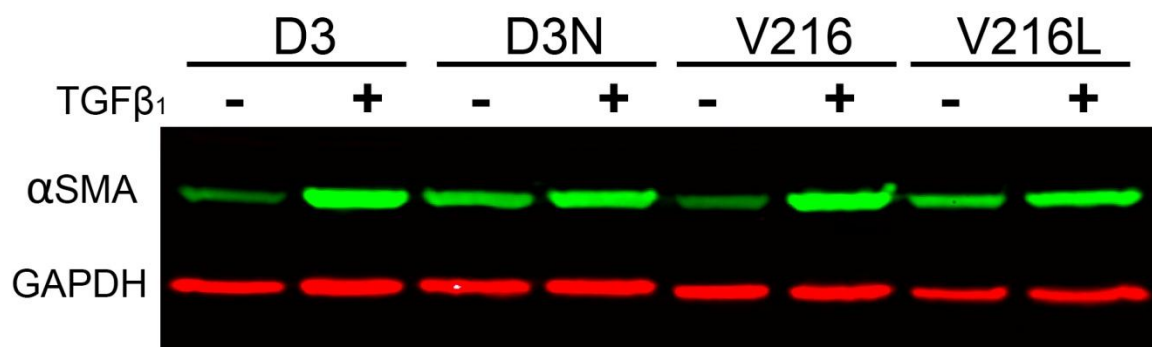


Figure 2.9 Reduced smooth muscle actin expression in mutant expressing fibroblasts

The expression of alpha smooth muscle actin was evaluated by Western blot in D3, D3N, V216 and V216L fibroblasts exposed to $TGF\beta_1$ for four days. The expression of alpha smooth muscle actin was significantly increased in D3 and V216 fibroblasts after $TGF\beta_1$ treatment. The fold change in alpha smooth muscle actin expression after $TGF\beta_1$ treatment was also significantly larger in the D3 and V216 fibroblasts when compared to the D3N and V216L fibroblasts. * $p < 0.05$.



in the levels of alpha smooth muscle actin were observed from mutant Cx43 expressing fibroblasts with each additional passage when compared to control fibroblasts. However, the fold-change in alpha smooth muscle actin expression after exogenous administration of TGF β ₁ between control and ODDD fibroblasts cells was significantly different. This result demonstrates that the expression of mutant Cx43 affects the differentiation of fibroblasts into myofibroblasts. Collectively, these studies would suggest that ODDD-patients may have compromised wound healing as mutant Cx43 expressing fibroblasts display defects in their ability to proliferate, migrate, and express alpha smooth muscle actin.

2.4 Discussion

2.4.1 Understanding ODDD

Since the discovery that ODDD was specifically linked to mutations in the *GJAI* gene encoding Cx43 (Paznekas et al., 2003), there has been an expansion of interest in understanding how Cx43 mutants lead to disease. Given the ubiquitous expression of Cx43 in the human body including vital organs, it was somewhat puzzling that patients harboring Cx43 mutants did not have even more disease burden. One possibility was that the wide array of missense mutations found within the *GJAI* gene only mildly compromises the functional status of Cx43 in forming intercellular channels. However, this explanation is not likely correct as all the ODDD-linked mutants examined to date have moderate to severe deficiencies in forming intercellular gap junction channels when expressed in GJIC-deficient cells (Dorsett-Martin, 2004; McLachlan et al., 2005). However, these *in vitro* studies do not ideally mimic the human condition due primarily to the difficulty in expressing Cx43 mutants and the wild-type Cx43 counterparts at the 1:1 ratio expected to be found in ODDD patients with autosomal dominant *GJAI* gene mutations. With the generation of mouse models of ODDD this genetic limitation was overcome and three ODDD-linked Cx43 mutants were also found to be dominant to

endogenous Cx43 resulting in a reduction in overall Cx43 function in many tissues (Dobrowolski et al., 2008; Flenniken et al., 2005; Kalcheva et al., 2007). Even in these mutant mouse studies, there was still a requirement to extrapolate the findings to the human disease condition. In the present study we report on the first efforts to design and study human models of ODDD with the anticipation that findings in these models will extend our understanding of ODDD as a disease and to further determine the functional role of Cx43.

2.4.2 Clinical presentation of ODDD in two patients with distinct GJA1 gene mutations

Clinically, ODDD is a complex disease as no two patients appear to have identical disease burdens. While nearly all patients have craniofacial bone deformities, fusion of digits, and thin enamel, the plethora of symptoms beyond these are highly diverse and linked to defects in any number of organs that include the heart, skin, as well as a wide array of conditions that are likely entrenched in neurogenic defects (Paznekas et al., 2009). In the present study we obtained clinical histories and dermal fibroblasts from two patients with ODDD. Importantly, we were also fortunate to have obtained dermal fibroblasts from the parent (mother) / child (daughter) of these patients which allows for all analytical tests to be matched to individuals sharing similar genetic profiles thus eliminating variance often seen in unrelated controls. Furthermore, in this study we control for any changes in Cx43 status through multiple cell passages by always using fibroblasts from control and disease conditions at the same cell passage. Collectively, we believe we established the best possible scenario to assess Cx43 and gap junctions in control and mutant-expressing human dermal fibroblasts. Moreover, we complement our approach by including *in vivo* wound repair studies using the G60S (*Gja1*^{Jrt/+}) mouse model of ODDD.

2.4.3 Cx43 and GJIC status in control and mutant fibroblasts

Previous *in vitro* studies using reference cell lines strongly suggest that all over-expressed Cx43 mutants dramatically reduce GJIC and act as dominant-negatives on co-expressed

Cx43 (Churko et al., 2010; McLachlan et al., 2005). In the case where the V216L mutant was expressed in reference cells that lack connexins, the V216L expressing cells fail to form functional intercellular channels (McLachlan et al., 2005). However, whether these or any other ODDD-linked mutants in human cells naturally harboring the mutants can affect GJIC had not been tested. In our studies we found that human fibroblasts harboring the D3N or V216L mutant have reduced GJIC. Interestingly, the V216L mutant appears to be twice as potent at reducing GJIC compared to the D3N mutant suggesting that the impact of the autosomal dominant mutation on the coupling status in ODDD patient may be dependent on the site of the mutation. This finding is in keeping with our previous study where the G21R mutant was found to be twice as potent at reducing GJIC as a G138R mutant when ectopically expressed and examined in reference cell systems (Gong et al., 2007). Since both the D3N and G21R mutations are found on the N-terminus of Cx43, these results may suggest that mutants within this domain are more potent than mutations found in at least some other regions of Cx43. It is notable that the N-terminal domain of some connexins has been reported to be involved in transjunctional voltage gating (Purnick et al., 2000), oligomerization of connexins into connexons (Lagree et al., 2003), and even in plugging the gap junction pore (Maeda et al., 2009; Oshima et al., 2007) highlighting the functional importance of this domain.

In vitro studies using ectopically expressed Cx43 mutants have suggested that there are two clear trafficking phenotypes where Cx43 mutants are either trapped within a secretory compartment such as the endoplasmic reticulum or Golgi apparatus (e.g. fs230, fs260, G60S mutants) or where the mutant traffics to the cell surface and assembles into non-functional gap junction plaques (e.g., G21R, G138R) (Churko et al., 2010; Gong et al., 2006). While the D3N and V216L mutants can form gap junction plaques, a population of the V216L mutant, in particular, localized to the Golgi apparatus. Impaired trafficking of the V216L mutant may also act to inhibit the delivery of wild type Cx43 to the cell surface and partly explain how this particular mutant contributes to a disease phenotype.

2.4.4 Cellular consequences of reduced Cx43 function in dermal fibroblasts

Given that patient-derived dermal fibroblasts exhibit a significant reduction in GJIC and that wound healing is delayed in G60S mutant mice, we sought to determine if the function of dermal fibroblasts is compromised (Greenhalgh, 2005; Kretz et al., 2004). Interestingly, it has been reported that transient knockdown of Cx43 in the skin by siRNAs or antisense leads to enhanced wound healing (Mori et al., 2006; Qiu et al., 2003) but chronic down regulation of Cx43 had not previously been tested. Furthermore, the reduction of total Cx43 in a knockdown study is mechanistically distinct from the expression of a functionally dominant Cx43 mutant as exhibited in an ODDD patient as a plethora of Cx43 binding partners may remain engaged (Toth et al., 2010). Since Cx43 may play distinct roles at the various stages of wound repair and within cell types (e.g., lymphatic endothelial cells, keratinocytes, fibroblasts) involved in wound healing, temporal knockdown of Cx43 may be beneficial during the early stages of wound healing while potentially detrimental during a later stage. For instance, acute down regulation of Cx43 at the wound edge over a 24-48 h period leads to increased keratinocyte and fibroblast migration (Mori et al., 2006; Wright et al., 2009). In addition, keratinocytes were shown to play a significant role in accelerating the healing of incisional tail wounds in mice with decreased levels of Cx43 levels (Kretz et al., 2003). Furthermore, transient antisense-induced knockdown of Cx43 leads to improved wound healing in the skin (Qiu et al., 2003) and cornea (Nakano et al., 2008) but functional recovery of Cx43 is thought to be necessary for the final stages of wound healing. Conversely, chronic expression of truncated Cx43 has been shown to be extremely detrimental as these mice die shortly after birth due to epidermal barrier defects (Maass et al., 2004). In our mouse studies, chronic reduction in overall functional Cx43 levels delayed wound healing and suggests that some ODDD patients may have a subclinical delay in overall wound healing.

In the present study we demonstrated that ODDD fibroblasts are deficient in their ability to proliferate, migrate and differentiate when compared to their respective familial matched control fibroblasts. Collectively, these cell characteristics are intimately involved in regulating the efficacy of wound repair. Interestingly, the defect in G60S

mouse fibroblast migration was only observed to occur when skin explants were cultured on fibronectin and collagen type I. It will be interesting to determine how Cx43 mutants impact the expression and localization of adhesion proteins involved in the attachment of fibroblasts to these substrates.

We have previously reported that the over-expression of several Cx43 mutants in reference cell lines reduces the phosphorylation state of total Cx43 (Churko et al., 2010; McLachlan et al., 2005). Importantly, the P₂ phosphorylation state of Cx43 is correlated with the presence of functional gap junctions (Solan and Lampe, 2005). In the present study, both the D3N and V216L mutants significantly decreased the levels of the P₂ phosphorylated species. Thus, it appears that both mutants are acting to partially inhibit the complete assembly of gap junction plaques which manifests as an overall reduction in GJIC as we have shown. Interestingly, in control fibroblasts, the P₂ species of Cx43 increased after TGFβ₁ treatment, indicative of a greater number of fully assembled gap junctions, but this increase was not observed in fibroblasts harboring ODDD-linked mutants. TGFβ₁ is critical in wound repair and acts to stimulate alpha smooth muscle actin and the formation of myofibroblasts (Brenmoehl et al., 2009; Greenhalgh, 2005). Quantification of alpha smooth muscle actin revealed that Cx43 mutant expressing fibroblasts are deficient in regulating the differentiation of fibroblasts into myofibroblasts. Mechanistically, the delay in wound repair observed in our mutant mice is likely linked, at least in part, to a deficiency in the ability of fibroblasts to differentiate into myofibroblasts.

In summary, this is the first study documenting and employing a human model of ODDD. Here we isolated and characterized human dermal fibroblasts from two ODDD families which included both affected and unaffected family members. We also employed a punch biopsy assay to demonstrate a delay in wound course in our mouse model for ODDD. Since fibroblast contraction plays a more important role in rodent wound healing (Dorsett-Martin, 2004; Greenhalgh, 2005) and given the limited number of patients studied and the lack of correlative data, we cannot generalize our results to all ODDD patients. However, since our V216L and D3N expressing primary fibroblast do exhibit impaired proliferation, migration, and differentiation, it is quite likely that this condition

remains present but unreported or subclinical and would only be revealed in patients that have severe skin wounds where dermal fibroblasts play a more active role.

2.5 References

- Brenmoehl, J., S.N. Miller, C. Hofmann, D. Vogl, W. Falk, J. Scholmerich, and G. Rogler. 2009. Transforming growth factor-beta 1 induces intestinal myofibroblast differentiation and modulates their migration. *World J Gastroenterol.* 15:1431-1442.
- Churko, J.M., S. Langlois, X. Pan, Q. Shao, and D.W. Laird. 2010. The potency of the fs260 connexin43 mutant to impair keratinocyte differentiation is distinct from other disease-linked connexin43 mutants. *Biochem J.* 429:473-483.
- Dobrowolski, R., P. Sasse, J.W. Schrickel, M. Watkins, J.S. Kim, M. Rackauskas, C. Troatz, A. Ghanem, K. Tiemann, J. Degen, F.F. Bukauskas, R. Civitelli, T. Lewalter, B.K. Fleischmann, and K. Willecke. 2008. The conditional connexin43G138R mouse mutant represents a new model of hereditary oculodentodigital dysplasia in humans. *Hum Mol Genet.* 17:539-554.
- Dorsett-Martin, W.A. 2004. Rat models of skin wound healing: a review. *Wound Repair Regen.* 12:591-599.
- Flenniken, A.M., L.R. Osborne, N. Anderson, N. Ciliberti, C. Fleming, J.E. Gittens, X.Q. Gong, L.B. Kelsey, C. Lounsbury, L. Moreno, B.J. Nieman, K. Peterson, D. Qu, W. Roscoe, Q. Shao, D. Tong, G.I. Veitch, I. Voronina, I. Vukobradovic, G.A. Wood, Y. Zhu, R.A. Zirngibl, J.E. Aubin, D. Bai, B.G. Bruneau, M. Grynepas, J.E. Henderson, R.M. Henkelman, C. McKerlie, J.G. Sled, W.L. Stanford, D.W. Laird, G.M. Kidder, S.L. Adamson, and J. Rossant. 2005. A Gja1 missense mutation in a mouse model of oculodentodigital dysplasia. *Development.* 132:4375-4386.
- Goldberg, G.S., J.F. Bechberger, and C.C. Naus. 1995. A pre-loading method of evaluating gap junctional communication by fluorescent dye transfer. *Biotechniques.* 18:490-497.
- Gong, X.Q., Q. Shao, S. Langlois, D. Bai, and D.W. Laird. 2007. Differential potency of dominant negative connexin43 mutants in oculodentodigital dysplasia. *J.Biol.Chem.* 282:19190-19202.
- Gong, X.Q., Q. Shao, C.S. Lounsbury, D. Bai, and D.W. Laird. 2006. Functional characterization of a GJA1 frameshift mutation causing oculodentodigital dysplasia and palmoplantar keratoderma. *J Biol Chem.* 281:31801-31811.
- Greenhalgh, D.G. 2005. Models of wound healing. *J Burn Care Rehabil.* 26:293-305.
- Kalcheva, N., J. Qu, N. Sandeep, L. Garcia, J. Zhang, Z. Wang, P.D. Lampe, S.O. Suadicani, D.C. Spray, and G.I. Fishman. 2007. Gap junction remodeling and cardiac arrhythmogenesis in a murine model of oculodentodigital dysplasia. *Proc Natl Acad Sci U S A.* 104:20512-20516.

- Kizana, E., C.Y. Chang, E. Cingolani, G.A. Ramirez-Correa, R.B. Sekar, M.R. Abraham, S.L. Ginn, L. Tung, I.E. Alexander, and E. Marban. 2007. Gene transfer of connexin43 mutants attenuates coupling in cardiomyocytes: novel basis for modulation of cardiac conduction by gene therapy. *Circ Res.* 100:1597-1604.
- Kretz, M., C. Euwens, S. Hombach, D. Eckardt, B. Teubner, O. Traub, K. Willecke, and T. Ott. 2003. Altered connexin expression and wound healing in the epidermis of connexin-deficient mice. *J Cell Sci.* 116:3443-3452.
- Kretz, M., K. Maass, and K. Willecke. 2004. Expression and function of connexins in the epidermis, analyzed with transgenic mouse mutants. *Eur J Cell Biol.* 83:647-654.
- Lagree, V., K. Brunschwig, P. Lopez, N.B. Gilula, G. Richard, and M.M. Falk. 2003. Specific amino-acid residues in the N-terminus and TM3 implicated in channel function and oligomerization compatibility of connexin43. *J Cell Sci.* 116:3189-3201.
- Maass, K., A. Ghanem, J.S. Kim, M. Saathoff, S. Urschel, G. Kirfel, R. Grummer, M. Kretz, T. Lewalter, K. Tiemann, E. Winterhager, V. Herzog, and K. Willecke. 2004. Defective epidermal barrier in neonatal mice lacking the C-terminal region of connexin43. *Mol.Biol.Cell.* 15:4597-4608.
- Maeda, S., S. Nakagawa, M. Suga, E. Yamashita, A. Oshima, Y. Fujiyoshi, and T. Tsukihara. 2009. Structure of the connexin 26 gap junction channel at 3.5 Å resolution. *Nature.* 458:597-602.
- McLachlan, E., J.L. Manias, X.Q. Gong, C.S. Lounsbury, Q. Shao, S.M. Bernier, D. Bai, and D.W. Laird. 2005. Functional characterization of oculodentodigital dysplasia-associated Cx43 mutants. *Cell Commun Adhes.* 12:279-292.
- Mori, R., K.T. Power, C.M. Wang, P. Martin, and D.L. Becker. 2006. Acute downregulation of connexin43 at wound sites leads to a reduced inflammatory response, enhanced keratinocyte proliferation and wound fibroblast migration. *J Cell Sci.* 119:5193-5203.
- Nakano, Y., M. Oyamada, P. Dai, T. Nakagami, S. Kinoshita, and T. Takamatsu. 2008. Connexin43 knockdown accelerates wound healing but inhibits mesenchymal transition after corneal endothelial injury in vivo. *Invest Ophthalmol Vis Sci.* 49:93-104.
- Oshima, A., K. Tani, Y. Hiroaki, Y. Fujiyoshi, and G.E. Sosinsky. 2007. Three-dimensional structure of a human connexin26 gap junction channel reveals a plug in the vestibule. *Proc Natl Acad Sci U S A.* 104:10034-10039.
- Paznekas, W.A., S.A. Boyadjiev, R.E. Shapiro, O. Daniels, B. Wollnik, C.E. Keegan, J.W. Innis, M.B. Dinulos, C. Christian, M.C. Hannibal, and E.W. Jabs. 2003. Connexin 43 (GJA1) mutations cause the pleiotropic phenotype of oculodentodigital dysplasia. *Am J Hum Genet.* 72:408-418.

- Paznekas, W.A., B. Karczeski, S. Vermeer, R.B. Lowry, M. Delatycki, F. Laurence, P.A. Koivisto, L. Van Maldergem, S.A. Boyadjiev, J.N. Bodurtha, and E.W. Jabs. 2009. GJA1 mutations, variants, and connexin 43 dysfunction as it relates to the oculodentodigital dysplasia phenotype. *Hum Mutat.* 30:724-733.
- Penuela, S., R. Bhalla, X.Q. Gong, K.N. Cowan, S.J. Celetti, B.J. Cowan, D. Bai, Q. Shao, and D.W. Laird. 2007. Pannexin 1 and pannexin 3 are glycoproteins that exhibit many distinct characteristics from the connexin family of gap junction proteins. *J Cell Sci.* 120:3772-3783.
- Purnick, P.E., D.C. Benjamin, V.K. Verselis, T.A. Bargiello, and T.L. Dowd. 2000. Structure of the amino terminus of a gap junction protein. *Arch Biochem Biophys.* 381:181-190.
- Qiu, C., P. Coutinho, S. Frank, S. Franke, L.Y. Law, P. Martin, C.R. Green, and D.L. Becker. 2003. Targeting connexin43 expression accelerates the rate of wound repair. *Curr.Biol.* 13:1697-1703.
- Richardson, R.J., S. Joss, S. Tomkin, M. Ahmed, E. Sheridan, and M.J. Dixon. 2006. A nonsense mutation in the first transmembrane domain of connexin 43 underlies autosomal recessive oculodentodigital syndrome. *J Med Genet.* 43:e37.
- Simek, J., J. Churko, Q. Shao, and D.W. Laird. 2009. Cx43 has distinct mobility within plasma-membrane domains, indicative of progressive formation of gap-junction plaques. *J Cell Sci.* 122:554-562.
- Solan, J.L., and P.D. Lampe. 2005. Connexin phosphorylation as a regulatory event linked to gap junction channel assembly. *Biochim Biophys Acta.* 1711:154-163.
- Solan, J.L., and P.D. Lampe. 2009. Connexin43 phosphorylation: structural changes and biological effects. *Biochem J.* 419:261-272.
- Stephens, P., E.J. Wood, and M.J. Raxworthy. 1996. Development of a multilayered in vitro model for studying events associated with wound healing. *Wound Repair Regen.* 4:393-401.
- Toth, K., Q. Shao, R. Lorentz, and D.W. Laird. 2010. Decreased levels of Cx43 gap junctions result in ameloblast dysregulation and enamel hypoplasia in Gja1Jrt/+ mice. *J Cell Physiol.* 223:601-609.
- van Steensel, M.A., L. Spruijt, d.B.I. van, R.S. Bladergroen, M. Vermeer, P.M. Steijlen, and G.M. van. 2005. A 2-bp deletion in the GJA1 gene is associated with oculo-dento-digital dysplasia with palmoplantar keratoderma. *Am.J.Med.Genet.A.* 132A:171-174.
- Vreeburg, M., E.A. de Zwart-Storm, M.I. Schouten, R.G. Nellen, D. Marcus-Soekarman, M. Devies, M. van Geel, and M.A. van Steensel. 2007. Skin changes in oculo-

dento-digital dysplasia are correlated with C-terminal truncations of connexin 43. *Am J Med Genet A*. 143:360-363.

Wright, C.S., M.A. van Steensel, M.B. Hodgins, and P.E. Martin. 2009. Connexin mimetic peptides improve cell migration rates of human epidermal keratinocytes and dermal fibroblasts in vitro. *Wound Repair Regen*. 17:240-249.

Chapter 3

3 Mutant Cx43 enhances keratinocyte proliferation without impacting keratinocyte migration

Fibroblasts derived from ODDD patients were shown to be impaired in their ability to proliferate, migrate and differentiate when compared to the familial matched control fibroblasts. However, keratinocytes also play a critical role in wound healing and mutant Cx43 may also impair the ability of keratinocytes to repair cutaneous wounds. Given that primary human keratinocytes are difficult to obtain and culture, this chapter will assess the ability of primary keratinocytes derived from the G60S mouse model of ODDD to proliferate, migrate and differentiate.

A version of this chapter is in preparation:

Churko, J.M., McDonald,A., Shao, Q., Laird., D.W. Mutant Cx43 Enhances Keratinocyte Proliferation without Impacting Keratinocyte Migration.

3.1 Introduction

A gap junction channel is composed of six oligomerized connexin (Cx) subunits which dock with six connexin subunits from a neighboring cell. These channels coalesce into tightly packed arrays known as gap junctions (reviewed in Sohl and Willecke, 2004). Gap junctions regulate the intercellular passage of small metabolites from cell to cell and various Cx43 mutants have been shown to disrupt cell to cell communication (Churko et al., 2010; McLachlan et al., 2005). Mutant Cx43 expression has been specifically linked to the disease called oculodentodigital dysplasia (ODDD) (Paznekas et al., 2003) and patients with ODDD commonly develop fusion of the digits and malformations of the bones, eyes and teeth (Paznekas et al., 2009). To study how mutant Cx43 leads to this disease, three mouse models have been engineered which also develop malformations similar to those seen in ODDD patients (Dobrowolski et al., 2008; Flenniken et al., 2005; Kalcheva et al., 2007). Specifically, we have used the ODDD mouse model expressing a G60S mutant Cx43 to study how mutant Cx43 impacts the development and function of the eyes (Tsui et al., 2011), teeth (Toth et al., 2010), and heart (Manias et al., 2008). However, mutant Cx43 may also disrupt skin homeostasis and the regeneration of the epidermis since Cx43 has previously been shown to be highly expressed during epidermal development and in the steady-state adult epidermis (Goliger and Paul, 1994).

During rodent epidermal development, Cx43 is expressed at E12-14 in the outer periderm and inner basal layer (Risek et al., 1992). At E17-E20, Cx43 expression can be seen in the stratum basale as well as the stratum spinosum layers but not in the stratum granulosum (Risek et al., 1992). In comparison to the mouse epidermis however, the human epidermis expresses little Cx43 within the stratum basale and stratum granulosum, but high levels of Cx43 were observed within the stratum spinosum (Salomon et al., 1994). In addition, Cx43 has also been shown to be regulated during epidermal wound healing. Twenty-four hours after injury, Cx43 expression is downregulated at the wounded edge (Brandner et al., 2004; Goliger and Paul, 1995; Lampe et al., 1998) and the S368 phosphorylated species of Cx43 is specifically expressed in the stratum basale (Richards et al., 2004). Two-three days after wounding occurred, Cx43 was reported to be absent at the wound border and at six days after wounding, Cx43 expression was

observed in the reformed epidermis (Brandner et al., 2004; Goliger and Paul, 1995). Since the expression of Cx43 dynamically changes during cutaneous wound healing, Cx43 expression is hypothesized to modulate the ability of keratinocytes to repair the damaged epithelium. To test this hypothesis, siRNAs and mimetic peptides against Cx43 have been used to transiently modulate wound healing. When Cx43 levels were inhibited by an antisense oligodeoxynucleotide against Cx43 (Mori et al., 2006) or when blocking the interaction between gap junction channels using a gap junction mimetic peptide, Gap27 (Pollok et al., 2010), an increase in keratinocyte proliferation occurred at the wounded edge. In addition, rodent wounds treated with Cx43 siRNAs and antisense Cx43 were reported to heal faster (Mori et al., 2006; Qiu et al., 2003).

While these studies have shown transient decreases in Cx43 expression and function can accelerate wound healing, chronic reductions in Cx43 gap junction function had not previously been studied until recently. By using the G60S ODDD mouse model we recently showed that full excision wounds performed on the backs of G60S mice healed slower than WT control littermate mice (Churko et al., 2011). In addition, fibroblasts derived from the G60S mice and from patients with ODDD were shown to display defects in fibroblast proliferation, migration, and differentiation (Churko et al., 2011). However, mouse wounds heal primarily through contraction and this delay in wound healing may not translate to a beneficial advantage in human wound healing. In addition, keratinocytes also play a significant role in wound healing and how mutant Cx43 impacts keratinocyte proliferation, migration and differentiation has not been investigated to date. To investigate if mutant Cx43 impacts keratinocyte dependent wound healing, we used primary keratinocyte cultures from mice expressing the G60S mutant and assessed the ability of these keratinocytes to proliferate, migrate and differentiate.

3.2 Materials and methods

3.2.1 Cell lines and mice

All animal experiments were approved by the Animal Use Subcommittee of the University Council on Animal Care at the University of Western Ontario. Mice expressing the mutant Cx43 were generated from an N-ethyl-N-nitrosourea mutagenesis

screen. This screen revealed a mouse with a point mutation within the *Gjal* gene encoding Cx43 and resulted in a glycine to serine substitution at amino acid position 60 (G60S). These mice were subsequently bred onto a mixed C57BL/6J and C3H/HeJ background (Flenniken et al., 2005). Adult G60S mice were distinguished from WT mice by the presence of fused digits and were genotyped for confirmation of the mutation.

Rat epidermal keratinocytes (REKs) were previously isolated and characterized by Baden and Kubilus (Baden and Kubilus, 1983). REKs were engineered to express the full length Cx43, G21R, G60S, G138R, fs230 and fs260 mutant Cx43 fused with GFP and cultured as previously described (Churko et al., 2010).

3.2.2 Wound healing assay

Mouse wounds were created as previously described with some notable differences (Churko et al., 2011). Full length incisions one inch long were created on the back of anesthetized WT and G60S mice with a scalpel blade. Either twenty-four hours, three days, or nine days after wounding, mice were euthanized with CO₂ inhalation. The wounded tissue was excised and processed for immunohistochemical analysis as described below.

3.2.3 Immunofluorescent labeling of human and mouse skin

The derivation and use of human skin biopsies was approved by the Office of Research Ethics at the University of Western Ontario and by the University of Utah Research Ethics Board. Skin biopsies were derived from a patient with ODDD (expressing a pD3N mutant Cx43) as well as a control skin biopsy from a relative not affected by ODDD (D3). Cx43 was previously genotyped from fibroblasts derived from these patients (Churko et al., 2011). To obtain mouse skin samples, mice were euthanized by CO₂ inhalation and the dorsal back surface was shaved using electric clippers. A 1 cm² piece of skin was cut from the back of WT and G60S mice and fixed in 4% formalin. Mouse and human skin biopsies were tissue processed, paraffin embedded, sectioned into 5 μm sections, and hydrated as previously described in Langlois et al (Langlois et al., 2010). Antigen retrieval was performed by simmering tissue sections in 1.8 mM citric acid and

8.2 mM of sodium citrate for 10 minutes. Tissue sections were permeabilized with 0.2% Triton X-100 in PBS for 12 minutes. A blocking solution containing 2% bovine serum albumin (BSA) and 0.2% Tween-20 in PBS was placed on the tissue section for 30 minutes. Primary antibody labeling was performed using anti-Cx43 (Cat# C6219, Sigma Aldrich, St. Louis, MO) diluted 1:500 in the blocking solution overnight at 4°C. The following day, tissue sections were washed 3X with PBS containing 0.2% Tween-20 for 5 minutes each wash. Cx43 localization was detected using Alexa Fluor 488 goat anti-rabbit IgG (Cat# A11008, Invitrogen, Carlsbad, CA) for Cx43 localization in human and mouse epidermis (Figure 1). For other immunofluorescent labeling, Alexa Fluor 555 goat anti-rabbit (Cat# A21429, Invitrogen, Carlsbad, CA) was used to detect primary Cx43 labeling at a dilution of 1:500 and CK14 was detected using Alexa Fluor 488 goat anti-mouse IgG (Cat# A11017, Invitrogen, Carlsbad, CA) at a dilution of 1:500. Secondary antibodies were incubated for 1 hour at room temperature and washed 3X (5 min each) with PBS containing 0.2% Tween-20. Nuclear staining was performed using Hoechst 33342 (Cat# 3570, Molecular Probes, Eugene, OR at a dilution of 1:1000) for 5 minutes and washed once with water for 5 minutes. Airvol was used to mount a coverslip over the tissue sections and a Zeiss LSM 510 microscope was used for imaging.

3.2.4 Primary keratinocyte culture

The back skin was dissected from postnatal day 2 littermates and rinsed in DPBS (Cat# 14190-136, Invitrogen, Carlsbad, CA) containing 5 µg/mL gentamycin (Cat# 14190-136, Invitrogen, Carlsbad, CA). The dissected skin was placed dermal side down in a well of a 6 well plate containing 2 mL of 25 µg/mL dispase (Cat# 17105-041, Invitrogen, Carlsbad, CA) diluted in Ca⁺² and Mg⁺² free HBSS (Cat# 14170-112, Invitrogen, Carlsbad, CA). The 6-well tissue culture dish was then placed on a rocker overnight at 4°C. The following morning, the epidermis was separated from the dermis with tweezers and the epidermis was placed into 2 mL trypsin (Cat# 25200-056, Invitrogen, Carlsbad, CA) for 5 min. The undigested epidermis was removed from the trypsin and 5 mL of keratinocyte serum free media (Keratinocyte-SFM) 1X (Cat# 17005-042 Invitrogen, Carlsbad, CA) and 1 mL of trypsin soybean inhibitor (Cat# 17075-029, Invitrogen, Carlsbad, CA) was added to the trypsin containing the dissociated keratinocyte

suspension. The keratinocytes were centrifuged into a pellet and resuspended into Keratinocyte-SFM. Keratinocytes were then plated on tissue culture wells precoated with collagen I (1.5 mg/ml, Cat# 354236, BD Biosciences, Bedford, MA). To induce keratinocyte differentiation, 1.4 mM calcium chloride was added to the Keratinocyte-SFM media. To verify the purity of primary keratinocyte cultures (and to visualize the expression of Cx43 in low calcium and high calcium conditions) immunocytochemistry labeling was performed. Primary keratinocytes were fixed with a mixture of 80% methanol/20% acetone for 5 min, blocked with blocking solution for 30 minutes, and labeled with anti-CK14 (Cat# MS-115-P, Neomarkers, Fremont, CA) and anti-Cx43 antibodies overnight. Secondary antibody labeling, nuclei labeling, and coverslip mounting was performed as described above.

3.2.5 Electrophysiology

The dual whole-cell patch clamp technique was applied to assess the electrical coupling level between paired wild-type and G60S keratinocytes. For conductance measurements both cells were initially held at 0 mV, and a 30 mV impulse (V_j) was injected into cell one while transjunctional current (I_j) was recorded from cell two. Then the gap junctional conductance was calculated according to Ohm's law. During the recordings, the keratinocytes were continuously perfused with a bath solution containing (mM) NaCl (135.0), KCl (5.0), HEPES (10.0), $MgCl_2$ (1), $CaCl_2$ (2), $BaCl_2$ (1), CsCl (2), Na pyruvate (2), D-glucose (5). Recording pipettes were filled with (mM) CsCl (130), EGTA (10), $CaCl_2$ (0.5), Mg-ATP (5), HEPES (10) and pipette resistance was between 2-5 m Ω . Signals were recorded using two Axopatch 200B amplifiers, low-pass filtered at 5 kHz and digitized at 10 kHz. * $P < 0.05$.

3.2.6 Proliferation Assays

Proliferation of REKs expressing either full length Cx43 (Cx43-GFP) or G60S-GFP was compared to vector control expressing REKs using a BrdU incorporation assay. REKs were seeded at a density of 5×10^4 onto coverslips in a 6 well plate. After 24 hours, fresh culture media containing 10 μ M of BrdU was placed onto the growing REKs for four

hours. After four hours, the coverslips were removed from 6 well plates and washed 2X with PBS. Each coverslip was fixed using a mixture of 80% methanol/20% acetone and washed an addition 2X with PBS. 2N HCL was then placed onto each coverslip for 20 minutes and then washed 2X with PBS. Immunofluorescent labeling was then performed using anti-BrdU antibody (G3G4, Developmental Studies Hybridoma Bank at a 1:100 dilution) overnight followed by incubation with a goat anti-mouse Alexa fluor 555 secondary antibody. Coverslips were mounted with Airvol and 5 - 10 random fields of view per N were taken using a Zeiss Meta 510 confocal microscope.

The proliferation of primary keratinocytes from wild type and mutant mice was quantified by cell counting. Primary keratinocytes were seeded at a cell density of 5×10^4 cells per well in a 12 well plate. Three, six and nine days after initial cell plating, 400 μ L of trypsin was added to the culture wells to dissociate the adherent cells. After five minutes, 10 μ L of the dissociated cells were mixed with 10 μ L of trypan blue (0.4%, Cat# T10282, Invitrogen, Carlsbad, CA) and 10 μ L of this mixed sample was injected into a chamber of the Cell Counting Chamber Slides (Cat# C10228, Invitrogen, Carlsbad, CA). Cell quantification was then performed by using the Countess Automated Cell Counter (Cat# C10227, Invitrogen, Carlsbad, CA).

3.2.7 Migration

REKs and primary keratinocytes were seeded at a cell density of 1×10^4 cells per culture well in a 12-well tissue culture dish. After two to three days in growth medium, the culture media was removed and a 1,000 μ L pipette tip was scraped down the center of the culture well. In REK cultures, REKs were washed 2X with Opti-MEM (Cat# 11058-021, Invitrogen, Carlsbad, CA) and 1 mL of Opti-MEM with or without serum was added to each culture well. In primary keratinocyte cultures, the culture wells were washed 2 x with Keratinocyte-SFM (1X) media. To prevent differentiation of the primary cultures, primary keratinocytes were imaged with 1 mL of Keratinocyte-SFM (1X) added to each culture well. Time-lapse imaging was performed using a Zeiss LSM 510 microscope equipped with Axiovision software. Time-lapse monolayer closure images were acquired

every 10 min for 11 hr in REK cultures or every 10 min for 12 hours in primary keratinocyte cultures.

3.2.8 Western blots

Western blots were performed as previously described (Penuela et al., 2007) with the use of the following primary antibodies: anti-Cx43 (Cat# C6219, Sigma Aldrich, St. Louis, MO), pan anti-cytokeratin (1:1000; Cat# ab7753 Abcam, Cambridge, MA), anti-involucrin (1:1000; Cat# PRB-140C, Covance, Princeton, NJ), anti-GAPDH (1:5000; Cat# MAB374, Millipore, Billerica, MA), anti-CK14 (1:1000; Cat# MS-115-P, Neomarkers, Fremont, CA). Primary antibodies were detected using Alexa Fluor 680 (1:5,000; Cat # A21076, Invitrogen) or IRDye 800 (1:5,000; Cat# 611-132-122; Rockland, Gilbertsville, PA) goat anti-rabbit and anti-mouse secondary antibodies in conjunction with the LiCor imaging system.

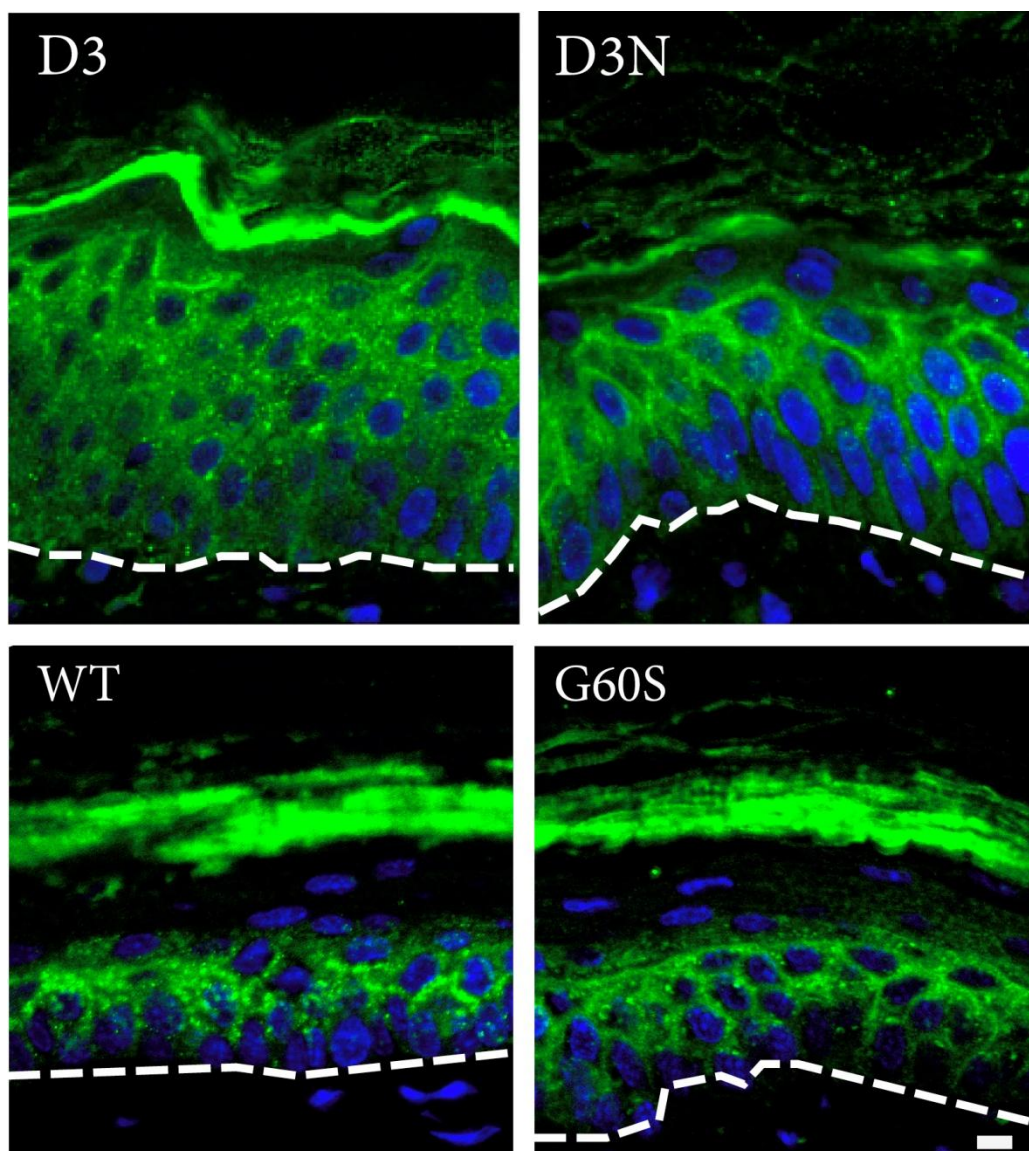
3.3 Results

3.3.1 Mutant Cx43 disrupts the overall localization pattern of Cx43 in mutant mouse and patient epidermis

Cx43 is highly expressed within both the human and mouse epidermis but the role it plays in this highly differentiated tissue is only beginning to be understood. To visualize mutant Cx43 in the epidermis, we labeled Cx43 in the epidermis from an ODDD patient expressing the pD3N mutant as well as in the mouse epidermis expressing the G60S mutant Cx43 (**Fig. 3.1**). In the epidermis from the patient expressing the D3N mutant, Cx43 was diffusely localized within the stratum spinosum and did not localize as a punctate profile indicative of gap junction plaques. A reduction in the punctate plaque localization was also observed in the epidermis from mice expressing the G60S Cx43 mutant. However in the control human epidermis (D3) and in the epidermis from WT mice, punctate Cx43 labeling could be seen within the epidermis.

Figure 3.1 Reduced Cx43 punctate localization in a human D3N patient skin biopsy and in skin obtained from G60S mutant mice

Cx43 (green) immunofluorescent localization was performed on skin biopsies obtained from a patient expressing the D3N mutant as well as from the patient's unaffected parent (D3). Cx43 localization in the D3N patient revealed less punctate Cx43 localization when compared to the D3 control epidermis. Cx43 immunofluorescent labeling of the G60S mouse epidermis also revealed a similar reduction in punctate Cx43 localization when compared to the epidermis from WT littermate control mice. Dashed line represents the division of the epidermis to the dermis. Intense unspecific staining was also observed in the upper stratum corneum layer. Nuclei were stained with Hoechst and are pseudocoloured blue. Bar= 10 μ m.



Since this change in localization pattern observed in both human and mouse epidermis may indicate that mutant Cx43 impairs Cx43 cellular trafficking, we sought to investigate if mutant Cx43 expression affects the dynamic Cx43 trafficking which occurs during wound healing. To evaluate this possibility, Cx43 immunofluorescent localization was performed one, three, and nine days after incisional wounds were created on the backs of WT and G60S mice (**Fig. 3.2**). One day after wounding, we observed a decrease in the expression of Cx43 at the wound edge from WT mice but Cx43 levels appeared to be slightly higher at the wound edge in the G60S mouse epidermis. Three days after wounding however, abundant Cx43 was observed in cells bordering the wound edge and Cx43 was primarily localized within intracellular compartments. Nine days of wounding, Cx43 returned to the similar punctate profile observed in the uninjured epidermis in WT mice and Cx43 was again diffusely localized in the epidermis from mutant mice.

3.3.2 Mutant Cx43 inhibits gap junctional intercellular communication and enhances the proliferation of primary mouse keratinocytes

Since the localization of Cx43 is impaired in G60S mouse epidermis during steady-state and during wound healing, we sought to determine if primary keratinocytes derived from G60S mice are impaired in their ability to proliferate, migrate, and differentiate as required during wound healing. Primary keratinocytes were isolated from both WT and G60S mice and the purity of the keratinocyte cultures were assessed by immunofluorescent labeling of a keratinocyte marker, cytokeratin 14 (CK14) (**Fig. 3.3**). In both cases over 97% percent of the cells isolated labeled with CK14. Cx43 localization studies revealed that keratinocytes from mutant mice had a reduced number of Cx43 gap junction plaques. To determine if this decrease in gap junction plaques translated into reduced gap junctional communication between keratinocytes, dual patch clamp analysis was performed on WT and G60S derived mouse keratinocytes. The primary keratinocytes derived from G60S mice had significantly reduced transjunctional conductance when compared to keratinocytes derived from WT mice suggesting that the expression of mutant Cx43 impairs gap junctional coupling.

Figure 3.2 Cx43 is maintained localized within intracellular compartments during the wound healing process in G60S mutant mice

Immunofluorescent localization of Cx43 revealed that the expression of Cx43 is downregulated at the wounded edge (beneath the labeled clot) one day after injury in WT mice. Three days after injury, Cx43 was predominantly localized within intracellular compartments of cells at the proliferative edge in WT mice. Nine days after injury, Cx43 localized into punctate plaque structures between keratinocytes in WT mice. However, in mutant mice Cx43 remained localized to intracellular compartments or diffusely localized at the cell surface during all stages of the wound healing process (see enlarged panel). Nuclei were stained with Hoechst and are pseudocoloured blue. Bar = 50 μm .

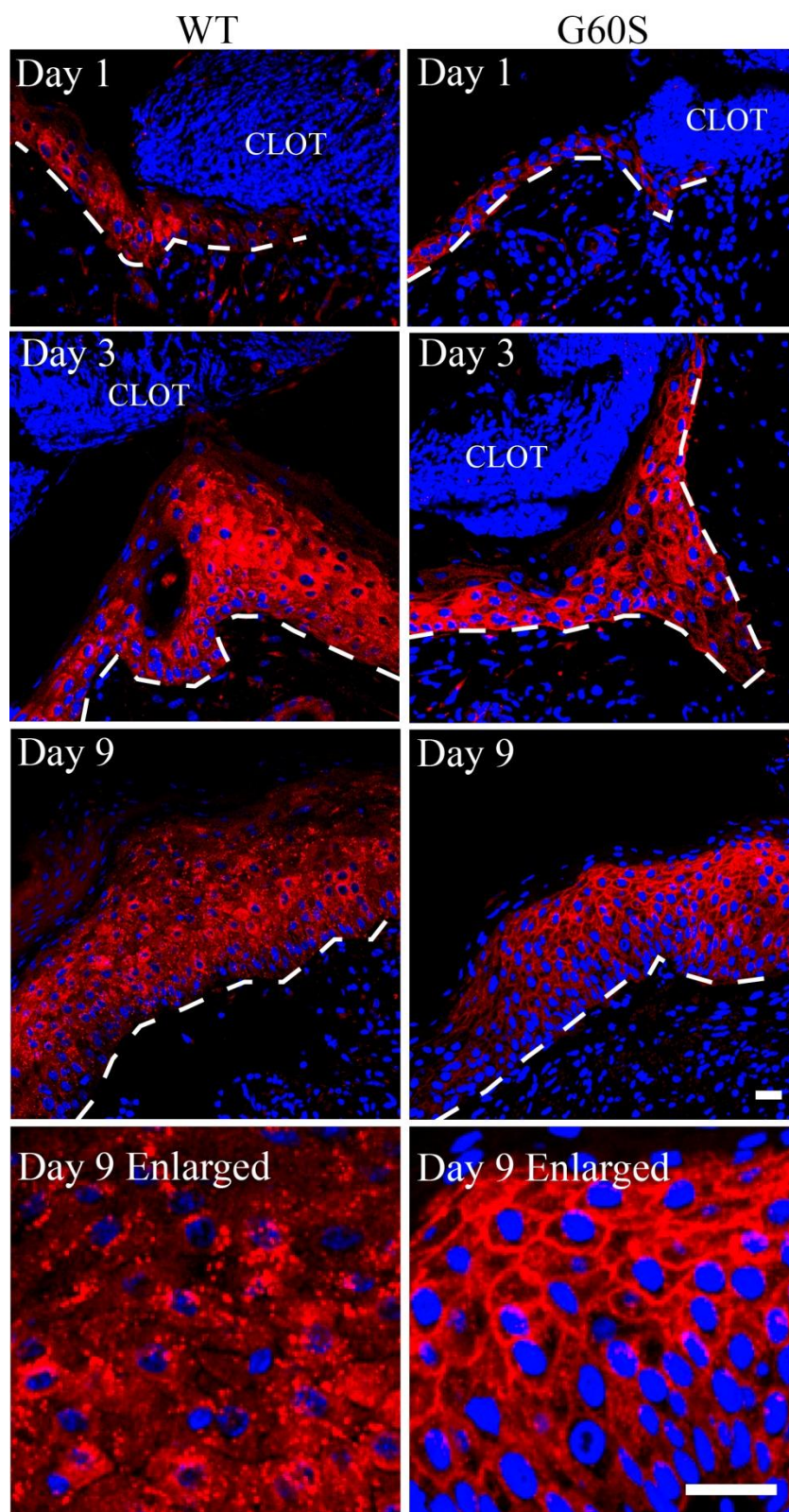
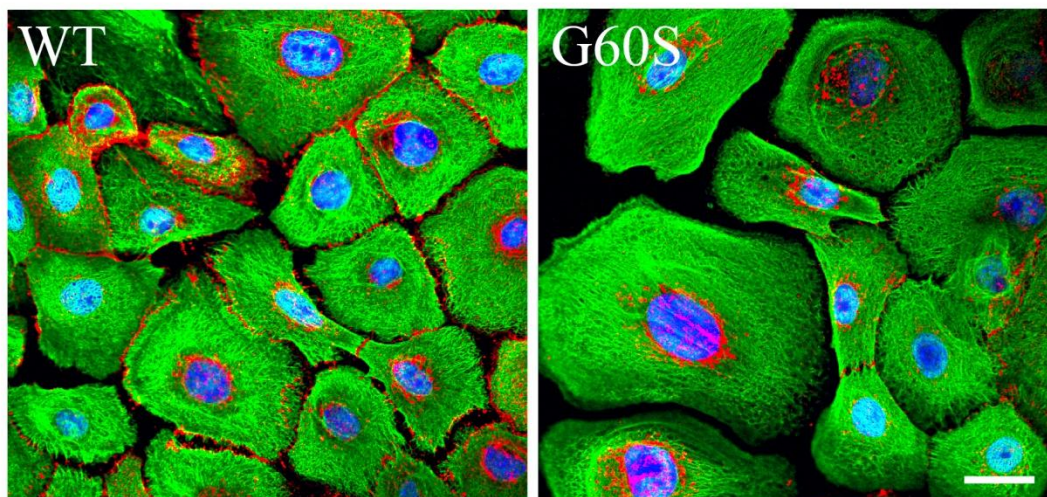


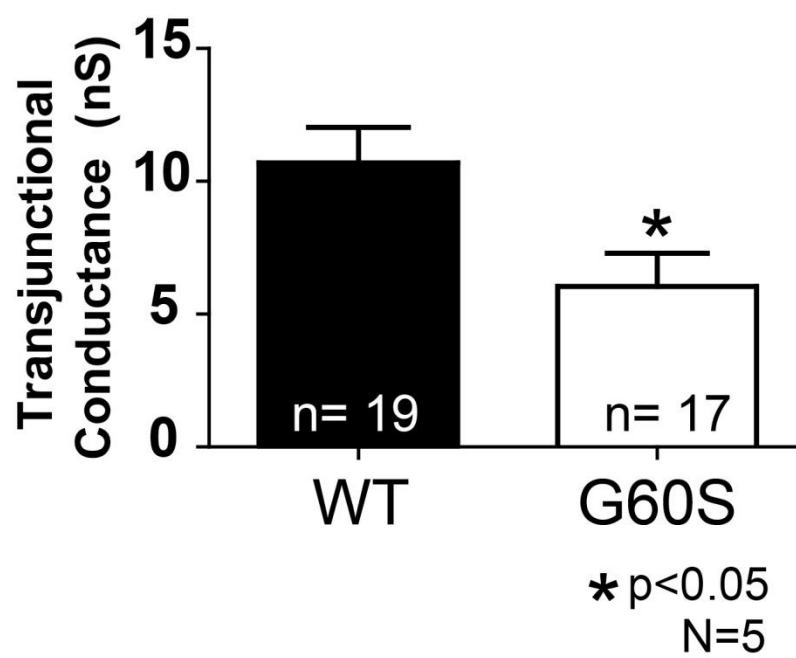
Figure 3.3 Mutant G60S Cx43 impairs the localization of Cx43 and decreases the transjunctional conductance in primary keratinocytes

A. Primary keratinocytes co-labeled for CK14 (green) and Cx43 (red) revealed that keratinocytes derived from G60S mice had reduced Cx43 localized at the areas of cell to cell apposition. B. Gap junctional coupling of paired wild-type or G60S keratinocytes revealed a significant decrease in the transjunctional conductance in cells from mutant mice as revealed by the dual whole-cell patch clamp technique. Bar = 20 μm .

A



B



To determine if mutant Cx43 expression impacts the proliferation of keratinocytes, we performed BrdU labeling on rat epidermal keratinocytes (REKs) expressing full length Cx43 (Cx43-GFP), G60S mutant Cx43 (G60S-GFP) or on vector control (V) infected REKs (**Fig. 3.4**). Cx43-GFP overexpression in REKs significantly lowered the proportion of nuclei which labeled for BrdU while mutant G60S-GFP expression increased the percent of BrdU labeled nuclei. This suggests that exogenous expression of mutant G60S Cx43 can enhance the proliferation of rat keratinocytes and overexpression of wild-type Cx43 lowers the proliferative ability of keratinocytes. In addition, cell counts revealed that keratinocytes from G60S mice proliferated faster than WT keratinocytes.

3.3.3 Migration and the ability of keratinocytes to differentiate is not affected by the expression of the G60S mutant

To determine if mutant Cx43 can impact the ability of keratinocytes to migrate, a scrape wound assay was performed on monolayer keratinocyte cultures derived from WT and G60S mice (**Fig. 3.5**). No significant difference was observed between the distances that keratinocytes derived from WT or G60S mice migrated. Scrape wound assays were also performed on REKs expressing different Cx43 variants either in the presence or the absence of serum and no differences were observed between any REK cell line assayed (**Fig 3.6**).

Primary keratinocyte from WT and G60S mice were also assayed for their ability to differentiate. Under low calcium conditions, WT mouse derived keratinocytes expressed abundant Cx43 gap junction plaques localized to the areas of cell to cell apposition while Cx43 was predominantly localized within the cell in keratinocytes derived from G60S mice. After two and four days under high calcium conditions, Cx43 expression at the areas of cell to cell apposition appeared to decrease in both WT and G60S derived keratinocytes while intracellular pools of Cx43 could still be observed in the keratinocytes derived from G60S mice.

Figure 3.4 Mutant G60S Cx43 expression enhances keratinocyte proliferation and overexpression of wild-type Cx43 reduces proliferation

A. REKs were engineered to express either the G60S mutant (G60S-GFP) or full length Cx43 (Cx43-GFP) tagged with green fluorescent protein. REKs were also infected with the empty viral vector (V). Proliferative events were quantified by determining the percent BrdU labeled nuclei compared to the total Hoechst stained nuclei. B. Cell counts on WT and G60S primary keratinocytes cultured for nine days revealed that G60S primary keratinocytes proliferated faster when compared to keratinocytes derived from WT mice.

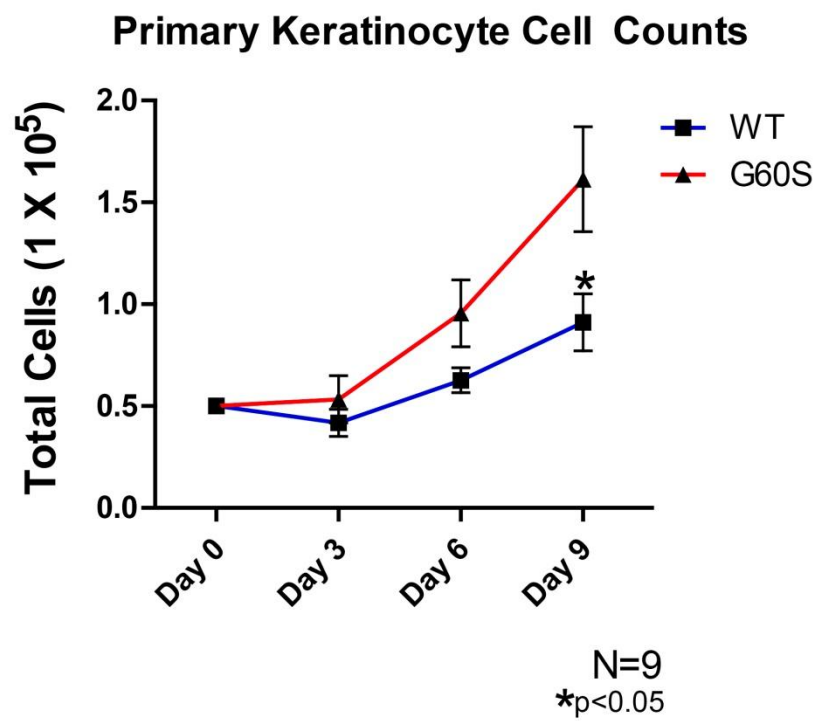
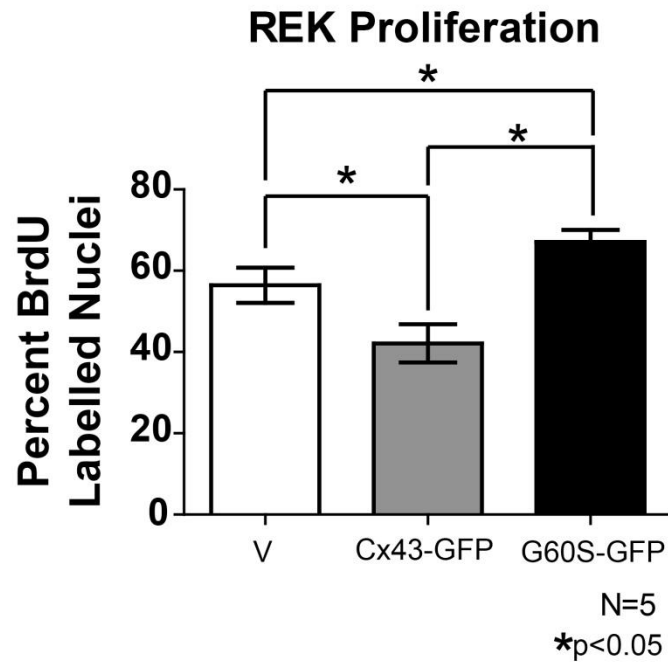


Figure 3.5 Mutant G60S Cx43 expression does not change the migration of primary keratinocytes

Scrape wounds were performed on primary keratinocytes derived from WT and G60S mice and closure of the scraped monolayer was assessed by time lapse imaging. Primary keratinocytes derived from WT and G60S mice migrated equal distances after 12 hours. Bar = 100 μm .

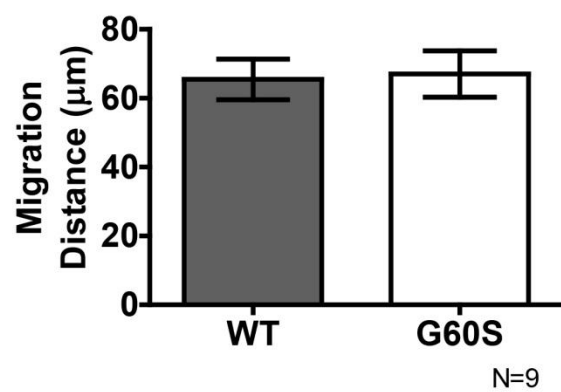
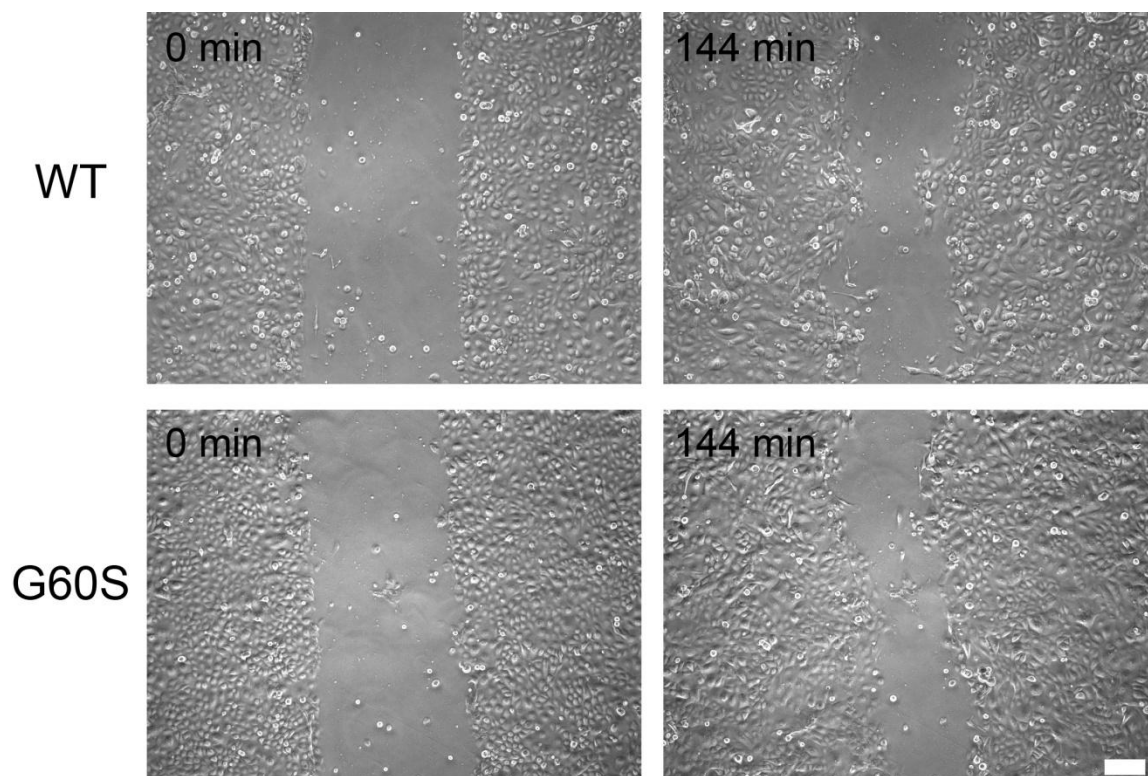
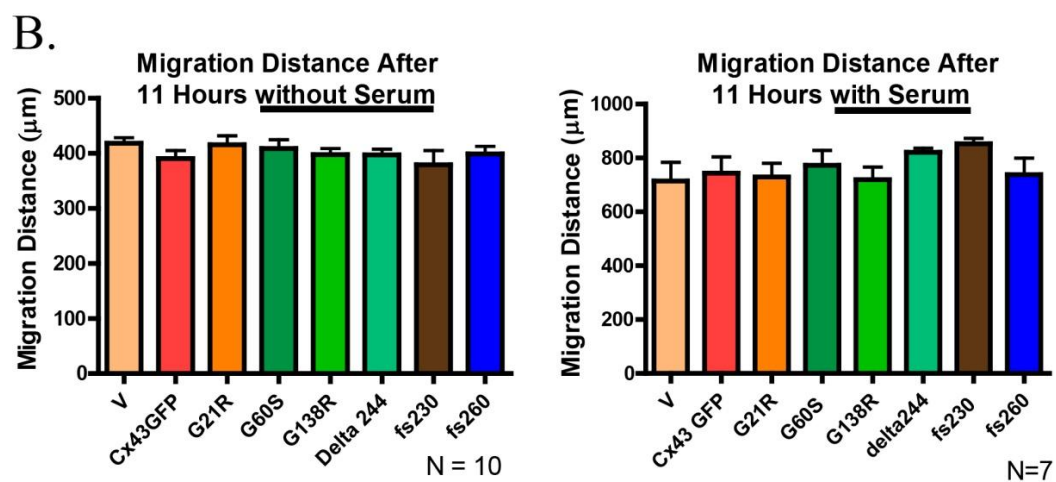
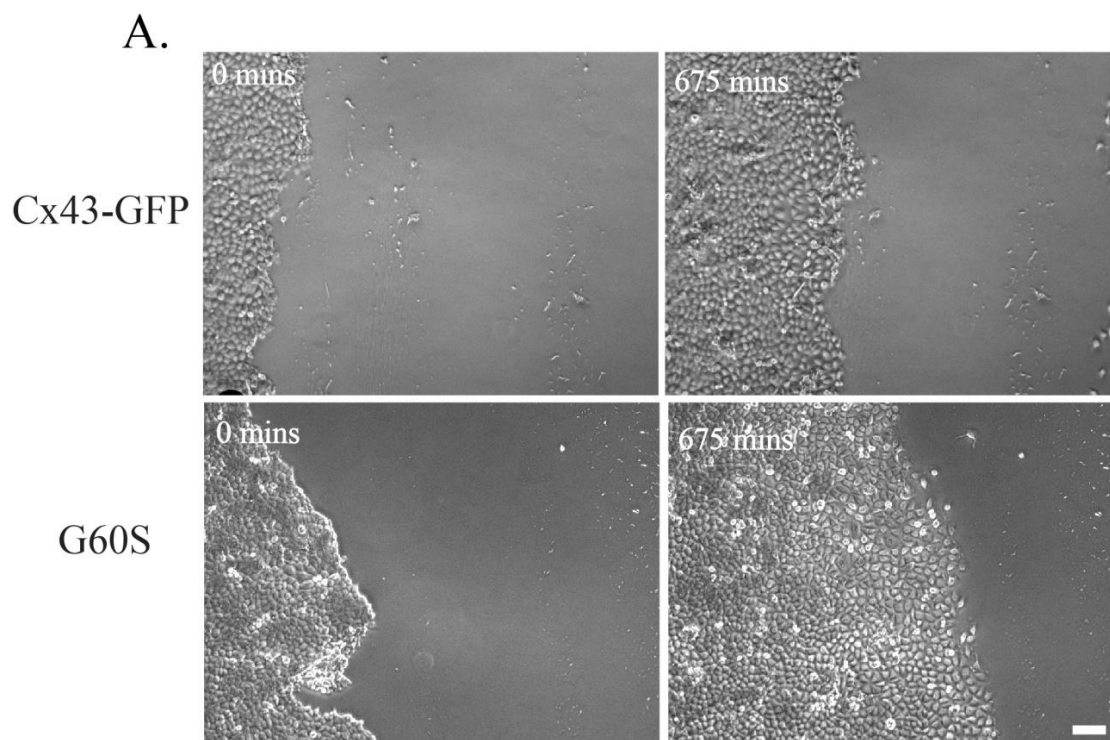


Figure 3.6 Rat epidermal keratinocytes engineered to express ODDD mutants exhibited similar levels of migration

REKs were engineered to express ODDD mutants (G21R, G60S, G138R, fs230, fs260) as well as full length Cx43 (Cx43-GFP) or a C-terminal truncated mutant with two additional mutations ($\Delta 244^*$). A. Scrape wound assays were performed on monolayer cultures and time-lapse imaging was performed to compare the migration competence of each of these cell lines. Images of Cx43-GFP and G60S-GFP expressing cells are presented immediately after scraping and approximately 11 hours after the scrape wound was performed. B. Quantification of the migration distance keratinocytes transverse over 11 hours with or without serum was not significantly different between the REK cell lines. Bar = 100 μm .



Under low calcium conditions, Western blots revealed high levels of Cx43 representing multiple Cx43 phosphorylated states (**Fig. 3.7**) and, interestingly, the levels of Cx43 were significantly higher in keratinocytes derived from G60S mice. After keratinocytes were cultured in high calcium conditions for two or four days however, Cx43 levels were significantly lowered in keratinocytes derived from both WT and G60S mice. To assess the extent which keratinocytes had differentiated under high calcium conditions, Western blots were performed to quantify the levels of a keratinocyte differentiation marker, total-cytokeratin, and a protein which is expressed in undifferentiated basale keratinocytes, CK14 (Matic et al., 2005). Analysis of all keratins or CK14 did not reveal any significant expression differences between keratinocytes obtained from WT or mutant mice. However, when examining the expression of an additional marker of differentiation, involucrin, keratinocytes derived from G60S mice expressed significantly higher levels of involucrin under low calcium conditions and after 2 days, but not 4 days under high calcium culturing conditions.

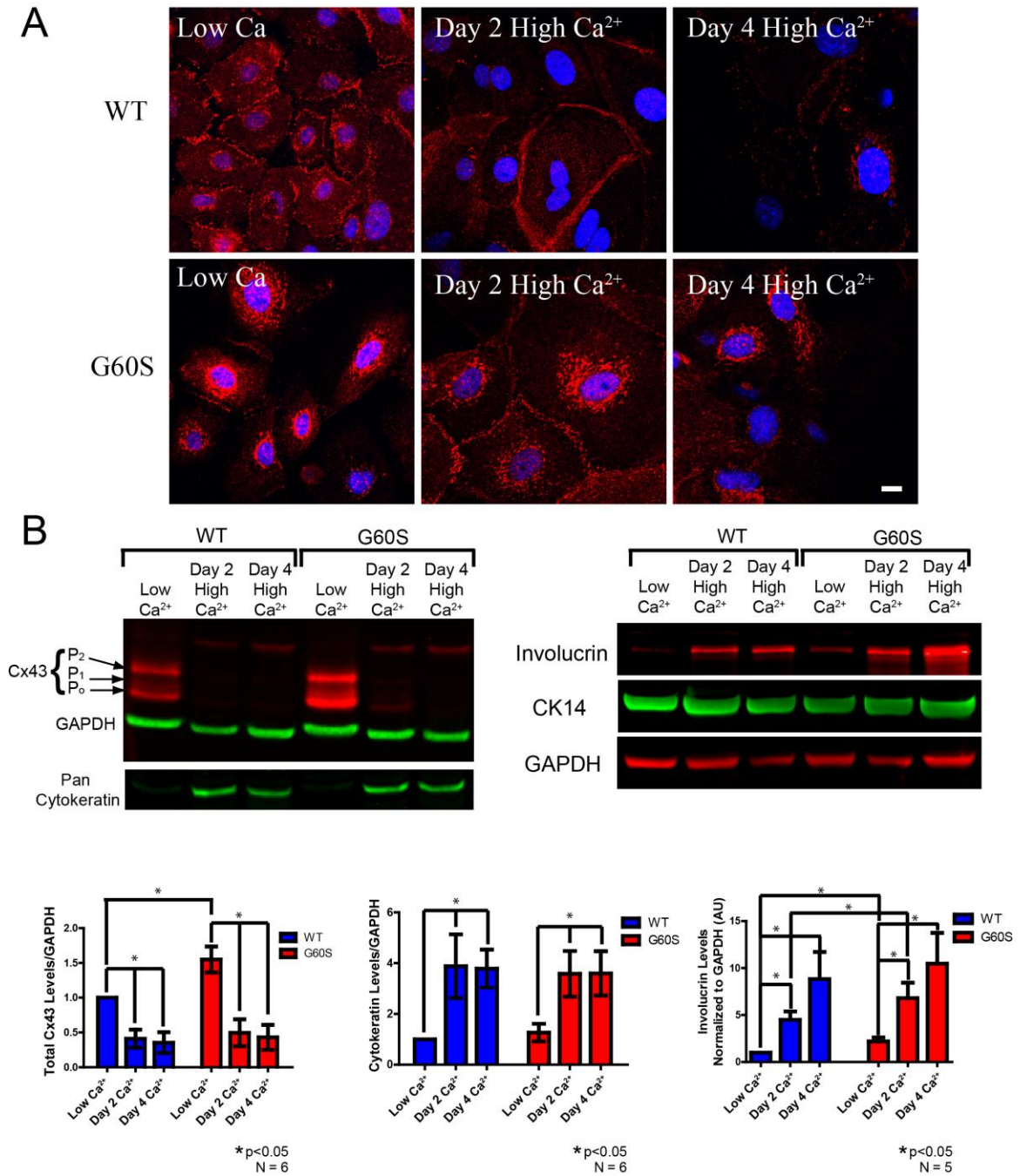
3.4 Discussion

Wound healing involves a combined effort between multiple cell types including fibroblasts and keratinocytes. In wound healing, both fibroblasts and keratinocytes must efficiently proliferate, migrate, and differentiate to rebuild the structural and functional integrity of the skin (Hackam and Ford, 2002; Werner et al., 2007). Connexins are thought to play a valuable role in the wound healing process since they have been shown to affect the proliferation (Song et al., 2010; Vinken et al., 2011), migration (Olk et al., 2009; Santiago et al., 2010) and differentiation (Belliveau et al., 2006; McLachlan et al., 2008) of multiple cells types.

Knockdown studies which transiently lower Cx43 expression have demonstrated that wounds heal faster when Cx43 levels are lowered (Mori et al., 2006; Qiu et al., 2003). However, we have previously demonstrated that wounds in mice expressing mutant G60S Cx43 did not heal as fast as their WT counterpart (Churko et al., 2011). Fibroblasts in this

Figure 3.7 Keratinocyte Cx43 levels decrease under high calcium conditions

A. Immunofluorescent labeling of Cx43 was performed on keratinocytes derived from WT and G60S mice under low and high calcium conditions. Under low calcium conditions, a large proportion of Cx43 was expressed in the areas of cell to cell apposition in the WT keratinocytes while intracellular labeling of Cx43 was observed in keratinocytes derived from G60S mice. After calcium was added to the culture media cell surface Cx43 plaques were greatly reduced. B. Western blots revealed that the addition of calcium to the culture media significantly reduced the levels of Cx43 in keratinocytes derived from both WT and G60S mice. Total cytokeratin and CK14 levels were not significantly different between WT and G60S mice under low or high calcium culture conditions. Involucrin levels were significantly higher in keratinocytes derived from G60S mice under low calcium conditions and at two days but not four days after calcium was added to the culture media. Bar= 10 μ m.



study were shown to have impaired proliferation, migration and differentiation. In addition, Cx43 has been shown to be dynamically regulated in keratinocytes during wound healing (Brandner et al., 2004; Goliger and Paul, 1995; Lampe et al., 1998) and mutant Cx43 may also impair the ability of keratinocytes to heal wounds. In the current study, we assessed the ability of keratinocytes expressing either wild-type or mutant Cx43 to proliferate, migrate and differentiate to determine if mutant Cx43 impairs the role that keratinocytes play during wound healing.

To date, the localization of Cx43 in any ODDD patient tissues has not been investigated. Here we have attained a punch biopsy from a patient with ODDD (expressing the D3N mutant) as well as from a family matched control. The reduction in Cx43 gap junctions observed in the ODDD patient epidermis could indicate that mutant Cx43 impairs proper cellular trafficking of Cx43 or it destabilizes the cell surface population of Cx43 that assembles into gap junction plaques. Mislocalized Cx43 was also observed in primary keratinocytes derived from G60S mice. It is possible that mislocalized Cx43 may affect the ability of Cx43 to bind to one or more of its multiple protein binding partners (reviewed in Laird, 2010). For example, Cx43 has been shown to compete with Smad2/3 to bind to microtubules (Dai et al., 2007). If the interaction between mutant Cx43 and microtubules is impaired, it is possible that more Smad2/3 may bind microtubules thus dysregulating the overall signaling action of Smad2/3. This may also have significant consequences in TGF β ₁ signaling since TGF β ₁ signaling activates Smad2/3. In addition, mislocalized Cx43 would be expected to reduce the overall coupling status of contacting mutant containing keratinocytes as we have determined to be the case. If the function of gap junction channels is reduced, keratinocytes may not efficiently transport metabolites and signaling molecules required for differentiation (e.g. calcium (Kimyai-Asadi et al., 2002)) and thus keratinocytes may be impaired in their ability to differentiate. However, since WT and G60S expressing Cx43 keratinocytes differentiated to a similar degree, mutant G60S co-expressed with wild-type Cx43 may allow sufficient metabolite/ion transport through gap junction channels to differentiate.

In this study, keratinocytes from G60S mice have a reduction in Cx43 gap junction plaque formation and this cellular status may result in a selective advantage in epidermal

wound healing. As previously reported by others and demonstrated in the current study, Cx43 levels decrease in cells bordering the wound edge twenty-four hours after injury (Brandner et al., 2004; Goliger and Paul, 1995; Lampe et al., 1998). Three days after injury however, abundant Cx43 was localized within the intracellular environment but Cx43 was still prohibited from forming gap junctions. At this stage of wound healing, keratinocytes are rapidly proliferating and migrating under the coagulum. Since keratinocytes from mutant mice maintain Cx43 within intracellular compartments for an extended, or even an indefinite period of time, this condition may further accelerate the wound healing response. In addition, since connexins are naturally removed from the plasma membrane prior to cell division (Solan and Lampe, 2009), the reduction of plasma membrane localized Cx43 expression in mutant expressing keratinocytes may further promote proliferation. This could also explain how lowering Cx43 levels by anti-sense oligonucleotide enhances keratinocyte proliferation (Mori et al., 2006). Here we have also observed that mutant G60S Cx43 expression in both REKs and in primary keratinocytes enhances the proliferation of keratinocytes. In addition, the expression of full-length Cx43 into REKs lowered the ability of REKs to proliferate when compared to vector control cells. However, it is unclear whether it is the physical presence of Cx43 on the plasma membrane or the functional coupling mediated through gap junction channels regulates this change in proliferation.

While keratinocyte proliferation is one of the earliest steps in wound healing, keratinocytes must also migrate under the coagulum to repopulate the wounded area. Fibroblasts derived from G60S mice and from patients with ODDD revealed a significant delay in migration (Churko et al., 2011). However, scratch wound assays performed on REKs expressing various Cx43 mutants and on primary keratinocytes derived from WT and G60S mice did not reveal any differences in cell migration. The ability of mutant Cx43 to impair migration in fibroblasts but not in keratinocytes suggests that there are clear cell type differences. Interestingly, the migration rate in both human (Wright et al., 2009) and mouse (Kandyba et al., 2008) keratinocytes were enhanced when treated with a connexin mimetic peptide, Gap27. Since Gap27 is proposed to block the interaction between connexons on the cell surface, coating the plasma membrane with Gap27 may also block the interaction between other cell adhesion proteins or between different

connexons expressed in keratinocytes. Therefore, the increase in migration observed when keratinocytes were treated with Gap27 may be due to the nonspecific interactions with other protein complexes expressed on the plasma membrane.

Previously, low calcium conditions have been shown to promote the expression of Cx43 and high calcium conditions have been shown to decrease the levels of Cx43 during keratinocyte differentiation (Brissette et al., 1994). In our study, keratinocytes derived from both WT and G60S mice were shown to express abundant Cx43 under low calcium conditions and primary keratinocytes derived from G60S mice expressed significantly more Cx43 when compared to primary keratinocytes derived from WT mice. This finding is quite unique since total Cx43 expression and the levels of the phosphorylated Cx43 species were shown to be lower in whole skin extracted from G60S mice (Langlois et al., 2007). It is possible that multiple cell passages may lead to an increase in Cx43 expression over time or keratinocytes derived from G60S mice may compensate for the loss of gap junction dependent communication by upregulating the overall levels of Cx43. In addition, given that keratinocytes derived from G60S mice exhibited reduced coupling and that the phosphorylated species of Cx43 observed in Western blots is associated with the functional plasma membrane localized pool of Cx43 (Solan and Lampe, 2005), the increase in total Cx43 expression observed in our keratinocytes derived from G60S mice is suspected to be due to an increase in the P₀ (intracellular pool of Cx43) band species. This is also supported by our immunofluorescent data which revealed a large intracellular pool of Cx43 in keratinocytes derived from G60S mice.

Under high calcium conditions however, keratinocytes derived from both WT and G60S responded similarly by lowering their expression of Cx43 at two and four days. In addition, no difference was observed in the expression of a cytokeratin differentiation marker between keratinocytes derived from WT and G60S mice after calcium-induced differentiation. However, freshly isolated keratinocytes derived from G60S mice may be somewhat better primed for differentiation since involucrin levels were elevated under low calcium and after two days under high calcium. While keratinocytes expressing mutant Cx43 may be initially primed to differentiate, this differentiation advantaged was nullified by day four of high calcium treatment. This finding is also supported by

previous Western blots which showed no significant difference in the levels of involucrin expression between skin extracts derived from adult WT and G60S mice (Langlois et al., 2007).

In general, there are few reports that suggest mutant Cx43 expression impairs skin differentiation. With over 62 different mutants reported to cause ODDD (Paznekas et al., 2009), only two patients expressing either the fs260 (van Steensel et al., 2005) or fs230 (Vreeburg et al., 2007) Cx43 mutants led to the development of palmar plantar hyperkeratosis. While the majority of Cx43 mutants have not been reported to affect skin physiology, some Cx43 mutants (e.g. fs260 and fs230 mutants) may be more potent at causing skin disease and impairing wound healing. Organotypic epidermal cultures engineered to express the fs260 mutant drastically reduced the endogenous levels of both Cx43 and Cx26 and disrupted the organotypic epidermal architecture (Churko et al., 2010). Since the fs260 mutant lacks a large portion of the C-terminal domain, the C-terminal domain is hypothesized to play an important role in skin differentiation. In support of this hypothesis, mice engineered to express a C-terminal truncation of Cx43 have also been shown to die prematurely due to epidermal barrier defects (Maass et al., 2004).

The ability of each mutant to impair skin homeostasis may also be cell type dependent. Mutant Cx43 drastically impaired the ability of fibroblasts to proliferate, migrate and differentiate however in this study, keratinocytes expressing mutant Cx43 did not demonstrate a significant difference in migration and did not show severe differentiation differences. Given that fibroblasts have been shown to express Cx43, Cx45 and Cx40 (Wright et al., 2009) while keratinocytes have been reported to express Cx43, Cx26, Cx30, Cx30.3, Cx31, Cx31.1, Cx37, Cx40, Cx57 (Goliger and Paul, 1994; Richard, 2000) the multitude of connexins expressed in keratinocytes may compensate for mutant Cx43. Functional compensation of connexins in the epidermis has previously been documented as an upregulation of Cx30 expression was observed within the epidermis of mice with reduced levels of Cx43 (Kretz et al., 2003).

In conclusion, the expression of mutant Cx43 may impart patients with a wound healing advantage when the wounds are superficial and restricted primarily to the epidermis. Under these conditions patient keratinocytes would be expected to proliferate faster and close over the wounded area. However, since mutant Cx43 has been shown to impair fibroblast proliferation, migration and differentiation, larger wounds requiring drastic dermal remodeling may not heal as fast in ODDD patients.

3.5 References

- Baden, H.P., and J. Kubilus. 1983. The growth and differentiation of cultured newborn rat keratinocytes. *J. Invest Dermatol.* 80:124-130.
- Belliveau, D.J., M. Bani-Yaghoub, B. McGirr, C.C. Naus, and W.J. Rushlow. 2006. Enhanced neurite outgrowth in PC12 cells mediated by connexin hemichannels and ATP. *J Biol Chem.* 281:20920-20931.
- Brandner, J.M., P. Houdek, B. Husing, C. Kaiser, and I. Moll. 2004. Connexins 26, 30, and 43: differences among spontaneous, chronic, and accelerated human wound healing. *J Invest Dermatol.* 122:1310-1320.
- Brissette, J.L., N.M. Kumar, N.B. Gilula, J.E. Hall, and G.P. Dotto. 1994. Switch in gap junction protein expression is associated with selective changes in junctional permeability during keratinocyte differentiation. *Proc Natl Acad Sci U S A.* 91:6453-6457.
- Churko, J.M., S. Langlois, X. Pan, Q. Shao, and D.W. Laird. 2010. The potency of the fs260 connexin43 mutant to impair keratinocyte differentiation is distinct from other disease-linked connexin43 mutants. *Biochem J.* 429:473-483.
- Churko, J.M., Q. Shao, X. Gong, K.J. Swoboda, D. Bai, J. Sampson, and D.W. Laird. 2011. Human dermal fibroblasts derived from oculodentodigital dysplasia patients suggest that patients may have wound healing defects. *Hum Mutat.*
- Dai, P., T. Nakagami, H. Tanaka, T. Hitomi, and T. Takamatsu. 2007. Cx43 mediates TGF-beta signaling through competitive Smads binding to microtubules. *Mol Biol Cell.* 18:2264-2273.
- Dobrowolski, R., P. Sasse, J.W. Schrickel, M. Watkins, J.S. Kim, M. Rackauskas, C. Troatz, A. Ghanem, K. Tiemann, J. Degen, F.F. Bukauskas, R. Civitelli, T. Lewalter, B.K. Fleischmann, and K. Willecke. 2008. The conditional connexin43G138R mouse mutant represents a new model of hereditary oculodentodigital dysplasia in humans. *Hum Mol Genet.* 17:539-554.
- Flenniken, A.M., L.R. Osborne, N. Anderson, N. Ciliberti, C. Fleming, J.E. Gittens, X.Q. Gong, L.B. Kelsey, C. Lounsbury, L. Moreno, B.J. Nieman, K. Peterson, D. Qu, W. Roscoe, Q. Shao, D. Tong, G.I. Veitch, I. Voronina, I. Vukobradovic, G.A. Wood, Y. Zhu, R.A. Zirngibl, J.E. Aubin, D. Bai, B.G. Bruneau, M. Grynepas, J.E. Henderson, R.M. Henkelman, C. McKerlie, J.G. Sled, W.L. Stanford, D.W. Laird, G.M. Kidder, S.L. Adamson, and J. Rossant. 2005. A Gja1 missense mutation in a mouse model of oculodentodigital dysplasia. *Development.* 132:4375-4386.
- Goliger, J.A., and D.L. Paul. 1994. Expression of gap junction proteins Cx26, Cx31.1, Cx37, and Cx43 in developing and mature rat epidermis. *Dev. Dyn.* 200:1-13.

- Goliger, J.A., and D.L. Paul. 1995. Wounding alters epidermal connexin expression and gap junction-mediated intercellular communication. *Mol.Biol.Cell.* 6:1491-1501.
- Hackam, D.J., and H.R. Ford. 2002. Cellular, biochemical, and clinical aspects of wound healing. *Surg Infect (Larchmt)*. 3 Suppl 1:S23-35.
- Kalcheva, N., J. Qu, N. Sandeep, L. Garcia, J. Zhang, Z. Wang, P.D. Lampe, S.O. Suadicani, D.C. Spray, and G.I. Fishman. 2007. Gap junction remodeling and cardiac arrhythmogenesis in a murine model of oculodentodigital dysplasia. *Proc Natl Acad Sci U S A.* 104:20512-20516.
- Kandyba, E.E., M.B. Hodgins, and P.E. Martin. 2008. A murine living skin equivalent amenable to live-cell imaging: analysis of the roles of connexins in the epidermis. *J Invest Dermatol.* 128:1039-1049.
- Kimyai-Asadi, A., L.B. Kotcher, and M.H. Jih. 2002. The molecular basis of hereditary palmoplantar keratodermas. *J.Am.Acad.Dermatol.* 47:327-343.
- Kretz, M., C. Euwens, S. Hombach, D. Eckardt, B. Teubner, O. Traub, K. Willecke, and T. Ott. 2003. Altered connexin expression and wound healing in the epidermis of connexin-deficient mice. *J Cell Sci.* 116:3443-3452.
- Laird, D.W. 2010. The gap junction proteome and its relationship to disease. *Trends Cell Biol.* 20:92-101.
- Lampe, P.D., B.P. Nguyen, S. Gil, M. Usui, J. Olerud, Y. Takada, and W.G. Carter. 1998. Cellular interaction of integrin alpha3beta1 with laminin 5 promotes gap junctional communication. *J Cell Biol.* 143:1735-1747.
- Langlois, S., J.M. Churko, and D.W. Laird. 2010. Optical and biochemical dissection of connexin and disease-linked connexin mutants in 3D organotypic epidermis. *Methods Mol Biol.* 585:313-334.
- Langlois, S., A.C. Maher, J.L. Manias, Q. Shao, G.M. Kidder, and D.W. Laird. 2007. Connexin levels regulate keratinocyte differentiation in the epidermis. *J Biol Chem.* 282:30171-30180.
- Maass, K., A. Ghanem, J.S. Kim, M. Saathoff, S. Urschel, G. Kirfel, R. Grummer, M. Kretz, T. Lewalter, K. Tiemann, E. Winterhager, V. Herzog, and K. Willecke. 2004. Defective epidermal barrier in neonatal mice lacking the C-terminal region of connexin43. *Mol.Biol.Cell.* 15:4597-4608.
- Manias, J.L., I. Plante, X.Q. Gong, Q. Shao, J. Churko, D. Bai, and D.W. Laird. 2008. Fate of connexin43 in cardiac tissue harbouring a disease-linked connexin43 mutant. *Cardiovasc Res.* 80:385-395.

- Matic, M., C. Pullis, M.G. Golightly, and S.R. Simon. 2005. Analysis of connexin 43 expression on keratinocytes using flow cytometry. *Methods Mol Biol.* 289:193-200.
- McLachlan, E., J.L. Manias, X.Q. Gong, C.S. Lounsbury, Q. Shao, S.M. Bernier, D. Bai, and D.W. Laird. 2005. Functional characterization of oculodentodigital dysplasia-associated Cx43 mutants. *Cell Commun Adhes.* 12:279-292.
- McLachlan, E., I. Plante, Q. Shao, D. Tong, G.M. Kidder, S.M. Bernier, and D.W. Laird. 2008. ODDD-linked Cx43 mutants reduce endogenous Cx43 expression and function in osteoblasts and inhibit late stage differentiation. *J Bone Miner Res.* 23:928-938.
- Mori, R., K.T. Power, C.M. Wang, P. Martin, and D.L. Becker. 2006. Acute downregulation of connexin43 at wound sites leads to a reduced inflammatory response, enhanced keratinocyte proliferation and wound fibroblast migration. *J Cell Sci.* 119:5193-5203.
- Olk, S., G. Zoidl, and R. Dermietzel. 2009. Connexins, cell motility, and the cytoskeleton. *Cell Motil Cytoskeleton.* 66:1000-1016.
- Paznekas, W.A., S.A. Boyadjiev, R.E. Shapiro, O. Daniels, B. Wollnik, C.E. Keegan, J.W. Innis, M.B. Dinulos, C. Christian, M.C. Hannibal, and E.W. Jabs. 2003. Connexin 43 (GJA1) mutations cause the pleiotropic phenotype of oculodentodigital dysplasia. *Am J Hum Genet.* 72:408-418.
- Paznekas, W.A., B. Karczeski, S. Vermeer, R.B. Lowry, M. Delatycki, F. Laurence, P.A. Koivisto, L. Van Maldergem, S.A. Boyadjiev, J.N. Bodurtha, and E.W. Jabs. 2009. GJA1 mutations, variants, and connexin 43 dysfunction as it relates to the oculodentodigital dysplasia phenotype. *Hum Mutat.* 30:724-733.
- Penuela, S., R. Bhalla, X.Q. Gong, K.N. Cowan, S.J. Celetti, B.J. Cowan, D. Bai, Q. Shao, and D.W. Laird. 2007. Pannexin 1 and pannexin 3 are glycoproteins that exhibit many distinct characteristics from the connexin family of gap junction proteins. *J Cell Sci.* 120:3772-3783.
- Pollok, S., A.C. Pfeiffer, R. Lobmann, C.S. Wright, I. Moll, P.E. Martin, and J.M. Brandner. 2010. Connexin 43 mimetic peptide Gap27 reveals potential differences in the role of Cx43 in wound repair between diabetic and non-diabetic cells. *J Cell Mol Med.*
- Qiu, C., P. Coutinho, S. Frank, S. Franke, L.Y. Law, P. Martin, C.R. Green, and D.L. Becker. 2003. Targeting connexin43 expression accelerates the rate of wound repair. *Curr.Biol.* 13:1697-1703.
- Richard, G. 2000. Connexins: a connection with the skin. *Exp.Dermatol.* 9:77-96.

- Richards, T.S., C.A. Dunn, W.G. Carter, M.L. Usui, J.E. Olerud, and P.D. Lampe. 2004. Protein kinase C spatially and temporally regulates gap junctional communication during human wound repair via phosphorylation of connexin43 on serine368. *J. Cell Biol.* 167:555-562.
- Risek, B., F.G. Klier, and N.B. Gilula. 1992. Multiple gap junction genes are utilized during rat skin and hair development. *Development.* 116:639-651.
- Salomon, D., E. Masgrau, S. Vischer, S. Ullrich, E. Dupont, P. Sappino, J.H. Saurat, and P. Meda. 1994. Topography of mammalian connexins in human skin. *J Invest Dermatol.* 103:240-247.
- Santiago, M.F., P. Alcami, K.M. Striedinger, D.C. Spray, and E. Scemes. 2010. The carboxyl-terminal domain of connexin43 is a negative modulator of neuronal differentiation. *J Biol Chem.* 285:11836-11845.
- Sohl, G., and K. Willecke. 2004. Gap junctions and the connexin protein family. *Cardiovasc Res.* 62:228-232.
- Solan, J.L., and P.D. Lampe. 2005. Connexin phosphorylation as a regulatory event linked to gap junction channel assembly. *Biochim Biophys Acta.* 1711:154-163.
- Solan, J.L., and P.D. Lampe. 2009. Connexin43 phosphorylation: structural changes and biological effects. *Biochem J.* 419:261-272.
- Song, D., X. Liu, R. Liu, L. Yang, J. Zuo, and W. Liu. 2010. Connexin 43 hemichannel regulates H9c2 cell proliferation by modulating intracellular ATP and [Ca²⁺]. *Acta Biochim Biophys Sin (Shanghai).* 42:472-482.
- Toth, K., Q. Shao, R. Lorentz, and D.W. Laird. 2010. Decreased levels of Cx43 gap junctions result in ameloblast dysregulation and enamel hypoplasia in Gja1Jrt/+ mice. *J Cell Physiol.* 223:601-609.
- Tsui, E., K.A. Hill, A.M. Laliberte, D. Paluzzi, I. Kisilevsky, Q. Shao, J.G. Heathcote, D.W. Laird, G.M. Kidder, and C.M. Hutnik. 2011. Ocular pathology relevant to glaucoma in a Gja1Jrt/+ mouse model of human oculodentodigital dysplasia. *Invest Ophthalmol Vis Sci.*
- van Steensel, M.A., L. Spruijt, d.B.I. van, R.S. Bladergroen, M. Vermeer, P.M. Steijlen, and G.M. van. 2005. A 2-bp deletion in the GJA1 gene is associated with oculodento-digital dysplasia with palmoplantar keratoderma. *Am.J.Med.Genet.A.* 132A:171-174.
- Vinken, M., E. Decrock, E. De Vuyst, R. Ponsaerts, C. D'Hondt, G. Bultynck, L. Ceelen, T. Vanhaecke, L. Leybaert, and V. Rogiers. 2011. Connexins: sensors and regulators of cell cycling. *Biochim Biophys Acta.* 1815:13-25.

- Vreeburg, M., E.A. de Zwart-Storm, M.I. Schouten, R.G. Nellen, D. Marcus-Soekarman, M. Davies, M. van Geel, and M.A. van Steensel. 2007. Skin changes in oculo-dento-digital dysplasia are correlated with C-terminal truncations of connexin 43. *Am J Med Genet A*. 143:360-363.
- Werner, S., T. Krieg, and H. Smola. 2007. Keratinocyte-fibroblast interactions in wound healing. *J Invest Dermatol*. 127:998-1008.
- Wright, C.S., M.A. van Steensel, M.B. Hodgins, and P.E. Martin. 2009. Connexin mimetic peptides improve cell migration rates of human epidermal keratinocytes and dermal fibroblasts in vitro. *Wound Repair Regen*. 17:240-249.

Chapter 4

4 The ability of the fs260 Cx43 mutant to impair keratinocyte differentiation is distinct from other disease-linked Cx43 mutants

In the previous chapter we found that mutant G60S Cx43 expression negligibly affected the ability of primary mouse keratinocytes to differentiate. However ODDD patients expressing the frame-shift mutations (fs230 and fs260) develop skin disease and thus these mutants may be more potent at affecting the differentiation of the skin. In addition, primary keratinocyte cultures grown in monolayer may not truly represent epidermal differentiation since the epidermis is composed of multiple layers representing different keratinocyte differentiation states. In this chapter we extended our evaluation of the ability of keratinocytes expressing mutant Cx43 to differentiate by assessing three-dimensional organotypic epidermal cultures expressing skin disease linked and non-skin disease linked ODDD mutant Cx43.

A version of this chapter has been published:

Churko, J.M., Langlois, S., Pan, X., Shao, Q., Laird, D.W. (2010) The potency of the fs260 connexin43 mutant to impair keratinocyte differentiation is distinct from other disease-linked connexin43 mutants. *Biochemical Journal.*, 429 (3):473-83.

4.1 Introduction

Direct cell to cell communication relies heavily on the passage of small molecules through gap junctions (Beyer et al., 1987). Structurally, gap junctions are composed of connexin proteins which oligomerize in the Golgi apparatus to form connexons (Vanslyke et al., 2009). Connexons are transported to the cell surface and dock with connexons from an adjacent cell to form functional channels (Goodenough et al., 1996). Given that connexins and gap junctions have a half-life of only 1-5 hours both *in vitro* and *in vivo*, constant regulatory control of connexin translation, oligomerization, delivery to the cell surface and assembly are all critical for the proper regulation of gap junctional intercellular communication (GJIC). When regulatory processes involved in the life cycle of connexins become disrupted, GJIC is compromised and disease may result. For example, disease-linked mutations in the gene encoding connexin43 (Cx43) has been shown to sequester endogenous and mutant Cx43 in intracellular compartments (Gong et al., 2006), and inhibit the passage of small molecules through gap junction channels and hemichannels (Lai et al., 2006; McLachlan et al., 2005). Clinically, germ line mutations in nine connexin gene family members lead to human diseases that include skin diseases (e.g. Cx26, Cx43) (Richard, 2005), cataracts (e.g. Cx45, Cx50) (White et al., 1999), deafness (e.g. Cx26) (Petit, 2006), arrhythmias (e.g. Cx40, Cx43) (Gutstein et al., 2001), Charcot Marie Tooth disease (e.g. Cx32) (Scherer et al., 1999) and oculodentodigital dysplasia (ODDD) (e.g. Cx43) (Paznekas et al., 2009).

ODDD was first described as a disease displaying craniofacial abnormalities (microphthalmia, dental anomalies, small nose and hypotrichosis), type III syndactyly, and missing toe phalanges (Gillespie, 1964). Since its initial characterization, spastic paraparesis, cerebral white matter abnormalities (Gutmann et al., 1991) and ectodermal abnormalities (Kelly et al., 2006; Kjaer et al., 2004; Paznekas et al., 2009) have also been associated with ODDD. ODDD is a rare condition as less than 1000 cases having been fully documented although now that the genetic link to the disease is known; the number of reported cases is likely to grow substantially. To date, ODDD is associated with 62 familial or sporadic mutations in the gene encoding Cx43 with the majority (~85%) being dominant missense mutations (Paznekas et al., 2009). Functional assays employing some

of these mutations have found that the mutants encoded are dominant-negative and result in a drastic reduction in normal Cx43 function (Gong et al., 2006; McLachlan et al., 2005). These mutations are associated with a wide array of phenotypic outcomes and generally, domain specific mutations were not found to correlate with a specific ODDD symptom. For example, ODDD has been diagnosed in patients having mutations in the N-terminal (e.g. Y17S, G21R), first extracellular loop (e.g. A40V, G60S, P59S), cytoplasmic loop (e.g. V96M, G138R), second extracellular loop (e.g. H194P) and C-terminal tail (fs230, fs260) (Paznekas et al., 2009). While most of these mutations often result in syndactyly and cranial facial abnormalities, two ODDD mutants that truncate the C-terminal tail (fs230 and fs260) have been reported to additionally cause the skin disease palmar plantar hyperkeratosis (van Steensel et al., 2005; Vreeburg et al., 2007). While both of these mutants have been reported to cause palmar plantar hyperkeratosis, a newly identified patient expressing the fs230 mutant did not exhibit this skin disease phenotype (Alao et al., 2010). Importantly, the fs260 mutant has a polypeptide extension of 46 non-connexin related amino acids before a stop codon is encountered while the fs230 mutant has only a 6 amino acid extension prior to reaching a stop codon (van Steensel et al., 2005). Thus, although these two mutants both lack the C-terminal tail they differ extensively in non-connexin polypeptide sequence that may contribute to the disease phenotype in the skin.

Palmar plantar hyperkeratosis has been linked to a wide array of abnormal processes. Palmar plantar hyperkeratosis involves a thickening of the epidermis in the friction and weight bearing surfaces of the palms and the plantar region of the feet (Chopra et al., 1997). Congenitally, palmar plantar hyperkeratosis can also be caused by mutations in the genes which code for epidermal proteins. Mutant keratin 1, keratin 10 (Kimonis et al., 1994), Cx26 (Vohwinkel's syndrome)(de Zwart-Storm et al., 2008) and desmosomal proteins (Bragg et al., 2008) have all been reported to be genetically linked to palmar plantar hyperkeratosis. In the case of Cx43 mutations, it is currently not known whether the mechanism by which Cx43 mutants cause palmar plantar hyperkeratosis is somehow associated to these other skin disease-linked proteins. However, it has previously been shown that a mutant Cx26 which causes palmar plantar hyperkeratosis can have transdominant effects on Cx43 (Rouan et al., 2001). Thus, it may also be possible that

mutant Cx43 causes palmar plantar hyperkeratosis through transdominant effects on Cx26. It is also reasonable to assume that, since keratins, desmosomes and tight junctions are all responsible for maintaining the integrity of the epidermal barrier, Cx43 mutants that disrupt any one of these components may lead to disruptions in the membrane barrier and contribute to palmar plantar hyperkeratosis. In the present study we examined the mechanism by which mutations in the gene encoding Cx43 can affect skin differentiation and how some mutations associated with ODDD, but not others, can lead to skin disease.

4.2 Materials and methods

4.2.1 Cell lines

Rat epidermal keratinocytes (REKs) were originally characterized by Baden and Kubilus (Baden and Kubilus, 1983) and were grown in REK growth medium composed of Dulbecco's modified Eagle's medium (DMEM) supplemented with 2 mM L-glutamine, 10% fetal bovine serum, 100 µg/ml streptomycin and 100 U/ml penicillin

4.2.2 Transfection and infection

Transfection of packaging 293 cells was carried out using the previously reported and characterized AP2 vector encoding full length Cx43 (Cx43-GFP) or the Cx43 mutants, G21R, G60S, G138R, Δ244 with mutations G58R and S158A (Δ244^{*}) (Simek et al., 2009) and fs260. In addition, a fs230 mutation was also created using a Qiagen QuikChange Site-Directed Mutagenesis Kit with Forward 5'-ATCATTGAACTCTTCTGTTTTCTTCAAGGGCGTTAAGGATCGGG and Reverse 5'-CCCGATCCTTAACGCCCTTGAAGAAAACAGAAGAGTTCAATGAT primers for human Cx43 pcDNA3.1. Untagged fs230 pcDNA3.1 was used to rule-out effects caused by the GFP tag. The mutant fs230 sequence was then fused in frame into a EGFP-N1 (Clontech Lab., Inc) vector and further incorporated into a AP2 vector using the Forward 5'-ATCTCGACATGGGTGACTGGAGCGC and Reverse 5'-GGTGGATCCGGACGCCCTTGAAGAA primers. The fs230-GFP mutant construct encodes the first 229 amino acids of Cx43, six amino acids resulting from the frame shift (CFLEGR), seven amino acid linkers (PDPPLAT) and the EGFP protein sequence.

To perform transfections of packaging 293 cells, 2.5 mL of Opti-MEM was placed into two separate 5 mL tubes. 10 µg of the AP2 vector was placed into one tube while 15 µL of lipofectamine 2000 was added to the second tube. Within 5 minutes, both tubes were combined and were incubated for 20 mins. Packaging cells in a 100 mm culture dish were then washed two times in Opti-Mem medium and the combined lipofectamine/AP2 vector solution was administered onto the growing packaging 293 cells. After six hours, the lipofectamine solution was aspirated and the packaging cells were grown overnight in low glucose DMEM supplemented with 10% FBS, 10 µg/mL tetracycline, 20 µg/mL G418. The next day, 5 mL of fresh REK growth media was placed onto the transfected packaging cells and viral collections were made every day for four days. Collected viral media was concentrated by centrifugation in sealed 5.1 mL tubes for 90 mins in a Beckman TL100 ultracentrifuge at 4°C at 25,000 rpm (Beckman Instruments, Palo Alto, CA). After centrifugation, the viral pellet was resuspended in 0.5 mL of REK growth media and stored at -80°C.

REKs were grown to 20% confluence and the viron containing supernatant was exposed to the cells overnight and 5 µg/ml of polybrene was also added to the media. The next day, fresh media was placed onto each REK infected cell line and these cell lines were passed five times before being visualized under a confocal microscope. Each REK cell line was successfully transduced with 95-100% of all cells expressing the Cx43 mutants.

4.2.3 Antibodies and imaging

Immunofluorescence was performed by incubating the cells overnight with an anti-C-terminal Cx43 antibody (P4G9; from the Fred Hutchinson Cancer Research Center Antibody Development Group, Seattle, WA) at a dilution of 1:200; an anti-GP130 antibody (to denote the Golgi apparatus) (GP130, Stressgen, Ann Arbor, MI) at a dilution of 1:250; an anti-PDI antibody (to denote the endoplasmic reticulum) (Stressgen, Ann Arbor, MI) at a dilution of 1:500; and an anti-E-cadherin (Zymed (Invitrogen), 18-0223, Carlsbad, CA), anti-claudin-1 (Zymed (Invitrogen), 71-7800, Carlsbad, CA) and anti-occludin (Zymed (Invitrogen), 71-1500, Carlsbad, CA) to view proteins involved in tight junction and cadherin based adhesion at a dilution of 1:250. For secondary antibody

labeling, anti-mouse Alexa 555 (Invitrogen, A21425, 1:500), or anti-rabbit Alexa 555 (Invitrogen, A21429, 1:500) antibodies were used. DAPI staining was also performed to visualize nuclei and immunolocalization imaging was performed using a Zeiss 510 META confocal microscope (Zeiss, Toronto, ON). Endogenous Cx43 plaques were labeled with the P4G9 anti-Cx43 antibody and immunofluorescent images of equal cell culture area were acquired from both the vector control and the fs230 expressing REKs. An experimenter blinded to the identity of each cell line was asked to count the number of punctate structures present at sites of cell-cell apposition in each image. A gap junction plaque was defined as a punctate immunolabeled structure of a size greater than 0.1 μm . The total number of nuclei (as revealed by DAPI staining) was also counted and the number of punctate structures was divided by the total number of nuclei per image to get the average number of gap junction plaques per cell.

Primary antibodies for Western blot analysis were used as follows: C-terminal Cx43 (Sigma, 1:5000), N-terminal Cx43 (from the Fred Hutchinson Cancer Research Center Antibody Development Group, Seattle, WA; dilution of 1:500), p368 Cx43 (Cell Signaling Technologies, 3511, 1:1000), E-cadherin (Zymed, 18-0223, 1:1000), occludin (Zymed, 71-1500, 1:1000), loricrin (Covance, PRB13-145P, 1:1000), Cx26 (Zymed, #71-0500, 1:1000), CK14 (Neomarkers MS-115-P, 1:1000), claudin-1 (Zymed, 71-7800, 1:1000) and GAPDH (Millipore, MAB374, 1:15,000). Primary antibodies were diluted in 5% Blotto (Santa Cruz) or 3% bovine serum albumin (for p368 Cx43 antibody) and nitrocellulose membranes were incubated with each antibody overnight. Depending on the antibody used, primary antibody detection was performed using mouse or rabbit IgG IRdye 800 (Rockland Immunochemicals, PA) and mouse or rabbit IgG Alexa 680 (Invitrogen, Burlington, ON) secondary antibodies. Imaging and densitometry was performed using the Odyssey software packaged with the Odyssey infrared imaging system (Licor) and data values were graphed using Graphpad Prism v4.0.

4.2.4 Microinjection

REKs were grown to a confluent monolayer and single cells were pressure-microinjected with 5% Lucifer yellow (Molecular Probes) using an Eppendorf microinjection system

coupled to a Leica inverted epifluorescent microscope. One minute after microinjection of Lucifer yellow dye, the incidence of dye transfer was determined where dye transfer to one or more adjacent cells was deemed positive dye transfer.

4.2.5 Organotypic culture

Culture inserts with a 3.0 μm pore size (BD, Bedford, MA) were coated with a collagen I substrate by mixing 4.25 mL of type I collagen (BD, Bedford, MA) with 0.5 mL of 10X HBSS with Phenol Red (Sigma), 50 μL of 1.0M HEPES (Gibco) and 75-100 μL of 1M NaOH. Collagen was polymerized by incubation at 37°C for two hours. The collagen layer was then washed with REK growth medium and REKs were plated at a density of 1.5×10^5 per well in the upper chamber and 2 mL of REK growth medium was placed in the lower chamber. After three days, media from the upper chamber was removed to expose the confluent REKs to air and to induce differentiation. Cultures were fed daily by replacing the lower chamber media with 2 mL of fresh REK growth media. After two weeks under differentiation conditions, REKs were processed for histological and Western blot analysis.

4.2.6 Histological analysis

Two week organotypic epidermis was fixed with 3.8% formalin for five hours. After five hours, samples were stored at 4°C in PBS. Tissue processing, embedding, sectioning (5 μm sections) and haemotoxylin & eosin staining was performed as previously described (Langlois et al., 2010).

4.2.7 Acetone induced injury

Acetone induced injury was performed as previously described (Ajani et al., 2007). After one week under differentiation conditions, organotypic epidermal cultures were left untreated or treated with 0.5 mL of 100% acetone for 30 seconds. Acetone was then washed off and the cultures were placed back in the incubator. Acetone treatment was repeated following three days of recovery. Four days after the organotypic cultures were allowed to respond to the acetone insult, they were processed for histological analysis.

4.2.8 Scrape loaded dye transfer assay

As previously describe in Lai et al (Lai et al., 2006), monolayer cultures of REKs were washed once with Hanks Balanced Salt Solution (HBSS) and a scrape was made down the center of each culture plate using a 1 mL pipette tip. Wells were washed once with HBSS and 1.5 mg/mL sulforhodamine B diluted in HBSS was added to the scraped monolayer. After ten min on ice, cultures were rinsed with PBS and evaluated under a fluorescence microscope. As a control, 2 mg/mL rhodamine-dextran, which cannot pass through gap junctions, was used in a separate set of wells to control for fluorescence uptake due to cell death. Since the specific fluorescence generated from GFP-tagged Cx43 and mutant variants was high, this prevented the use a dye which fluoresces with the same emission as GFP. The area of fluorescence in both groups were outlined and calculated using ImageJ and the area of dye transfer in the rhodamine-dextran group was subtracted from the area of dye transfer in the sulforhodamine group and graphed.

4.2.9 Transepithelial resistance

Transepithelial resistance measurements were taken as previously reported (Langlois et al., 2007). Briefly, 1.5×10^4 REKs were seeded on a 3.0 μm pore transwell insert (BD, Bedford, MA). After 24 hr a Millicel-ERS voltmeter (Millipore) was used to measure resistance in ohms. Measurements were taken for five consecutive days and the measurements from days 2-4 were averaged and graphed.

4.2.10 Statistics

All statistical tests were performed and graphed using GraphPad Prism 4.0 software. Given the multiple variability factors, assay comparisons between full length Cx43 expressing REKs and each individual mutant REK cell line created were performed using a t-test with a statistical cut off at $p < 0.05$.

4.3 Results

4.3.1 Localization and functional characterization of REKs expressing mutant Cx43

Rat epidermal keratinocytes (REKs) were engineered to express Cx43 or Cx43 mutants associated with ODDD to determine how only a subset of Cx43 mutants can cause skin disease. Two frame-shift mutants that have been reported to cause ODDD and palmar plantar hyperkeratosis (fs230, and fs260) (van Steensel et al., 2005; Vreeburg et al., 2007) and one previously characterized Cx43 trafficking mutant was included in the study (Simek et al., 2009). In addition, a mouse G60S mutant (Flenniken et al., 2005) that results in a phenotype mimicking the ODDD condition, and further represents a mutation in the 1st extracellular loop region of Cx43, was also included. The missense human G21R and G138R mutants were selected since these mutants represent amino acid changes in Cx43 motifs within the N-terminal tail and cytoplasmic loop domain, respectively. Finally, controls included a REK cell line that expressed the empty viral vector as well as an REK cell line that expressed full length Cx43. To assist in Cx43 localization, all Cx43 variants were tagged with GFP at the C-terminal which has been shown to have minor effects on Cx43 distribution and function (Laird et al., 2001).

Localization of the Cx43 variants when expressed in REKs revealed that almost all cells were in fact expressing the Cx43 variants (**Fig. 4.1**). Similar to the full-length Cx43 and endogenous Cx43, the G21R and G138R mutants exhibited a cell surface distribution with abundant gap junction plaques. The G60S mutant, on the other hand, revealed few plaques with the bulk of the mutant retained within intracellular compartments. Both the $\Delta 244^*$ and fs230 mutants exhibited an ER-like phenotype with little to no evidence of gap junction plaques. Finally, the fs260 mutant was predominantly expressed in the perinuclear region which we have previously shown to be localized within the endoplasmic reticulum and the Golgi apparatus (Gong et al., 2006). To determine which subcellular organelle retained the fs230 mutant, fs230 expressing REKs were immunolabeled for the endoplasmic reticulum resident protein, protein disulphide isomerase (PDI), and the resident Golgi protein, gp130 (**Fig. 4.2A**). Only a small fraction

Figure 4.1 Cx43 mutants display different localization profiles in rat epidermal keratinocytes.

REKs were engineered by retroviral infection to stably express GFP-tagged full length (Cx43), two ODDD mutants that cause skin disease (fs230 and fs260), a C-terminal truncation with two additional mutations ($\Delta 244^*$), as well as three ODDD-linked mutants not associated with skin disease (G21R, G60S and G138R). Full length Cx43, as well as G21R, and G138R mutants, traffic to the plasma membrane and display large gap junctions while G60S, $\Delta 244^*$, fs230 and fs260 mutant expression is largely confined to intracellular compartments. Endogenous Cx43 was detected by immunolabeling (red) and nuclei were labeled with DAPI (blue). Bar = 10 μm .

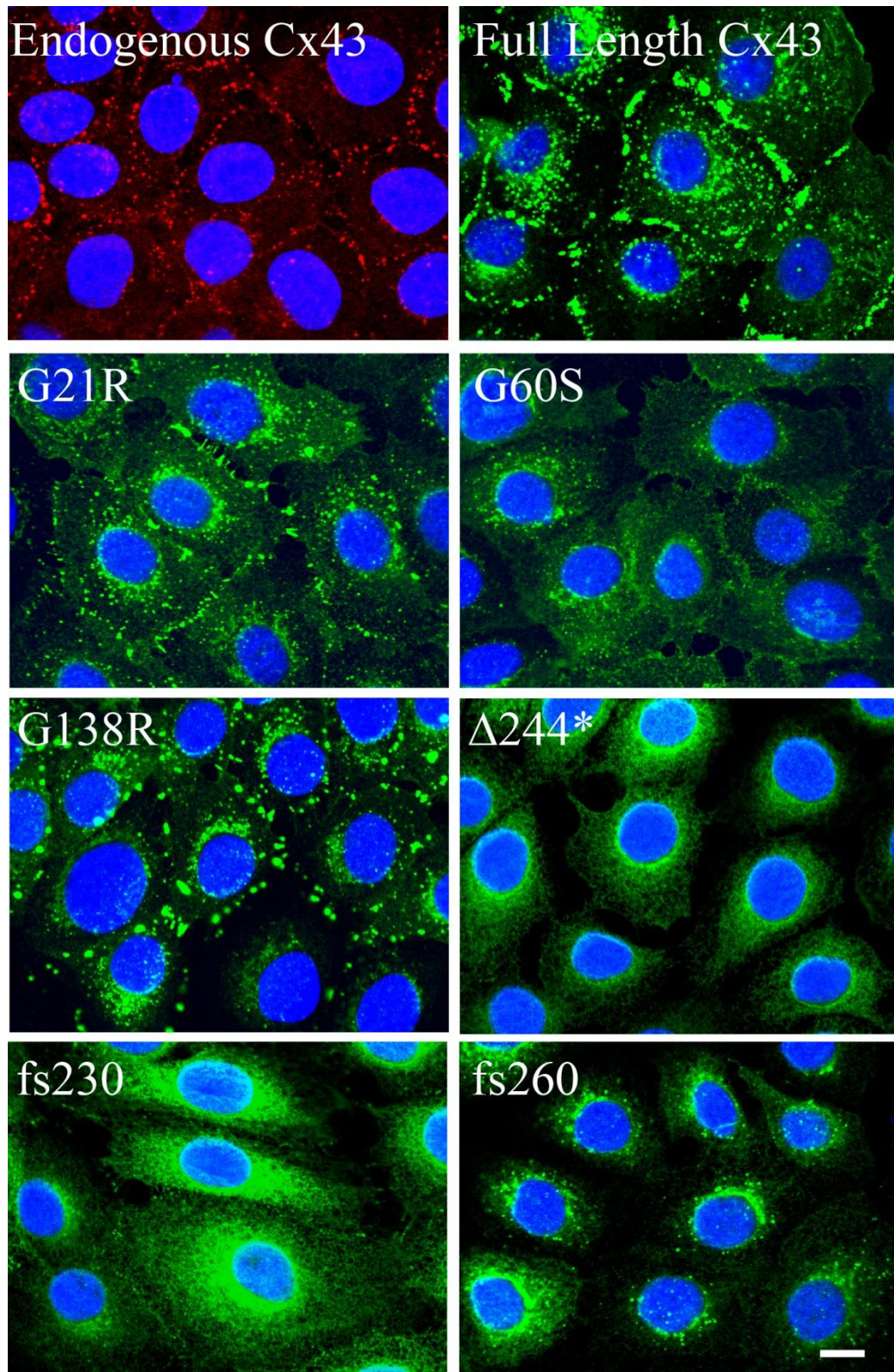
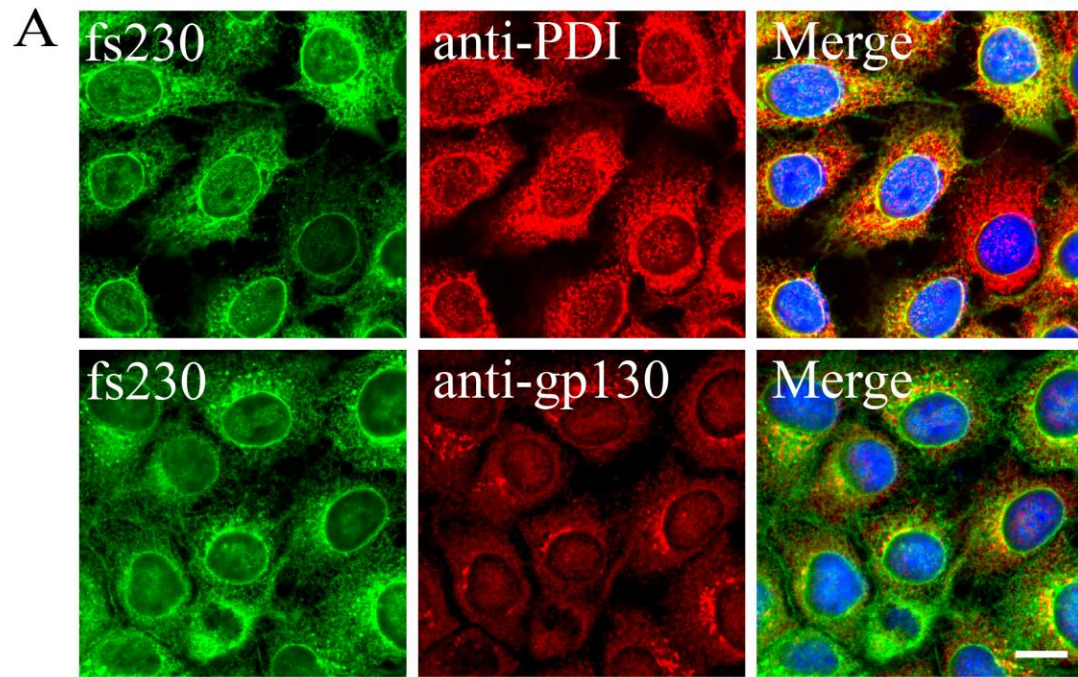
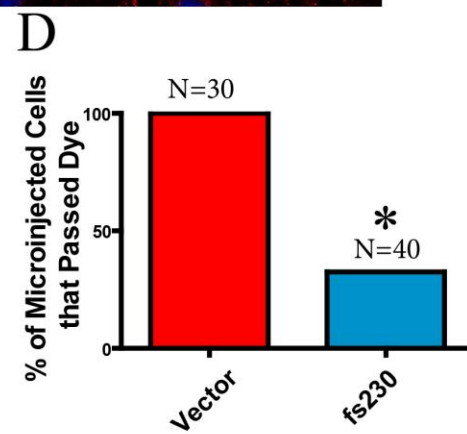
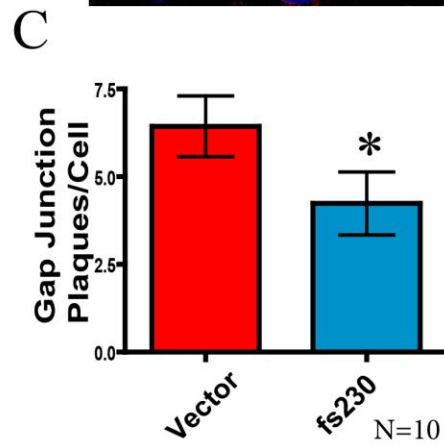
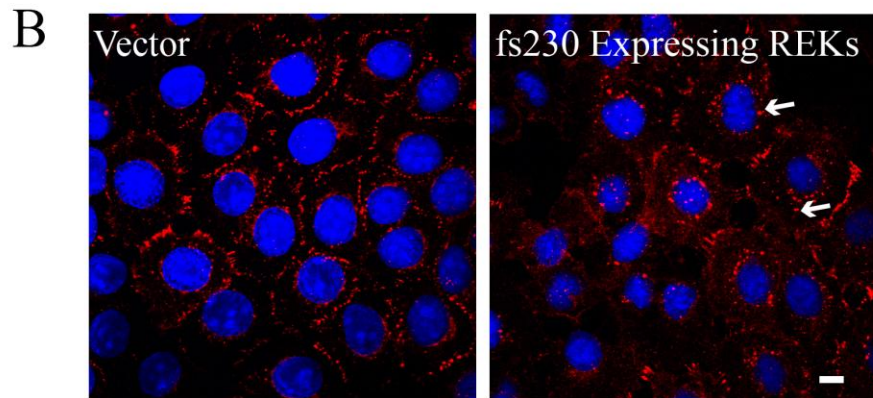


Figure 4.2 The fs230 mutant is predominantly localized within the endoplasmic reticulum and reduces the number of endogenous gap junctions and the extent of GJIC.

A. fs230 expressing REKs were labeled with antibodies specific for protein disulfide isomerase (PDI; ER resident protein) or gp130 (Golgi marker). The bulk of fs230 colocalized primarily with PDI. B. Both vector control and fs230 expressing REKs were immunolabeled with a C-terminal specific anti-Cx43 antibody that detected only endogenous Cx43. C. fs230 expressing REKs exhibited a 34% decrease in endogenous Cx43 plaques formation when compared to vector control REKs. D. Lucifer yellow dye was microinjected into both vector control and fs230 expressing REKs. All vector control REKs passed Lucifer yellow dye while only 33% of fs230 expressing REKs passed dye to neighboring cells. * $p < 0.05$. Nuclei were stained with DAPI (blue). Bar = 10 μm .



Anti- C-terminal Cx43



of the fs230 mutant was localized to the Golgi apparatus while a large population of the mutant was retained within the endoplasmic reticulum. Since the majority of the ODDD mutants examined thus far have been found to be dominant negative to endogenous Cx43 (McLachlan et al., 2005), the frequency of endogenous Cx43 gap junction plaques were assessed after labeling with an antibody directed to C-terminal domain of Cx43 that is lacking in the fs230 mutant variant. Compared to cells expressing an empty vector, the number of detectable endogenous Cx43 gap junction plaques was reduced when the fs230 mutant was expressed (**Fig. 4.2B, C**). To determine if the fs230 mutant expressing REKs could functionally pass Lucifer yellow dye to their neighboring cell, Lucifer yellow dye was injected into REKs expressing the empty vector or the fs230 mutant (**Fig. 4.2D**). Incidence of dye transfer revealed that 33% of the fs230 mutant expressing REKs and 100% of vector control REKs passed dye. This result suggests that the over-expressed fs230 mutant is also dominant-negative to the endogenous Cx43 protein.

To further evaluate the gap junction functional status of each REK cell line created, a dye transfer assay was performed on a wounded monolayer (**Fig. 4.3**). Scraped monolayers were either treated with a small dye (sulforhodamine B) which can pass through gap junctions (**Fig. 4.3A**) or, as a negative control, a large dye (rhodamine dextran) which cannot spread from one cell to another via gap junctions. In each ODDD mutant Cx43 expressing cell line, with the exception of the $\Delta 244^*$ expressing REKs, there was a significant decrease in the area of dye spread when compared to REKs expressing the full length Cx43 (**Fig. 4.3B**). These results suggest that all mutants (except $\Delta 244^*$) have the capacity to inhibit the function of endogenous Cx43 consistent with previous reports (Gong et al., 2007; Langlois et al., 2007; McLachlan et al., 2005).

4.3.2 Organotypic epidermal differentiation is affected by REKs expressing mutant Cx43

Given that the G21R, G60S, G138R, fs230, and fs260 mutants inhibit overall gap junction coupling in REKs, we sought to determine if this reduced cell coupling state could affect epidermal differentiation (**Fig. 4.4**). Surprisingly, all REK cell lines possess the ability to differentiate and establish multiple cellular layers (**Fig. 4.4A**). A basal layer,

Figure 4.3 Cx43 mutants reduce dye transfer in REKs.

A. To assess the ability of REKs to transfer dye to neighboring cells, a scrape assay was performed using a gap junction permeable dye, sulforhodamine. B. With the exception of $\Delta 244^*$, there was a significant reduction in dye spread in mutant expressing REKs compared to Cx43 over expressing REKs. v = empty vector. $*p < 0.05$. Bar = 100 μm .

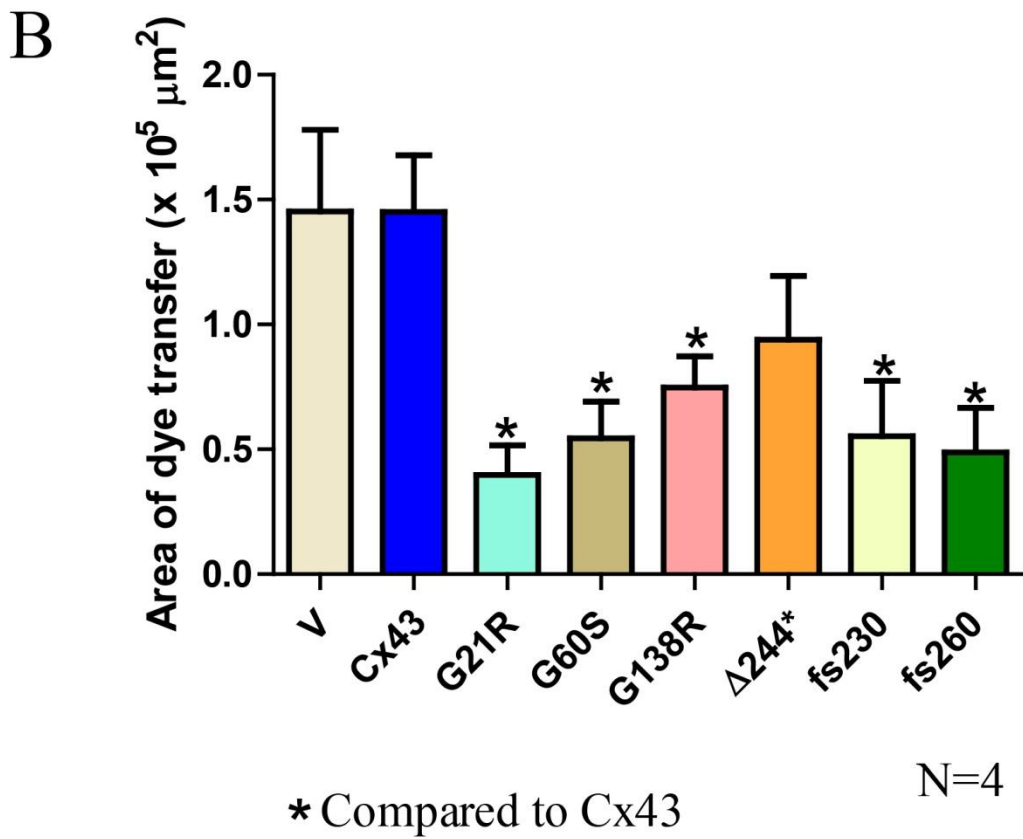
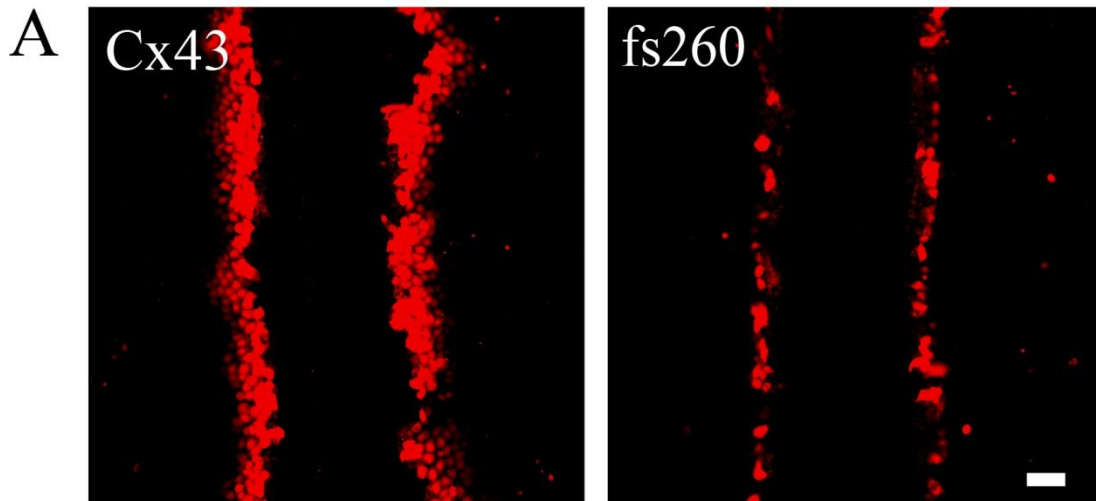
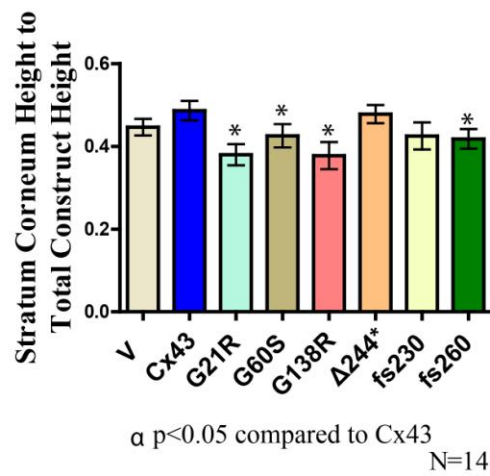
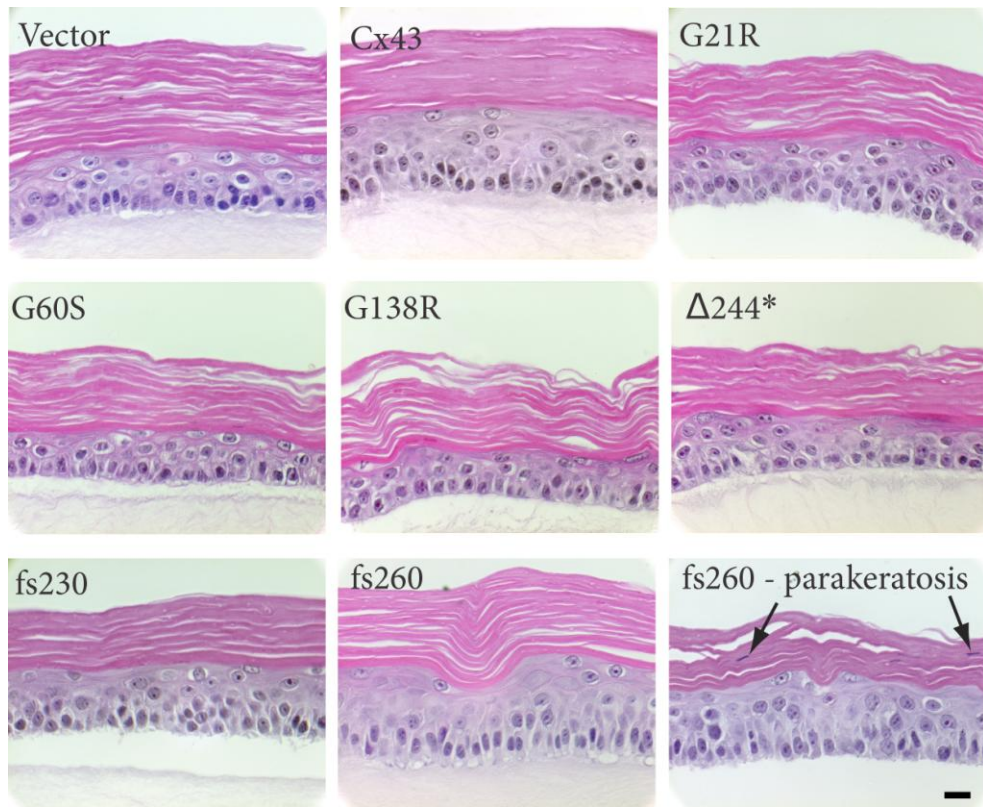


Figure 4.4 Cx43 mutant expressing REKs differentiate into organotypic epidermis.

REKs were plated onto collagen type I coated well inserts and media from the upper chamber was removed to allow REKs to differentiate and stratify. After two weeks of organotypic differentiation, all mutant expressing Cx43 REK cell lines differentiated. To determine the extent of organotypic differentiation, histological sections of each organotypic culture were stained with haematoxylin and eosin, imaged, and the upper stratum corneum and lower vital layer thicknesses were measured. When comparing the stratum corneum height to total epidermal height, there was a significant decrease found in the G21R, G60S, G138R, and fs260 expressing cultures when compared to organotypic cultures derived from Cx43 expressing REKs. In addition, parakeratosis was observed in the fs260 expressing cultures (arrows). * $p < 0.05$. Bar = 20 μm .



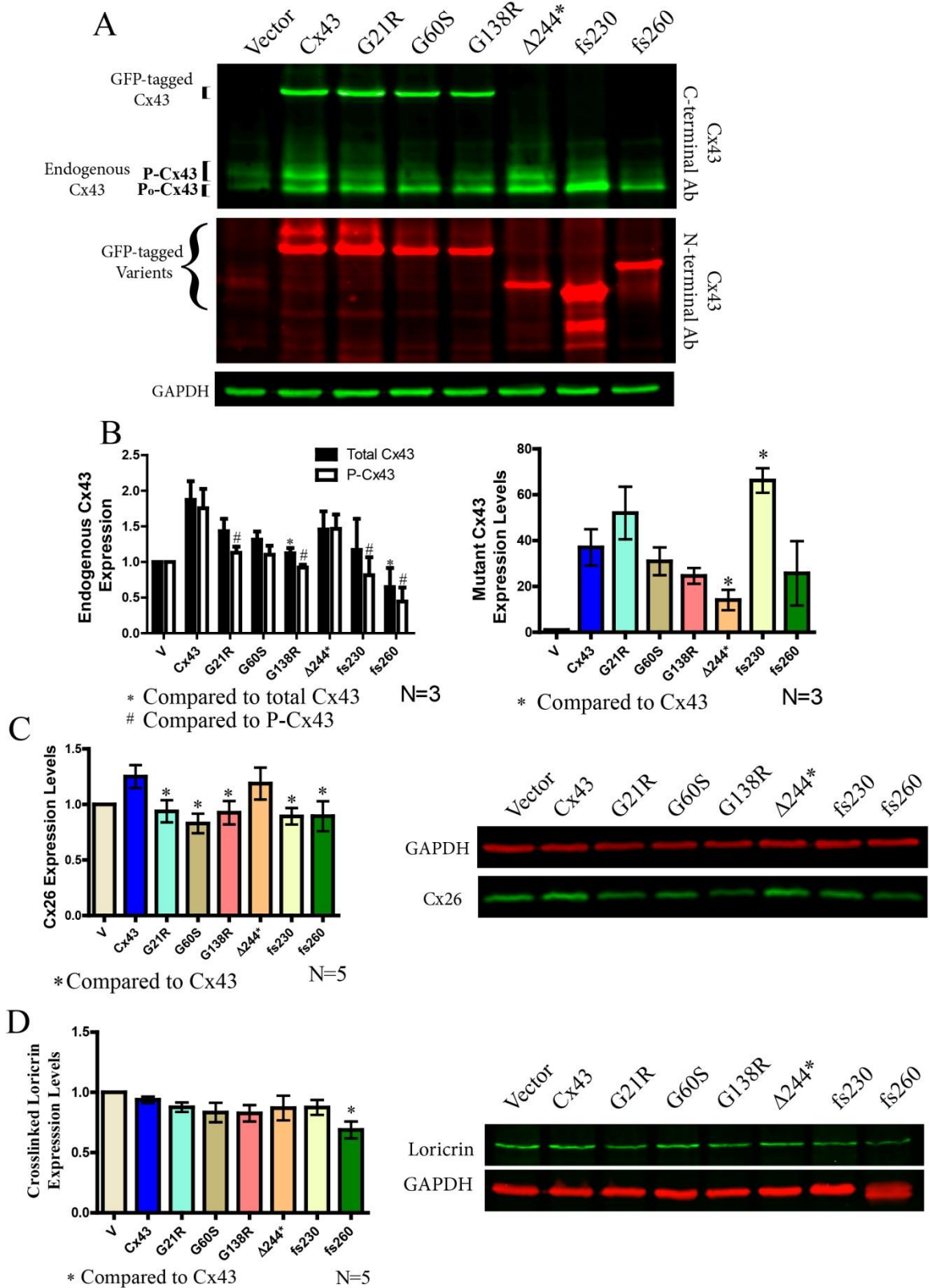
stratum spinosum, stratum granulosum and stratum corneum developed suggesting that epidermal formation can proceed with greatly reduced Cx43 gap junction function. Cx43 expressing REKs predominantly developed a tightly packed stratum corneum while in other REK cell lines, spaces were observed within the stratum corneum. In addition, nuclei were often observed in the stratum corneum of fs260 expressing REKs (typically called parakeratosis). The differentiation state was also analyzed by measuring the total organotypic architecture and stratum corneum layer thicknesses (corrected for the spaces in the stratum corneum) (**Fig. 4.4**). The stratum corneum thickness compared to the entire construct thickness was graphed and revealed that the G21R, G60S, G138R and fs260 organotypic epidermal cultures all developed a slightly thinner stratum corneum. This suggests that the expression of these ODDD-linked mutants in keratinocytes inhibits the formation of the stratum corneum.

4.3.3 Mutant Cx43 expression reduced the levels of phosphorylated Cx43, Cx26 and loricrin

Since endogenous Cx43 is co-expressed with the Cx43 variants during the differentiation process, the endogenous Cx43 content was examined in organotypic epidermal cultures (**Fig. 4.5A**). Western blots of organotypic epidermal cultures were performed using an antibody directed to the C-terminus of Cx43 which only detects endogenous Cx43, as well as an antibody directed to the N-terminus of Cx43 suitable for detecting all of the GFP-tagged Cx43 variants. As expected, all REK cell lines expressed the exogenous Cx43 variants to an approximately similar level as ectopic Cx43 with the exception that the $\Delta 244^*$ mutant was under-expressed and the fs230 mutant was over-expressed compared to the other mutants (**Fig. 4.5A, B**). It was notable the over-expression of GFP-tagged Cx43 resulted in an increase in the detectable levels of endogenous Cx43 suggesting that exogenous Cx43 was serving a role in stabilizing the endogenous population of Cx43 (**Fig. 4.5A, B**). Interestingly, the phosphorylated species of endogenous Cx43 (P-Cx43) was reduced (compared to Cx43 over-expressing cells) when the ODDD associated Cx43 mutants (G21R, G138R, fs230 and fs260) were co-expressed (**Fig. 4.5B**). Moreover, when Cx43 or the $\Delta 244^*$ mutant was over-expressed, there was an increase in Cx26 levels and this increase was not evident when any other ODDD

Figure 4.5 Assessment of endogenous and mutant Cx43, Cx26 and loricrin protein expression in organotypic epidermis.

Western blots were performed on REK cells lines after two weeks of differentiation. A. Anti-Cx43 N-terminal specific antibody was used to detect GFP-tagged mutant Cx43 variants while an anti-Cx43 C-terminal specific antibody was used to detect endogenous Cx43 expression. B. The G138R and fs260 expressing REKs had significantly lower total endogenous Cx43 levels when compared to full length Cx43 REKs. ODDD mutants also reduced the highly phosphorylated species of endogenous Cx43. Densitometry analysis of GFP-tagged Cx43 variants also revealed a significant decrease in the expression of the $\Delta 244^*$ mutant while the expression of the fs230 mutant was significantly elevated. In addition, Western blot analysis of Cx26 (C) revealed that all ODDD Cx43 mutants reduced the levels of Cx26 compared to cells expressing full length Cx43 while loricrin (D) was only reduced in fs260 expressing REKs. * $p < 0.05$.



linked mutant was over-expressed (**Fig. 4.5C**). Of all the mutants tested, only the fs260 mutant reduced the P_0 state of endogenous Cx43 when compared to ectopic Cx43 and this mutant was the only one to significantly inhibit the state of organotypic differentiation as assessed by a reduction in a key molecular marker of differentiation, loricrin (**Fig. 4.5D**).

4.3.4 Reduced barrier function in REKs expressing G60S, G138R, and fs260 Cx43 mutants

Since the epidermal barrier is important for proper epidermal function and Cx43 has been found to cross-talk with other junctional complexes (Li et al., 2009; Nagasawa et al., 2006), we assessed if mutant Cx43 expressing REKs can disrupt the transepithelial resistance (**Fig. 4.6**). Collectively, REKs which expressed the G60S, G138R and fs260 ODDD-linked mutants exhibited lower transepithelial resistance when compared to ectopic Cx43 expressing REKs (**Fig. 4.6A**). However, this reduction in transepithelial resistance was not due to expression level (**Fig. 4.6C, D**) or subcellular localization changes in occludin or claudin-1 or change in the cell adhesion protein, E-cadherin (**Fig. 4.6B**). In addition, reduced transepithelial resistance was not due to differences in cell death as revealed through the use of the multitox cell death assay (data not shown).

4.3.5 Organotypic epidermis expressing fs260 increased the vital layer thickness after acetone induced injury

We showed that organotypic cultures expressing the fs260 mutant developed a thinner stratum corneum thickness and exhibited parakeratosis. In addition, REKs expressing the fs260 mutant lowered the endogenous expression of Cx43, Cx26, loricrin and lowered the transepithelial resistance. Given these changes, REKs expressing this mutant may develop an aberrant epidermal barrier. To determine if the expression of mutant Cx43 in organotypic cultures can affect the epidermal cultures response to injury, an acetone induced injury and recovery assay was performed (**Fig. 4.7**). The stratum corneum in the full length Cx43 expressing REKs remained compact after acetone treatment while nuclei were enriched in the stratum corneum of fs260 expressing organotypic cultures (**Fig. 4.7A**). Since acetone treatment has been shown to induce a proliferative response

Figure 4.6 Cx43 mutant expressing REKs exhibited reduced transepithelial resistance

Cx43 mutant expressing REKs exhibited reduced transepithelial resistance when compared to Cx43 over expressing REKs in the absence of changes in the expression or localization of junctional proteins. A. Transepithelial resistance measurements of confluent monolayer cultures were taken daily for five days and the resistance from days 2-4 were averaged and graphed. B. E-cadherin, claudin1 and occludin were localized by immunofluorescent labeling in REKs over expressing GFP-tagged Cx43, G138R or fs260. Western blot analysis did not reveal any changes in the expression of occludin, E-cadherin, or claudin-1 (C and D). * $p < 0.05$.

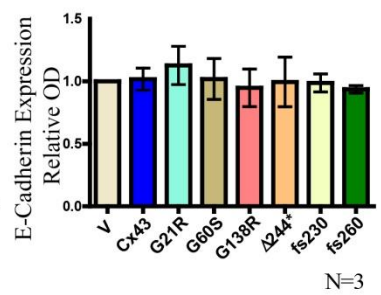
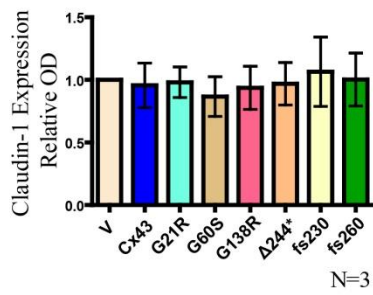
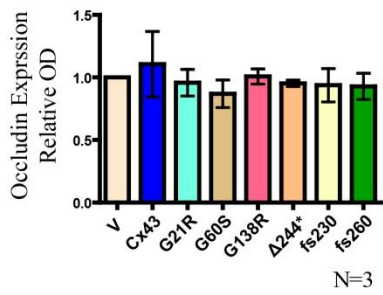
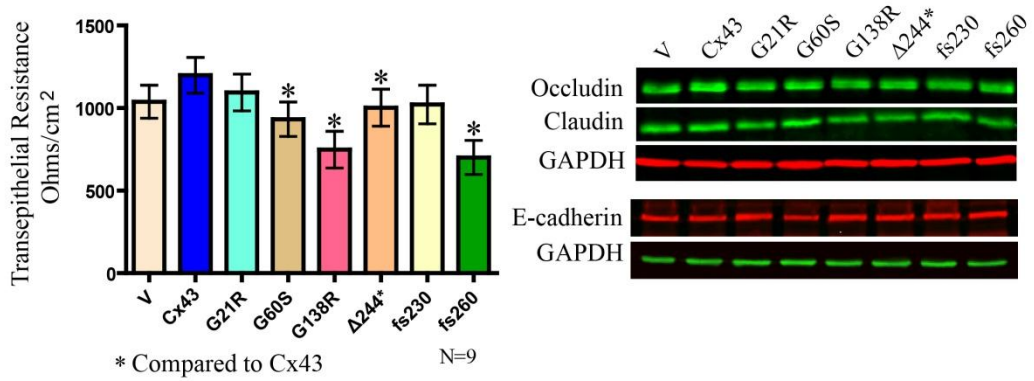
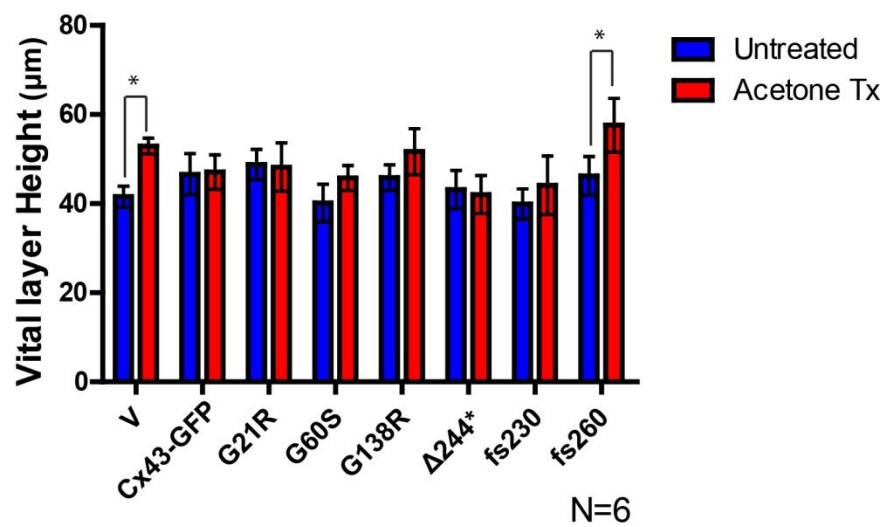
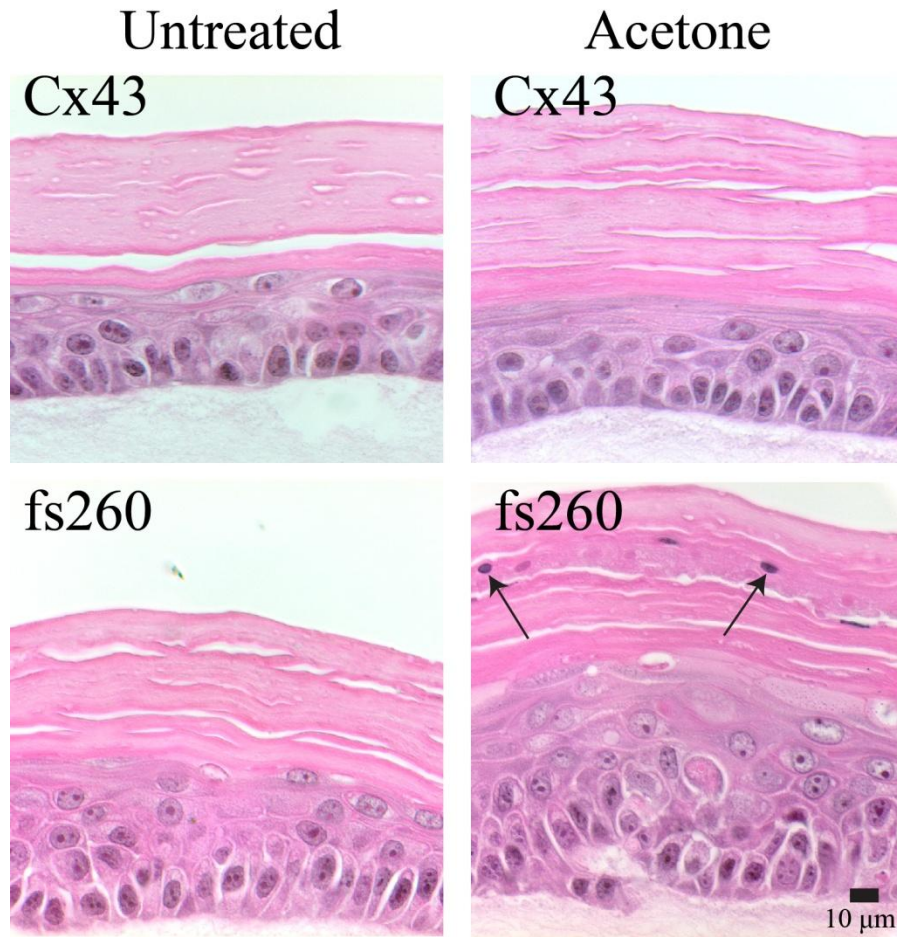


Figure 4.7 Acetone treatment increased the vital layer thickness in fs260 expressing organotypic cultures

A. Organotypic cultures of REKs expressing endogenous Cx43 or over expressing Cx43 or Cx43 mutants were left untreated or treated with acetone. Note that in fs260 expressing REK epidermis there were nuclei present in the stratum corneum (arrows). B. Vital layer measurements of all REK cell lines either untreated or treated with acetone revealed a significant increase in the vital layer thickness in both the vector and fs260 expressing REKs when compared to full length Cx43 expressing organotypic cultures. B. * $p < 0.05$. Bar = 10 μm .



(Ajani et al., 2007), vital layer thickness measurements were graphed between untreated and acetone treated organotypic epidermal cultures (**Fig. 4.7B**). While no differences were observed in the vital layer thickness in full length Cx43 expressing cultures, the fs260 expressing cultures formed a significantly larger vital layer thickness after treatment with acetone.

4.4 Discussion

4.4.1 Understanding skin disease in ODDD patients

Mutations in the gene encoding Cx43 have been conclusively linked to ODDD. Although there are currently 62 mutations that have been reported to cause ODDD (Paznekas et al., 2009), only the fs230 and fs260 Cx43 mutants have been reported to result in an additional skin disease phenotype (van Steensel et al., 2005; Vreeburg et al., 2007). In the case of the fs230 mutant, this is not always the case as a recent patient harboring this mutant exhibited no evidence of skin disease (Alao et al., 2010). The skin disease associated with these two mutants has been classified as palmar planter hyperkeratosis and the molecular etiology by which Cx43 mutations can cause skin disease remains unknown. To determine how select mutants can cause skin disease, various Cx43 constructs were expressed in REKs and assessed for their cellular localization, functional status, organotypic differentiation potential, transepithelial resistance, effect on endogenously expressed connexins, and finally response to chemical injury. In all assays performed, only the fs260 mutant expressing REKs consistently exhibit epidermal defects and we propose that the additive effects of these defects ultimately lead to palmar plantar hyperkeratosis.

4.4.2 Subcellular localization may reflect the disease burden of ODDD mutants

The fs230 and fs260 mutants are similar in that they result in C-terminal tail truncations but they differ dramatically in the extra non-connexin amino acid length. The fs230 mutant only has 6 extra amino acids (Vreeburg et al., 2007) while the fs260 mutant

possesses an additional 46 amino acids (van Steensel et al., 2005). While both of these mutants have been shown to be linked to palmar plantar hyperkeratosis, the fs230 mutant does not consistently cause this skin disease in all patients (Alao et al., 2010), which may be mechanistically linked to their primary subcellular residence. Immunofluorescent localization studies revealed that the fs230 mutant primarily resides in the endoplasmic reticulum. While the fs260 mutant is also found in the endoplasmic reticulum when it is expressed in REKs (Gong et al., 2006), a significant population escapes this compartments and reaches the Golgi apparatus (Gong et al., 2006). The importance of this finding is rooted in the fact that Cx43 oligomerization does not occur in the endoplasmic reticulum, possible though its interaction with ERp19 (Das et al., 2009), with final oligomerization being delayed until the Golgi apparatus (Musil and Goodenough, 1993). Thus, the bolus of the fs260 mutant in the Golgi apparatus would have an increased opportunity to oligomerize and inactivate co-expressed wild-type Cx43 by both preventing further transport to the cell surface and inhibiting channel function. Of all the frame-shift and missense Cx43 mutants examined to date, this characteristic of accumulating in the Golgi apparatus is unique to fs260. Thus, our results suggest that the fs230 mutant is not as potent in causing skin disease and this etiology may not manifest in all patients harboring this mutation as seems to be the case.

4.4.3 fs260 expressing REKs develop epidermal defects not observed by other ODDD mutants

A major advantage in using the REK cell line is the ability to model epidermal differentiation in culture. Surprisingly, all cell lines examined retain the ability to differentiate and form epidermal layers as found in thin skin. It was observed that the full length Cx43 expressing REKs did however form a very compact stratum corneum. Since proper calcium signalling in the upper stratum granulosum has been shown to facilitate the release of keratohyalin granules, cleave stratum corneum precursor proteins (profilagrin) and activate transglutaminases to crosslink proteins of the stratum corneum (loricrin) (Kimyai-Asadi et al., 2002), over-expression of functional Cx43 may enhance calcium signalling and facilitate the formation of this phenotype. Morphological evaluation of the organotypic epidermal cultures revealed that the stratum corneum layer

thickness was largest in the REK cell lines which expressed Cx43 variants (Cx43 and $\Delta 244^*$) that both maintained their dye transfer ability and the expression of the most phosphorylated Cx43 species. Since cells expressing both the Cx43 and $\Delta 244^*$ constructs developed a larger stratum corneum, we suggest that functional Cx43 levels can enhance the differentiation state of the epidermis. This is also supported by evidence that Cx43 is enhanced during restratification of the epidermis during development and after wound healing (Choudhry et al., 1997; Goliger and Paul, 1994; Kretz et al., 2003; Richards et al., 2004).

Given that a feature of hyperkeratosis is an enlarged stratum corneum, the observed decrease in the stratum corneum thickness in the fs260 expressing organotypic cultures was not expected. Since palmar plantar hyperkeratosis is only seen in a thick skin environment, our organotypic epidermal cultures may model a thin skin environment and not fully mimic the disease state found in thick skin. In addition, the relatively short time period used to establish organotypic epidermal cultures may only assess how mutant Cx43 affects the development of the epidermis and not represent the resulting steady state and maintenance after differentiation. Over time, keratinocytes expressing ODDD associated mutants may undergo unnecessary proliferative and regenerative events to result in an enlarged stratum corneum. The fs260 expressing organotypic epidermal cultures did however reveal nuclei present in the stratum corneum. This feature is however often observed in hyperkeratosis (Chopra et al., 1997) and suggests that the fs260 expressing keratinocytes may have a higher propensity to develop hyperkeratosis in vivo.

4.4.4 Cx26 cross-talk with Cx43 mutants

To biochemically assess the differentiation state of these organotypic cultures, Cx26, loricrin, and CK14 were evaluated using Western blot analysis. Cx26 is normally expressed in the stratum granulosum layer under terminal differentiation conditions and this expression was found to be lower in the ODDD mutant Cx43 expressing organotypic cultures as compared to REKs over-expressing full length Cx43. Mutant Cx26 has previously been shown to be transdominant to Cx43 (Rouan et al., 2001) and thus mutant

Cx43 may also be transdominant to Cx26. Since Cx26 mutants are strongly correlated with skin disease (hyperkeratosis) (Iossa et al., 2009; Maestrini et al., 1999; Uyguner et al., 2002), Cx43 mutants which reduce Cx26 levels may also contribute mechanistically to any resulting skin disease phenotype and also wound repair (Goliger and Paul, 1995).

4.4.5 Decreased levels of Cx43 may lead to epidermal barrier defects

Truncation of the C-terminal tail of Cx43 has previously been shown to disrupt the epidermal barrier in mice (Maass et al., 2004). To determine if the epidermal barrier function could also be affected in REKs expressing mutant Cx43, transepithelial resistance measurements and an acetone induced injury assay was performed on organotypic cultures derived from each REK cell line created. Although transepithelial resistance measurements assess the paracellular barrier formed by tight junctions, nevertheless, the introduction of Cx43 mutants lowered the transepithelial resistance values but had no effect on the levels or localization of claudin-1 or occludin, suggesting that the cross-talk between the gap junction status and tight junctions may be at the level of junction assembly and not at gene expression (de Carvalho et al., 2006). Given that the G60S, G138R, and fs260 mutants all moderately reduce transepithelial resistance, palmar plantar hyperkeratosis cannot be rooted solely to this finding. The fs260 mutant however did cause the greatest decrease in transepithelial resistance and since this mutant reduces the levels of phosphorylated Cx43 which is typically reflective of assembled gap junctions, other junctional complexes may be disrupted leaving the epidermis more prone to dysregulation when placed under stress. This in turn may lead to a proliferative response, an increase in epidermal thickness, and hyperkeratosis. Topical application of retinoic acid has been used to treat hyperkeratosis (Braun-Falco, 2009) and retinoic acid treatment has been shown to up regulate Cx43 expression (Guo et al., 1992; Masgrau-Peya et al., 1997). Thus, the up regulation of Cx43 may promote and stabilize the formation of junctional complexes and further maintain keratinocytes in a non-proliferative state.

To further determine if keratinocytes expressing mutant Cx43 have a normal epidermal barrier, acetone was administered to organotypic cultures and histological analysis was

performed after one week of injury. Acetone treatment has previously been shown to induce a proliferative response in organotypic cultures (Ajani et al., 2007). Organotypic cultures expressing full length Cx43 formed a compact epidermal barrier and no increase in the vital layer was seen as found in cultures that lacked Cx43 over expression. However, a significant increase in vital layer thickness was observed in fs260 expressing organotypic cultures. Collectively, these results suggest that Cx43, as well as most of the mutant variants of Cx43 but not fs260, can protect against acetone-induced injury.

While all mutations in the gene encoding Cx43 lead to ODDD, some mutations are clearly more potent leading to skin abnormalities. Typically, domain-specific Cx43 mutants all cause one or more measurable defects in processes related to epidermal differentiation. However, the fs260 mutant consistently caused quantifiable defects in REKs. In particular, organotypic cultures grown from cells expressing the fs260 mutant developed a thinner stratum corneum with nuclei often present and an enlarged vital layer when exposed to acetone. We proposed that the additive effects of these changes ultimately cause the skin disease phenotype observed in ODDD patients that express this mutant. Thus our findings demonstrate how one Cx43 mutant can cause increased disease burden over and above that caused by other Cx43 mutants.

4.5 References

- Ajani, G., N. Sato, J.A. Mack, and E.V. Maytin. 2007. Cellular responses to disruption of the permeability barrier in a three-dimensional organotypic epidermal model. *Exp.Cell Res.* 313:3005-3015.
- Alao, M.J., D. Bonneau, M. Holder-Espinasse, C. Goizet, S. Manouvrier-Hanu, A. Mezel, F. Petit, D. Subtil, C. Magdelaine, and D. Lacombe. 2010. Oculo-dento-digital dysplasia: lack of genotype-phenotype correlation for GJA1 mutations and usefulness of neuro-imaging. *Eur.J.Med.Genet.* 53:19-22.
- Baden, H.P., and J. Kubilus. 1983. The growth and differentiation of cultured newborn rat keratinocytes. *J.Invest Dermatol.* 80:124-130.
- Beyer, E.C., D.L. Paul, and D.A. Goodenough. 1987. Connexin43: a protein from rat heart homologous to a gap junction protein from liver. *J.Cell Biol.* 105:2621-2629.
- Bragg, J., C. Rizzo, and S. Mengden. 2008. Striate palmoplantar keratoderma (Brunauer-Fohs-Siemens syndrome). *Dermatol.Online.J.* 14:26.
- Braun-Falco, M. 2009. Hereditary Palmoplantar Keratodermas. *J.Dtsch.Dermatol.Ges.* 7:971-984.
- Chopra, A., Maninder, and S. Gill. 1997. Histopathological study of hyperkeratosis of palms and soles. *Indian Journal of Dermatology, Venereology, and Leprology.* 63:82-84.
- Choudhry, R., J.D. Pitts, and M.B. Hodgins. 1997. Changing patterns of gap junctional intercellular communication and connexin distribution in mouse epidermis and hair follicles during embryonic development. *Dev Dyn.* 210:417-430.
- Das, S., T.D. Smith, J.D. Sarma, J.D. Ritzenthaler, J. Maza, B.E. Kaplan, L.A. Cunningham, L. Suaud, M.J. Hubbard, R.C. Rubenstein, and M. Koval. 2009. ERp29 restricts Connexin43 oligomerization in the endoplasmic reticulum. *Mol.Biol.Cell.* 20:2593-2604.
- de Carvalho, A.D., S.W. de, and J.A. Morgado-Diaz. 2006. Morphological and molecular alterations at the junctional complex in irradiated human colon adenocarcinoma cells, Caco-2. *Int.J.Radiat.Biol.* 82:658-668.
- de Zwart-Storm, E.A., H. Hamm, J. Stoevesandt, P.M. Steijlen, P.E. Martin, G.M. van, and M.A. van Steensel. 2008. A novel missense mutation in GJB2 disturbs gap junction protein transport and causes focal palmoplantar keratoderma with deafness. *J.Med.Genet.* 45:161-166.

- Flenniken, A.M., L.R. Osborne, N. Anderson, N. Ciliberti, C. Fleming, J.E. Gittens, X.Q. Gong, L.B. Kelsey, C. Lounsbury, L. Moreno, B.J. Nieman, K. Peterson, D. Qu, W. Roscoe, Q. Shao, D. Tong, G.I. Veitch, I. Voronina, I. Vukobradovic, G.A. Wood, Y. Zhu, R.A. Zirngibl, J.E. Aubin, D. Bai, B.G. Bruneau, M. Grynepas, J.E. Henderson, R.M. Henkelman, C. McKerlie, J.G. Sled, W.L. Stanford, D.W. Laird, G.M. Kidder, S.L. Adamson, and J. Rossant. 2005. A Gja1 missense mutation in a mouse model of oculodentodigital dysplasia. *Development*. 132:4375-4386.
- Gillespie, F.D. 1964. A Hereditary Syndrome: "Dysplasia Oculodentodigitalis". *Arch.Ophthalmol.* 71:187-192.
- Goliger, J.A., and D.L. Paul. 1994. Expression of gap junction proteins Cx26, Cx31.1, Cx37, and Cx43 in developing and mature rat epidermis. *Dev.Dyn.* 200:1-13.
- Goliger, J.A., and D.L. Paul. 1995. Wounding alters epidermal connexin expression and gap junction-mediated intercellular communication. *Mol.Biol.Cell.* 6:1491-1501.
- Gong, X.Q., Q. Shao, S. Langlois, D. Bai, and D.W. Laird. 2007. Differential potency of dominant negative connexin43 mutants in oculodentodigital dysplasia. *J.Biol.Chem.* 282:19190-19202.
- Gong, X.Q., Q. Shao, C.S. Lounsbury, D. Bai, and D.W. Laird. 2006. Functional characterization of a GJA1 frameshift mutation causing oculodentodigital dysplasia and palmoplantar keratoderma. *J Biol Chem.* 281:31801-31811.
- Goodenough, D.A., J.A. Goliger, and D.L. Paul. 1996. Connexins, connexons, and intercellular communication. *Annu.Rev.Biochem.* 65:475-502.
- Guo, H., P. Acevedo, F.D. Parsa, and J.S. Bertram. 1992. Gap-junctional protein connexin 43 is expressed in dermis and epidermis of human skin: differential modulation by retinoids. *J.Invest Dermatol.* 99:460-467.
- Gutmann, D.H., E.H. Zackai, D.M. Donald-McGinn, K.H. Fischbeck, and J. Kamholz. 1991. Oculodentodigital dysplasia syndrome associated with abnormal cerebral white matter. *Am.J.Med.Genet.* 41:18-20.
- Gutstein, D.E., G.E. Morley, H. Tamaddon, D. Vaidya, M.D. Schneider, J. Chen, K.R. Chien, H. Stuhlmann, and G.I. Fishman. 2001. Conduction slowing and sudden arrhythmic death in mice with cardiac-restricted inactivation of connexin43. *Circ.Res.* 88:333-339.
- Iossa, S., V. Chinetti, G. Auletta, C. Laria, L.M. De, M. Rienzo, P. Giannini, M. Delfino, A. Ciccodicola, E. Marciano, and A. Franze. 2009. New evidence for the correlation of the p.G130V mutation in the GJB2 gene and syndromic hearing loss with palmoplantar keratoderma. *Am.J.Med.Genet.A.* 149A:685-688.

- Kelly, S.C., P. Ratajczak, M. Keller, S.M. Purcell, T. Griffin, and G. Richard. 2006. A novel GJA 1 mutation in oculo-dento-digital dysplasia with curly hair and hyperkeratosis. *Eur J Dermatol.* 16:241-245.
- Kimonis, V., J.J. DiGiovanna, J.M. Yang, S.Z. Doyle, S.J. Bale, and J.G. Compton. 1994. A mutation in the V1 end domain of keratin 1 in non-epidermolytic palmar-plantar keratoderma. *J.Invest Dermatol.* 103:764-769.
- Kimyai-Asadi, A., L.B. Kotcher, and M.H. Jih. 2002. The molecular basis of hereditary palmoplantar keratodermas. *J.Am.Acad.Dermatol.* 47:327-343.
- Kjaer, K.W., L. Hansen, H. Eiberg, P. Leicht, J.M. Opitz, and N. Tommerup. 2004. Novel Connexin 43 (GJA1) mutation causes oculo-dento-digital dysplasia with curly hair. *Am J Med Genet A.* 127A:152-157.
- Kretz, M., C. Euwens, S. Hombach, D. Eckardt, B. Teubner, O. Traub, K. Willecke, and T. Ott. 2003. Altered connexin expression and wound healing in the epidermis of connexin-deficient mice. *J Cell Sci.* 116:3443-3452.
- Lai, A., D.N. Le, W.A. Paznekas, W.D. Gifford, E.W. Jabs, and A.C. Charles. 2006. Oculodentodigital dysplasia connexin43 mutations result in non-functional connexin hemichannels and gap junctions in C6 glioma cells. *J.Cell Sci.* 119:532-541.
- Laird, D.W., K. Jordan, T. Thomas, H. Qin, P. Fistouris, and Q. Shao. 2001. Comparative analysis and application of fluorescent protein-tagged connexins. *Microsc.Res.Tech.* 52:263-272.
- Langlois, S., J.M. Churko, and D.W. Laird. 2010. Optical and biochemical dissection of connexin and disease-linked connexin mutants in 3D organotypic epidermis. *Methods Mol Biol.* 585:313-334.
- Langlois, S., A.C. Maher, J.L. Manias, Q. Shao, G.M. Kidder, and D.W. Laird. 2007. Connexin levels regulate keratinocyte differentiation in the epidermis. *J Biol Chem.* 282:30171-30180.
- Li, M.W., D.D. Mruk, W.M. Lee, and C.Y. Cheng. 2009. Connexin 43 and plakophilin-2 as a protein complex that regulates blood-testis barrier dynamics. *Proc.Natl.Acad.Sci.U.S.A.* 106:10213-10218.
- Maass, K., A. Ghanem, J.S. Kim, M. Saathoff, S. Urschel, G. Kirfel, R. Grummer, M. Kretz, T. Lewalter, K. Tiemann, E. Winterhager, V. Herzog, and K. Willecke. 2004. Defective epidermal barrier in neonatal mice lacking the C-terminal region of connexin43. *Mol.Biol.Cell.* 15:4597-4608.
- Maestrini, E., B.P. Korge, J. Ocana-Sierra, E. Calzolari, S. Cambiaghi, P.M. Scudder, A. Hovnanian, A.P. Monaco, and C.S. Munro. 1999. A missense mutation in connexin26, D66H, causes mutilating keratoderma with sensorineural deafness

- (Vohwinkel's syndrome) in three unrelated families. *Hum.Mol.Genet.* 8:1237-1243.
- Masgrau-Peya, E., D. Salomon, J.H. Saurat, and P. Meda. 1997. In vivo modulation of connexins 43 and 26 of human epidermis by topical retinoic acid treatment. *J.Histochem.Cytochem.* 45:1207-1215.
- McLachlan, E., J.L. Manias, X.Q. Gong, C.S. Lounsbury, Q. Shao, S.M. Bernier, D. Bai, and D.W. Laird. 2005. Functional characterization of oculodentodigital dysplasia-associated Cx43 mutants. *Cell Commun Adhes.* 12:279-292.
- Musil, L.S., and D.A. Goodenough. 1993. Multisubunit assembly of an integral plasma membrane channel protein, gap junction connexin43, occurs after exit from the ER. *Cell.* 74:1065-1077.
- Nagasawa, K., H. Chiba, H. Fujita, T. Kojima, T. Saito, T. Endo, and N. Sawada. 2006. Possible involvement of gap junctions in the barrier function of tight junctions of brain and lung endothelial cells. *J.Cell Physiol.* 208:123-132.
- Paznekas, W.A., B. Karczeski, S. Vermeer, R.B. Lowry, M. Delatycki, F. Laurence, P.A. Koivisto, L. Van Maldergem, S.A. Boyadjiev, J.N. Bodurtha, and E.W. Jabs. 2009. GJA1 mutations, variants, and connexin 43 dysfunction as it relates to the oculodentodigital dysplasia phenotype. *Hum Mutat.* 30:724-733.
- Petit, C. 2006. From deafness genes to hearing mechanisms: harmony and counterpoint. *Trends Mol.Med.* 12:57-64.
- Richard, G. 2005. Connexin disorders of the skin. *Clin.Dermatol.* 23:23-32.
- Richards, T.S., C.A. Dunn, W.G. Carter, M.L. Usui, J.E. Olerud, and P.D. Lampe. 2004. Protein kinase C spatially and temporally regulates gap junctional communication during human wound repair via phosphorylation of connexin43 on serine368. *J.Cell Biol.* 167:555-562.
- Rouan, F., T.W. White, N. Brown, A.M. Taylor, T.W. Lucke, D.L. Paul, C.S. Munro, J. Uitto, M.B. Hodgins, and G. Richard. 2001. trans-dominant inhibition of connexin-43 by mutant connexin-26: implications for dominant connexin disorders affecting epidermal differentiation. *J.Cell Sci.* 114:2105-2113.
- Scherer, S.S., L.J. Bone, S.M. Deschenes, A. Abel, R.J. Balice-Gordon, and K.H. Fischbeck. 1999. The role of the gap junction protein connexin32 in the pathogenesis of X-linked Charcot-Marie-Tooth disease. *Novartis.Found.Symp.* 219:175-185.
- Simek, J., J. Churko, Q. Shao, and D.W. Laird. 2009. Cx43 has distinct mobility within plasma-membrane domains, indicative of progressive formation of gap-junction plaques. *J Cell Sci.* 122:554-562.

- Uyguner, O., T. Tukel, C. Baykal, H. Eris, M. Emiroglu, G. Hafiz, A. Ghanbari, N. Baserer, M. Yuksel-Apak, and B. Wollnik. 2002. The novel R75Q mutation in the GJB2 gene causes autosomal dominant hearing loss and palmoplantar keratoderma in a Turkish family. *Clin.Genet.* 62:306-309.
- van Steensel, M.A., L. Spruijt, d.B.I. van, R.S. Bladergroen, M. Vermeer, P.M. Steijlen, and G.M. van. 2005. A 2-bp deletion in the GJA1 gene is associated with oculo-dento-digital dysplasia with palmoplantar keratoderma. *Am.J.Med.Genet.A.* 132A:171-174.
- Vanslyke, J.K., C.C. Naus, and L.S. Musil. 2009. Conformational maturation and post-ER multisubunit assembly of gap junction proteins. *Mol.Biol.Cell.* 20:2451-2463.
- Vreeburg, M., E.A. de Zwart-Storm, M.I. Schouten, R.G. Nellen, D. Marcus-Soekarman, M. Davies, M. van Geel, and M.A. van Steensel. 2007. Skin changes in oculo-dento-digital dysplasia are correlated with C-terminal truncations of connexin 43. *Am J Med Genet A.* 143:360-363.
- White, T.W., M.R. Deans, J. O'Brien, M.R. Al-Ubaidi, D.A. Goodenough, H. Ripps, and R. Bruzzone. 1999. Functional characteristics of skate connexin35, a member of the gamma subfamily of connexins expressed in the vertebrate retina. *Eur.J.Neurosci.* 11:1883-1890.

Chapter 5

5 The G60S Connexin43 Mutant Regulates Hair Growth and Hair Fiber Morphology in a Mouse Model of Human Oculodentodigital Dysplasia

Hair development relies on the proper signaling between modified epithelial keratinocytes and dermal fibroblasts (reviewed in Botchkarev and Paus, 2003). Since fibroblasts derived from ODDD patients and organotypic epidermal cultures expressing ODDD mutants displayed defects in their ability to differentiate, in vivo development and differentiation of the hair follicle may also be impaired by the expression of mutant Cx43. In addition, since ODDD patients have often been cited as developing hair defects, mutant Cx43 expression in the hair follicle is hypothesized to affect hair follicle structure, growth, and regeneration. This chapter evaluates the ability of mutant Cx43 to impair hair follicle structure, growth, and regeneration by using the G60S mouse model of ODDD and by studying hair samples derived from ODDD patients.

A version of this chapter is in press:

Churko, J.M., Chan, J., Pan, X., Shao, Q., Laird., D.W. Mice Expressing the G60S Mutant Cx43 Develop Similar Hair Abnormalities Commonly Presented by Oculodentodigital Dysplasia Patients (*Journal of Investigative Dermatology*, in press)

5.1 Introduction

A gap junction channel is composed of two connexin hexamers which allow direct intercellular communication between two contacting cells. These channels proceed to cluster into tightly packed arrays known as gap junctions. Connexin43 (Cx43) has been implicated in a wide variety of physiological events that include the synchronous beating of the heart (Jalife et al., 1999), bone development (Civitelli, 2008), and epidermal differentiation (Churko et al., 2010; Langlois et al., 2007). However, our current knowledge on the role of Cx43 in hair follicle differentiation and hair growth is limited.

In the skin, Cx43 is reported to be expressed in keratinocytes, dermal fibroblasts, the arrector pili muscle, sweat glands, sebaceous glands, and the hair follicle (Choudhry et al., 1997). In addition, Cx43 has also been reported to be expressed in the inner and outer root sheath, the dermal papilla, and the proliferating matrix in the rat hair follicle (Risek et al., 1992). While the expression of Cx43 within each histological distinct cellular layer of the hair follicle has been reported, to our knowledge, there are no studies that examine how Cx43 is linked to hair growth, the structure of the hair fiber or hair regeneration. In the present study we assess these physiological events in a mouse model of a Cx43-linked disease.

Oculodentodigital dysplasia (ODDD) is a disease associated with mutations in the gene that encodes Cx43. The majority of ODDD patients develop craniofacial defects, teeth abnormalities and syndactyly of the digits (Paznekas et al., 2003). In addition to these common developmental defects, poor hair growth or hair abnormalities is observed in approximately 25% of these patients (Paznekas et al., 2009). These same patients are also often reported to have hair that is dry, dull, thin, curly and sparse (Gorlin et al., 1963; Kelly et al., 2006; Kjaer et al., 2004; Paznekas et al., 2009; Sugar et al., 1966; Thoden et al., 1977). Hair fiber abnormalities were reported as early as 1977 in an ODDD patient who developed monilethrix and pili annuli changes in their hair fibers (Thoden et al., 1977). In addition, hair fibers from a patient expressing the L11P mutant were recently reported to develop a nodule/beaded appearance along the hair shaft (Kelly et al., 2006).

Given that a sub-populations of ODDD patients develop these hair abnormalities, Cx43 is proposed be involved in the differentiation and growth of hair.

Several mutant mouse lines (G60S, I130T and G138R) have now been established that mimic ODDD (Dobrowolski et al., 2008; Flenniken et al., 2005; Kalcheva et al., 2007). To date, the only reported hair defect in these mouse models are seen in the G138R mouse where ~30% of the mutant mice are born with sparse hair and this phenotype becomes more apparent in adulthood (Dobrowolski et al., 2008). However, it is not known whether any of these mouse models of ODDD also mimic other hair abnormalities present in ODDD patients. This study is the first to use a mutant mouse model as well as hair samples obtained from ODDD patients to examine the role of Cx43 in hair development, growth, and structure.

5.2 Materials and methods

5.2.1 Skin tissue collection

All animal experiments were approved by the Animal Use Subcommittee of the University Council on Animal Care at the University of Western Ontario. The G60S mice were developed by Dr. Janet Rossant at the Centre for Modeling Human Disease (University of Toronto, ON) (Flenniken et al., 2005). Dorsal neck and back skin samples from 5 WT and 5 G60S six- to eight-week old male mice from either untreated or epilation treated mice were dissected and placed in fixative solution of 4% formalin for 4 hours before being transferred into phosphate buffered saline (PBS). Paraffin embedded samples were cross sectioned at 5 μ m thickness. Tissue sections used to determine the hair follicle density were subjected to hematoxylin and eosin staining while tissue sections used to determine the localization of Cx43 were further immunolabeled.

5.2.2 Hematoxylin and eosin staining to determine hair follicle density

Skin sections were deparaffinized in xylene via 3 changes at 3 minute intervals followed by immersing in a series of ethanol solutions (100%, 100%, 100%, 95%, and 70%) for 3 minutes each. Sections were then stained in hematoxylin (Lerner Laboratories, Pittsburg,

PA) solution for 5 minutes followed by tap water for 5 minutes after rinsing. Slides were quickly dipped 8 times in acid ethanol (1% HCl in 70% ethanol) before staining with eosin (Lerner Laboratories, Pittsburg, PA) solution for 5 min. Slides were then put in ethanol (95% and 100%) for 3 changes each of 3 minutes followed by xylene for 3 changes of 5 minutes each and mounted using Cytoseal® 60 (Thermo Scientific, Waltham, MA). Slides were imaged using a Zeiss Axioplan 2IE microscope (Zeiss, AxioVision 4.7.2 software).

5.2.3 Cx43, phosphorylated histone H3 and cytokeratin 15 immunolabeling

Skin sections from untreated, WT Day 6 post-epilation and G60S Day 9 post-epilation mice were deparaffinized in xylene and passed through a series of ethanol solutions (95%, 95%, 70%, 70%, 50%, and 50%) for 2 minutes each. Sections were washed in PBS before antigen retrieval treatment with aqueous 1.8 mM citric acid and 8.2 mM sodium citrate solution in boiling water for 10 minutes. Sections were permeabilized with 0.2% Triton X-100 in PBS for 12 minutes, washed with 0.2% Tween-20 in PBS, and blocked with 2% BSA (Sigma-Aldrich, St. Louis, MO) in PBS containing 0.2% Triton X-100 for 30 min. Primary antibodies: rabbit anti-Cx43 polyclonal antibody (Sigma-Aldrich, St. Louis, MO) at a 1:500 dilution, cytokeratin 15 (CK15, Cat# ab17765, clone SPM190, Abcam, Cambridge, MA) at a 1:4 dilution or phospho-histone H3 (Ser28) antibody (Cat# 9713, Cell Signaling, Danvers, MA) at a 1:400 dilution in blocking buffer were incubated for 1 hour at room temperature. Alexa Fluor 555 (Invitrogen, Carlsbad, CA) goat anti-rabbit secondary antibody or Alexa Fluor 488 (Invitrogen, Carlsbad, CA) goat anti-mouse secondary was used at a dilution of 1:250 in blocking buffer for 1 hour. Nuclei were stained with DAPI dye (1:1000; Molecular Probes, Eugene, OR) for 5 min. Before mounting with Airvol (Air-products and Chemicals, Allentown, PA), sections were washed 1X with PBS for 3 minutes and 1X with water. To quantify phospho-histone H3 positive cells, 150 WT and 178 G60S mouse hair follicles were imaged from mouse skin six and nine days after epilation occurred. DAPI labeled nuclei and phospho-histone H3 labeled nuclei surrounding the dermal papilla were counted and the percent of phospho-histone H3 labeled nuclei were graphed.

5.2.4 Hair growth experiment

Four male WT and four male G60S six- to eight-week old mice (littermate grouping) were used to determine the hair growth rate. Mice were first anaesthetized using 5% isoflurane in combination with oxygen before the dorsal hair was shaved using electric clippers (Oster Golden A5 2-speed universal motor clipper). Initial shaving was performed to prepare the skin surface for either epilation or depilation treatments. For epilation treatment (complete removal of hair fiber and bulb), approximately 1-square inch of a NAIR® wax strips was used to remove the hair fiber and bulb. In a separate set of mice, the bulb region was kept intact and the visible hair fiber was removed using a NAIR® Hair Removal Cream containing calcium thioglycolate (depilation treatment). Hair length measurements were performed by plucking an average of 35 hairs from the post-treated (Day 12, 15, 18) regions following initial epilation or depilation treatment (Day 0). Hair fibers were mounted on slides using glycerol/water (4:1 v/v) solution. Hair fiber lengths were measured by first taking photographs using a Zeiss Axioplan 2IE microscope with camera (Zeiss AxioVision 4.7.2 software) and then using computer software (ImageJ 1.42) to manually determine lengths of individual hair fibers.

5.2.5 Analysis of coat hair

Adult dorsal hair was plucked using tweezers from the lateral non-treated region of adult mice coat hair (8 to 11 week old male mice). For adult hair length and diameter measurements, hair fibers were mounted using glycerol/water (4:1 v/v) solution. For finer analysis of hair under higher magnification, hair fibers were mounted using Cytoseal® 60 (Thermo Scientific, Waltham, MA). Photographs were taken using a Zeiss Axioplan 2IE microscope (Zeiss AxioVision 4.7.2 software) and measurements were made manually using computer software (ImageJ 1.42). Determination of pelage hair subtype of at least 200 hairs per mouse was done visually using light microscope under low magnification (2X).

5.2.6 Ultrastructural analysis

To analyze the hair samples from WT and G60S mice, scissors were used to gently cut the dorsal coat hair fibers. Human hair samples were obtained from ODDD patients with consent and under a University of Western Ontario approved research ethics protocol. Three separate hairs from both a mother and a son expressing the G143S mutant along with a three hairs from a patient expressing the T154A mutant Cx43 were obtained. Tweezers were then used to transfer the hairs to an aluminum stub coated with a sticky tape. The proximal region of the hair was handled to ensure handling did not damage the imaged region of the hair fiber. To analyze the proximal bulb and hair fiber region of WT and G60S mice, the mice were shaved using electric clippers (Oster Golden A5 2-speed universal motor clipper) and a Nair wax strip was used to epilate the embedded hair fiber and bulb. The wax strip was then cut into approximately 7 mm square pieces and placed onto the aluminum stubs. Stubs were then sputter-coated (Polaron THERMO, SC7620) with a 5 nm layer of Au/Pd. Hairs were then examined using a Hitachi S3000N scanning electron microscope (Hitachi Science Systems, Hitachinaka-Shi, Japan) at 15 kV and at a working distance of 15 mm

5.2.7 Statistical analysis

At least four mice were used per WT or G60S group for all experiments. Statistical analysis was done using Student's *t* test or ANOVA test and $p < 0.05$ was considered significant. All statistics were performed using GraphPad Prism version 4.02 for Windows (GraphPad Software).

5.3 Results

Since Cx43 was previously reported to be expressed in the skin (Choudhry et al., 1997; Risek et al., 1992), we sought to determine if Cx43 localization was altered in mice harboring a mutant form of Cx43. Immunofluorescent localization of Cx43 in skin taken from the backs of WT mice was consistent with previous reports (Choudhry et al., 1997; Risek et al., 1992) and Cx43 was also found to be localized to various regions of the hair follicle. During anagen, high Cx43 expression could be observed in the hair matrix

(HM), the outer root sheath (ORS) [basale, suprabasal, the companion layer (Cl)], the inner root sheath (IRS) [Huxle (Hx) and the cuticle (iCu) layer] and low Cx43 levels were observed in the dermal papilla (DP) and the connective tissue sheath (CTS) (**Fig 5.1**). Hair follicles were also co-labeled for Cx43 and a bulge stem cell marker cytokeratin 15 (CK15). Little Cx43 was found to be present in CK15-positive cells (**Fig 5.1c**). In hair follicles from WT mice, Cx43 localized to punctate plaque-like structures while the localization of Cx43 within the hair follicles of mutant mice was more diffused in appearance (**Fig. 5.1a, inserts**).

To determine if the observed difference in Cx43 localization in mutant mice might adversely affect the development and differentiation of the hair follicle, we analyzed hair follicle density, growth rates, and hair fiber structure in both WT and mutant mice. Visually, there was a decrease in hair density (hypotrichosis) in a subset of mutant mice (~20%) and this observation was most evident in the neck region of aged mice (**Fig. 5.2a**). The coat hair from these mice also appeared dull and had a “wooly” appearance. To empirically determine if mutant mice develop hypotrichosis, tissue sectioning of the neck and back skin was performed and the number of hair follicles per epidermal length was analyzed. Quantification of the number of hair follicles of 6-8 week old mice however, did not reveal any statistically significant differences between WT and mutant mice in either the neck or back region (**Fig. 5.2b**).

Since Cx43 is expressed in zig zag, guard, awl, and auchene hair follicle subtypes we sought to determine if Cx43 mutant expression could selectively impact the development of different hair subtypes. Within the WT and G60S mice (**Fig. 5.3a**), we found no significant differences between the proportion of any hair subtype suggesting that the Cx43 mutant does not selectively impact the differentiation of different mouse hair subtypes. When analyzing the different subtypes by light microscopy, hair fibers taken from the G60S mice revealed slight notching (arrows) as well as some twisted regions along the hair fiber (**Fig. 5.3b**). A notable difference in the size of the hair derived from the mutant mice was also observed. By quantifying both the length and thickness (diameter) of the most abundant hair subtypes (zigzag and awl), we found a statistically

Figure 5.1 Cx43 expression in the mouse hair follicle

A. Cx43 immunolabeling revealed that Cx43 is highly expressed in the hair matrix (HM) while little Cx43 expression was observed in the dermal papilla (DP). Cx43 gap junctions formed between cells in WT hair follicles while Cx43 was diffusely localized in mutant mouse follicles (inserts). B. Above the bulb region, Cx43 is expressed in multiple layers of the hair follicle. Med= medula, Cor= cortex, Cu= cuticle layer of the hair shaft, iCu= cuticle layer of the inner root sheath, Hx= Huxle layer, He= Henle layer, IRS= inner root sheath, Cl= companion layer of the outer root sheath (ORS), CTS= connective tissue sheath. C. Little Cx43 localized with CK15-positive cells in the hair bulge region (inserts). SG= sebaceous gland, HS= hair shaft. Bars= 20 μ m.

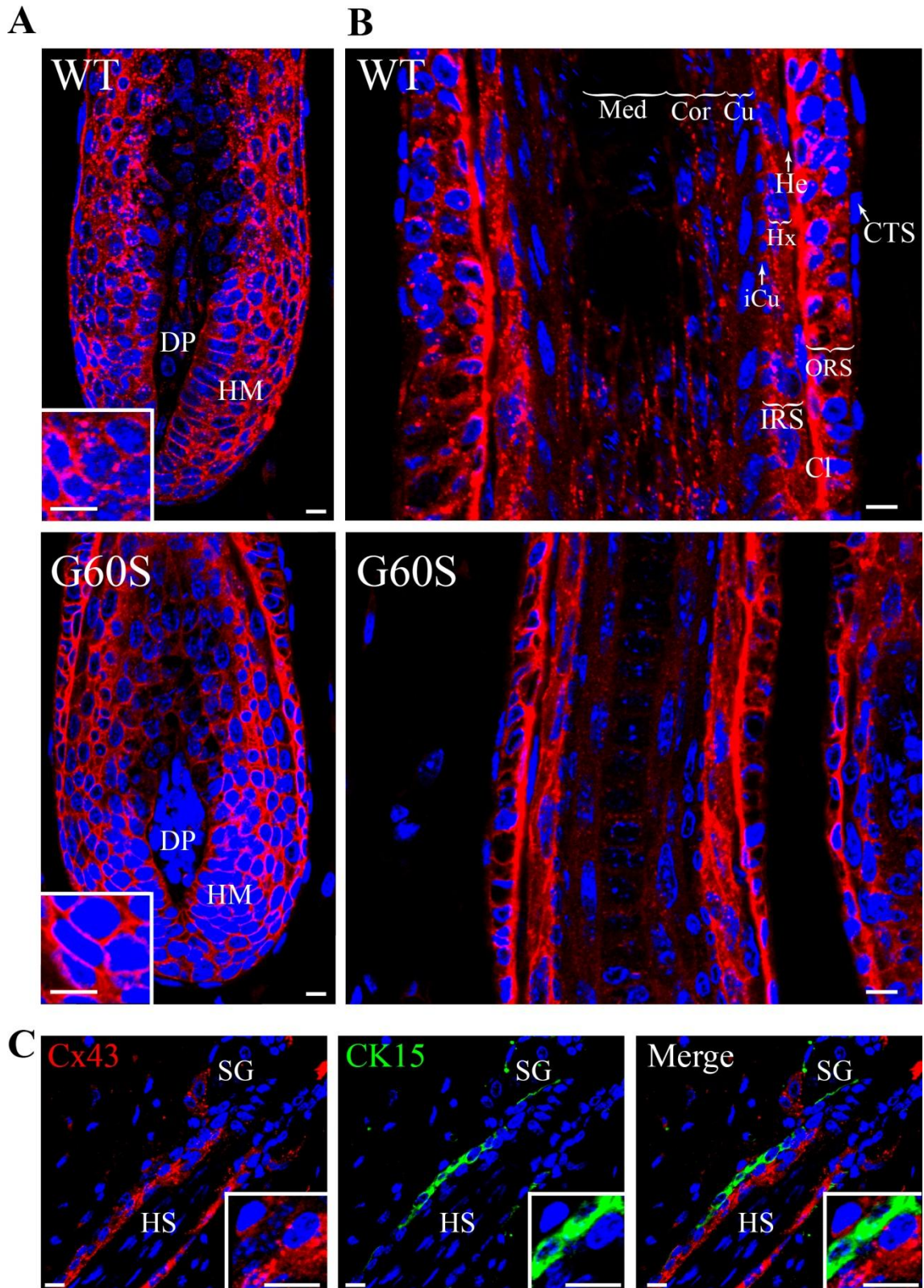


Figure 5.2 A subset of G60S mutant mice have sparse hair in the back and neck regions but overall hair density in mutant mice remains unchanged from wild type mice.

A. In approximately 20% of G60S mice, a decrease in hair follicle density could visually be observed. B. Quantification of the number of hair follicles per field of view after hematoxylin and eosin staining; however, revealed no significant difference in the adult hair follicle density of mutant mice. N=5. Bar= 100 μ m.

A



B

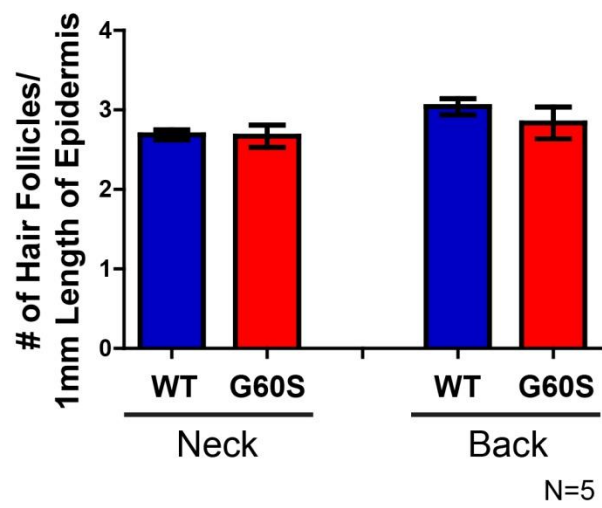
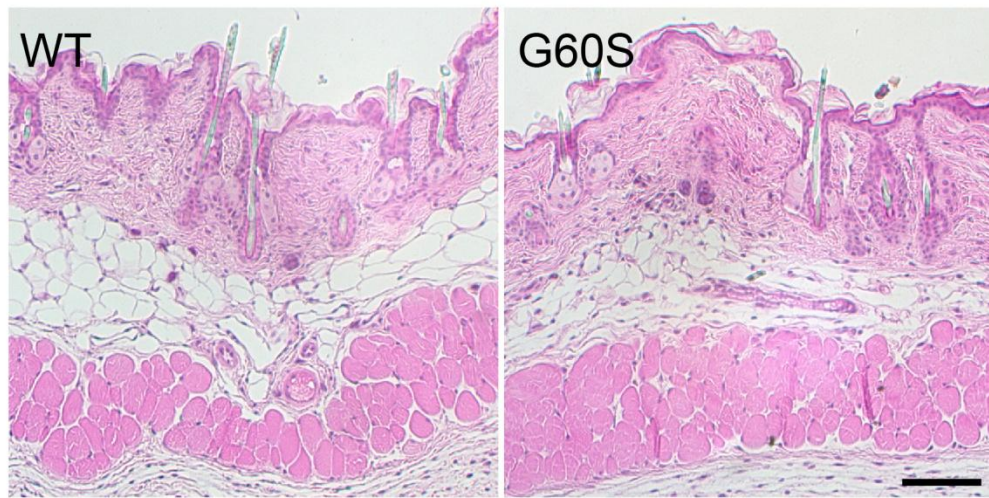
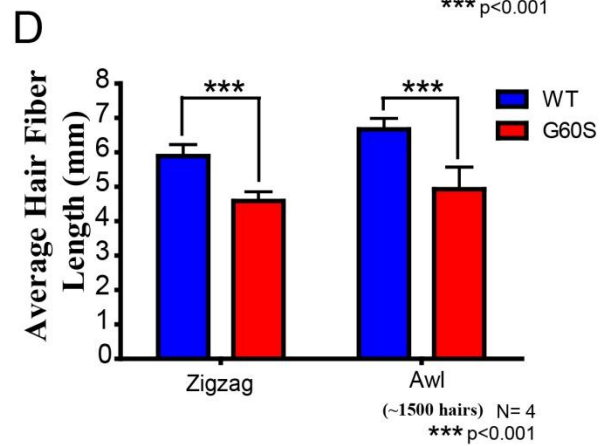
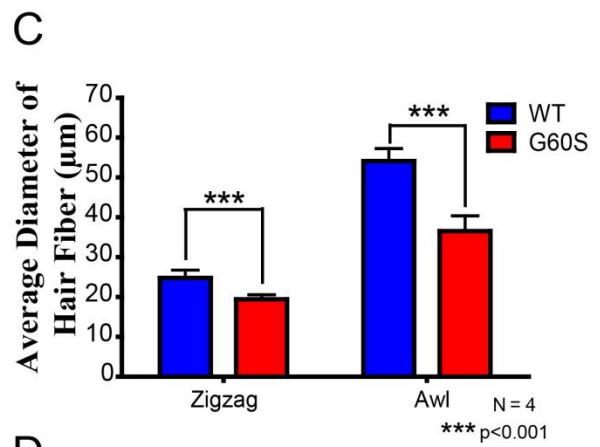
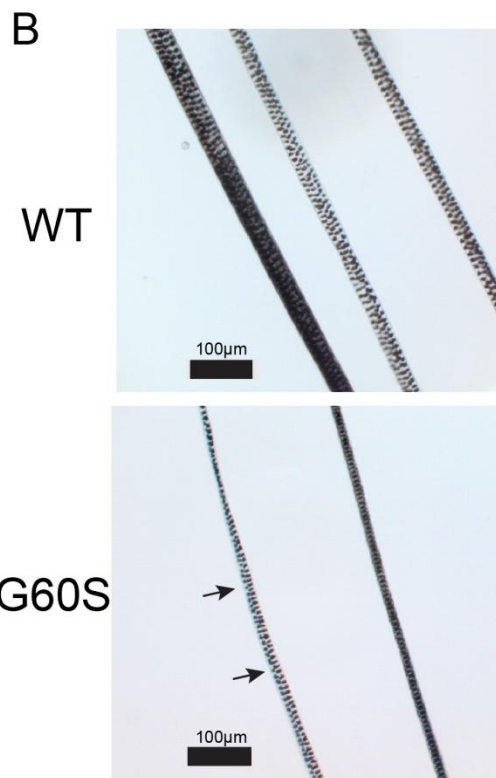
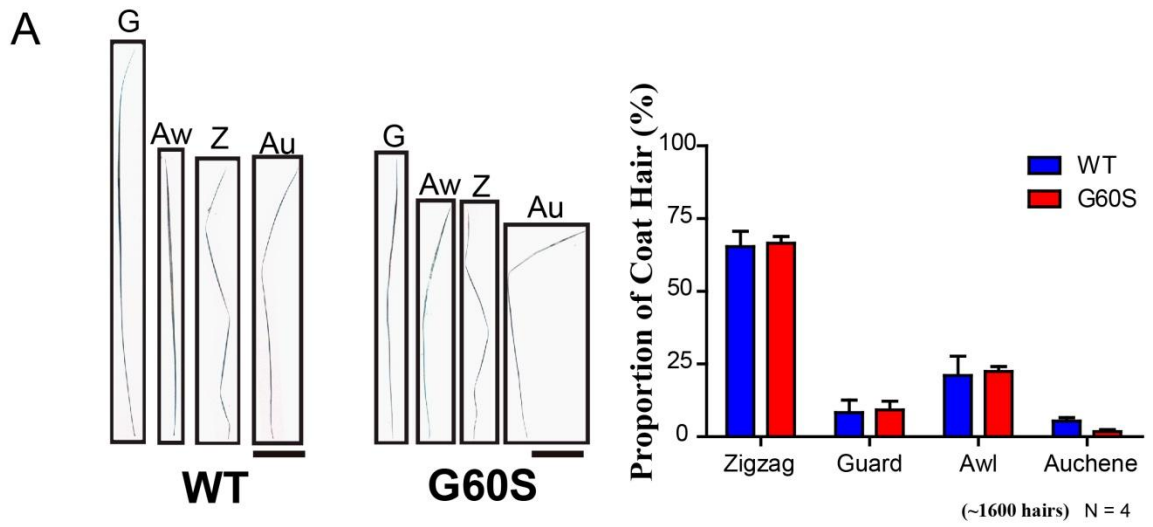


Figure 5.3 G60S mutant mice have the same frequency of hair subtypes as WT mice but develop thinner and shorter hair fibers

A. Fifty hairs from both WT (N=4) and G60S (N=4) mice were identified as being either zigzag (Z), guard (G), awl (Aw), or auchene (Au). There were no significant differences observed between the proportion of hair subtype between G60S and WT mice. B. Hair fiber diameter (C) and length (D) measurements were taken from four WT and four G60S mice (250 hairs measured). Hair fibers derived from G60S mice were significantly shorter (** $p < 0.001$, N=4) and thinner (** $p < 0.001$, N=4) when compared to WT mice. Bar= 1 mm in panel A and 100 μm in panels B.



significant decrease in both the thickness (**Fig. 5.3c**) and length (**Fig. 5.3d**) of mutant mouse hair.

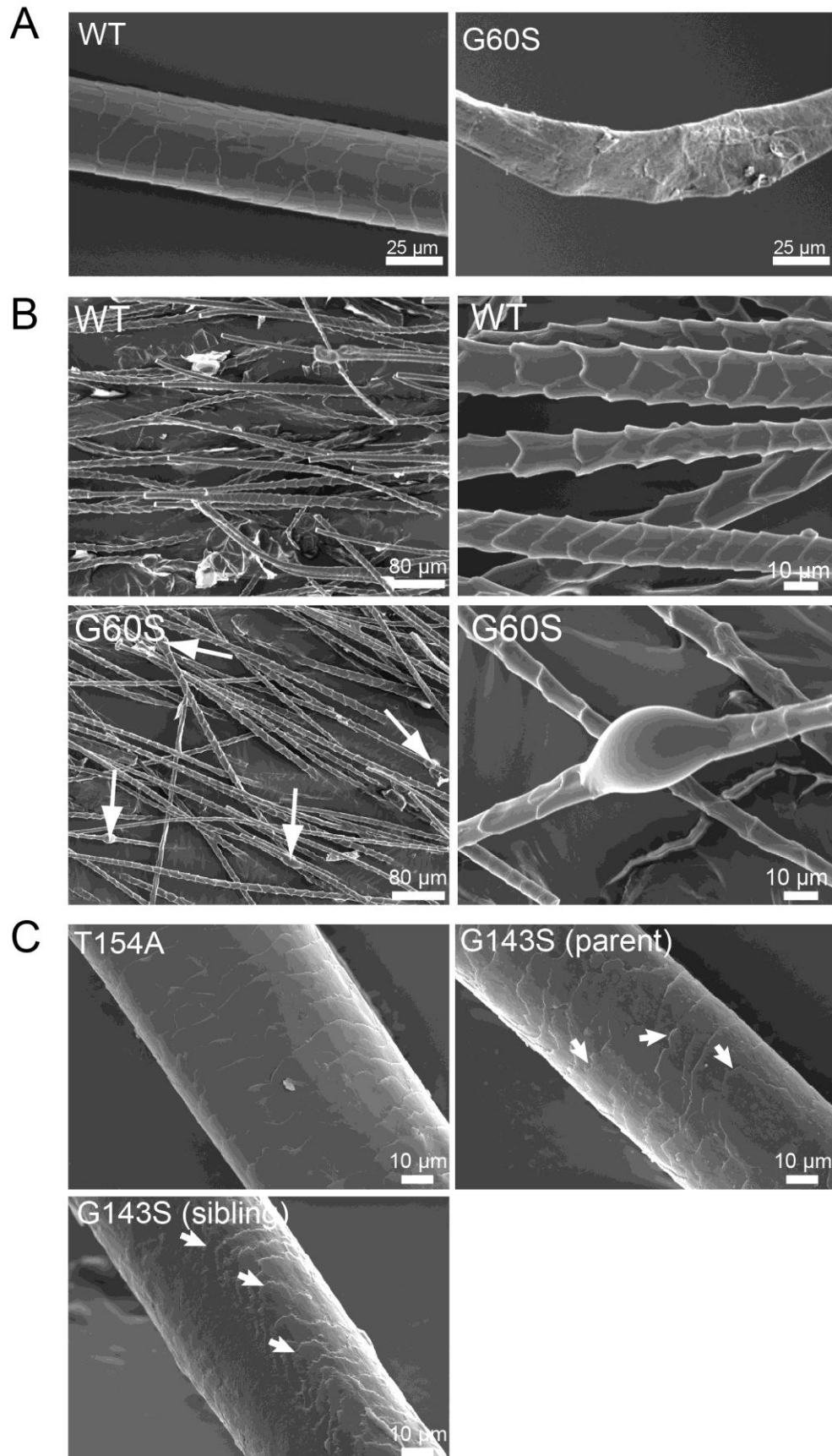
To analyze the ultrastructure of the hair fiber, scanning electron microscopy was performed on WT and G60S mouse hair fibers (**Fig. 5.4**). Both the distal (**Fig. 5.4a**) and the proximal region (**Fig. 5.4b**) of the hair fiber was imaged to distinguish between the hair fiber morphology from newly formed hair (proximal region) to that of hair fibers which may have undergone greater exposure to environmental stresses (distal region). In comparing the distal hair fiber region from eight week old WT and G60S mutant mice, the WT hair fibers contained well-formed scaling with little to no observable cuticle degradation. However, when analyzing the distal hair fiber from mutant mice, we found severe cuticle degradation. Some hair fibers even completely lacked this cuticle layer and the underlying cortical layer could be observed (**Fig. 5.4a**). To analyze the proximal region of the hair fiber, the dorsal coat hair was epilated, and the epilated hairs were analyzed again by scanning electron microscopy (**Fig. 5.4b**). Normal cuticle scales were evident in the proximal hair fibers taken from mutant mice but surprisingly, hair fiber nodule formation was observed (arrows). These nodules were not uniform, irregularly spaced, and could span 2-5 cuticle scale lengths.

An ultrastructural analysis of scalp hair obtained from ODDD patients harboring the T154A or G143S mutant was also performed by scanning electron microscopy (**Fig. 5.4c**). A female ODDD patient expressing the T154A mutant self-reported that her hair was thick, dry and fast growing while a patient with the G143S Cx43 mutant described her, and her son's, hair as curly and thin. Ultrastructural examination revealed no overt hair fiber abnormalities in a patient expressing the T154A mutant while the hair fibers from both the mother and son expressing the G143S mutant revealed significant scale weathering with irregular scale borders (**Fig. 5.4c** arrows).

Another common condition reported in ~25% of patients with ODDD is that their hair grows slowly (Paznekas et al., 2009). To determine if G60S mutant mice also mimic the human ODDD cases of slow growing hair, hair fiber length measurements were performed on WT and G60S mice hair that was previously epilated or depilated with the

Figure 5.4 Structural defects are observed in hair fibers from human ODDD patients and in the G60S mouse.

A. The distal region of the hair fiber from WT and G60S mice was compared by scanning electron microscopic analysis. Hair fibers from the G60S mice revealed significant weathering in the cuticle layer. B. The proximal region of the hair fiber was also evaluated under low and high magnification by scanning electron microscopy to reveal nodules along many hair fibers (arrows). C. Cuticle weathering was also observed in patients expressing the G143S mutant. Scanning electron microscopic examination of the T154A hair fibers did not reveal any significant structural abnormalities. However, hair from two patients (parent and sibling) expressing the G143S mutant revealed cuticle weathering.



application of calcium thioglycolate (Nair cream) (**Fig. 5.5**). Images of hair regrowth were evaluated on the day of treatment (Day 0) and Day 6, 9, 12, 15, and 18 after epilation (**Fig. 5.5a**). Hair length measurements after epilation (**Fig. 5.5b**) and depilation (**Fig. 5.5c**) revealed that hair fibers plucked from the G60S mice were consistently shorter than hair fibers plucked from the WT mice. In addition, after epilation treatment, the WT mice hair re-grew uniformly while hair growth from the backs of mutant mice was not synchronized (**Fig. 5.5d**). The largest delay in re-growth was determined to be within the neck (cranial) region of these mice.

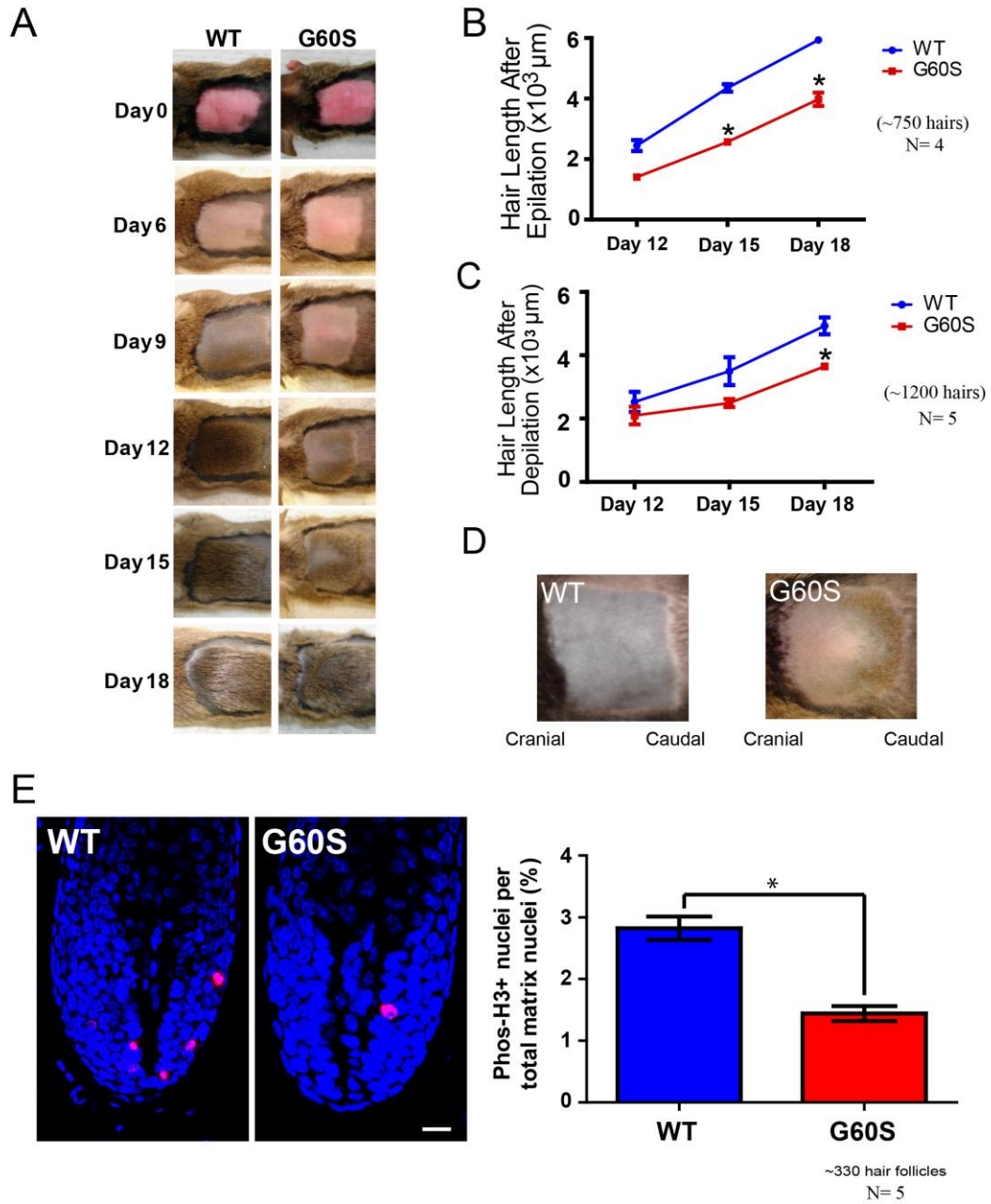
Since G60S mutant mouse hair fibers grew slower than WT hair fibers, we investigated if the mitotic output was lower in hair follicles from mutant mice. WT and G60S mouse anagen hair follicles from skin regions previously epilated (day 6 and day 9 after epilation) were labeled with the M-phase specific marker phosphorylated-histone H3 and the percentage of the phosphorylated-histone H3-positive nuclei in the hair matrix was quantified (**Fig. 5.5e**). In WT mouse hair follicles, there were significantly more phosphorylated-H3-positive nuclei when compared to hair follicles from G60S mutant mice. In addition, there was significantly more cells (nuclei) in the WT mouse hair matrix ($p < 0.05$, average nuclei \pm SEM: WT = 106 ± 02.8 , G60S = 86 ± 2.1 , N=5, n=328 follicles analyzed) while no differences were observed in the amount of dermal papilla nuclei (average nuclei \pm SEM: WT = 10.15 ± 0.45 , G60S = 10.07 ± 0.35 , N=5, n=328 follicles analyzed).

5.4 Discussion

Cx43 is the most widely expressed connexin within the human body and it has been reported to regulate many developmental processes (Elias and Kriegstein, 2008; Hatler et al., 2009; Nagata et al., 2009; Toth et al., 2010). Cx43 is expressed in the follicular and interfollicular epidermis however; the various roles that Cx43 may play in regulating these compartments have not been characterized. Given that the expression of mutant Cx43 in some patients leads to structural hair fiber abnormalities (Adamski et al., 1994; Kelly et al., 2006; Thoden et al., 1977) and slow growing, thin, dry and dull hair (Gorlin et al., 1963; Kjaer et al., 2004; Paznekas et al., 2009; Sugar et al., 1966), we postulated

Figure 5.5 Hair regrowth is delayed in G60S mice.

A. The backs from WT and G60S mice were imaged at Day 0, 6, 9, 12, 15, and 18 after epilation. Regrowth of hair was quantified by measuring the length of plucked hairs Day 12, 15, and 18 after epilation (B, $*p < 0.05$, N=4) or depilation (C, $*p < 0.05$, N=5). D. Asynchronous regrowth was observed in the neck region (cranial region) of G60S mice after epilation when compared to WT littermates. After both treatments, hair regrowth in mutant mice was delayed by approximately three days. E. Assessment of cell proliferation revealed that G60S hair follicles had significantly less phospho-histone H3-positive (Phos-H3+) cells in the hair matrix. ($*p < 0.05$, N=5). Bars= 50 μm .



that Cx43 may play a key role in hair development and growth. In this study, we found that Cx43 in mutant mice has a distinct Cx43 localization profile within the hair follicle, displays hair fiber structural abnormalities and grows slower. While the G60S mutant has not been reported in the human population (Paznekas et al., 2009), these mice display many similar hair defects also associated with ODDD patients. In addition, ultrastructural analysis of hair fibers from ODDD patients expressing the G143S mutant, but not the T154A mutant, also displayed cuticle degradation.

Cx43 was localized in a punctate pattern at sites of cell-cell apposition in WT mouse hair follicles while a diffuse pattern was observed in cells from the hair follicles of G60S mice. There appeared to be a notable reduction in gap junction plaques in mutant mice, and by definition a predicted reduction in gap junctional intercellular communication, but this is somewhat difficult to conclude with certainty as a putative up-regulation of Cx43 could mask the punctate gap junction plaque profile. We previously observed significantly reduced gap junctional coupling when the G60S mutant was expressed in reference cell lines that contained or lacked endogenous Cx43 (Churko et al., 2010; McLachlan et al., 2005) as well as in primary cardiomyocytes (Manias et al., 2008) or osteoblasts (McLachlan et al., 2008) obtained from G60S mutant mice. Thus, it is highly likely that resident cell types of the hair follicle also have reduced gap junctional coupling, which could in turn impact the growth and development of the hair follicle and the hair fiber. However, in theory, mutant Cx43 may also impact hair growth and differentiation by other mechanisms such as disrupting the gap junction proteome (Laird, 2010).

Although hair abnormalities have been reported in some patients with ODDD, this is not the case for all ODDD patients suggesting that some Cx43 mutants may be more potent in altering hair growth and differentiation. This concept is supported in a previous study which demonstrated that keratinocytes expressing the frame-shift 260 mutant was more potent than several missense Cx43 mutants at altering cell coupling levels, epidermal organotypic formation, and transepithelial resistance (Churko et al., 2010). Alternatively, patient disease heterogeneity may extend beyond these criteria as phenotype variability is also seen in mutant mice. For instance, it has been reported that only 1/3rd of sibling mice

expressing the G138R Cx43 mutant develop slow growing and sparse hair (Dobrowolski et al., 2008). This variability was also observed in our study as a subset of mice (~20%) expressing the G60S mutant exhibited visually less hair density near the neck region. However, when the entire mutant mouse population was considered, no hair density differences were observed between G60S and WT mice. In the G60S mice, hair re-growth was asynchronous and delayed by approximately 3 days. Our results suggest that Cx43 is linked to mechanisms which regulate the outward growth of the hair fiber since hair growth was delayed after both epilation and depilation treatment. The bulge cell population in human hair follicle development has been reported to express Cx43 (Arita et al., 2004), however another group reported that mouse bulge stem cells do not express Cx43 (Matic and Simon, 2003). Consistent with the latter report, we also observed little Cx43 expression in CK15 (bulge stem cell marker) expressing cells suggesting that the telogen-anagen transition in G60S mutant mice may be unaffected. As Cx43 expression increases in hair follicle growth (anagen), mutant Cx43 may impair the formation and growth of the hair follicle. Proliferation analysis in cells which highly express Cx43 (the hair matrix) revealed that the total mitotic output was lower in G60S mouse hair follicles. This could also explain the delay in hair re-growth observed in the G60S mice and why G60S mice develop significantly shorter and thinner hair fibers. However, since Cx43 is also expressed in the dermal papilla, it is not known whether mutant Cx43 expression in this region impairs the signaling interactions that occur between the dermal papilla and the hair follicle epithelium.

Scanning electron microscopy revealed cuticle degradation in both family members expressing the G143S mutant, but these same structural defects were not observed from the hair sample derived from a patient expressing the T154A mutant. A patient expressing the G143S mutant self-reported that their hair was thin and curly while the patient expressing the T154A self-reported that their hair was thick and grew fast. Since slow growing hair is often reported as a hair abnormality associated with ODDD and since only ~25% of patients with ODDD report any hair abnormalities, we were not surprised that the hair fibers from the T154A patient documented in this study appeared normal. Nevertheless, cuticle weathering was observed in the patients expressing the G143S mutant and this defect was consistent with previous reports which linked Cx43

mutants with hair fiber structural defects such as monilethrix, pili annuli, nodule/beaded and cuticle weathering (Adamski et al., 1994; Kelly et al., 2006; Thoden et al., 1977). Similar to hair fiber bulging and cuticle weathering as seen in a patient with ODDD (Adamski et al., 1994), the proximal region of the hair fiber from some mutant mice formed nodules at irregular intervals while the distal portion of the mutant mouse hair fibers showed extreme cuticle layer weathering. This defect was sometimes so severe that the underlying cortical layer was exposed. Since keratinization defects have been reported in ODDD patients (Kelly et al., 2006; Paznekas et al., 2003; van Steensel et al., 2005; Vreeburg et al., 2007), improper keratinization may also explain the cuticle weathering and nodule formation observed in the mutant mice. In the absence of proper keratinization, the hair fiber may be prone to structural defects and premature degradation.

Given that loss-of-function mutant Cx43 expression delays hair re-growth in mutant mice, future studies should address the question as to whether Cx43 overexpression would enhance hair follicle health and the rate of hair growth. In addition, since a reduction in functional Cx43 leads to a decline in the health of the hair fiber shaft, elevating the expression of Cx43 during hair growth may also improve the structural integrity of the developing hair fiber.

5.5 References

- Adamski, H., J. Chevrant-Breton, S. Odent, M. Patoux-Pibouin, B. Le Marec, A. Laudren, and M. Urvoy. 1994. [Hair dysplasia in oculo-dento-digital syndrome. Apropos of a mother-daughter case]. *Ann Dermatol Venereol.* 121:694-699.
- Arita, K., M. Akiyama, Y. Tsuji, J.R. McMillan, R.A. Eady, and H. Shimizu. 2004. Gap junction development in the human fetal hair follicle and bulge region. *Br J Dermatol.* 150:429-434.
- Botchkarev, V.A., and R. Paus. 2003. Molecular biology of hair morphogenesis: development and cycling. *J Exp Zool B Mol Dev Evol.* 298:164-180.
- Choudhry, R., J.D. Pitts, and M.B. Hodgins. 1997. Changing patterns of gap junctional intercellular communication and connexin distribution in mouse epidermis and hair follicles during embryonic development. *Dev Dyn.* 210:417-430.
- Churko, J.M., S. Langlois, X. Pan, Q. Shao, and D.W. Laird. 2010. The potency of the fs260 connexin43 mutant to impair keratinocyte differentiation is distinct from other disease-linked connexin43 mutants. *Biochem J.* 429:473-483.
- Civitelli, R. 2008. Cell-cell communication in the osteoblast/osteocyte lineage. *Arch Biochem Biophys.* 473:188-192.
- Dobrowolski, R., P. Sasse, J.W. Schrickel, M. Watkins, J.S. Kim, M. Rackauskas, C. Troatz, A. Ghanem, K. Tiemann, J. Degen, F.F. Bukauskas, R. Civitelli, T. Lewalter, B.K. Fleischmann, and K. Willecke. 2008. The conditional connexin43G138R mouse mutant represents a new model of hereditary oculodentodigital dysplasia in humans. *Hum Mol Genet.* 17:539-554.
- Elias, L.A., and A.R. Kriegstein. 2008. Gap junctions: multifaceted regulators of embryonic cortical development. *Trends Neurosci.* 31:243-250.
- Flenniken, A.M., L.R. Osborne, N. Anderson, N. Ciliberti, C. Fleming, J.E. Gittens, X.Q. Gong, L.B. Kelsey, C. Lounsbury, L. Moreno, B.J. Nieman, K. Peterson, D. Qu, W. Roscoe, Q. Shao, D. Tong, G.I. Veitch, I. Voronina, I. Vukobradovic, G.A. Wood, Y. Zhu, R.A. Zirngibl, J.E. Aubin, D. Bai, B.G. Bruneau, M. Grynopas, J.E. Henderson, R.M. Henkelman, C. McKerlie, J.G. Sled, W.L. Stanford, D.W. Laird, G.M. Kidder, S.L. Adamson, and J. Rossant. 2005. A Gja1 missense mutation in a mouse model of oculodentodigital dysplasia. *Development.* 132:4375-4386.
- Gorlin, R.J., L.H. Miskin, and G.J. St. 1963. Oculodentodigital dysplasia. *J Pediatr.* 63:69-75.
- Hatler, J.M., J.J. Essner, and R.G. Johnson. 2009. A gap junction connexin is required in the vertebrate left-right organizer. *Dev Biol.* 336:183-191.

- Jalife, J., G.E. Morley, and D. Vaidya. 1999. Connexins and impulse propagation in the mouse heart. *J Cardiovasc Electrophysiol.* 10:1649-1663.
- Kalcheva, N., J. Qu, N. Sandeep, L. Garcia, J. Zhang, Z. Wang, P.D. Lampe, S.O. Suadicani, D.C. Spray, and G.I. Fishman. 2007. Gap junction remodeling and cardiac arrhythmogenesis in a murine model of oculodentodigital dysplasia. *Proc Natl Acad Sci U S A.* 104:20512-20516.
- Kelly, S.C., P. Ratajczak, M. Keller, S.M. Purcell, T. Griffin, and G. Richard. 2006. A novel GJA 1 mutation in oculo-dento-digital dysplasia with curly hair and hyperkeratosis. *Eur J Dermatol.* 16:241-245.
- Kjaer, K.W., L. Hansen, H. Eiberg, P. Leicht, J.M. Opitz, and N. Tommerup. 2004. Novel Connexin 43 (GJA1) mutation causes oculo-dento-digital dysplasia with curly hair. *Am J Med Genet A.* 127A:152-157.
- Laird, D.W. 2010. The gap junction proteome and its relationship to disease. *Trends Cell Biol.* 20:92-101.
- Langlois, S., A.C. Maher, J.L. Manias, Q. Shao, G.M. Kidder, and D.W. Laird. 2007. Connexin levels regulate keratinocyte differentiation in the epidermis. *J Biol Chem.* 282:30171-30180.
- Manias, J.L., I. Plante, X.Q. Gong, Q. Shao, J. Churko, D. Bai, and D.W. Laird. 2008. Fate of connexin43 in cardiac tissue harbouring a disease-linked connexin43 mutant. *Cardiovasc Res.* 80:385-395.
- Matic, M., and M. Simon. 2003. Label-retaining cells (presumptive stem cells) of mice vibrissae do not express gap junction protein connexin 43. *J Investig Dermatol Symp Proc.* 8:91-95.
- McLachlan, E., J.L. Manias, X.Q. Gong, C.S. Lounsbury, Q. Shao, S.M. Bernier, D. Bai, and D.W. Laird. 2005. Functional characterization of oculodentodigital dysplasia-associated Cx43 mutants. *Cell Commun Adhes.* 12:279-292.
- McLachlan, E., I. Plante, Q. Shao, D. Tong, G.M. Kidder, S.M. Bernier, and D.W. Laird. 2008. ODDD-linked Cx43 mutants reduce endogenous Cx43 expression and function in osteoblasts and inhibit late stage differentiation. *J Bone Miner Res.* 23:928-938.
- Nagata, K., K. Masumoto, G. Esumi, R. Teshiba, K. Yoshizaki, S. Fukumoto, K. Nonaka, and T. Taguchi. 2009. Connexin43 plays an important role in lung development. *J Pediatr Surg.* 44:2296-2301.
- Paznekas, W.A., S.A. Boyadjiev, R.E. Shapiro, O. Daniels, B. Wollnik, C.E. Keegan, J.W. Innis, M.B. Dinulos, C. Christian, M.C. Hannibal, and E.W. Jabs. 2003. Connexin 43 (GJA1) mutations cause the pleiotropic phenotype of oculodentodigital dysplasia. *Am J Hum Genet.* 72:408-418.

- Paznekas, W.A., B. Karczeski, S. Vermeer, R.B. Lowry, M. Delatycki, F. Laurence, P.A. Koivisto, L. Van Maldergem, S.A. Boyadjiev, J.N. Bodurtha, and E.W. Jabs. 2009. GJA1 mutations, variants, and connexin 43 dysfunction as it relates to the oculodentodigital dysplasia phenotype. *Hum Mutat.* 30:724-733.
- Risek, B., F.G. Klier, and N.B. Gilula. 1992. Multiple gap junction genes are utilized during rat skin and hair development. *Development.* 116:639-651.
- Sugar, H.S., J.P. Thompson, and J.D. Davis. 1966. The oculo-dento-digital dysplasia syndrome. *Am J Ophthalmol.* 61:1448-1451.
- Thoden, C.J., S. Ryoppy, and P. Kuitunen. 1977. Oculodentodigital dysplasia syndrome. Report of four cases. *Acta Paediatr Scand.* 66:635-638.
- Toth, K., Q. Shao, R. Lorentz, and D.W. Laird. 2010. Decreased levels of Cx43 gap junctions result in ameloblast dysregulation and enamel hypoplasia in Gja1Jrt/+ mice. *J Cell Physiol.* 223:601-609.
- van Steensel, M.A., L. Spruijt, d.B.I. van, R.S. Bladergroen, M. Vermeer, P.M. Steijlen, and G.M. van. 2005. A 2-bp deletion in the GJA1 gene is associated with oculo-dento-digital dysplasia with palmoplantar keratoderma. *Am.J.Med.Genet.A.* 132A:171-174.
- Vreeburg, M., E.A. de Zwart-Storm, M.I. Schouten, R.G. Nellen, D. Marcus-Soekarman, M. Davies, M. van Geel, and M.A. van Steensel. 2007. Skin changes in oculo-dento-digital dysplasia are correlated with C-terminal truncations of connexin 43. *Am J Med Genet A.* 143:360-363.

Chapter 6

6 Discussion

Cx43 modulates the correct development and function of various organs (Laird, 2010; Santiago et al., 2010; Toth et al., 2010; Tsui et al., 2011). The goal of this thesis was to determine how mutant Cx43 affects the development and differentiation of the skin. With the combinatory use of mouse, cell lines and organotypic models, this thesis examined how Cx43 can modulate keratinocyte and dermal fibroblast proliferation, migration, and differentiation. We have also studied the G60S Cx43 mutant mouse model for hair defects often observed in ODDD patients. In this section I will address the wider implications of our findings.

6.1 G60S mice exhibit a delay in wound healing

We have determined that wounds heal slower in G60S mice compared to WT littermates. This is particularly interesting since topical knockdown of Cx43 in the skin has been shown to accelerate wound healing (Ghatnekar et al., 2009; Mori et al., 2006; Qiu et al., 2003). Administration of topical anti-sense Cx43 during wound healing may have only significantly lowered Cx43 in the superficial epidermal layer and not effectively lowered Cx43 levels in the deep dermal layer. Since the G60S mutant mouse contains a germ line mutation in the gene encoding Cx43, all cells expressing Cx43 would also express mutant Cx43. Fibroblasts do express Cx43, are present in the deep dermal layer, and also play a pivotal role in wound healing (Hackam and Ford, 2002; Werner et al., 2007). In this thesis we have demonstrated that mutant Cx43 expression in human fibroblasts hinders fibroblast proliferation, migration and differentiation (Churko et al., 2011) and cumulatively, the delay in wound healing in the G60S mice might specifically be attributed to the role that dermal fibroblasts play in wound healing.

Topical administration of Cx43 anti-sense also transiently lowers the total levels of Cx43 whereas the G60S mice have overall chronically lower functional levels of Cx43. Transient knockdown of Cx43 in the wound area has proven to be beneficial in the initial

proliferation and migration stages of wound healing but unless Cx43 anti-sense treatment is repeated daily, functional Cx43 levels return to normal to support the keratinocyte differentiation stage of wound healing. In our studies, mutant Cx43 enhanced the proliferation of keratinocytes but negligibly affected the calcium-induced differentiation of primary keratinocytes. However, in the organotypic epidermal cultures, some Cx43 mutants were shown to impair epidermal differentiation given that the expression of some Cx43 mutants generally lowered the transepithelial resistance values, Cx26 levels and affected the size of the stratum corneum. In addition, fs260 expression was particularly potent at lowering the levels of endogenous Cx43 and disrupting the stratum corneum architecture. Langlois et al also demonstrated that exogenous administration of Cx43 shRNA to organotypic cultures disrupts the organotypic tissue architecture to further emphasize that extreme changes in Cx43 levels can impair epidermal differentiation (Langlois et al., 2007). Collectively, these findings suggest that the functional state of Cx43 may be more vital in the stratification of the epidermis and certain Cx43 mutants may also be more potent at disrupting the three-dimensional organization of the epidermis. In cases where mutant Cx43 drastically lowers the total and functional levels of Cx43, skin disease and defects in wound healing may result.

The anatomical site of wounding may also favor the role that keratinocytes or fibroblasts play during wound healing. Since the back skin in rodents is loosely adherent, wound contraction plays a significant role in healing full-thickness excisional wounds (Reid et al., 2004). Thus wound healing assessed in our mutant mice would be highly dependent on fibroblast contraction. In contrast, head skin in mice is tightly adherent to the underlying bone and fibroblast dependent contraction would be expected to play a lesser role (Reid et al., 2004). Human skin, like the skin localized to the head area in mice, is strongly adherent to the underlying bones/connective tissue and human wound healing is more dependent on the formation of new tissue and not contraction (Davidson, 1998). Therefore, it would be interesting to determine if head wounds performed on the G60S mice would also demonstrate a delay in wound healing. In addition, it would be interesting to determine if wounds, which primarily damaged the epidermal layer (topical abrasions) in G60S mice, also impact the rate of wound healing. Given that keratinocytes

expressing mutant Cx43 enhanced their proliferation, it is possible that wounds which primarily damage the epithelium heal faster.

6.2 Combined use of multiple ODDD models

Overexpression of mutant Cx43 in rat epidermal cells was performed to determine how mutant Cx43 impacts the endogenous Cx43 expression levels and GJIC. Overexpression of ODDD-linked Cx43 mutants in these cells significantly inhibited the passage of dye through gap junction channels suggesting that mutant Cx43 impairs the function of gap junction channels. Interestingly, by assessing the organotypic epidermal growth of rat epidermal cells expressing various Cx43 mutants, we have also determined that some mutants are more potent at impairing the functional and differentiation properties of rat epidermal cells. Specifically, the G138R and fs260 mutants significantly lowered endogenous Cx43 levels whereas other ODDD mutants had no effect. In addition, organotypic epidermal cultures grown from REKs expressing mutant fs260 also formed nuclei in the stratum corneum whereas this phenotype was not seen in organotypic epidermal models grown from other ODDD mutant expressing REKs. The unique disease burden of the fs260 mutant suggests that all ODDD patients may develop various levels of disease burden. This is particularly evident in the only two reported cases where patients expressing the fs260 (and fs230) have been shown to develop palmar plantar hyperkeratosis (van Steensel et al., 2005; Vreeburg et al., 2007).

While it is difficult to control the dosage of mutant Cx43 being expressed in these organotypic models, we have also investigated primary cultures derived from G60S mice and primary fibroblast cultures from patients with ODDD to ensure that mutant Cx43 to wild-type Cx43 expression is properly controlled at a 1:1 ratio. In addition, to better understand human ODDD and to rule-out species differences, we examined the G60S mouse model of ODDD and compared our results with assays performed using human ODDD patient cells and tissues. By comparing the ability of mouse and human fibroblasts expressing mutant Cx43 to migrate, we found that both mouse and human fibroblasts demonstrate impaired migration. Future studies on primary cultures and tissues derived from multiple patients expressing various ODDD mutants will be

important to evaluate how mutant Cx43 causes common ODDD symptoms and how specific Cx43 mutants may be more potent at causing disease.

Given the complexity of tissue development, it may be necessary to study the development of organs *in vivo*. Hair follicle development is one such example which needs an *in vivo* environment to effectively progress and we have used G60S mice to demonstrate that mutant Cx43 expression delays hair growth and causes hair fibers structural defects. Studying hair development *in vivo* also added an additional level of complexity since only a subpopulation of littermate matched mice demonstrate defects in their coat appearance. Given that hypotrichosis was only observed in a subset of G60S mice, hair defects in these mice are not fully penetrant suggesting that additional genes may work in a multifactorial manner to affect hair development. In addition, since observable differences could only be seen in aged mice (2-3 months), future studies using the *in vivo* environment will be important to determine how the ODDD disease manifests with age.

6.3 Cell type differences

Since wound healing involves an interplay between keratinocytes, dermal fibroblasts, immune cells, endothelial cells and other cell types (Yamaguchi and Yoshikawa, 2001), it is important to separately assess each cell type and to determine what role each cell type plays in the wound healing process. By separately assessing keratinocytes and dermal fibroblasts for their ability to proliferate, migrate, and differentiate, we have found that keratinocytes and fibroblasts react differently when mutant Cx43 is expressed. Interestingly, mutant G60S Cx43 expression in mouse primary keratinocytes enhances proliferation while the expression of D3N and V216L mutant Cx43 in human dermal fibroblast hinders proliferation. Since mutant Cx43 could both enhance and reduce proliferation, the roles that Cx43 plays in tissue homeostasis or function may also be dependent on the cell type assessed. For example, given that ODDD patients commonly develop defects in their bones, digits, and eyes, perturbation in the expression and function of Cx43 in osteoblasts, digit mesenchymal cells and corneal epithelial cells may be more potent at causing developmental defects when compared to other cell types.

Other organs and cells types expressing mutant Cx43 may also contribute to the delay in wound healing we observed. For example, macrophages express Cx43 and are known to infiltrate into the wound area and modulate wound healing (Martin and Leibovich, 2005; Rodero and Khosrotehrani, 2010). Specifically, macrophages secrete TGF β ₁ and this growth factor is important for the differentiation of fibroblasts into myofibroblasts which occurs during wound healing (Rodero and Khosrotehrani, 2010). Since mutant Cx43 may also impair the function of other cell types involved in wound healing, further examination into other cell types involved in wound healing would lead to a greater understanding of the role that Cx43 plays in wound healing.

One possible explanation as to why Cx43 may differentially affect each cell type may be proteomic expressional differences between cell types. Given that Cx43 interacts with multiple proteins (reviewed in Laird, 2010), expression of a subset of proteins unique to keratinocytes may be required for specific keratinocyte functions. For example, keratinocytes require cell to cell contacts through tight junctions to maintain a proper epithelial barrier (Niessen, 2007). Connexins are also found within the same adhesive domains as tight and adherens junctions (reviewed in Laird, 2010) and wild-type expression of connexins may facilitate this adhesive environment. Since ODDD mutants expressed in rat epidermal keratinocytes lowered the transepithelial resistance values, indicating a reduction in tight junction adhesion, mutant Cx43 may disrupt cell to cell adhesion between keratinocytes and impair the epithelial barrier formed by keratinocytes. Fibroblasts however, sparsely populate the dermis and disruption of cell to cell adhesion in these cells may not be as important as the adhesive environment required by keratinocytes.

Keratinocytes and fibroblasts also express different integrin subunits which differentially affect the ability of each cell type to adhere to specific extracellular matrix proteins. Keratinocytes residing on the basement membrane interact with laminin 332 through connections with α 6 β 4 integrin (Lampe et al., 1998). Under wound healing conditions however, keratinocytes interact with laminin 332 through α 3 β 1 integrin and express, α 5 β 5 and α 5 β 1 integrins (De Luca et al., 1994; Lampe et al., 1998). In contrast, fibroblasts express α 1 β 1, α 2 β 1, and α 11 β 1 integrins which facilitates fibroblasts adherence to

collagen (Eckes et al., 2006). Since the interaction between integrins and extracellular matrix proteins regulate migration (De Luca et al., 1994), mutant Cx43 may selectively disrupt specific integrin subunit interactions and effectively impair the migration of cells expressing these integrin subunits. In our study, the migration of primary keratinocytes derived from G60S mice did not differ when compared to keratinocytes derived from WT mice. However, fibroblasts derived from G60S mice did not migrate as well as fibroblasts derived from WT mice when plated on collagen type I and fibronectin. This suggests that mutant Cx43 may selectively impair the interaction between $\alpha 1\beta 1$ or $\alpha 11\beta 1$ integrins since keratinocytes do not express these integrin subunit combinations. The link between integrin interactions and gap junction communication is also supported in a study which demonstrated that keratinocytes plated on laminin 332 promoted gap junction communication in comparison to keratinocytes plated on collagen and fibronectin (Lampe et al., 1998).

6.4 Therapeutic implications

It is apparent that connexins affect skin physiology. By studying how connexin expression modulates the function of keratinocytes and fibroblasts, connexin manipulation in the skin may be important in mitigating connexin-linked skin diseases and enhancing wound healing. Given that the skin is a readily accessible organ, connexin levels may be manipulated with the topical administration of therapeutic creams.

In treating Cx43-related skin disorders, it is important to consider whether it is more appropriate to overexpress wild-type Cx43 or to inhibit the expression of mutant Cx43. Our results have shown that human fibroblasts derived from ODDD patients have reduced intercellular conductance levels and it remains to be determined whether overexpression of wild-type Cx43 in cells expressing mutant Cx43 could raise the coupling status and improve defects (e.g. slow growing hair, syndactyly, microcornea) associated with ODDD. However, the exogenously expressed Cx43 may be rendered non-functional since the endogenously expressed mutant Cx43 may continue to disrupt connexin trafficking and channel function.

Determining how various Cx43 mutants cause skin disorders will be important in deciding the proper therapeutic action to take. For example, if palmar plantar hyperkeratosis is caused by the mutant ability to disrupt cell to cell adhesion between keratinocytes, over expression of Cx43 may strengthen the weakened contacts between keratinocytes. If however, palmar plantar hyperkeratosis is caused by a deficient transport of metabolites through gap junction channels, increasing wild-type Cx43 expression may prove ineffectual since mutant Cx43 may continue to impair channel function. In addition knowing how mutant Cx43 affects the skin of ODDD patients may have wider implications for the general population. Since the function of Cx43 channels are indeed impaired in ODDD patients (Churko et al., 2011), understanding how a decrease in gap junction function affects skin physiology will be important to evaluate the role of Cx43 in disease free skin.

6.5 References

- Churko, J.M., Q. Shao, X. Gong, K.J. Swoboda, D. Bai, J. Sampson, and D.W. Laird. 2011. Human dermal fibroblasts derived from oculodentodigital dysplasia patients suggest that patients may have wound healing defects. *Hum Mutat.*
- Davidson, J.M. 1998. Animal models for wound repair. *Arch Dermatol Res.* 290 Suppl:S1-11.
- De Luca, M., G. Pellegrini, G. Zambruno, and P.C. Marchisio. 1994. Role of integrins in cell adhesion and polarity in normal keratinocytes and human skin pathologies. *J Dermatol.* 21:821-828.
- Eckes, B., M.C. Zweers, Z.G. Zhang, R. Hallinger, C. Mauch, M. Aumailley, and T. Krieg. 2006. Mechanical tension and integrin alpha 2 beta 1 regulate fibroblast functions. *J Invest Dermatol Symp Proc.* 11:66-72.
- Ghatnekar, G.S., M.P. O'Quinn, L.J. Jourdan, A.A. Gurjarpadhye, R.L. Draughn, and R.G. Gourdie. 2009. Connexin43 carboxyl-terminal peptides reduce scar progenitor and promote regenerative healing following skin wounding. *Regen Med.* 4:205-223.
- Hackam, D.J., and H.R. Ford. 2002. Cellular, biochemical, and clinical aspects of wound healing. *Surg Infect (Larchmt).* 3 Suppl 1:S23-35.
- Laird, D.W. 2010. The gap junction proteome and its relationship to disease. *Trends Cell Biol.* 20:92-101.
- Lampe, P.D., B.P. Nguyen, S. Gil, M. Usui, J. Olerud, Y. Takada, and W.G. Carter. 1998. Cellular interaction of integrin alpha3beta1 with laminin 5 promotes gap junctional communication. *J Cell Biol.* 143:1735-1747.
- Langlois, S., A.C. Maher, J.L. Manias, Q. Shao, G.M. Kidder, and D.W. Laird. 2007. Connexin levels regulate keratinocyte differentiation in the epidermis. *J Biol Chem.* 282:30171-30180.
- Martin, P., and S.J. Leibovich. 2005. Inflammatory cells during wound repair: the good, the bad and the ugly. *Trends Cell Biol.* 15:599-607.
- Mori, R., K.T. Power, C.M. Wang, P. Martin, and D.L. Becker. 2006. Acute downregulation of connexin43 at wound sites leads to a reduced inflammatory response, enhanced keratinocyte proliferation and wound fibroblast migration. *J Cell Sci.* 119:5193-5203.
- Niessen, C.M. 2007. Tight junctions/adherens junctions: basic structure and function. *J Invest Dermatol.* 127:2525-2532.

- Qiu, C., P. Coutinho, S. Frank, S. Franke, L.Y. Law, P. Martin, C.R. Green, and D.L. Becker. 2003. Targeting connexin43 expression accelerates the rate of wound repair. *Curr.Biol.* 13:1697-1703.
- Reid, R.R., H.K. Said, J.E. Mogford, and T.A. Mustoe. 2004. The future of wound healing: pursuing surgical models in transgenic and knockout mice. *J Am Coll Surg.* 199:578-585.
- Rodero, M.P., and K. Khosrotehrani. 2010. Skin wound healing modulation by macrophages. *Int J Clin Exp Pathol.* 3:643-653.
- Santiago, M.F., P. Alcamí, K.M. Striedinger, D.C. Spray, and E. Scemes. 2010. The carboxyl-terminal domain of connexin43 is a negative modulator of neuronal differentiation. *J Biol Chem.* 285:11836-11845.
- Toth, K., Q. Shao, R. Lorentz, and D.W. Laird. 2010. Decreased levels of Cx43 gap junctions result in ameloblast dysregulation and enamel hypoplasia in Gja1Jrt/+ mice. *J Cell Physiol.* 223:601-609.
- Tsui, E., K.A. Hill, A.M. Laliberte, D. Paluzzi, I. Kisilevsky, Q. Shao, J.G. Heathcote, D.W. Laird, G.M. Kidder, and C.M. Hutnik. 2011. Ocular pathology relevant to glaucoma in a Gja1Jrt/+ mouse model of human oculodentodigital dysplasia. *Invest Ophthalmol Vis Sci.*
- van Steensel, M.A., L. Spruijt, d.B.I. van, R.S. Bladergroen, M. Vermeer, P.M. Steijlen, and G.M. van. 2005. A 2-bp deletion in the GJA1 gene is associated with oculodento-digital dysplasia with palmoplantar keratoderma. *Am.J.Med.Genet.A.* 132A:171-174.
- Vreeburg, M., E.A. de Zwart-Storm, M.I. Schouten, R.G. Nellen, D. Marcus-Soekarman, M. Davies, M. van Geel, and M.A. van Steensel. 2007. Skin changes in oculodento-digital dysplasia are correlated with C-terminal truncations of connexin 43. *Am J Med Genet A.* 143:360-363.
- Werner, S., T. Krieg, and H. Smola. 2007. Keratinocyte-fibroblast interactions in wound healing. *J Invest Dermatol.* 127:998-1008.
- Yamaguchi, Y., and K. Yoshikawa. 2001. Cutaneous wound healing: an update. *J Dermatol.* 28:521-534.

Appendices

Copyright and Permission

Human Mutation

JOHN WILEY AND SONS LICENSE
TERMS AND CONDITIONS

Jun 02, 2011

This is a License Agreement between Jared M Churko ("You") and John Wiley and Sons ("John Wiley and Sons") provided by Copyright Clearance Center ("CCC"). The license consists of your order details, the terms and conditions provided by John Wiley and Sons, and the payment terms and conditions.

License Number

2680851317855

License date

Jun 02, 2011

Licensed content publisher

John Wiley and Sons

Licensed content publication

Human Mutation

Licensed content title

Human dermal fibroblasts derived from oculodentodigital dysplasia patients suggest that patients may have wound-healing defects

Licensed content author

Jared M. Churko, Qing Shao, Xiang-qun Gong, Kathryn J. Swoboda, Donglin Bai, Jacinda Sampson, Dale W. Laird

Licensed content date

Apr 1, 2011

Start page

456

End page

466

Type of use

Dissertation/Thesis

Requestor type

Author of this Wiley article

Format

Electronic

Portion

Full article
Will you be translating?
No
Order reference number
Total
0.00 USD
Terms and Conditions

TERMS AND CONDITIONS

This copyrighted material is owned by or exclusively licensed to John Wiley & Sons, Inc. or one of its group companies (each a "Wiley Company") or a society for whom a Wiley Company has exclusive publishing rights in relation to a particular journal (collectively "WILEY"). By clicking "accept" in connection with completing this licensing transaction, you agree that the following terms and conditions apply to this transaction (along with the billing and payment terms and conditions established by the Copyright Clearance Center Inc., ("CCC's Billing and Payment terms and conditions"), at the time that you opened your Rightslink account (these are available at any time at <http://myaccount.copyright.com>)

Terms and Conditions

1. The materials you have requested permission to reproduce (the "Materials") are protected by copyright.
2. You are hereby granted a personal, non-exclusive, non-sublicensable, non-transferable, worldwide, limited license to reproduce the Materials for the purpose specified in the licensing process. This license is for a one-time use only with a maximum distribution equal to the number that you identified in the licensing process. Any form of republication granted by this licence must be completed within two years of the date of the grant of this licence (although copies prepared before may be distributed thereafter). The Materials shall not be used in any other manner or for any other purpose. Permission is granted subject to an appropriate acknowledgement given to the author, title of the material/book/journal and the publisher and on the understanding that nowhere in the text is a previously published source acknowledged for all or part of this Material. Any third party material is expressly excluded from this permission.
3. With respect to the Materials, all rights are reserved. Except as expressly granted by the terms of the license, no part of the Materials may be copied, modified, adapted (except for minor reformatting required by the new Publication), translated, reproduced, transferred or distributed, in any form or by any means, and no derivative works may be made based on the Materials without the prior permission of the respective copyright owner. You may not alter, remove or suppress in any manner any copyright, trademark or other notices displayed by the Materials. You may not license, rent, sell, loan, lease, pledge, offer as security, transfer or assign the Materials, or any of the rights granted to you hereunder to any other person.
4. The Materials and all of the intellectual property rights therein shall at all times remain the exclusive property of John Wiley & Sons Inc or one of its related companies (WILEY) or their respective licensors, and your interest therein is only that of having possession of and the right to reproduce the Materials pursuant to Section 2 herein during the continuance of this Agreement. You agree that you own no right, title or interest in or to the Materials or any of the intellectual property rights therein. You shall have no rights hereunder other than the license as provided for above in Section 2. No right, license or interest to any trademark, trade name, service mark or

other branding ("Marks") of WILEY or its licensors is granted hereunder, and you agree that you shall not assert any such right, license or interest with respect thereto.

5. NEITHER WILEY NOR ITS LICENSORS MAKES ANY WARRANTY OR REPRESENTATION OF ANY KIND TO YOU OR ANY THIRD PARTY, EXPRESS, IMPLIED OR STATUTORY, WITH RESPECT TO THE MATERIALS OR THE ACCURACY OF ANY INFORMATION CONTAINED IN THE MATERIALS, INCLUDING, WITHOUT LIMITATION, ANY IMPLIED WARRANTY OF MERCHANTABILITY, ACCURACY, SATISFACTORY QUALITY, FITNESS FOR A PARTICULAR PURPOSE, USABILITY, INTEGRATION OR NON-INFRINGEMENT AND ALL SUCH WARRANTIES ARE HEREBY EXCLUDED BY WILEY AND ITS LICENSORS AND WAIVED BY YOU.

6. WILEY shall have the right to terminate this Agreement immediately upon breach of this Agreement by you.

7. You shall indemnify, defend and hold harmless WILEY, its Licensors and their respective directors, officers, agents and employees, from and against any actual or threatened claims, demands, causes of action or proceedings arising from any breach of this Agreement by you.

8. IN NO EVENT SHALL WILEY OR ITS LICENSORS BE LIABLE TO YOU OR ANY OTHER PARTY OR ANY OTHER PERSON OR ENTITY FOR ANY SPECIAL, CONSEQUENTIAL, INCIDENTAL, INDIRECT, EXEMPLARY OR PUNITIVE DAMAGES, HOWEVER CAUSED, ARISING OUT OF OR IN CONNECTION WITH THE DOWNLOADING, PROVISIONING, VIEWING OR USE OF THE MATERIALS REGARDLESS OF THE FORM OF ACTION, WHETHER FOR BREACH OF CONTRACT, BREACH OF WARRANTY, TORT, NEGLIGENCE, INFRINGEMENT OR OTHERWISE (INCLUDING, WITHOUT LIMITATION, DAMAGES BASED ON LOSS OF PROFITS, DATA, FILES, USE, BUSINESS OPPORTUNITY OR CLAIMS OF THIRD PARTIES), AND WHETHER OR NOT THE PARTY HAS BEEN ADVISED OF THE POSSIBILITY OF SUCH DAMAGES. THIS LIMITATION SHALL APPLY NOTWITHSTANDING ANY FAILURE OF ESSENTIAL PURPOSE OF ANY LIMITED REMEDY PROVIDED HEREIN.

9. Should any provision of this Agreement be held by a court of competent jurisdiction to be illegal, invalid, or unenforceable, that provision shall be deemed amended to achieve as nearly as possible the same economic effect as the original provision, and the legality, validity and enforceability of the remaining provisions of this Agreement shall not be affected or impaired thereby.

10. The failure of either party to enforce any term or condition of this Agreement shall not constitute a waiver of either party's right to enforce each and every term and condition of this Agreement. No breach under this agreement shall be deemed waived or excused by either party unless such waiver or consent is in writing signed by the party granting such waiver or consent. The waiver by or consent of a party to a breach of any provision of this Agreement shall not operate or be construed as a waiver of or consent to any other or subsequent breach by such other party.

11. This Agreement may not be assigned (including by operation of law or otherwise) by you without WILEY's prior written consent.

12. Any fee required for this permission shall be non-refundable after thirty (30) days from receipt.

13. These terms and conditions together with CCC's Billing and Payment terms and conditions (which are incorporated herein) form the entire agreement between you and WILEY concerning this licensing transaction and (in the absence of fraud) supersedes all prior agreements and representations of the parties, oral or written. This Agreement may not be amended except in writing signed by both parties. This Agreement shall be binding upon and inure to the benefit of the parties' successors, legal representatives, and authorized assigns.

14. In the event of any conflict between your obligations established by these terms and conditions and those established by CCC's Billing and Payment terms and conditions, these terms and conditions shall prevail.

15. WILEY expressly reserves all rights not specifically granted in the combination of (i) the license details provided by you and accepted in the course of this licensing transaction, (ii) these terms and conditions and (iii) CCC's Billing and Payment terms and conditions.

16. This Agreement will be void if the Type of Use, Format, Circulation, or Requestor Type was misrepresented during the licensing process.

17. This Agreement shall be governed by and construed in accordance with the laws of the State of New York, USA, without regards to such state's conflict of law rules. Any legal action, suit or proceeding arising out of or relating to these Terms and Conditions or the breach thereof shall be instituted in a court of competent jurisdiction in New York County in the State of New York in the United States of America and each party hereby consents and submits to the personal jurisdiction of such court, waives any objection to venue in such court and consents to service of process by registred or certified mail, return receipt requested, at the last known address of such party. . BY CLICKING ON THE "I ACCEPT" BUTTON, YOU ACKNOWLEDGE THAT YOU HAVE READ AND FULLY UNDERSTAND EACH OF THE SECTIONS OF AND PROVISIONS SET FORTH IN THIS AGREEMENT AND THAT YOU ARE IN AGREEMENT WITH AND ARE WILLING TO ACCEPT ALL OF YOUR OBLIGATIONS AS SET FORTH IN THIS AGREEMENT. v1.4

Biochemical Journal

For terms and conditions for online usage of journals published by Portland Press Ltd, please visit the following websites:

[Biochemical Journal](#)
[Clinical Science](#)
[Bioscience Reports](#)
[Biochemical Society Transactions](#)
[Biology of the Cell](#)
[Biotechnology and Applied Biochemistry](#)
[ASN NEURO](#)
[Cell Biology International](#)
[Essays in Biochemistry](#)
[Biochemical Society Symposia](#)

[Licensing enquiries](#)

The guidelines below refer to articles published in the following journals, published by Portland Press Limited:

<i>ASN NEURO</i>	<i>Cell Biology International</i>
<i>Biochemical Journal</i>	<i>Cell Biology International Reports</i>
<i>Biochemical Society Symposia</i>	<i>Cell Signalling Biology</i>
<i>Biochemical Society Transactions</i>	<i>Clinical Science</i>
<i>Biology of the Cell</i>	<i>Essays in Biochemistry</i>
<i>Bioscience Reports</i>	<i>The Biochemist</i>
<i>Biotechnology and Applied Biochemistry</i>	

Authors of articles published in the above journals

Authors do NOT usually need to contact Portland Press Limited to request permission to reuse their own material, as long as the material is properly credited to the original publication. It is usual to provide the citation of the original publication thus:

“This research was originally published in Journal Name. Author(s), Title. Journal Name. Year; Volume: pp-pp © copyright holder”

The copyright holder for each publication is as follows:

© the Biochemical Society	© Portland Press Limited
<i>Biochemical Journal</i>	<i>ASN NEURO</i>
<i>Biochemical Society Symposia</i>	<i>Biology of the Cell</i>
<i>Biochemical Society Transactions</i>	<i>Biotechnology and Applied Biochemistry</i>
<i>Bioscience Reports</i>	<i>Cell Biology International</i>
<i>Clinical Science</i>	<i>Cell Biology International Reports</i>
<i>Essays in Biochemistry</i>	<i>Cell Signalling Biology</i>

The Biochemist

Provided the original publication of the article, or portion of the article, is properly cited, Authors retain the following non-exclusive rights:

1. **To reproduce their article in whole or in part in any printed volume (book or thesis) of which they are the Author or Editor**
2. To reproduce their article in whole or in part at the Author's current academic institution for teaching purposes
3. To reuse figures, tables, illustrations or photos from the article in commercial or non-commercial works created by them
4. To post a copy of the Immediate Publication (i.e. the Accepted Manuscript*) at the Author's Institutional Repository, 6 months after publication, provided that this is linked to the article on the journal website (e.g. through the DOI).

In addition, authors of Opt2Pay articles, or authors of articles published in the open access journals *ASN NEURO* and *Cell Biology International Reports*, may post the Version of Record** to their Institutional Repository. Portland Press Limited will deposit the Version of Record in PubMed Central on behalf of the author, where applicable.

Requests for non-commercial use

Other parties wishing to use reuse an article in whole or in part for educational purposes (e.g. in lectures or tutorials) may do so at no cost providing the original source is attributed, as outlined above.

You may also reproduce an article in whole or in part in your thesis at no cost providing the original source is attributed.

If you wish to copy and distribute an article in whole for teaching (e.g. in a course pack), please contact your librarian who will advise you on the various clearance options available.

STM Permission Guidelines

Portland Press Limited is a signatory of the [STM Permission Guidelines](#), which aims to reduce the administration involved in clearing permissions.

Publishers who are also signatories to the STM Permission Guidelines may re-use work published in Portland Press Limited journals, without contacting us, as long as the work is appropriately used and attributed as stated in the Guidelines.

All other usage requests, including Books

For all other requests please download and complete the [permission request form](#) and send by email or fax to:

(e) permissions@portlandpress.com

(f) +44 (0) 20 7685 2469

*Accepted Manuscript – (also known as Immediate Publication) - the version of the article that has been accepted for publication and includes the revisions made following Peer Review.

**Version of Record - the version of the article, after processes such as copyediting, proof corrections, layout and typesetting have been applied.

Please see the [NISO/ALPSP guidelines](#) for a full description of these terms.

Journal of Investigative Dermatology

If you are the author of this content (or his/her designated agent) please read the following. Since 2003, ownership of copyright in original research articles remains with the Authors*, and provided that, when reproducing the Contribution or extracts from it, the Authors acknowledge first and reference publication in the Journal, the Authors retain the following non-exclusive rights:

1. **To reproduce the Contribution in whole or in part in any printed volume (book or thesis) of which they are the author(s).**
2. They and any academic institution where they work at the time may reproduce the Contribution for the purpose of course teaching.
3. To reuse figures or tables created by them and contained in the Contribution in other works created by them.
4. To post a copy of the Contribution as accepted for publication after peer review (in Word or Tex format) on the Author's own web site, or the Author's institutional repository, or the Author's funding body's archive, six months after publication of the printed or online edition of the Journal, provided that they also link to the Journal article on NPG's web site (eg through the DOI).

NPG encourages the self-archiving of the accepted version of your manuscript in your funding agency's or institution's repository, six months after publication. This policy complements the recently announced policies of the US National Institutes of Health, Wellcome Trust and other research funding bodies around the world. NPG recognizes the efforts of funding bodies to increase access to the research they fund, and we strongly encourage authors to participate in such efforts.

Authors wishing to use the published version of their article for promotional use or on a web site must request in the normal way.

If you require further assistance please read NPG's online author reuse guidelines.

Note: British Journal of Cancer and Clinical Pharmacology & Therapeutics maintain copyright policies of their own that are different from the general NPG policies. Please consult these journals to learn more.

* Commissioned material is still subject to copyright transfer conditions

Ethics Approvals



Office of Research Ethics

The University of Western Ontario
 Room 4180 Support Services Building, London, ON, Canada N6A 5C1
 Telephone: (519) 661-3036 Fax: (519) 850-2466 Email: ethics@uwo.ca
 Website: www.uwo.ca/research/ethics

Use of Human Subjects - Ethics Approval Notice

Principal Investigator: Dr. D.W. Laird
Review Number: 12102E
Review Date: January 5, 2010
Protocol Title: Assessment of a local family with oculodentodigital dysplasia
Department and Institution: Anatomy, University of Western Ontario
Sponsor:
Ethics Approval Date: January 5, 2010
Documents Reviewed and Approved: Revised Study End Date
Documents Received for Information:

Review Level: Expedited
Revision Number: 4
Approved Local # of Participants: 20
Expiry Date: January 31, 2014

This is to notify you that The University of Western Ontario Research Ethics Board for Health Sciences Research Involving Human Subjects (HSREB) which is organized and operates according to the Tri-Council Policy Statement: Ethical Conduct of Research Involving Humans and the Health Canada/ICH Good Clinical Practice Practices: Consolidated Guidelines; and the applicable laws and regulations of Ontario has reviewed and granted approval to the above referenced revision(s) or amendment(s) on the approval date noted above. The membership of this REB also complies with the membership requirements for REB's as defined in Division 5 of the Food and Drug Regulations.

The ethics approval for this study shall remain valid until the expiry date noted above assuming timely and acceptable responses to the SREB's periodic requests for surveillance and monitoring information. If you require an updated approval notice prior to that time you must request it using the UWO Updated Approval Request Form.

During the course of the research, no deviations from, or changes to, the protocol or consent form may be initiated without prior written approval from the HSREB except when necessary to eliminate immediate hazards to the subject or when the change(s) involve only logistical or administrative aspects of the study (e.g. change of monitor, telephone number). Expedited review of minor change(s) in ongoing studies will be considered. Subjects must receive a copy of the signed information/consent documentation.

Investigators must promptly also report to the HSREB:

- changes increasing the risk to the participant(s) and/or affecting significantly the conduct of the study;
- all adverse and unexpected experiences or events that are both serious and unexpected;
- new information that may adversely affect the safety of the subjects or the conduct of the study.

If these changes/adverse events require a change to the information/consent documentation, and/or recruitment advertisement, the newly revised information/consent documentation, and/or advertisement, must be submitted to this office for approval.

Members of the HSREB who are named as investigators in research studies, or declare a conflict of interest, do not participate in discussion related to, nor vote on, such studies when they are presented to the HSREB.

Chair of HSREB: Dr. Joseph Gilbert
 FDA Ref. #: IRB 00000940

Ethics Officer to Contact for Further Information

<input type="checkbox"/> Janice Sutherland (jsutherl@uwo.ca)	<input type="checkbox"/> Elizabeth Wambolt (ewambolt@uwo.ca)	<input checked="" type="checkbox"/> Grace Kelly (grace.kelly@uwo.ca)	<input type="checkbox"/> Denise Grafton (dgrafton@uwo.ca)
---	---	---	--

This is an official document. Please retain the original in your files.

cc: ORE File
 LHRI



11.01.09

***This is the 3rd Renewal of this protocol**
 *A Full Protocol submission will be required in 2010

Dear Dr. **Laird**

Your Animal Use Protocol form entitled:

The role of gap junction in diseases

has had its yearly renewal approved by the Animal Use Subcommittee.

This approval is valid from **11.01.09 to 10.31.10**

The protocol number for this project remains as **2006-101**

1. This number must be indicated when ordering animals for this project.
2. Animals for other projects may not be ordered under this number.
3. If no number appears please contact this office when grant approval is received.
If the application for funding is not successful and you wish to proceed with the project, request that an internal scientific peer review be performed by the Animal Use Subcommittee office.
4. Purchases of animals other than through this system must be cleared through the ACVS office. Health certificates will be required.

REQUIREMENTS/COMMENTS

Please ensure that individual(s) performing procedures on live animals, as described in this protocol, are familiar with the contents of this document.

The holder of this *Animal Use Protocol* is responsible to ensure that all associated safety components (biosafety, radiation safety, general laboratory safety) comply with institutional safety standards and have received all necessary approvals. Please consult directly with your institutional safety officers.

c.c. W Lagerwert

The University of Western Ontario

Animal Use Subcommittee / University Council on Animal Care
 Health Sciences Centre, ● London, Ontario ● CANADA N6A 5C1
 PH: 519-661-2111 ext. 86770 ● FL 519-661-2028 ● www.uwo.ca/animal

Curriculum Vitae

Education Background

- PhD Candidate, University of Western Ontario, London, ON, 2007- Current
Department: Anatomy and Cell Biology
Supervisor: Dr. Dale Laird
Thesis Topic: Mutant Connexin43 in skin development and disease
- MSc degree, University of Western Ontario, London, ON, 2004-2006
Department: Anatomy and Cell Biology
Supervisor: Dr. Peter Merrifield
Thesis Topic: Muscle satellite cell lineage and differentiation
- Hons BSc degree, McMaster University, Hamilton, ON, 2000-2004
Program: Honors Biology and Psychology- Graduated with Distinction

Scholarships/Awards

International/National

- Alexander Graham Bell NSERC- \$70,000, London, ON, 2009-2011
- ASCB/JSCB/Riken CDB Travel Award- \$1,000, Kyoto, Japan, 2009
- International Gap Junction Conference Travel Award- €500, Ghent, Belgium, 2011

Provincial

- Ontario Graduate Scholarship- \$15,000, London, ON, 2008-2009
- General Proficiency Award Saskatchewan Education- \$400, Yorkton, SK, 2000

Local

- Graduate Thesis Research Award- \$437, London, ON, 2011
- Anatomy and Cell Biology PhD Entrance Scholarship- \$2000, London, ON, 2007
- Schulich Graduate Scholarship, London, ON, 2007
- Western Graduate Research Scholarship, London, ON, 2007
- Schulich Enhancement Scholarship, London, ON, 2007
- Schulich School of Medicine and Dentistry Travel Award-\$1000, London, ON, 2006
- Anatomy and Cell Biology Altman Award-\$250, London, ON, 2005
- Special University Scholarship (University of Western Ontario), London, ON, 2005
- Anatomy and Cell Biology Graduate Entrance Scholarship- \$1000, London, ON, 2004
- McMaster University Entrance Scholarship- \$1000, Hamilton, ON, 2000
- Co-operative Association Student Award, Yorkton, SK, 2000

Publications

Peer Reviewed Publications

- **Churko, J.M.**, McDonald,A., Shao, Q., Laird., D.W. 3 Mutant Cx43 enhances keratinocyte proliferation without impacting keratinocyte migration. (*in preparation*)

- **Churko, J.M.**, Chan, J., Pan, X., Shao, Q., Laird, D.W. Mice Expressing the G60S Mutant Cx43 Develop Similar Hair Abnormalities Commonly Presented by Oculodentodigital Dysplasia Patients (*Journal of Investigative Dermatology*, in press)
- **Churko, J.M.**, and Shao, Q., Gong, X., Swoboda, K.J., Bai, D., Sampson, J., and Laird, D.W. (2011) Human dermal fibroblasts derived from oculodentodigital dysplasia patients suggest that patients may have wound-healing defects. *Human Mutation*, Apr;32(4):456-66.
- **Churko, J.M.**, Langlois, S., Pan, X., Shao, Q., Laird, D.W. (2010) The potency of the fs260 connexin43 mutant to impair keratinocyte differentiation is distinct from other disease-linked connexin43 mutants. *Biochemical Journal.*, 429 (3):473-83.
- Celetti S.J., Cowan K.N., Penuela S, Shao Q, **Churko J**, Laird D.W. (2010) Implications of Pannexin 1 and Pannexin 3 in Keratinocyte Differentiation. *Journal of Cell Science* 123(Pt 8):1363-72.
- Gehi, R.B., Penuela S., **Churko J.M.**, Shao, Q., and Laird D.W. (2010) Panx1 and Panx3 Delivery, Cell Surface Dynamics and Cytoskeletal Interactions. *Journal of Biological Chemistry*, 285(12):9147-60.
- Simek J., **Churko, J.**, Shao, Q., Laird, D.W. (2009). Cx43 demonstrates distinct mobility within plasma membrane domains indicative of progressive gap junction plaque formation. *Journal of Cell Science*. Feb 15;122(Pt 4):554-62.
- Manias, J.L., Plante, I., Gong, X.Q., Shao, Q., **Churko, J.**, Bai, D., Laird, D.W. (2008). Fate of Cx43 in Cardiac Tissue Harboring a Disease-Linked Cx43 Mutant. *Cardiovascular Research*. Dec 1;80(3):385-95.

Invited Book Chapters

- **Churko, J.M.**, Laird, D.W., (2010) “Gap junctions as a Cellular Domain” in Cellular Domains edited by Ivan Robert Nabi, John Wiley & Sons, Inc. N.J. (in press)
- Langlois, S., **Churko, J.M.**, and Laird, D.W. (2008) “Optical and biochemical dissection of connexin and disease-linked connexin mutants in 3D organotypic epidermis” In: *Epidermal Cells: Methods and Protocols*, Second Edition, Kursad Turksen, Ed. The Humana Press Inc. N.J.

Local and International Meetings

- Churko, J.M., Shao, Q., Sampson, J., Laird, D.W. (2010) Subclinical skin disease in oculodentodigital dysplasia patients as revealed by organotypic cultures, mutant mouse models and patient derived fibroblasts. International Gap Junction Conference 2011. Ghent, Belgium, Aug. 6-11. (Ph.D., International conference)
 - *This abstracts is invited for a platform session to be presented on August 9th.*

- Churko, J.M., Shao, Q., Sampson, J., Laird, D.W. (2010) Cutaneous Wound Healing Defects Associated with Mutant Cx43 Expression. American Society of Cell Biology. Philadelphia, PA; Dec. 11-15. (Ph.D., International conference)
- Churko, J.M., Shao, Q., Sampson, J., Flanigan, K.M. Swoboda, K.J., Laird, D.W. (2009) Delayed wound healing in mouse and human models of oculodentodigital dysplasia suffering from compromised Cx43 gap junctions. ASCB/JSCB/Riken CDB Meeting, Kyoto, Japan: Sept. 21-23.
- Churko, J.M., Chan, J., Shao, Q., Laird D.W. (2009) Hair follicle development and epidermal differentiation in mice and organotypic epidermal cultures expressing mutant Cx43. International Gap Junction Conference. Sedona, AZ.; July. 25-30.
- Churko, J., Shao, Q. C., Sampson, J., Flanigan, K., Swoboda, K., Laird, D. W. Mapping oculodentodigital dysplasia-linked genetic mutations in Cx43 to an epidermal phenotype using cell, mouse, and human reference models. American Society of Cell Biology. San Francisco, CA; Dec. 12-17, 2008.
 - *This abstract was invited for a platform session in a Sub-Group meeting which was presented on December 13th.*
- Q. Shao, J. Churko, J. Sampson, K.M. Flanigan, K.J. Swoboda, and D.W. Laird (2008) “Aberrant Cx43 localization and function in cells and tissues obtained from oculodentodigital dysplasia patients mimic findings from mutant mouse models of Cx43-linked disease. 48th American Society for Cell Biology Meeting, San Francisco, CA
- Churko, J., Clow, C., Conway, K. and Merrifield, P.A.* Fiber-Type Specific Expression of Contractile Protein Isoforms in Different Myogenic Lineages and Cell Lines. EMBO Conference Series. Conference I, The Molecular and Cellular Mechanisms Regulating Skeletal Muscle Development and Regeneration. Sant Feliu de Guixols, Spain; Sept. 24-29, 2008.
- Churko, J., Shao, Q., Laird, D.W. (2008) An oculodentodigital dysplasia-linked frame-shift Cx43 mutant is retained within the endoplasmic reticulum of keratinocytes and exhibits dominant-negative properties. Margaret P. Moffat Graduate Research Day, London, ON; May 2008.
- Churko, J. and Merrifield, P.A. (2006). Regulating myogenic differentiation through p38 signalling in C2C12 cells. Frontiers in Myogenesis Conference, Pine Mountain, GA. 2006
- Churko, J. and Merrifield, P.A. (2005). Early p38 activation in C2C12 myoblasts maintains myoblast proliferation, while later p38 activation is required for fusion. 45th Annual meeting of the American Society for Cell Biology, San Francisco, CA; Dec 2005.
- Churko, J. and Merrifield, P.A. (2005). Satellite cells from neonatal rat muscle co-express multiple myosin heavy chain isoforms in vitro. 45th Annual meeting of the American Society for Cell Biology, San Francisco, CA; Dec 2005

- Churko, J., Mehta, S., Punch, V. and Merrifield, P.A. (2005). Origin and Fate of Muscle Satellite Cells in Developing Rat Hindlimb Muscle. FASEB Summer Research Conference on Skeletal Muscle Satellite and Stem Cells, Tucson, AZ; June 11-16, 2005.
- Churko, J. Mehta, S., Punch, V. and Merrifield, P.A. (2005). Identification, isolation and characterization of satellite cells from developing rat hindlimb muscles. Margaret P. Moffat Graduate Research Day, London, ON; May 2005
- Awarded Altman Award for best poster presentation
- Churko, J. Mehta, S., Punch, V. and Merrifield, P.A. (2005). Identification, isolation and characterization of satellite cells from developing rat hindlimb muscles Great Lakes Mammalian Meeting, Toronto, ON; Dec 2005.

Teaching Experience

- Mentored 4th year Undergraduate Honors Thesis Projects
Xinyue Pan – 2009
Jason Chan – 2008
- Teaching Assistant for Medical Science Honors Thesis Course, (University of Western Ontario), London, ON, 2009-2011
- Lab Coordinator for Anatomy 319, (University of Western Ontario), London, ON, 2006,08-09
- Teaching Assistant for Anatomy 319, (University of Western Ontario), London, ON, 2005

Platform Presentations

- International Gap Junction Conference, Ghent, Belgium, Aug 9, 2011
 - Talk entitled "Subclinical skin disease in oculodentodigital dysplasia patients as revealed by organotypic cultures, mutant mouse models and patient derived fibroblasts"
- Gap Junction Research Day, London, ON, Jan 14, 2011
 - Talk entitled "Hair abnormalities associated with the expression of mutant Connexin43"
- Anatomy and Cell Biology Seminar Series, London, ON, May 7, 2010
 - Talk entitled "The role of Cx43 in skin disease and wound healing"
- American Society of Cell Biology Conference, San Francisco, CA, December 13, 2008
 - Platform session in a Sub-Group meeting
 - Talk entitled "Mapping oculodentodigital dysplasia-linked genetic mutations in the GJA1 gene to phenotypic outcomes using cell, mouse and human reference models"
- Western Research Forum, London, ON, 2006
 - Talk entitled "Muscle Satellite Cells and the Expression of MyHCs"
- Lawson Health Research Institute Research Days, London, ON, 2005
 - Talk entitled "Identification, isolation and characterization of satellite"

Other Contributions

Leadership Roles

Elected student representative on Anatomy and Cell Biology Graduate Affairs Committee, 2007

Elected President of the McMaster Biology and Psychology Society, Hamilton, ON, 2003

Community Outreach/Volunteer

“Movember”- Raised funds for Prostate Cancer Research, London, ON, 2010

Anatomy and Cell Biology Recruitment Event, London, ON, 2008, 2009

Schulich Graduate Open House, London, ON, 2007, 2009

Canadian Cancer Society Relay for Life, London, ON, 2005, 2006, 2008, 2009

Mentor for Big Brothers of London, London, ON, 2006-2008

Let's Talk Science Volunteer, London, ON, 2005-2007, 2009

Lawson Affiliation of Fellows and Students, London, ON, 2004-2006

Captain of Labatt 24 Hour Relay (raised >\$2300 for the London hospitals), London, ON, 2005

Easter Seals, "Tee Up for Easter Seals Golf Tournament," Dundas, ON, 2005

Canadian Medical Hall of Fame Discovery Days (Moderator), London, ON, 2005

May at Mac- Promoted Psychology at McMaster, Hamilton, ON, 2005

Canadian Foundation for AIDS Research, Bloor Street Entertains, Toronto, ON, 2004

Exercise Assistant for disabled individuals at the McMaster University Hamilton, ON, 2004

Rick Hansen: Wheels in Motion 5 km Race, Hamilton, ON, 2003

Prevention of Colorectal Cancer 5K race, Hamilton, ON, 2002

Taught Tae Kwon Do on a First Nations Reserve, Fort Qu'Appelle, SK, 1999

Boys on the move- After School Sports for Grade 4-6, Yorkton, SK, 1998